Développment et Croissance de la Musculature Épaxial et du Membre chez les Amniotes

Gauthier Toulouse

Université Claude Bernard Lyon 1

THESE de DOCTORAT DE
L'UNIVERSITE CLAUDE BERNARD LYON 1

Ecole Doctorale N° 340
Biologie Moléculaire, Intégrative et Cellulaire

Biologie du développement

Soutenue publiquement le 21/10/2024, par :

Gauthier Toulouse

Development and Growth of Limb and Epaxial Musculature in Amniotes

---

Devant le jury composé de :

Chédotal Alain	PU-PH	Université Claude Bernard Lyon1	Président
Duprez Delphine	DR CNRS	Institut de Biologie Paris Seine	Rapporteure
Maire Pascal	DR Inserm	Institut Cochin	Rapporteur
Kardon Gabrielle	Professor	University of Utah	Examinatrice
Pourquié Olivier	Professor	Harvard Medical School	Examinateur
Buckingham Margaret	Honorary Professor	Institut Pasteur	Examinatrice
Marcelle Christophe	PU	Université Claude Bernard Lyon1	Directeur de thèse
Le Grand Fabien	DR CNRS	Institut NeuroMyoGène	Invité

À mon grand-père, Noël

Acknowledgments

First and foremost, I would like to deeply thank all the members of my thesis jury for graciously accepting the responsibility of evaluating my Ph.D. thesis. I am deeply honored to present my work to each one of you, not only because of your remarkable expertise in myogenesis but also because of the respect and admiration I hold for you as scientists.

Thanks to William Jarrassier and Fabien Le Grand for helping me set up and conduct the analysis of the scRNA-seq experiment.

Thanks to Miyuki Suzuki and Marianne Bronner from Caltech for providing the *Pleurodeles waltl* specimens; thanks to Anna Iouchmanov and Douglas Menke from the University of Georgia for providing the *Anolis sagrei* specimens; and thanks to Marie-Élise Schwartz from Tefor Paris-Saclay for providing the *Xenopus laevis* samples. Thanks to Alain Chédotal and Joséphine Blevinal from Institute de la Vision for their help with the light-sheet imaging.

Thanks to Martin Scaal for his help with all the anatomical references, and especially for the chicken dissections.

Merci à Christophe de m'avoir accueilli dans son équipe de recherche pour me permettre d'effectuer mes travaux de thèse.

Merci à Julie de m'avoir fait me sentir aussi bien dans cette équipe dès le début et de m'avoir transmis le flambeau de l'électroporation.

Merci à Chloé pour les nombreuses aides avec la culture cellulaire, mais surtout pour le soutien mutuel dès le début de nos thèses respectives, au laboratoire ou en dehors.

Merci à Inès pour sa grande implication dans le projet des muscles épaxiaux, qui, sans son travail, ne serait sans doute encore qu'à ses prémices.

Merci à Clémence pour sa bonne humeur, son soutien et son énergie positive au quotidien.

Merci à Yoann pour sa patience et son écoute.

Merci à Valérie pour son aide au de tous les jours, tout son travail pour veiller à une bonne organisation et une bonne cohésion d'équipe, son aide pour les *in situ Cxcr4*, et plus particulièrement pour m'avoir inculqué de solides bases de clonage durant mes débuts dans l'équipe.

Merci à Émilie pour son écoute, sa culture, et les nombreuses discussions scientifiques ainsi que sur le monde académique en général.

Merci à Zoé de m'avoir aidé à faire avancer le projet sur les muscles épaxiaux et surtout pour m'avoir aidé à mettre en place les greffes de somites.

Merci à tous les membres de l'équipe Marcelle, présents ou passés, que j'ai pu croiser ici ou en Australie : Marie-Julie, Hila, Lina, Nadège, Olivier, Claire, Clémence L., Erwan, Kathrin, Alizée.

Merci à toute l'équipe du CIQLE, plus particulièrement à Denis, pour m'avoir aidé tout au long de ma thèse avec le SP5, et à Bruno pour le scanner de lames et sa grande écoute.

Merci à Thierry et Fabien pour vos commentaires élogieux et bienveillants lors de mes comités de suivi de thèse.

Merci à Julien pour les discussions scientifiques et son expertise précieuse en matière d'imagerie 3D.

Merci à toutes les personnes, du côté recherche ou administratif au laboratoire, qui ont pu m'aider à un moment ou à un autre, même pour le plus petit des services.

Merci à toute ma famille et plus particulièrement à mes parents qui ont toujours cru en moi et m'ont toujours soutenu moralement et financièrement à chaque étape de mes études. Merci à ma grand-mère Arlette et mon grand-père Noël de m'avoir donné ce goût pour l'observation de la nature. Merci à mon grand-père Robert pour son soutien vis-à-vis de mes différents voyages.

Merci à Margaux de m'avoir rejoint en cours de route dans cette aventure. Je suis sûr qu'il nous en reste encore plein d'autres à vivre ensemble.

Abbreviation List

AP: Antero-posterior
AL: Anterior lip
bHLH: Basis helix-loop-helix
BMP: Bone morphogenetic protein
BSA: Bovine serum albumin
CNCC: Cranial neural crest cell
COL2: Collagen 2
CPM: Cardiopharyngeal mesoderm
CR: Carapacial ridge
DML: Dorso-medial lip
DTA: Diphteria toxin A
DV: Dorso-ventral
EC: Endothelial cells
ECi: Ethyl Cinnamate
ECM: Extra-cellular matrix
eGFP: Enhanced green fluorescent protein
EMT: Epithelio-mesenchymal transition
ERK: Extracellular signal-regulated kinases
EtOH: Ethanol
FGF: Fibroblast growth factor
FISH: Fluorescent *in situ* hybridization
HCR: Hybridization Chain Reaction
GEF: Guanine nucleotide exchange factor
iPS: Induced pluripotent stem cells
HH: Hamburger-Hamilton
LEC: Lymphatic endothelial cell
LPM: Lateral plate mesoderm
MCT: Muscle connective tissue
MetOH: Methanol
MRF: Muscle regulatory factor
mRNA: Messenger ribonucleic acid
MyHC: Myosin Heavy Chain
NC: Notochord
NCC: Neural crest cell
NT: Neural tube
PA: Pharyngeal arch
PBS: Phosphate buffer saline
PS: Phosphatidyl serine or Primitive streak
PSM: Pre-somitic mesoderm
RA: Retinoic acid
RT: Room temperature
SMA: Smooth muscle actin
vSMC: Vascular smooth muscle cell
VLL: Ventro-lateral lip
VNP: Venus-NLS-PEST
WB: Washing buffer
WM: Wholemount
WT: Wild-type

For axis orientation:
A: Anterior
P: Posterior
L: Left or Lateral
R: Right
M: Medial
D: Dorsal
V: Ventral

Summary

The trunk and limb muscles of amniotes originate from **somites**, which are spherical assemblies of epithelial cells lining each side of the neural tube. Somites are generated in the pre-somitic mesoderm (PSM) through a periodic process known as **somitogenesis**. During somitogenesis, clusters of cells at the anterior end of the PSM undergo repeated epithelialization throughout embryonic life to form the somites. These structures are formed in pairs along the antero-posterior axis, representing the earliest sign of **segmentation**, or **metamerization**, of the embryo.

Once formed, somites experience dramatic cellular and molecular changes in response to signals from surrounding tissues. The ventral portion undergoes an **epithelial-to-mesenchymal transition** (EMT) to form the **sclerotome**, while the dorsal portion remains epithelial and differentiates into a structure known as the **dermomyotome**. The sclerotome provides precursors for the bones, cartilage, and tendons of the axial musculoskeletal system, while the dermomyotome gives rise to all the muscles of the trunk and limbs, the hypoglossal system, and the diaphragm. The dermomyotome also generates the dermal cells of the back and the brown fat in mammals. Additionally, both regular and lymphatic endothelial cells, along with their associated mural cells, originate from the somitic lineage.

Vertebrate musculature is broadly divided into two main categories: **hypaxial** muscles and **epaxial** muscles. Hypaxial muscles include those of the body wall, limbs, associated pectoral or pelvic girdle, the hypoglossal system, and the diaphragm. The epaxial muscles, on the other hand, comprise the deep muscles of the trunk and neck. Regarding their development, both hypaxial and epaxial muscles rely on several intricate processes during pre-natal life: (1) a cellular determination of undifferentiated muscle progenitors toward the myogenic lineage, (2) the fusion of theses differentiated myogenic cells to form multinucleated myofibers (3) the formation and patterning of newly formed myofibers into functional muscle bundles, a process often referred to as **primary myogenesis** (4) the growth of these muscle bundles through the addition of nuclei to primary myofibers and the formation of new myofibers, known as **secondary myofibers**, while a population of stem progenitors is set aside to form adult muscle stem cells, known as satellite cells.

During limb myogenesis, muscle precursors from somites at specific levels migrate laterally and invade the growing limb bud, where they proliferate and differentiate to form all the musculature of the limb and associated girdle. Throughout this process, migrating myogenic progenitors are exposed to a variety of signals that regulate their proliferation, migration, and early and late differentiation. Although significant progress has been made in understanding these steps over the past two decades, particularly regarding intrinsic and extrinsic cues, the role of the Wnt-TCF/LEF signaling pathway remains controversial. While its early function during somite and dermomyotome development is well-documented, its precise role in limb myogenesis is ambiguous.

In this manuscript, I addressed this question by using a newly destabilized transcriptional reporter for the Wnt-TCF/LEF signaling pathway and chicken embryo somite electroporation. I demonstrated that TCF/LEF activity is restricted to a population of **early differentiated myoblasts** within the limb bud. As developmental timing progresses, muscle progenitors abruptly **cease their response** to TCF/LEF, coinciding with the individualization of the first muscle bundles from a homogeneous muscle anlage. By designing a **dynamic and inducible lineage tracing tool**, I showed that only a sub-population of early progenitors responds to TCF/LEF. Fate mapping revealed that TCF/LEF-responding cells preferentially form the **first fibers of the muscle bundles**, while non-responding cells seem to be reserved for the later formation of **secondary myotubes and satellite cells**. Genetic

perturbation of TCF/LEF transcription in early myoblasts revealed that while their myogenic differentiation and proliferation were unaffected, their **migration** was significantly impacted. Further scRNA-seq analysis indicated that TCF/LEF-responding myoblasts have higher transcript levels of genes involved in cellular migration, such as ***Cxcr4*****,** that appears to be regulated by TCF/LEF signaling. These results suggest that TCF/LEF is essential for an early limb myogenic population that forms the first myofibers of the limb, known as the primary myofibers.

In vivo early myogenic differentiation has been extensively studied in the epaxial compartment within the early somite, leading to a detailed blueprint of early epaxial myogenesis. The segmented somites give rise to **repeated** early myotomes along the antero-posterior axis, with small myofibers spanning only over one segment. However, in adult amniotes, several epaxial muscle bundles extend over the **entirety of the back or the neck**. Due to their anatomical complexity and the technical limitations of imaging late embryos and fetuses, the late development and patterning of these muscles remains a mystery.

In the second part of my Ph.D., I investigated the **late morphogenesis of the epaxial musculature** using light sheet 3D imaging and **single-somite electroporation** in chicken embryos. I demonstrated that the segmented myotome first adopts a **chevron-shaped** structure, with myofibers from a defined segment shifting and elongating along the antero-posterior axis. This phenomenon appears to occur at the same stages in all amniotes, while myotomes remain segmented throughout the life of Lissamphibia. Additionally, I showed that both myofibers and muscle progenitors from a defined segment can be detected up to **seven vertebrae** away from the segment of origin, and that they can contribute to distinct muscle bundles. Furthermore, I developed an experimental system to **differentially label two adjacent somites**, allowing me to determine the spatiotemporal dynamics of segment mixing that leads to the formation of mosaic myofibers. This part is currently ongoing.

More generally, these two projects have demonstrated several key points:

(1) When studying a signaling pathway, **dynamical tools** are essential to characterize the detailed response of the system, avoiding incorrect assumptions that might arise from only studying inhibition or activation of the pathway. Questions like "Where, when, which cells, how many, and for how long?" should be fundamental when studying a signaling pathway in a defined system.
(2) A **global response** to a signaling pathway, rather than just focusing on one gene, can be used to trace different populations during development.
(3) Solid **anatomical references** are crucial for understanding the morphogenetic events underlying the formation of a defined organ.
(4) **A 3D view** of an embryonic system is highly informative and provides valuable insights into the developmental process.

Keywords: Myogenesis, somite, chicken embryo, electroporation, limb development, primary myogenesis, TCF/LEF, epaxial muscles, metamerization.

Résumé

Les muscles du tronc et des membres des amniotes proviennent des somites, qui sont des assemblages sphériques de cellules épithéliales situées de chaque côté du tube neural. Les somites sont générés dans le mésoderme pré-somitique (PSM) par un processus périodique appelé somitogenèse. Pendant la somitogenèse, des groupes de cellules à l'extrémité antérieure du PSM s'épithélialisent de façon répétée tout au long de la vie embryonnaire pour former les somites. Ces structures associées paire le long de l'axe antéro-postérieur, représentent le premier signe de segmentation, ou métamérisation, de l'embryon.

Une fois formés, les somites subissent d'importants changements cellulaires et moléculaires en réponse aux signaux des tissus environnants. La portion ventrale subit une transition épithélio-mésenchymateuse (EMT) pour former le sclérotome, tandis que la portion dorsale reste épithéliale et se différencie en une structure appelée dermomyotome. Le sclérotome fournit les précurseurs des os, du cartilage et des tendons du système musculo-squelettique axial, tandis que le dermomyotome donne naissance à tous les muscles du tronc et des membres, du système hypoglosse et du diaphragme. Le dermomyotome génère également les cellules dermiques du dos et la graisse brune chez les mammifères. De plus, les cellules endothéliales régulières et lymphatiques, ainsi que leurs cellules murales associées, proviennent de la lignée somitique.

La musculature des vertébrés est généralement divisée en deux grandes catégories : les muscles hypaxiaux et les muscles épaxiaux. Les muscles hypaxiaux comprennent ceux de la paroi abdominale, des membres, des ceintures pectorale ou pelvienne associées, du système hypoglosse et du diaphragme. Les muscles épaxiaux, quant à eux, comprennent les muscles profonds du tronc et du cou. En ce qui concerne leur développement, les muscles hypaxiaux et épaxiaux dépendent de plusieurs processus complexes au cours de la vie prénatale : (1) une détermination cellulaire de progéniteurs musculaires indifférenciés vers la lignée myogénique, (2) la fusion de ces cellules myogéniques différenciées pour former des myofibres multinucléées (3) la formation et la structuration de myofibres nouvellement formées en faisceaux musculaires fonctionnels, un processus souvent appelé myogenèse primaire (4) la croissance de ces faisceaux musculaires par l'ajout de noyaux aux myofibres primaires et la formation de nouvelles myofibres, appelées myofibres secondaires, tandis qu'une population de progéniteurs souches est mise de côté pour former des cellules souches musculaires adultes, appelées cellules satellites.

Au cours de la myogenèse des membres, les précurseurs musculaires des somites à des niveaux spécifiques migrent latéralement et envahissent le bourgeon du membre en croissance, où ils prolifèrent et se différencient pour former toute la musculature du membre et de la ceinture associée. Tout au long de ce processus, les progéniteurs myogéniques sont exposés à une variété de signaux qui régulent leur prolifération, leur migration et leur différenciation précoce et tardive. Bien que des progrès significatifs aient été réalisés dans la compréhension de ces étapes au cours des deux dernières décennies, en particulier en ce qui concerne les signaux intrinsèques et extrinsèques, le rôle de la voie de signalisation Wnt-TCF/LEF reste controversé. Alors que sa fonction précoce au cours du développement des somites et du dermomyotome est bien documentée, son rôle précis dans la myogenèse des membres est ambigu.

Dans ce manuscrit, j'ai abordé cette question en utilisant un nouveau rapporteur transcriptionnel déstabilisé pour la voie de signalisation Wnt-TCF/LEF et l'électroporation des somites d'embryons de poulet. J'ai démontré que l'activité TCF/LEF est limitée à une population de myoblastes précoces au sein du bourgeon du membre. Au fur et à mesure que le développement progresse, les

progéniteurs musculaires cessent brusquement leur réponse à TCF/LEF, ce qui coïncide avec l'individualisation des premiers faisceaux musculaires à partir d'une population homogène. En concevant un outil de lignage cellulaire dynamique et inductible, j'ai montré que seule une sous-population de progéniteurs précoces répond à TCF/LEF. L'étude du devenir de ces cellules a révélé que celles répondant à TCF/LEF forment préférentiellement les premières fibres des faisceaux musculaires, tandis que les cellules qui n'y répondent pas, semblent être réservées à la formation ultérieure de myotubes secondaires et de cellules satellites. La perturbation génétique de l'activité transcriptionnelle de TCF/LEF dans les myoblastes précoces a révélé que si leur différenciation myogénique et leur prolifération n'étaient pas impactées, leur migration était significativement affectée. Une analyse plus poussée en séquençage de l'ARN en cellule unique a indiqué que les myoblastes répondant à TCF/LEF ont des niveaux de transcription plus élevés de gènes reliés à la migration cellulaire, tels que *Cxcr4*, qui semble être régulé par la signalisation TCF/LEF. Ces résultats suggèrent que TCF/LEF est essentiel pour une population myogénique précoce qui forme les premières myofibres du membre, appelées myofibres primaires

La différenciation myogénique a été largement étudiée dans le compartiment épaxial du somite précoce, ce qui a conduit à un schéma détaillé de la myogenèse épaxiale quelque temps après la formation des somites. Les somites segmentés donnent naissance à des myotomes précoces répétés le long de l'axe antéro-postérieur, avec de petites myofibres ne s'étendant que sur un seul segment. Cependant, chez les amniotes adultes, plusieurs faisceaux musculaires épaxiaux s'étendent sur l'ensemble du dos ou du cou. En raison de leur complexité anatomique et des limites techniques de l'imagerie des gros embryons et des fœtus, le développement tardif et la structuration de ces muscles reste un mystère.Dans la deuxième partie de mon doctorat, j'ai étudié la morphogenèse tardive de la musculature épaxiale en utilisant l'imagerie 3D par feuille de lumière et l'électroporation d'un seul somite dans des embryons de poulet. J'ai démontré que le myotome segmenté adopte d'abord une structure en forme de chevron, avec des myofibres d'un segment défini se déplaçant et s'allongeant le long de l'axe antéro-postérieur. Ce phénomène semble se produire aux mêmes stades chez tous les amniotes, alors que les myotomes restent segmentés tout au long de la vie des amphibiens. De plus, j'ai montré que les myofibres et les progéniteurs musculaires d'un segment défini peuvent être détectés jusqu'à sept vertèbres du segment d'origine, et qu'ils peuvent contribuer à des faisceaux musculaires distincts. Enfin, j'ai développé un système expérimental pour marquer différemment deux somites adjacents, me permettant de déterminer la dynamique spatiotemporelle du mélange de segments qui conduit à la formation de myofibres mosaïques. Cette partie est actuellement en cours d'investigation.

Plus généralement, ces deux projets ont démontré plusieurs points clés :

(1) Lors de l'étude d'une voie de signalisation, des outils dynamiques sont essentiels pour caractériser la réponse du système, en évitant les hypothèses erronées qui pourraient découler de l'étude uniquement de l'inhibition ou de l'activation de la voie. Des questions telles que « Où, quand, quelles cellules, combien et pendant combien de temps ? » devraient être fondamentales lors de l'étude d'une voie de signalisation dans un système défini.
(2) Une réponse globale à une voie de signalisation, plutôt que de se concentrer uniquement sur l'expression d'un seul gène, peut être utilisée pour déterminer différentes populations au cours du développement.
(3) Des références anatomiques solides sont essentielles pour comprendre les événements morphogénétiques sous-jacents à la formation d'un organe défini.
(4) Une vue 3D d'un système embryonnaire est informative et fournit une approche précieuse sur le processus de développement étudié.

Mot clés : Myogenèse, somite, embryon de poulet, électroporation, développement du membre, myogenèse primaire, TCF/LEF, muscles épaxiaux, métamérie.

This Ph.D. thesis was prepared in the Mechanisms in Integrated Life Sciences (MeLiS) laboratory, Université Claude Bernard Lyon 1, CNRS UMR 5284 - INSERM U1314

Address:
Faculté de Médecine et de Pharmacie,
8 avenue Rockefeller
69008 Lyon, France

Introduction

Pre-somitic Mesoderm Formation and Somitogenesis

In this section I will briefly describe the cellular and molecular events leading to the formation of the precursors of all the axial and limb muscles (among other tissues), the somites, and the mechanisms responsible for their spatial patterning. As the somitogenesis is well-studied and quite complex, I will not try to depict an exhaustive list of all the molecular actors involved but instead a general overview of the process.

Gastrulation and Pre-somitic Mesoderm Formation

Gastrulation is an early major morphogenetic event in animal development. In vertebrates, during this process, a pluripotent single-layered epithelium, the **epiblast**, is restructured into three germ layers, the **ectoderm**, **mesoderm** and **endoderm** with restricted cell fate potentials. As most developmental stages, gastrulation is driven by four critical cell behaviors, i.e. cell division, cell differentiation, cell shape changes and cell movements.

Embryonically, all muscles of the trunk and limb derived from the **somite**, which are **repeated small sphere of epithelial cells flanking each side of the neural tube**. Somite organization is referred as **metameric** and serve as a blueprint for the stereotypical vertebrate body plan. They give rise to a great variety of cell types, among which the vertebrae, that exhibit an obvious metameric organization in the adult. Others somite-derived tissues exhibit metameric pattern, like the muscles and tendons articulating two adjacent vertebrae between them. More strikingly somites are able to instruct segmentation in non-somite derived tissues such as the peripheral nerves leading to what has been called the secondary segmentation. The precise number of somites is unique to each vertebrate, ranging from 31 in zebrafish, 44 in human or 52 in chicken, to approximatively 315 in the corn snake.

The mesoderm give rise to several tissues such as the uro-genital system, all musculoskeletal system, including muscle fibers, bones and tendons, the heart and the vasculature, with all its associated hematopoietic cell types. During gastrulation the mesoderm is subdivided into different mesodermal tissue, with specific location and destiny. Classically the trunk of an early amniote is composed of three different mesodermal tissues, the **paraxial mesoderm**, on each side of the neural tube, the **lateral plate mesoderm** on the lateral most-sides of the embryo and the **intermediate mesoderm** in between. The mesoderm of the most cranial region is often classified in different sub-mesodermal compartment but can be referred as the **cranial mesoderm**. Somites derive from the paraxial mesoderm. At the beginning of gastrulation, in the epiblast, the presumptive territory of the paraxial mesoderm is located bilaterally to the forming primitive streak that defines the future anteroposterior axis of the embryo. During **primitive streak** formation, these territories converge toward the streak and begin to ingress while undergoing an epithelial-mesenchymal transition (EMT). The first mesodermal precursors to ingress form the cranial mesoderm, which therefore lies at the anterior tip of the embryo. The cranial mesoderm does not form any somite but is responsible for the formation of nearly all the muscles of the head and neck. Then, the primitive streak begins to shrink and regress, and its anterior tip, which corresponds to the Spemann organizer of amniotes called **Hensen's node** or the node, moves posteriorly. In the chicken embryo, these mechanisms occur around Hamburger-Hamilton stage 4 (HH4) (18-19h after laying). At stage HH7, the regression of the primitive streak progressively forms more posterior levels of the paraxial mesoderm, corresponding to the somite precursors. Epiblast cells continue to ingress in the primitive streak and join the descendants of a

population of resident stem cells in the node to generate the paraxial mesoderm. At the end of this process, the paraxial mesoderm forms two strips of tissue bilaterally to the notochord and starts to form the first somite. Medial and lateral precursors of the PSM, and the somite later, are derived from the streak stem cells and the epiblast layer, respectively. In HH10 embryos (around 35h post laying), around 10 somites have formed, and the somite precursors now form a structure called the pre-somitic mesoderm (PSM). The PSM contains a newly form organizer named the **tail bud** that fulfill the production of somite progenitors. Whereas the primitive streak directly contributes to the formation of the most anterior somites, more posterior one derived from the tail bud. Somitogenesis from the tail bud therefore act in concert with axial elongation. (see (Chal and Pourquié, 2009). Somite are denominated with roman numerals, somite I being the last formed and somite II, the one just anterior etc. (Christ and Ordahl, 1995).

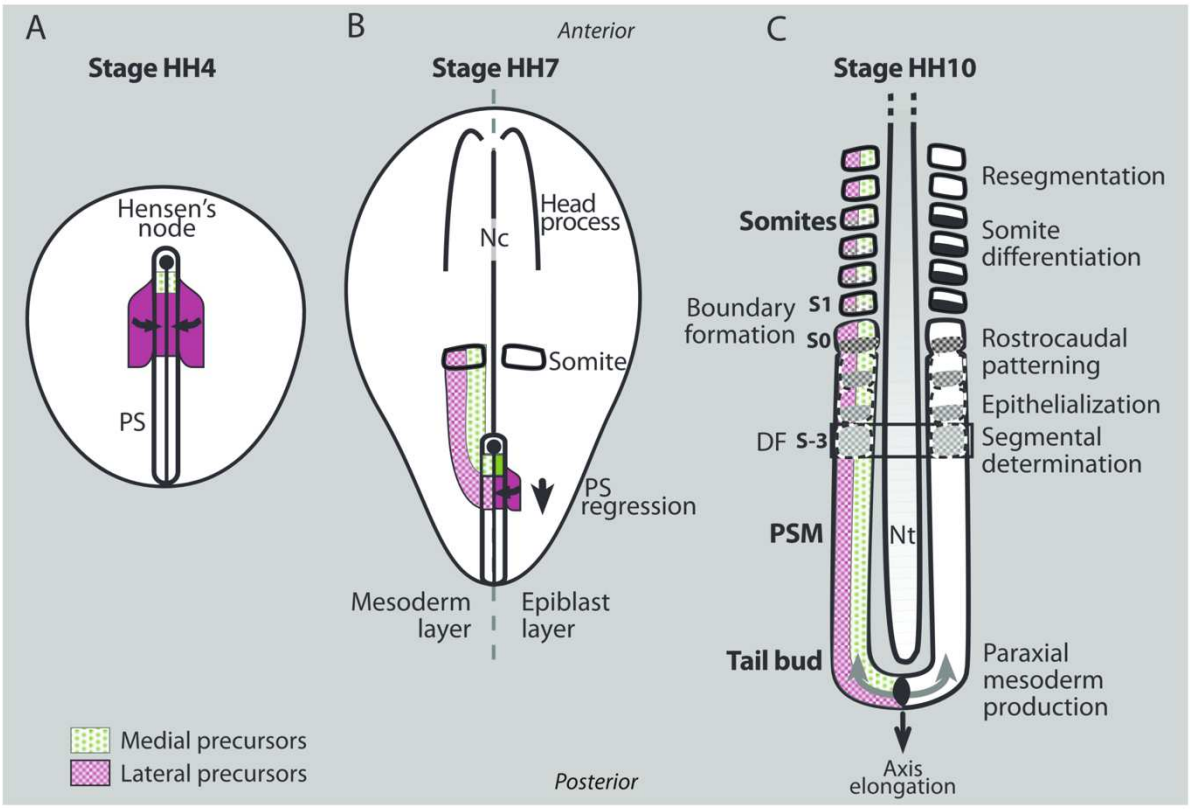

Figure 1. Paraxial mesoderm formation and segmentation in the chicken embryo. *From Chal and Pourquié, 2009. DF: Determination front, Nc: Notochord, Nt: Neural tube, PS: Primitive streak*

The Clock and Wavefront Model of Somitogenesis

The Clock

Somites are periodically generated from the PSM at a species-specific pace (for example, every 90 minutes in chickens, 120 minutes in mice, and around 5 hours in humans (Gomez et al., 2008; Miao et al., 2023). Theoretical works in the 70's have led to the hypothesis that the somites are formed through a mechanism referred as **"the clock and wavefront"** (Cooke and Zeeman, 1976). This model proposed that the periodicity of somites results from the action of a molecular oscillator (called the clock) traveling along the embryonic axis. In this model, the formation of a periodic segment is triggered during a defined permissive phase of the oscillation, while the oscillator is constantly displaced posteriorly by a wave of maturation, the wavefront, hence, ensuring the spacing

of the response to the oscillator. Years later, in 1997, Palmeirim et al. observed that the mRNA of *Hairy1,* a target of the **Notch signaling** pathway, was oscillating in the PSM of the chicken embryo (Palmeirim et al., 1997). Before forming a new somite, the PSM is therefore swiped by a wave of *Hairy1* expression. Temporally, *Hairy1* is first activated in the posterior most part of the PSM and progressively gets expressed in the more anterior PSM, giving the illusion of a traveling wave. This dynamical differential expression along the PSM was proposed to represent the clock of the clock and wavefront model. Several studies then have shown that other Notch targets, belonging to the same family of gene than *Hairy1*, the basic helix-loop-helix (bHLH) transcriptional repressors family (*Hes/Her/Hairy)* also exhibit a cyclic behavior in the fish, frog, chicken, and mouse PSM, indicating that the oscillator is conserved in vertebrates (see Chal and Pourquié, 2009 for a detailed review). Cyclic expression of other Notch pathway genes such as *Lfng* (Lunatic Fringe), which is a glycosyl-transferase that modifies the Notch receptor is detected but only in amniotes. All these genes are both target and inhibitors of the Notch signaling pathway, therefore, they establish a negative feedback loop, ensuring the dynamical activation of Notch in the PSM. Another group of cyclic genes linked to the **Wnt signaling** pathway were identified as cycling in the PSM. Two transcriptions factors, *Sp5* (Trans-acting transcription factor 5) and *Myc* (Myelocytomatosis oncogene) but also negative feedback inhibitors such as *Axin2* and *Dkk1* (Dickkopf WNT signaling pathway inhibitor 1). Finally, the last group of genes to oscillate are related to the **Fibroblast Growth Factor** (FGF) signaling pathway. Two negative feedback inhibitors of the FGF pathway, *Spry2* (Sprouty homologue 2) and *Dusp6* (Dual specificity phosphatase 6), show a clearly periodic profile. The FGF targets *Snai1* (Snail homologue 1), in mouse, and *Snai2*, in chicken, as well as the *Dusp4* negative feedback inhibitor of the FGF pathway, also exhibit periodic expression in mouse and chicken PSM. Furthermore, periodic phosphorylation of ERK (Extracellular signal-regulated kinase) in the mouse PSM supports periodic FGF signaling (see Dequéant and Pourquié, 2008 for a detailed review of all the interaction).

The Wavefront

The wavefront as described by Cooke and Zeeman, corresponds to a molecular mechanism that set a zone where cell located in this area undergo dramatic changes in their cell properties leading to somite formation, *in fine*. Molecularly, the determination front is positioned by antagonistic gradients of FGF, Wnt, and retinoic acid (RA) signaling, and regresses posteriorly as the embryo elongates along the anteroposterior axis. This gradient defines a transitional zone within the PSM, called the **determination front, in approximatively the position of the somite -II or -III**. In this zone, cells are in a poised state and wait for a pulsed signaling from the oscillating clock to rapidly switch and differentiate into somites. In the posterior PSM, cells are exposed to a high level of FGF and Wnt activity, and are maintained in an immature, undifferentiated state (Aulehla et al., 2008; Dubrulle et al., 2001; Dunty et al., 2008; Sawada et al., 2001; Vermot and Pourquié, 2005). **RA signaling** requires direct RA binding to its nuclear receptor, formed by a heterodimer of RA and Retinoid X receptors (RARs and RXRs). These receptors act as ligand-dependent transcriptional activators of genes that contain RA-response elements (RAREs). RA signaling is regulated by controlling the amount of biologically active RA. In amniotes, RA signaling forms a decreasing rostrocaudal gradient that is opposite to the FGF and Wnt gradients in the PSM, and therefore only the somites and the anterior most PSM are responding to RA signaling (Vermot and Pourquié, 2005). The segmentation of the PSM is therefore initiated when a wide-enough portion of the anterior PSM is positioned at the determination front formed by Wnt, FGF and RA gradients. The determination front is an imaginary line defined as the level at which PSM cells first acquire their segmental identity and is therefore conceptually similar to the wavefront. In addition to specify the determination front, RA also buffers the action of the left-right asymmetry in the embryo and ensures a coordinate formation of a pair of somite on each side of the embryo (Vermot and Pourquié, 2005). At the molecular level, the position of the determination front corresponds to the posterior boundary of the *Mesp2* (Mesoderm posterior 2) stripe that marks the first evidence of a segmental prepattern in the PSM. Synergistic action of *Tbx6* and of a pulse of Notch signaling downstream of the clock activates *Mesp2* in cells that have reached

the determination front during the preceding oscillation cycle, in a striped pattern (Dequéant and Pourquié, 2008). *Mesp* family genes (*Mesp1* and *-2* in the mouse and *Meso1* and *-2* in the chicken) code for bHLH transcription factors, which show a conserved expression pattern and function during somitogenesis. Notch signaling oscillations in the posterior PSM generate waves of NICD production that control *Lfng* expression in the mouse. When the NICD/*Lfng* wave reaches the determination front level, *Mesp2* becomes activated in the future segmental domain where it takes over *Lfng* regulation, thus stabilizing its expression in the *Mesp2* expression domain. Because *Lfng* negatively regulates Notch activation, this results in the creation of an interface between a *Mesp2*$^{+}$ domain (the future somitic domain) in which Notch activation is suppressed, and an adjacent posterior *Mesp2*$^{-}$ domain in which Notch is activated. This interface marks the presumptive somite boundary. Rostrocaudal somite polarity is subsequently established in the newly specified segment by repressing *Mesp2* expression in the future caudal compartment (which reactivates Notch and expresses *Dll1*), while maintaining *Mesp2* in the rostral compartment. *Ripply2* (Ripply transcriptional repressor 2) activation by *Mesp2* results in the termination of the segmentation program by a negative feedback loop mechanism. The rostrocaudal polarity of the newly formed somite is maintained by the antagonism between *Tbx18* and *Uncx4.1* (see (Chal and Pourquié, 2009). Therefore, as tightly intertwined with its own formation, the anteroposterior polarity of the somite is set very early during development, as confirmed by grafting experiments (Aoyama and Asamoto, 2000).

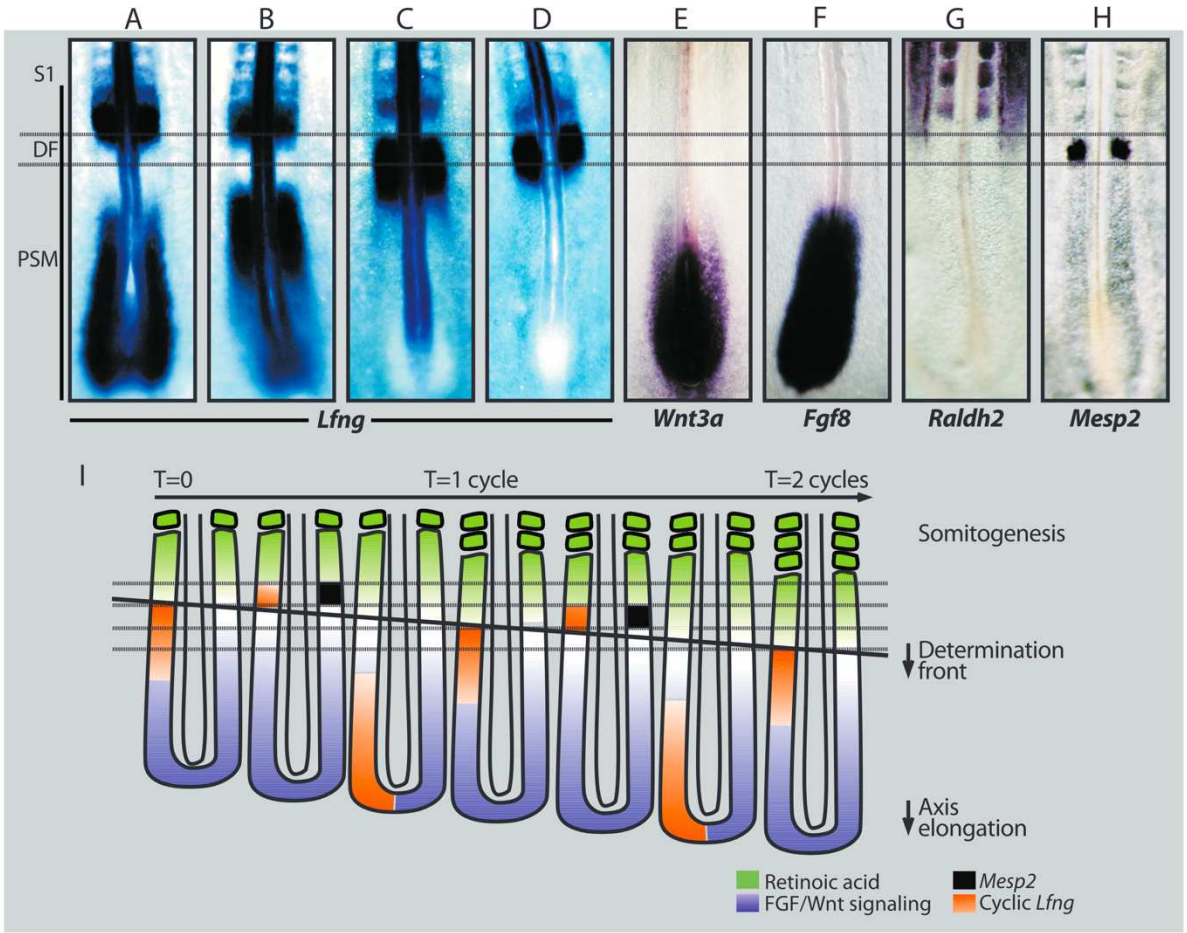

Figure 2. Clock and wavefront model of somitogenesis. *(A-H) Expression pattern of key genes involved in somitogenesis. Embryos from A,B,C and D all have 18 somites and represent the dynamic expression of lunatic fringe during one somite formation. (I) Model showing the progression of the determination front toward the posterior of the embryo, in concert with axis elongation. From Chal and Pourquié, 2009.*

Somite Epithelialization

The posterior PSM is a loose mesenchymal tissue. Somite boundary morphogenesis primarily involves a localized fissure that forms across the epithelialized anterior PSM tissue. As the cell reach the anterior PSM, they undergo a progressive mesenchymal-to-epithelial transition that involves changes in cell shape and cell-cell interactions. Epithelialization is associated with the deposition of a basal lamina on the outer surface of the forming somite. As the PSM cells epithelialize, they adopt an elongated and polarized shape, and their basolateral side encounters the nascent basal lamina on the outer surface of the forming somite while their apical domain establishes adherent junctions with mesenchymal cell in the center of the somite, somitocoele cells. Somitocoele cells remain mesenchymal during all step of somite formation. The MESP family of transcription factors connects the genetic prepattern to morphogenesis by controlling the expression of Eph receptor tyrosine kinases and Ephrin ligands. *EphA4* expression is restricted posteriorly to the forming boundary, whereas Ephrin ligand-encoding genes such as *EphrinB2* and *EphrinA1* become located anteriorly to the prospective boundary (Chal and Pourquié, 2009). The Eph–Ephrin interactions generate bidirectional signaling that facilitates the remodeling of the actin cytoskeleton and extracellular matrix (ECM) at the interface to form the inter-somitic fissure. The bHLH transcription factor *Paraxis* (*Tcf15*) is also necessary for somite epithelialization (Linker et al., 2005). N-cadherin is essential for proper somite formation, and the mouse null mutants exhibit significant defects in somite morphogenesis (Linask et al., 1998). In addition, the integrins, which link the cell with the surrounding ECM, are deeply involved as the space between somites is rapidly filled with a fibrillar fibronectin matrix and lined with laminin patches (Rifes and Thorsteinsdóttir, 2012). Moreover, the newly formed epithelial somite is wrapped in laminin and fibronectin sheets (Rifes and Thorsteinsdóttir, 2012). Mutant mice for *Itgav* (Integrin α5) and *Fn1* (Fibronectin1) exhibit severe defects in mesoderm formation and cell migration, resulting in disruption of somite formation (George et al., 1993; Georges-Labouesse et al., 1996; Goh et al., 1997; Yang et al., 1999). In the chicken embryo, fibronectin is produced mainly by the dorsal ectoderm, a tissue required for proper epithelialization of somites (Correia and Conlon, 2000; Palmeirim et al., 1998; Rifes et al., 2007).

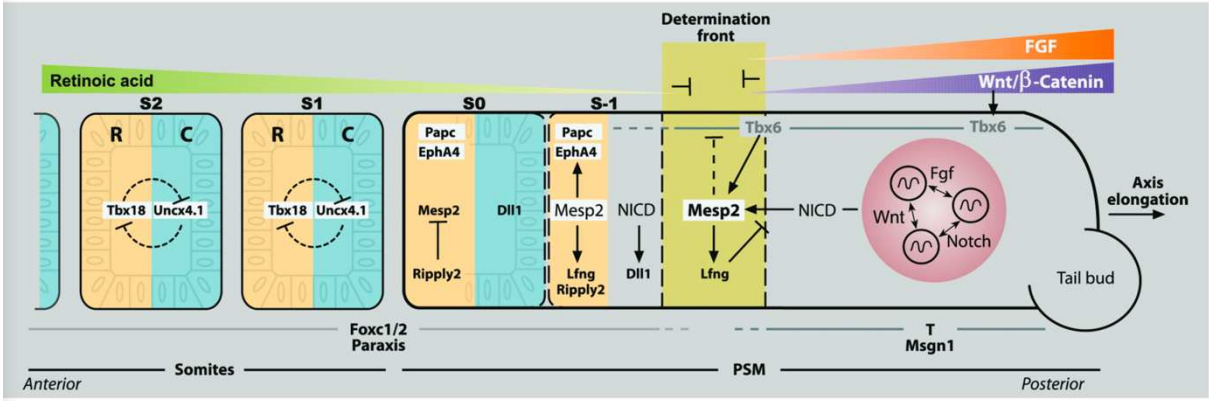

Figure 3. Genetic network involved in somite formation and rostro-caudal patterning. *The posterior PSM expresses a specific set of transcription factors including Brachyury (T), Tbx6, and Msgn1, and undergoes periodic activation of the Notch, Wnt, and Fgf signaling pathways driven by the segmentation clock. At the determination front level, synergistic action of Tbx6 and of the pulse of Notch signaling (NICD) downstream of the clock activates Mesp2 in cells that have reached the determination front during the preceding oscillation cycle, in a striped pattern. Mesp2 activates Lfng in the future segmental domain, creating an interface between a domain where Notch is activated (gray) and a domain where Notch is inhibited (green). This interface marks the presumptive somite boundary. Rostrocaudal somite polarity is subsequently established in the newly specified segment by repressing Mesp2 expression in the future caudal compartment (which reactivates Notch and expresses Dll1), while maintaining Mesp2 in the rostral compartment. Mesp2 then activates downstream targets such as EphA4 and Papc. Ripply2 activation by Mesp2 results in the termination of the segmentation program by a negative feedback loop mechanism. Concomitantly, PSM cells progressively acquire epithelial characteristics after the determination front. The anterior PSM expresses a distinct set of transcription factors including Paraxis and Foxc1 and -2. The rostrocaudal polarity of the newly formed somite is maintained by the antagonism between Tbx18 and Uncx4.1.*

Metabolic Regulation of Somitogenesis

Regulation of somite formation by cellular metabolism has recently emerged as a major factor modulating both the clock and the wavefront. A posterior-to-anterior gradient of glycolysis exist in the PSM of developing amniotes. Cells in the tailbud and posterior PSM exhibit a high level of **aerobic glycolysis**, compared with the anterior PSM, reminiscent of the signature of cancer cells experiencing the Warburg effect. FGF signaling defines this gradient by regulating the transcription of rate-limiting glycolytic enzymes (Oginuma et al., 2017). Disruption of the glycolytic gradient leads to defects in cell motility, axis elongation and PSM differentiation. On top of that, the glycolytic status of the PSM links FGF and Wnt signaling. High glycolysis in the posterior PSM leads to a higher intracellular pH. On the contrary, the reduced acidity in the anterior PSM creates a favorable chemical environment for non-enzymatic β-catenin acetylation, promoting WNT signaling for paraxial mesoderm specification (Oginuma et al., 2020). As mentioned hereinabove, the time for one somite production is species-specific, while it measures around 90min in chicken, or 2.5h in mice, the precise duration of the human clock was still unknown until recently. Using, ***in vitro* organoid models** recapitulating the PSM differentiation process of human embryo, Miao et al. were able to precisely measure the human clock to 5h (Miao et al., 2023). These *in vitro* models also offer incredible tools to easily compare the different in somite rate production between close species, such as mice and humans. Using these *in vitro* models, Diaz-Cuadros et al. studied the inter-species variation in the rate of embryonic development and demonstrate that the segmentation clock period is directly regulated by the metabolic rate of the cell (Diaz-Cuadros et al., 2023). Pharmacologically impairing the cellular **NAD^+/NADH redox balance** led to lowered rates of global protein translation and slow down clock oscillation, whereas increasing the ratio of NAD^+/NADH speeds up the clock. These quantitative results thus support a hierarchy wherein global metabolic rate determines both translation and biochemical reaction speed to control the tempo of the segmentation clock. In snake embryos, however, the segmentation clock rate is much faster relative to developmental rate than in other amniotes, leading to a greatly increased number of smallerized somites (Gomez et al., 2008). It would be interesting to determine if the snake "speed-up" clock is under the control of a specific metabolic program within the PSM or not.

Differentiation and Compartmentalization of the Somite

Somites can give rise to a great number of derivatives and need to be appropriately patterned by environmental cues to properly differentiate. The two main early derivative components of the somite are the **dermomyotome** and the **sclerotome**. The dermomyotome is an epithelial structure located on the dorsalmost part. The dermomyotome is the precursors for all muscle progenitors of the trunk, limb, tongue and hypoglossal muscles, in mammals it also contains diaphragm muscle progenitors. Besides, the dermomyotome also generates the **dermis** of the back and **endothelial** and **lymphatics** cells of both limb and trunk (Christ et al., 2007a). These limb endothelial cells have an **haemogenic potential** at a late fetal/young adult stage (Yvernogeau et al., 2019). Therefore, it can be assumed that the somite is also able to give rise to **hematopoietic stem cells** and therefore all blood and immune cells. The associated **connective tissue** of the most dorsal muscles, the epaxial muscles, has been proposed to also originate from the dermomyotome but it has never been clearly proven. The dermomyotome also provides the **scapula** with chondrocytes and osteoblasts in its posterior most part (Ruijin Huang et al., 2000a). Finally, in mammals at the level of the cervico-thoracic level it gives rise to the **brown adipocytes** and its associated connective tissues, while in birds at the sacral level, it contributes to the **lymph heart**, a muscular structure related to the lymphatic system, but the precise cell types remain unknown (Atit et al., 2006; Valasek et al., 2007). On the ventral side however, the epithelial somite undergoes an EMT and mixes with the mesenchymal somitocoele cells to form the sclerotome. This newly formed mesenchymal cell population contains precursors for **chondrocytes**, **osteoblasts** and **tenocytes** of the axial musculo-skeletal system and **occipital region**

(Draga and Scaal, 2024). It also gives rise to **pericytes** and **vascular smooth muscle cells** of the axial vasculature (Draga and Scaal, 2024). The sclerotome has been identified as the embryonic source of the **spinal meninges**, and nerve associated cells such as **perineurium** and **endoneurium**, however the proofs are sparse and lack molecular precisions. In addition, it has been recently found that at the limb level, a subset of the sclerotomal cell can migrate into the limb bud and participate to all these cell types, except for the meningeal one, into the limb bud (Arostegui et al., 2022). These two structures therefore give rises to a plethora of cell type and for that are subdivided into different sub-comportment with different cellular or anatomical destiny. These results are summarized in the following table, with in grey the lineage that remains to be more finely studied.

Dermomyotome-derivatives	Axial, limb, hypoglossal and diaphragm muscles
	Dorsal dermis
	Osteoblasts and chondrocytes of the scapula
	Lymph heart (birds)
	Brown fat (mammals)
	Endothelial and lymphatic endothelial cells
	Hematopoietic stem cells
	Muscle connective tissue
Sclerotome-derivatives	Osteoblast and chondrocytes of vertebrae, ribs and occipital bone
	Axial tendons
	Pericytes and vascular smooth muscle cells
	Osteoblasts, chondrocytes, tendons, pericytes and vascular smooth muscle cells of the limb
	Nerve-associated tissues (peri- and endoneurium)
	Meninges

Rostro-caudal Polarity

The rostrocaudal polarity of somite derivatives is mostly visible in the sclerotome, as the dermomyotome do not shown any morphological or functional sub-compartmentalization along the rostrocaudal axis. Nonetheless, it is the first axis to be determined as its origin is tightly linked to the process of somitogenesis itself. Aoyama and Asamoto used experimental embryology in chicken embryos to swap the different axis of newly formed somites and found out that even for the last formed somite, its rostrocaudal polarity was already determined (Aoyama and Asamoto, 2000). Confirming that the rostrocaudal polarity was determined before somite formation, within the PSM (see above for the molecular mechanisms).

Dorso-ventral Polarity

In the same set of experiments, Aoyama and Asamoto swapped the dorso-ventral polarity by inverting the somites along the dorsoventral axis. When swapped the somite formed an ectopic sclerotome under the epidermis (Aoyama and Asamoto, 2000). When the transplantations reversed only the dorsoventral axis, one day after the operation the two caudal somites (somite I and II) gave rise to normal dermomyotomes and sclerotomes, while the most rostral somite (somite III) gave rise to a sclerotome abnormally situated just beneath the ectoderm. When transplantations reversed only the dorsoventral axis, one day after the operation the two caudal somites gave rise to normal dermomyotomes and sclerotomes, while the most rostral somite gave rise to a sclerotome abnormally situated just beneath ectoderm. These results suggest that the dorsoventral axis was not determined when the somites were formed but began to be determined about three hours after their formation (in somite III). Moreover, when both the rostrocaudal and dorsoventral axes where swapped, the ectopic sub-ectodermal sclerotome conserved its craniocaudal polarity, confirming the cell autonomous determination of the craniocaudal axis of somite compared to the dorsoventral axis.

However, years later, Dockter and Ordahl revised these experiments with molecular markers of both the sclerotome and dermomyotome compartment. While they confirmed that dorsoventral inversion of stage I and II somite led to a normal development, with a dorsal dermomyotome and a ventral sclerotome, their somite III inversion led to a dermomyotome enchased between a sclerotome on the ventral side and an undifferentiated mesenchyme on the dorsal side. This suggested a delay between sclerotome and myotome specification, the dermomyotome being first specified compared to the sclerotome (Dockter and Ordahl, 2000). Altogether these results suggest that the dorsoventral polarity of the somite is quite plastic in the early stage and therefore seems to be dependent on environmental cues. Grafting of an additional notochord dorsal to the PSM compartment leads to a transformation of the dorsal dermomyotome into a sclerotome, cells from the dorsal somite undergo an EMT and the expression domains of sclerotomal markers such as the paired box family gene *Pax1* and *Pax9* are dorsally expanded, whereas dorsal markers such as the *Pax3* and *Pax7* are downregulated (Dietrich et al., 1998, 1997; Goulding et al., 1994). An additional floor plate can also convert the dermomyotome towards a sclerotomal fate (Pourquié et al., 1993). In the truncate and *Brachyury* curtailed mutant embryos, the notochord does not develop and *Pax1* expression is never activated, whereas the whole somite expresses *Pax3* (Dietrich et al., 1993). These ventralizing factors has been attributed to SHH from the notochord / floor plate module in both mouse and chicken (Dietrich et al., 1993). Using various grafting experiments, a few years later, Dietrich et al. proved that both the dorsal neural tube and the ectoderm were responsible for the dorsal expression of *Pax3*, and therefore the dorsalization of the somite (Dietrich et al., 1997). These two structures produce several Wnt ligands that have been shown to favorize the development and maintenance of the dermomyotome instead of the sclerotome (Wagner et al., 2000).

Medio-lateral Polarity

Even though the **medial** and **lateral** parts of the somite derive from different embryonic origins at the level of the Hensen's node, inversion of somite along the mediolateral axis has shown that the two halves of newly formed somites are largely interchangeable (Ordahl and Le Douarin, 1992). However, the two mediolateral halves of somites do not exhibit the same destiny. Only the lateralmost part contributes to the sclerotome, while the dorsolateral part will form the lateral and central part of the dermomyotome. On the other hand, the lateral somite only contributes to the formation of the lateral part of dermomyotome. The medial and central part of the dermomyotome will give rise to the dorsal muscles, the epaxial muscles, while the lateral part will give rise to muscles of the body wall, the limbs, tongue and hypoglossal and diaphragm muscles, named the hypaxial musculature. The two presumptive domains can be identified by the expression of specific marker such as ***Sim1*** (Single-minded family bHLH transcription factor 1) for the lateral domain. *Sim1* lateral expression in the somite is activated by **BMP4** secreted from the lateral plate mesoderm and inhibited more medially by the dorsal neural tube (Pourquié et al., 1996). The lateral expression of *Sim1* is maintained within the hypaxial dermomyotome at later stages. Conversely, another gene, Engrailed 1, ***En1***, is expressed in the medial most part of the somite (Cheng et al., 2004). At later stages *En1* becomes expressed in the central most part of the dermomyotome and formed a clear boundary with the lateral *Sim1* expression domain. The lateral plate mesoderm derived BMP4 signal constraints *En1* to a more medial position, while medial **SHH** from the **notochord/floor plate complex** and ***Wnt1*** from **the roof of the neural tube** positively regulate *En1* (Cheng et al., 2004). This differential expression is maintained in the dermomyotome where *Sim1* is still confined to the lateral domain, while *En1* is restricted to the central dermomyotome while the Wnt ligand ***Wnt11*** specifies the lateral most domain, called the **dorso-medial lip (DML)**. *Wnt11* expression is antagonized by SHH from the notochord/floor plate complex while BMP signal from the roof of the neural tube activates *Wnt1* and *Wnt3a* within the neural tube to regulate *Wnt11* expression in the DML (Marcelle et al., 1997). The BMP inhibitor **Noggin**, from the somite, constraints BMP signaling in the neural tube, avoiding any lateralization of the medial dermomyotome (Marcelle et al., 1997).

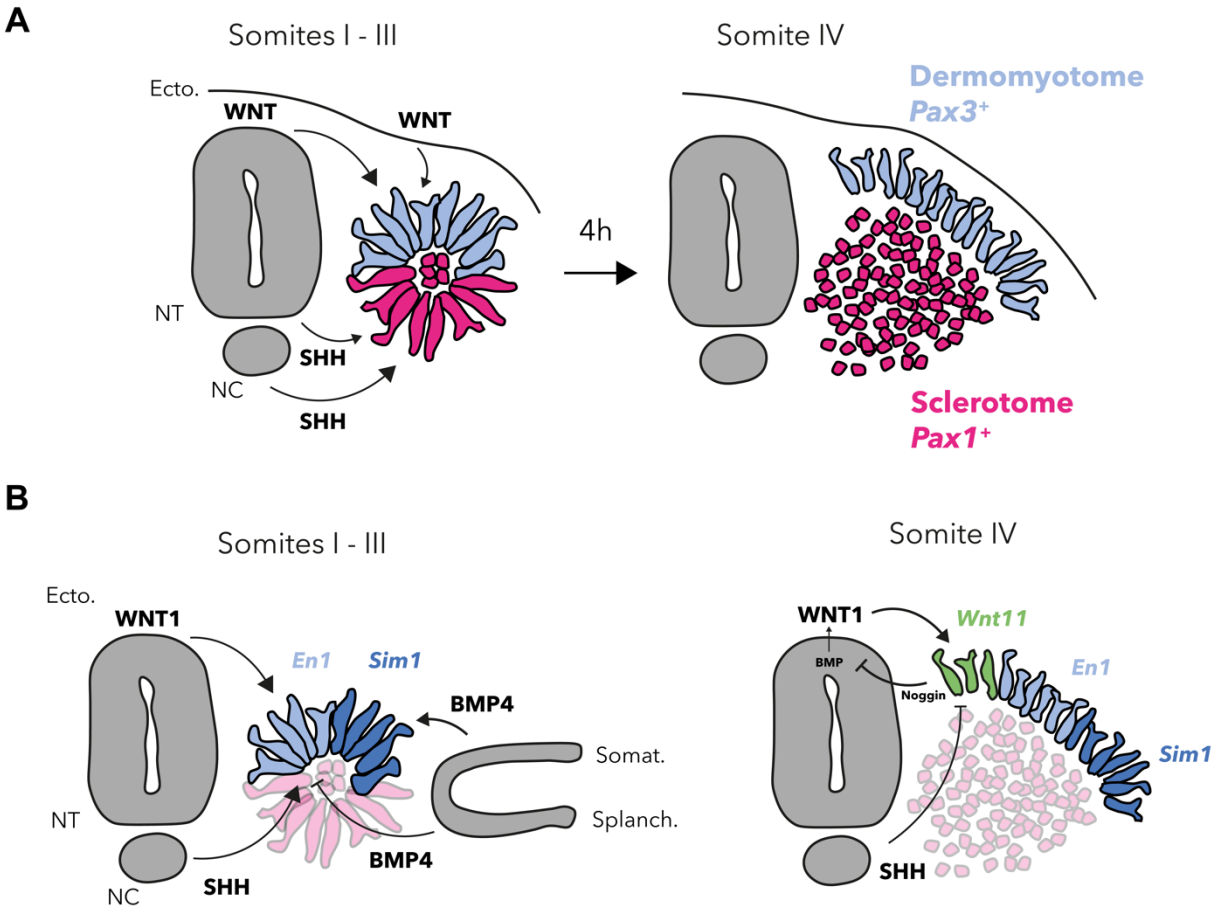

Figure 4. Early somite patterning. *(A) SHH from the floor plate/notochord complex specify the ventral part of the somite to become the Pax1⁺ sclerotome, while Wnt signaling from the ectodermis and the roof of the neural tube induces the specification of the dorsal Pax3⁺ dermomyotome. (B) Wnt, Bmp and Shh pattern the early and late medio-lateral polarity of the somite and the dermomyotome.*

Development of Myogenic and Non-myogenic Somitic Derivatives

In this chapter I will describe how different somitic compartments generate their respective derivatives, with an emphasis on the dermomyotome. If not specified, the mechanism described will be the one occurring during amniote development. I will try to give an exhaustive view of the anatomical, cellular, molecular and evolutionary mechanisms leading to the formation of epaxial and hypaxial musculature. The development of non-somitic muscles and connective tissues in the head will be portrayed in the next chapter. The mechanisms beyond muscle regeneration upon injury or during exercise will not be discussed. Embryonic origin of other non-muscle somite-derivatives will be depicted, with less molecular details, either because of a lack of space or knowledge.

Development of Dermomyotome-Derived Muscles

Dermomyotome Patterning and the Epaxial/Hypaxial Concept

At the end of the somite compartmentalization the dermomyotome form a square of epithelial cells above the mesenchymal sclerotome. It can be subdivided into three different domains: a medial most domain, the DML, characterized by the expression of *Wnt11*, a central domain, expressing *En1* and a lateral most domain expressing *Sim1*. At the cellular level, the dermomyotome can also be subdivided into different domains, the central dermomyotome and 4 borders, or lips, on each side, the **dorsomedial lip** (DML), the **ventrolateral lip** (VLL), the **anterior lip** (AL) and the **posterior lip** (PL) (Gros et al., 2004). Except for *Wnt11* whose expression in strictly restricted to the DML, the two other genes are not specific to any anatomical part of the dermomyotome. The **central dermomyotome**, *i.e.* all the epithelial cells between the DML and the VLL, are either expressing *En1* in the most medial part or *Sim1* in the lateral part (Ahmed et al., 2006). ***En1*** is not expressed in the DML and ***Sim1*** expression is very low in the VLL compared to the rest of the hypaxial dermomyotome. In contrast, the ALX homeobox 4, ***Alx4***, is expressed all over the central dermomyotome and not into the VLL or DML (Ahmed et al., 2006). Interestingly, when dissociated and co-cultivated *in vitro*, lateral and medial part of the dermomyotome segregate according to their medio-lateral origin, suggesting a differential cell adhesion capacity between these two populations that could explains their segregation *in vivo* (Cheng et al., 2004). In this regard, muscles are often categorized into two different groups, the **epaxial** and **hypaxial** muscles. The epaxial muscles represent the more dorsal axial muscles and are innervated by the dorsal rami of the motoneurons. On the contrary, the axial hypaxial muscles are located more ventrally and are innervated by the ventral rami of the motoneurons (Ahmed et al., 2017; Nagashima et al., 2020). In amniotes, epaxial muscles compose the deep back musculature, while the hypaxial muscles compose all the intercostal and abdominal muscles, limb and gridle-associated musculature, the tongue and the hypoglossal musculature (lower part of the neck), in addition to provide the diaphragm with muscle cell in mammals. In fishes, these two muscles groups are clearly distinct as they are separated by a horizontal septum. However, the simple muscle organization found in fishes is not conserved in amniotes and the delimitation is sparser. At the embryonic levels, the epaxial/hypaxial boundary can be observed in the early dermomyotome, with a clear delimitation between the $En1^+$ and $Sim1^+$ domain. Chicken somite electroporation also confirmed this view, as electroporation of the DML and VLL lead to the formation of epaxial and hypaxial-located myofibers, respectively (Gros et al., 2004). At the cellular level, these epithelial cells undergo an EMT and translocate one by one under the dermomyotome, into the transition zone, where they enter the myogenic program, and elongate in the antero-posterior axis (AP axis) to form myofibers. The assembly of myofibers from the four dermomyotome border is called

a **myotome**. This process takes place in all of the four borders of the dermomyotome (Gros et al., 2004; Rios et al., 2011). Nonetheless, the AL and PL, as they extend on both the medial and the lateral part of the somite, seem to give rise to both epaxial and hypaxial muscles, during development. In a second step, a **massive delamination of the central dermomyotome** fulfills both the epaxial and hypaxial myotome with muscle progenitors that will sustain the growth of the early myotome during later stages (Gros et al., 2005). In addition, some of these progenitors will be set aside before birth/hatching to form the adult muscle stem cells population, the satellite cells (Gros et al., 2005; Relaix et al., 2005). Therefore, epaxial and hypaxial muscles are both distinct by their embryonic origin and their innervation, even though recent works suggest that some nerves innervating the hypaxial muscles have a dorsal-like molecular signature (Nagashima et al., 2020). Adult muscles are mainly composed of myogenic cells (myofibers and satellite cells) but they also contain several others mesenchymal cell types, regrouped under the appellation of **muscle-associated connective tissue MCT** (Sefton and Kardon, 2019). Epaxial and hypaxial muscles also differ according to the embryonic origin of their MCTs. Hypaxial muscle MCT are derived from the **somatopleura of the lateral plate mesoderm** (LPM) while the epaxial muscles MCTs origin has been inputted to the dermomyotome. Based on this, Burke and Nowicki proposed a new classification for muscles, the **primaxial** and **abaxial** concept, in which primaxial muscles developed with MCT coming from the somites, while abaxial muscle developed with MCT coming from the lateral plate mesoderm (Burke and Nowicki, 2003). In this classification, all epaxial muscles are primaxial and therefore the two denominations are redundant in this case, while the hypaxial muscles can be divided into hypaxial-primaxial and hypaxial-abaxial muscles. Using a *Prx1*^{CRE} mice to label all LPM derivatives, they proposed the term **lateral somitic frontier** as an imaginary line that separates the muscle derived only from the somite, the primaxial muscles, with the muscle derived from both somites (myogenic cells) and the LPM (MCTs), the abaxial muscles (Durland et al., 2008). In this case, for instance the abdominal muscles are hypaxial-abaxial muscles, *i.e.* derived from the hypaxial myotome, innervated by the ventral rami and with LPM-derived MCT, while the intercostal musculature is hypaxial-primaxial, *i.e.* derived from the hypaxial myotome, innervated by the ventral rami and with somite-derived MCT (Durland et al., 2008). As said before, in addition to ventral body wall, hypaxial muscles composed all the muscle of the limbs, pectoral and pelvic girdle, hypoglossal muscles and diaphragm musculature in mammals. During development, limbs, girdle, tongue, hypoglossal and diaphragm muscles arise from **migrating muscle precursors (MMPs)** that only start they differentiation when reaching their final target tissues (Babiuk et al., 2003; Chevallier et al., 1977; Huang et al., 1999; Noden, 1983). This highly contrast with the formation of epaxial muscles that remains located within the back and do not undertake extensive lateral migration.

Myogenic Regulatory Factors (MRFs)

Even though the hierarchy, the presence or absence of some components may vary, amniotes myogenesis always leads to the activation of the same set of transcription factors, no matter the anatomical location. These genes belong to the basic helix-loop-helix domain-containing **myogenic regulatory factors** (MRFs), which includes myogenic factor 5 (***Myf5***), myogenic differentiation 1 (*Myod1*, also known as ***MyoD***), ***Mrf4*** (also known as *Myf6*) and myogenin (***MyoG***). MRFs are responsible for driving the expression of several genes necessary for the contracting properties of a mature skeletal muscle fiber. They act at multiple points in the muscle lineage to cooperatively establish the skeletal muscle phenotype through regulation of proliferation, irreversible cell cycle arrest and activation of sarcomeric- and muscle-specific genes to facilitate differentiation and sarcomere assembly. Their bHLH domain recognizes the **E-box** DNA sequence (CANNTG) that gives MRFs sequence specificity in the regulatory regions of the target genes (Hernández-Hernández et al., 2017). The function of these MFRs has been mostly studied using mouse transgenesis. *Myf5* and *MyoD* has been proposed to act redundantly, as inactivation of one or the other gene results in a relatively normal myogenesis, while the double knock-out leads to a complete lack of skeletal muscle (Braun et al., 1992; Rudnicki et al., 1993). Mutants for *MyoG* initiate myogenesis normally but exhibit

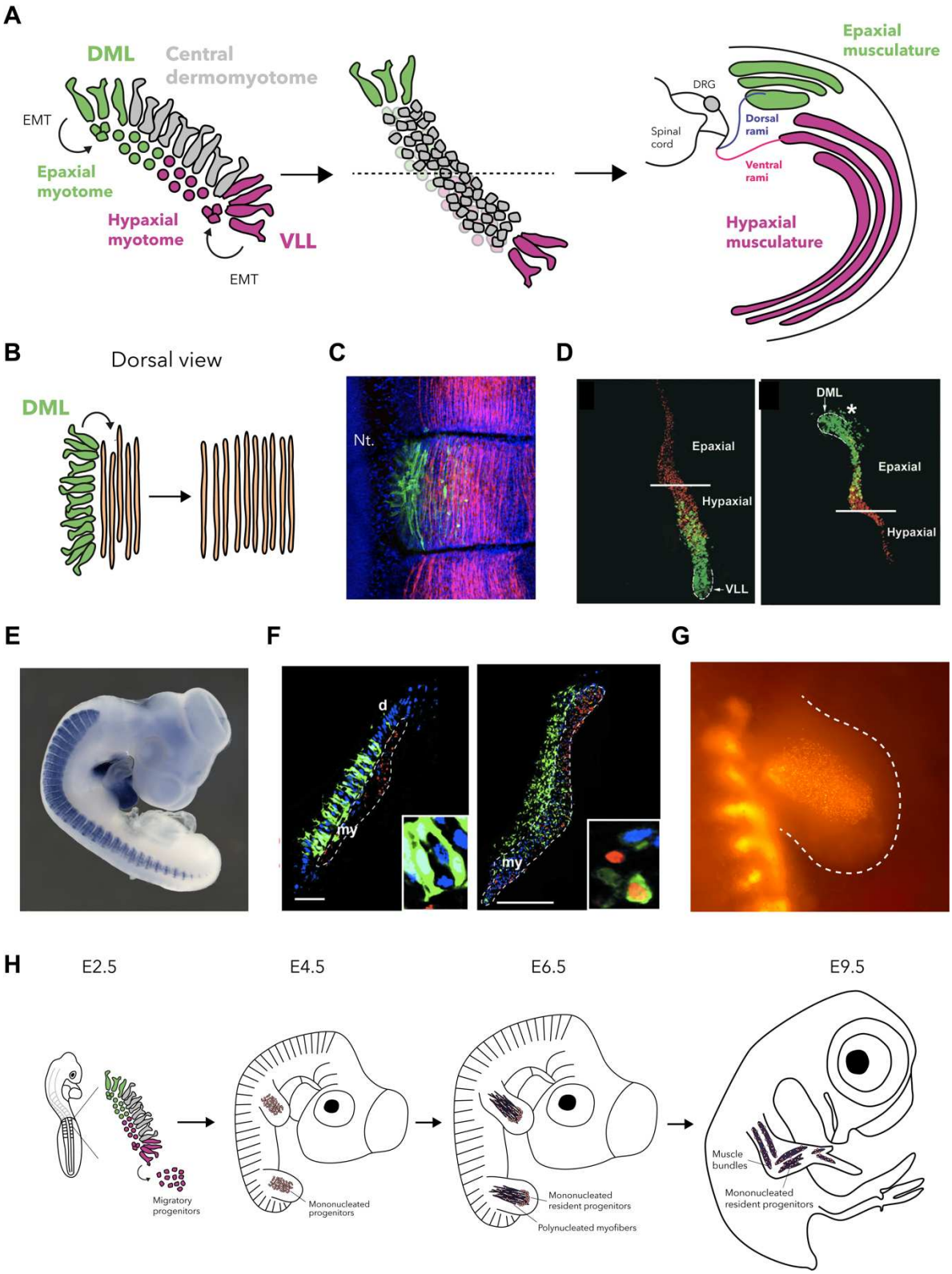

Figure 5. Epaxial and hypaxial myogenesis. *(A) Formation of the epaxial and hypaxial myotome and musculature. (B) Dorsal view of myogenesis in the DML. (C) Electroporation of eGFP in the DML, myofibers are stained in red and muscle progenitors in blue (Pax7). (D) Electroporation of either the VLL or the DML leading to the formation of the hypaxial or epaxial myotome, respectively, from Gros et al., 2005. (E) In situ hybridization of Myh7 depicting the formation of the early myotome in the trunk. (F) Electroporation of the central dermomyotome with a eGFP at E4.5 and E6.5 days, showing the entry of the muscle resident progenitors in the early myotome and their entry in the myogenic lineage (Pax7 in blue, MyoG in red, from Manceau et al., 2008). (G) Electroporation of the VLL of forelimb somite with a dTomato showing the invasion of the limb bud by myogenic progenitors. (H) Summary of the limb myogenesis in the chicken embryo.*

defects in the maturation of myofibers (Hasty et al., 1993; Nabeshima et al., 1993). Initial studies of *Mrf4* knockout mice similarly suggested that, like *MyoG*, *Mrf4* acts downstream of the redundant activities of *Myf5* and *MyoD,* during late myogenic differentiation (Patapoutian et al., 1995; Zhang et al., 1995). However, the original *Myf5* knockout was in fact a double knockout for *Myf5* and *Mrf4* as these two genes share the same locus. Indeed, strong evidences demonstrated that *Mrf4* can induce myogenesis in absence of both *Myf5* and *MyoD*, suggesting a bi-phasic role for *Mrf4* in both initiation and later differentiation of myogenic precursors (Kassar-Duchossoy et al., 2005). Giving the functional redundancy between *Myf5* and *MyoD* is has been suggest that these two genes were acting in parallel in two different myogenic lineages, explaining the compensation of myogenesis when one was knocked-out (Haldar et al., 2008; Kablar et al., 2003). However, a more recent study proved that this hypothesis was wrong, mainly due to issues with CRE efficiencies in deleting/labeling one or the other lineage (Comai et al., 2014). Furthermore, these two genes have a molecular different role in transcriptional activation of muscle-specific genes. The initial specification of the muscle lineage by *Myf5* occurs without significant induction of gene transcription. Transcription of the skeletal muscle program is then achieved by the subsequent expression of *MyoD*, which binds to the same sites as *Myf5*, indicating that each factor regulates distinct steps in gene initiation and transcription at a shared set of binding sites (Conerly et al., 2016).

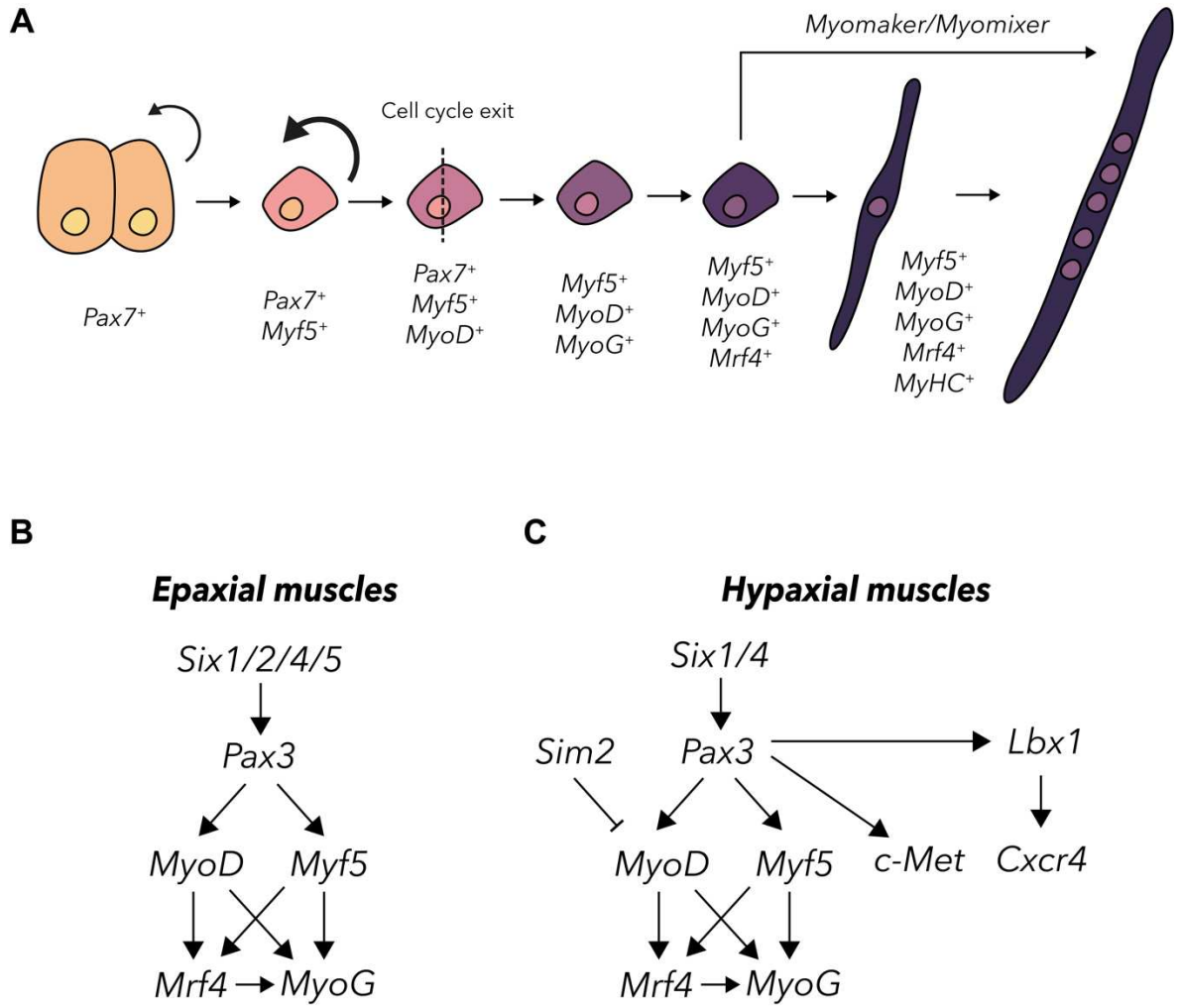

Figure 6. Myogenic differentiation*. (A) Activation of the different MRFs during myogenic differentiation. (B) GRN during epaxial muscles development. (C) GRN during hypaxial muscles development.*

Upstream Regulators

Two major upstream regulators of the MRFs are the paired-homeobox transcription factors ***Pax3*** and ***Pax7***. Mouse dermomyotomal cells express both *Pax3* and *Pax7*, with *Pax3* being more enriched in

the borders, and *Pax7* more in the central dermomyotome, in chick, however, the entirety of the dermomyotome is positive for both *Pax3* and *Pax7* (Kassar-Duchossoy et al., 2005; Otto et al., 2006). In mice, *Pax3* and *Pax7* do not appear to have the same function. The *Splotch* mutant for a loss-of-function in the *Pax3* gene does not develop any hypaxial muscle, the most striking phenotypes being the limb devoid of muscles, the epaxial musculature is less affected (Bober et al., 1994). On the other side, *Pax7* appears to be dispensable for embryonic muscle development, and can only compensate partially the function of *Pax3* in limb muscle precursors migration (Relaix et al., 2004; Seale et al., 2000). Double mutants for both *Pax3* and *Pax7* exhibit a more severe phenotypes compared to the *Splotch* animals, with only the early myotome developing (Relaix et al., 2005). Specific ablation of either *Pax3* or *Pax7* population, using CRE-mediated diphtheria toxin A (DTA) showed that the loss of the *Pax3* lineage is embryonically lethal and prevents the emergence of $Pax7^{+}$ cells, whereas ablation of *Pax7* expressing cells only lead to defects in later stages of development, with smaller myofibers (Hutcheson et al., 2009). This, and the enriched expression of *Pax7* in the central dermomyotome has led to a model in which *Pax7*-derived cell would be responsible for the growth of the muscles during fetal stages by giving rise to muscle resident progenitors and satellite cells, a process named **secondary myogenesis**. Besides, $Pax3^{+}/Pax7^{-}$ cells appears to mainly drive the early step of muscle formation, referred as the **primary myogenesis**. However, regarding the fact that *Pax3* and *Pax7* share the same spatiotemporal expression in chicken, a unified amniote theory for primary and secondary myogenesis remains to be drawn (discussed above).

Another family of genes is considered to be at the apex of the genetic regulatory cascade that drive myogenesis. These genes belong to the sine oculis-related homeobox family (Six). **SIX proteins** bind to the eyes-absent homologs ***Eya1*** and ***Eya2*** and translocate to the nucleus to activate target genes, such as *Pax3*, *MyoD*, *Mrf4* and *MyoG* (Grifone et al., 2005). *Six1*:*Six4* or *Eya1*:*Eya2* mutants are devoid of *Pax3* expression in the hypaxial dermomyotome and consequently do not form any limb and trunk hypaxial muscle (Grifone et al., 2007; Heanue et al., 1999). In addition, SIX proteins binding sites are found directly within the transcriptional regulatory sequences of both *Myf5* and *MyoG*, suggesting that in addition to act as upstream regulators, SIX proteins can also drive myogenesis conjointly with *Pax3* (Giordani et al., 2007; Spitz et al., 1998). In the double mutant for *Six1* and *Six4*, the epaxial muscles are the only one remaining. Interestingly, in the quadruple mutant *Six1:Six2:Six4:Six5*, even highly impaired, the epaxial muscle development still takes place but with a complete loss of $Pax7^{+}$ cells by the end of the fetal life, demonstrating that SIX homeoproteins are required for the maintenance of the $Pax7^{+}$ progenitor cells, but not essential for the onset of myogenesis at the epaxial level (Wurmser et al., 2023). These results are similar with the *Pax3/7* situation in early myotome development, where the double mutant for the two paired-box transcription factors only manage to initiate myogenesis, showing that a *Pax/Six*-independent myogenesis can be initiated at the axial level but cannot be maintained throughout fetal life. Wurmser et al., showed that SIX and HOX proteins can bind common DNA binding sites in the genome, and proposed that in absence of SIX or PAX proteins, *Hox* genes could drive the entry in the myogenic program.

Regulation of the Migrating Hypaxial Muscle Progenitors

As said throughout these lines, epaxial and hypaxial muscles do not always exhibit the same transcription factor requirements, one of the most striking being *Pax3* (Bober et al., 1994). Alongside *Pax3*, the Ladybird Homeobox 1, ***Lbx1*** is expressed in the lateral dermomyotome at the level of the limbs and in all the occipital and cervical dermomyotomes (Mennerich et al., 1998). These muscle progenitors leave the dermomyotome compartment to form the limbs, tongue, hypoglossal and diaphragm musculature. Therefore, *Lbx1* is restricted to myogenic precursors undergoing long range migration. While knockout of *Pax3* leads to an incomplete migration of myogenic precursors within the limb bud, in the $Lbx1^{-/-}$ mice, cell managed to delaminate from the dermomyotome but do not migrate properly and failed to enter the limb bud (Gross et al., 2000). Genetic analysis also revealed that *Lbx1* act downstream of *Pax3* (Mennerich et al., 1998). During limb bud colonization,

muscle progenitors split into two different pre-muscle masses, under the dorsal or the ventral epidermis. Interestingly, another transcription homolog to *Sim1*, *Sim2* has been shown to be specifically expressed in the VLL and then, only in the ventral muscle mass of the limb bud. *Sim2* binds to regulatory sequences of *MyoD* and therefore delays the entry of the ventral muscle mass in the myogenic program. This mechanism is dependent on the polarized expression of *Lmx1b*, a gene specifically expressed in the dorsal compartment of the limb bud, and is conserved between birds and mammals (Havis et al., 2012). This mechanism has been proposed to delay the differentiation of the ventral mass to increase its progenitor capacity, as ventral limb muscle are larger at later stages compared to dorsal ones. Others non-cell autonomous regulators are involved in migration, such as the ***c-Met*** tyrosine kinase receptor and its ligand, the **Hepatocyte Growth Factor (HGF)** (Bladt et al., 1995). The *Hgf* transcripts are present in limb mesenchyme and the expression of *c-Met* in myoblasts is essential for their migration into the limb bud, the tongue and diaphragm (Bladt et al., 1995; Dietrich et al., 1999). The connective tissue of the diaphragm is the main source of HFG, and therefore critical for the invasion of the myoblasts (Sefton et al., 2022). The chemokine receptor type 4, ***Cxcr4***, and its ligand the stromal-cell derived factor 1, ***Sdf1***, also known as *Cxcl12*, regulate migration of myoblasts within the limb bud (Vasyutina et al., 2005). Applying SDF1 coated bead directly into chick embryos directs the migration of these cell directly toward the ectopic source, moreover, *Cxcr4*$^{-/-}$ mice have severe defect of myogenic migration at both the occipital and limb levels. Replacement of neck PSM, that produce *Lbx1*$^{+}$ somites, by interlimb PSM, that produce *Lbx1*$^{-}$ somite, proved that not all the somites are able to generate *Lbx1*$^{+}$ MMPs and that this property is determined before somite formation, in the PSM. Furthermore, graft of LPM of any level in front of normally *Lbx1*$^{+}$ somite do not perturb its expression, while grafting of LPM medially induces the ectopic expression of *Lbx1* in the medial compartment, only at neck and limb level. Complementary grafts of interlimb PSM in the forelimb region lead to the formation of *Lbx1*$^{+}$ somites (Alvares et al., 2003). This demonstrate that the LPM is sufficient to induce the expression of *Lbx1*, no matter its axial level, but that it can only act into specific responsive somites along the AP axis. The signal coming from the LPM and/or the growing limb bud have been inputted to FGF signaling while the axial determination is based upon the *Hox* code (Alvares et al., 2003).

Terminal Myogenic Differentiation

MyoD coding sequence was first identified in a screen for genes regulating skeletal myogenesis as being sufficient to induce skeletal muscle differentiation in cells from many different lineages (Davis et al., 1987; Lassar et al., 1986). When expressed in primary fibroblasts or in a wide variety of other cell types, such as melanocytes, neuron, fat and liver cells, *MyoD* can convert these cells to the skeletal muscle lineage (Weintraub et al., 1989). At this time in the 80's, this was the first direct evidence that a single gene can initiate a complex program of differentiation, leading to the conclusion that *MyoD* acts as a **master switch** for the myogenic program. However, as said above, physiologically, *in vivo*, during muscle development, *MyoD* is not essential for myogenesis as others MRFs can substitute to it when knocked-out. *MyoD* presence in the cell leads to the robust expression of several muscle specific genes such as *MyoG*, M-cadherin, muscle creatine kinase (*Mck*) and several myosin heavy and light chains. In addition to this, *MyoD* also up-regulated the expression of the cyclin-dependent kinase inhibitor ***p21***, leading to irreversible exit of the cell cycle (see Berkes and Tapscott, 2005 for a detailed review of *MyoD*-mediated transcription). MYOD is strikingly more effective than *Myf5* at inducing differentiation-phase target genes. Indeed, MYF5 modifies the chromatin at its binding sites but does not robustly recruit Pol II or activate gene transcription, whereas MYOD binds the same sites but robustly recruits Pol II and activates gene transcription, therefore the two genes are recruited at the same locus but MYOD seems more decisive in triggering transcription compared to *Myf5* (Conerly et al., 2016).

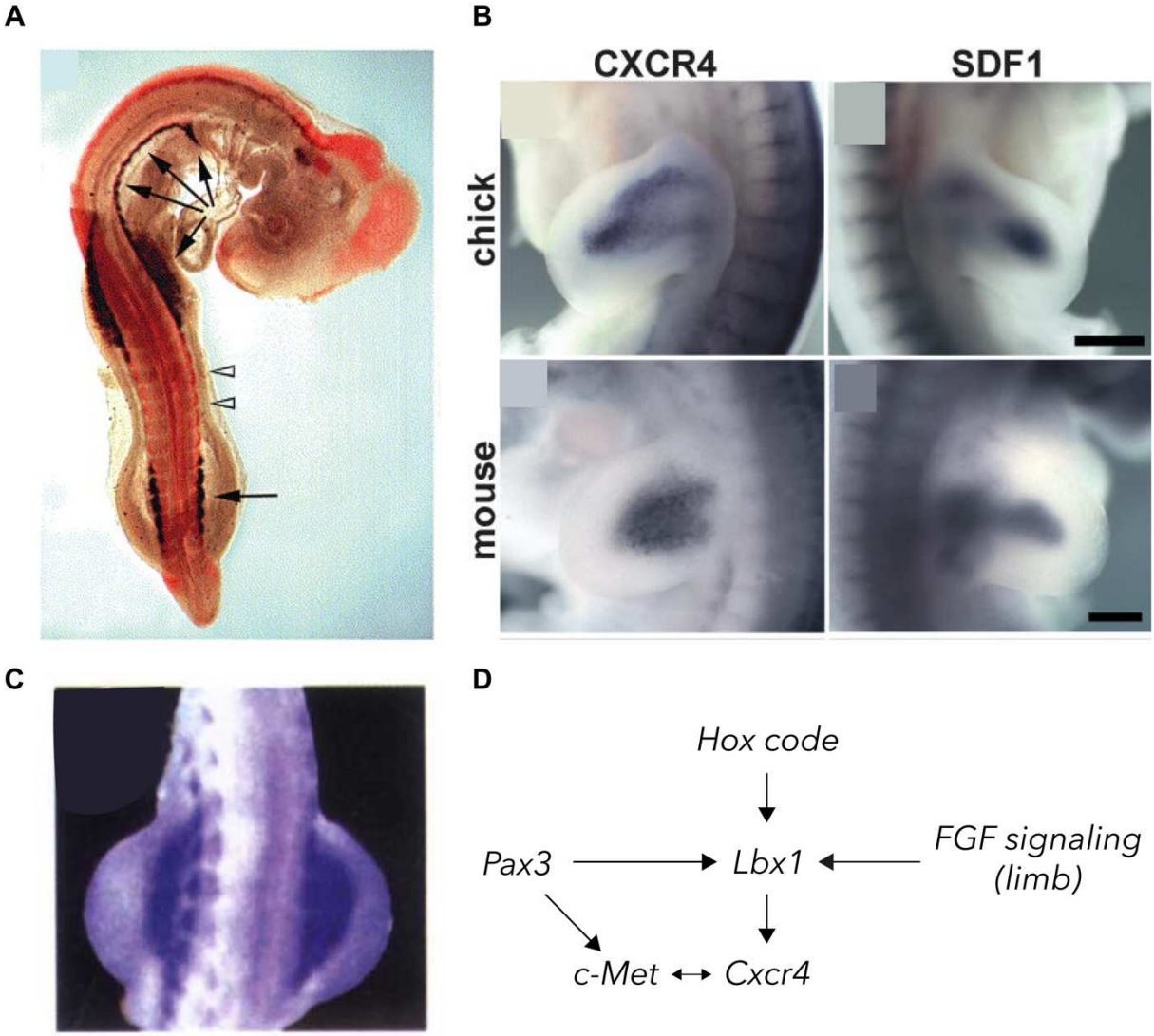

Figure 7. Genes involved in the myoblast migration. *(A) Expression of Lbx1 (purple) and Pax3 (Red) in E3 chicken embryo. Black arrowheads indicate Lbx1 expression in occipital, cervical, and limb somites, while interlimb somites do not exhibit any Lbx1 expression (from Alvares et al., 2003). (B) Expression of Cxcr4 and its ligand, Sdf1, in both chick and mouse limb bud (from Vasyutina et al., 2005) (C) Expression of cMet in mouse limb bud (Bladt et al., 1995). (D) GRN driving the expression of the migratory limb myoblasts component.*

MyoG knockout exhibits a widespread muscle loss, suggesting less functional redundancy than for others MFRs, even with MYOD (Hasty et al., 1993; Nabeshima et al., 1993). As for MYF5 and MYOD, MYOD and MYOG share a lot of common binding sites but differ in their respective molecular functions. For early muscle genes, MYOD is sufficient for near full expression, whereas, for late muscle genes, MYOD initiates regional histone modification but is not sufficient for gene expression (Cao et al., 2006). MYOG can bind efficiently to these genes without MYOD, and is essential to recruit and activate the transcription machinery for late muscle genes such as *Mymk* and *Mymg* (Adhikari et al., 2021). Moreover, *MyoG* appears critical to maintains *MyoD* expression, thus the two work in a positive feed-forward loop (Adhikari et al., 2021).

Genetic Regulation of Myoblast Fusion

Once fully mature, muscle progenitors elongated and fused together to form polynucleated myofibers. While several genes and signaling pathways have been demonstrated to be involved, only two genes are absolutely required for fusion, ***Myomaker*** (*Mymk*) and ***Myomerger*** (*Mymg*, also called *Myomixer* or *Minion*) (Bi et al., 2017; Millay et al., 2013; Quinn et al., 2017; Zhang et al., 2017). MYMK is a transmembranal protein, expressed at the surface of myoblasts during fusion and

downregulated right after. *Mymk* knockout embryos exhibit a normal expression of *MyoD* and *MyoG* transcripts, showing that *Mymk* acts downstream of these two genes, however, none of the mutant survived after post-natal day 7, because of an absence of polynucleated muscle fibers (Millay et al., 2013). Remarkably, *Mymk* overexpression in myoblasts enhances their fusogenic capacity and forced expression in fibroblasts promotes their heterologous fusion with myoblasts (Millay et al., 2013). The other gene absolutely required for myoblast fusion during development has been simultaneously discovered by three independent group and called *Myomerger/Myomixer/Minion* (Bi et al., 2017; Quinn et al., 2017; Zhang et al., 2017). Quinn et al. forced two fibroblastic cell lines to fuse together by both transducing them with *Mymk* but only one of them with *Mymg* (Quinn et al., 2017). Molecularly, *Mymk* and *Mymg* independently mediate distinct steps in the fusion process, *Mymk* is involved in membrane hemifusion whereas *Mymg* is necessary for fusion pore formation, therefore acting at the very last step of fusion (Millay, 2022). The *Mymk/Mymg* duo does not operate alone but instead cooperates with several molecular actors to drive the two plasmic membranes merging. **Actin cytoskeleton** is highly involved in this process and therefore, several actin remodelers are necessary for myoblast fusion, one of which being the ***Arp2/3* complex**. *Arp2/3* is regulated by several small GTPases during myoblast fusion, including ***Rac1*** and ***Cdc42*** (Vasyutina et al., 2009). The hydrolyzation of GTP by *Cdc42* and *Rac1* leads to their transformation into a GDP-bound inactive form, **Guanosine Exchange Factors proteins** (GEF) are therefore essential in the function of these small GTPases. The **DOCK1/ELMO** complex acts as a GEF for RAC1, specifically at the membrane of the pre-fusing myoblasts thanks to interaction with membrane-anchored proteins (Laurin et al., 2008; Sun et al., 2015). **Phosphatidylserine** (PS) translocation from the inner leaflet of the plasma membrane to the outer one is a classical marker of apoptotic cell. This event is seen as an "eat-me" signal for the phagocytic cells. Hochreiter-Hufford et al., demonstrated that a membrane protein involved in apoptosis, the Brain-Specific Angiogenesis Inhibitor 1, **BAI1**, regulates fusion by signaling through the DOCK1/Elmo/Rac1 module (Hochreiter-Hufford et al., 2013). During myoblast fusion *in vitro*, a fraction of myoblasts within the population undergoes apoptosis and exposes phosphatidylserine, an established ligand for BAI1. Mechanistically, apoptotic cells did not directly fuse with the healthy myoblasts, rather the apoptotic cells induce a contact-dependent signaling with neighbors to promote fusion among the healthy myoblasts. Therefore, myoblasts seem to have highjacked the apoptotic process to induce actin remodeling during fusion.

Signaling Pathways Regulating the Myogenic Program During Development

Once formed, somites and more particularly the dermomyotome must maintain their epithelial organization. This is achieved by the surrounding ectoderm that secretes **WNT6** which act on the dermomyotome via **TCF/LEF**, and more precisely *paraxis*, to maintain the **epithelial structure** of the dermomyotome (Linker et al., 2005). The first molecular evidence of myogenesis is the presence of *Myf5* mRNA in the presumptive dermomyotome of the newly formed somites (Williams and Ordahl, 1994). *MyoD* starts to be expressed later in the just formed DML of somite IV (Williams and Ordahl, 1994). Thus, the DML is the place where the first differentiated muscle cells are found. However, each lip of the dermomyotome is able to initiate myogenesis and contribute to the formation of the myotome (Gros et al., 2004). When separately labelled by electroporation in the chicken embryo, each lip has the capacity to give rise to elongated myocytes below the dermomyotome, but at different pace. In this study by Gros et al., thoracic somites I to V were electroporated and elongated myocytes were observed 14h, 24h or 28h for the DML, PL, and AL and VLL, respectively. The cells from each one of the dermomyotome borders therefore delaminate and migrate under the dermomyotome to elongate into the anteroposterior axis, with the cells from the DML being the very first. At the end of this process, around E4.5 in the chicken embryo, each myofiber of the myotome **spans over the entirety of the segment**, from the cranial to the caudal part of the previously existing somite. During this process the newly formed myofibers acquire additional nuclei by fusion with other myogenic cells, reaching up to 3 or 4 nuclei in thoracic myotomes of chicken by E5.5 (Sieiro-Mosti et al., 2014). Moreover, double-electroporation experiments shown that before E5.5 cells from DML do

not fuse together, but only to cells coming from the AL and PL borders (Sieiro-Mosti et al., 2014). This specific fusion pattern is allowed by a spatio-temporal regulation of the fusion pace by **Tgf-β signaling**. During early myogenesis, Tgf-β signaling acts as an **inhibitor of myogenic fusion** (Melendez et al., 2021). Tgf-β receptors function as heterodimers, with both TGFBR1 and TGFBR2 being necessary for linking Tgf-β ligands. During development, *Tgfbr1* is preferentially expressed in the DML while *Tgfbr2* is expressed in the AL and PL of the dermomyotome. Fusion between the DML-derived cells and PL/AL-derived cells leads to the formation of a functional Tgf-β receptors in the newly formed polynucleated fiber, therefore blocking its capacity to fuse with any other myoblasts. Recycling of the heterodimeric receptor via **RAB-dependent endocytosis** resets the system and allows a new round of fusion to take place (Melendez et al., 2021).

Around E4.5 in the chicken embryo or E10.5 in the mouse, a second wave of myogenesis appears that starts with the delamination of the entirety of the central dermomyotome into the early myotome (Gros et al., 2005). These progenitors will fulfill myogenesis until late stages and some of them will eventually be kept aside to form the satellite cell pools at post-hatching/post-natal stages (Gros et al., 2005; Relaix et al., 2005). Molecularly, the later timing of emergence of muscle resident progenitors is set up by **FGF signaling**. The early myotome is highly positive for ***Fgf8*** that signals to the above dermomyotome to trigger the activation of ***Snai1***, a regulator of **EMT**, through MAPK/ERK signaling (Delfini et al., 2009). During early stages, the central dermomyotome-derived progenitors do not fuse to the pre-existing myofibers formed by the DML, and form *de novo* myofibers (Sieiro-Mosti et al., 2014). Moreover, it has been partly demonstrated that the DML only gives rise to early myofibers and not resident muscle progenitors (Gros et al., 2005). For all these reasons, the myofibers coming from the different borders have been proposed to form what have been called a "primary myotome" that is invaded with muscle resident progenitors from the central dermomyotome that form *de novo* myofibers without fusing to the pre-existing myotome and form a so-called "secondary myotome", or more generally constitute the secondary myogenic wave. This view suggests that the borders do not contribute to the formation of resident muscle progenitors and therefore, the satellite cell pool, drawing a comparison with what happens in the limb bud with the $Pax3^{+}/Pax7^{-}$ and $Pax3^{+}/Pax7^{+}$ populations (see below for a detailed discussion of primary and secondary myogenesis).

The initiation of myogenesis within the DML has received a lot of interest. A particular mechanism of inter-tissular communication has been found in this context. The roof of the neural tube represents the territory of origin for the **neural crest cells (NCC)**, a migratory population of progenitors that formed various tissues including the melanocytes, Schwan cells and peripheral nerves. When getting out of the neural tube these cells express the notch ligand, ***Dll1***, while the DML cells express several **Notch** receptors. Upon their migration they enter in close contact with the DML cells and trigger Notch activation that *in fine* results in the entry into the myogenic lineage, via the transcription of *Myf5*, and their translocation into the transition zone, under the dermomyotome (Rios et al., 2011). As said above, Wnt ligands from the neural tube are important for the expression of *Wnt11* in the DML (Marcelle et al., 1997). Migrating neural crest have been shown to be decorated with the **WNT1** ligand and thus serve as a cargo between the neural tube and the DML to convey WNT molecules (Serralbo and Marcelle, 2014). This process is essential for *Wnt11* expression in the DML, which in instructs the proper **orientation** of the early DML-derived myofibers via the **planar cell polarity pathway** (PCP) (Gros et al., 2009). Interestingly, cells responding to Notch signaling in the DML also exhibit a high response to **TCF/LEF** (Sieiro et al., 2016). Indeed, the contact of $Dll1^{+}$ NCC with the DML transduces via a NICD/Snai1/GSK3/β-catenin cytoplasmic module that *in fine* couples DML-cell delamination with the TCF/LEF-dependent activation of *Myf5* (Sieiro et al., 2016). How this Notch/TCF/LEF pathway interferes, or not, with the regular Wnt ligand-dependent activation of *Wnt11* is unknown.

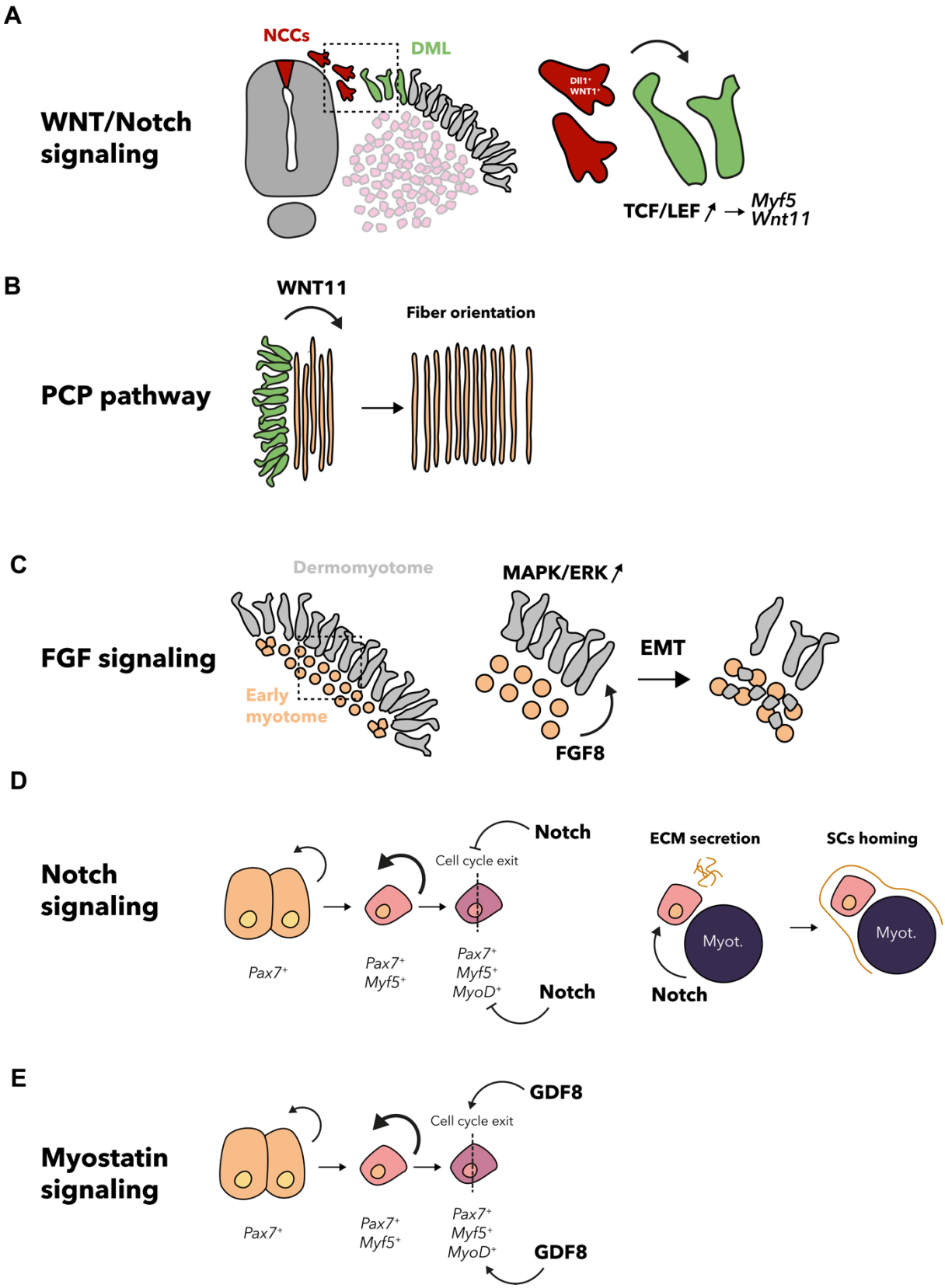

Figure 8. Signaling pathway regulating myogenic development. *(A) Migrating neural crest cells (NCCs) expose DLL1 and WNT1 ligand to the epithelial cells and activate TCF/LEF transcription into the epithelial cells. (B)WNT11 secreting from the DML instruct a proper fiber elongation along the A-P axis by activating the PCP pathway within newly formed myofibers. (C) FGF8 from the early myotome trigger the MAPK/ERK pathway in the surrounding dermomyotome and induce a massive EMT of the central dermomyotome. (D) Notch inhibits the cell cycle exit and MyoD activation and at later stages is essential for the secretion of several component of the satellite cell niche. (E) The myostatin promotes the cell cycle exit of early myobalsts progenitors and the activation of MyoD.*

The molecular regulation of the myogenic initiation in others borders of the dermomyotome is not known, but as they enter the myogenic program later, we could infer that the privileged interaction of the DML with the migratory neural crest cells offer a particular environment to enter the myogenic program earlier than other borders. Interestingly, Rios et al. showed that only a **transient** exposure to Notch signaling can lead to activation of myogenesis, as a **continuous** response to Notch leads to the complete inactivation of *Myf5* (Rios et al., 2011). These results are confirmed by several other studies in mice and chickens, in which Notch **dampens myogenesis during development**, by inhibiting *MyoD* expression and maintaining the cycling status of muscle progenitors (Delfini et al., 2000; Esteves De Lima et al., 2022, 2016; Hirsinger et al., 2001; Zalc et al., 2014). Moreover, during fetal stages, *Jag2* expression in myofibers, a ligand of Notch receptor, is under the control of muscle contraction thought a **YAP**-mediated mechanism. Thus, upon muscle contraction, a dialog starts between the myofibers and the surrounding myoblasts to inhibits their entry in the late myogenic program in order to maintain a sufficient muscle progenitors pool throughout fetal life (Esteves De Lima et al., 2016). In this regard, Notch signaling inhibits *Mymk* expression in terminally differentiated myogenic cells (Esteves De Lima et al., 2022). In accordance with this, mice fetuses mutant for the transcriptional effector of the Notch signaling pathway, *Rbpj*, within the muscle lineage display extremely reduced muscle masses due to the precocious exhaustion of the muscle progenitors pool (Vasyutina et al., 2007). Moreover, Notch signaling is necessary for the homing of the muscle progenitors under the basal lamina of the forming muscle by favorizing the secretion of various adhesion molecules (Bröhl et al., 2012). At early stages, in the VLL of the dermomyotome, Notch signaling is crucial for the decision between myogenic and endothelial lineage (see the section about endothelial development below). The **growth differentiation factor 8** (***Gdf8***, also known as ***Myostatin***) is a TGF-β related family member is specifically expressed in myogenic cells during development. *Gdf8*$^{-/-}$ adults mice weight two to three time more than wild-type one and exhibit a spectacular increase in their muscle mass, both resulting from **hyperplasia** (more muscle fibers) and **hypertropia** (larger muscle fibers) (McPherron et al., 1997). At post-natal stages, the increase of muscle mass following myostatin depletion is mainly done via hyperplasia, by modulating synthesis and turnover of structural muscle fiber proteins, with few to no effects on satellite cells proliferation and differentiation (Amthor et al., 2009). On the contrary, during embryonic development myostatin acts to regulate the balance between proliferation and differentiation of embryonic muscle progenitors by promoting their terminal differentiation through the activation of *p21* and *MyoD* (Manceau et al., 2008). Others member of the Tgf-β superfamily, such as the **BMP signaling** pathways are involved in muscle development. As said above, BMP4 is secreted by the lateral plate mesoderm. This lateral expression of BMP4 maintains the undifferentiated state of muscle progenitors within the hypaxial dermomyotome by inhibiting the expression of *MyoD* (Pourquié et al., 1996, 1995). At the medial level, BMP signaling from the neural tube inhibits myogenesis in the somite and expression of the BMP inhibitor, **Noggin**, in the DML precedes the activation of *Myf5* and *MyoD* (Reshef et al., 1998*).* Whitin the limb bud, *Bmp2* and *Bmp4* are expressed in the epidermis and the underlying mesenchyme (Amthor et al., 1998). Noggin is expressed in the center of the limb bud, in between the dorsal and ventral muscle masses. Upon limb epidermis removal, the expression of *Pax3* is drastically decreased compared to the one of *MyoD*, while grafting of beads soaked in BMP4 can restores the expression of *Pax3* and contains the *MyoD* one. Moreover, this effect seems to be mediated by **Shh**, as SHH bead grafting increases *Bmp2* domain expression and leads to an increase of *Pax3* expression and the downregulation of *MyoD*. Early limb migratory myoblasts are positive for the phospho-SMAD1/5/9 antibody, demonstrating an active response to BMP signaling (Asfour et al., 2023). Shutting down BMP signaling cell-autonomously with the overexpression of *Smad6*, a natural BMP inhibitor, specifically in *Lbx1*$^{+}$ migrating cells, disrupts their migration, via the regulation of *Hoxa11,* and trigger a more quicker entry in the myogenic lineage, leading *in fine*, to a loss of the most distal muscles (Wang et al., 2010).

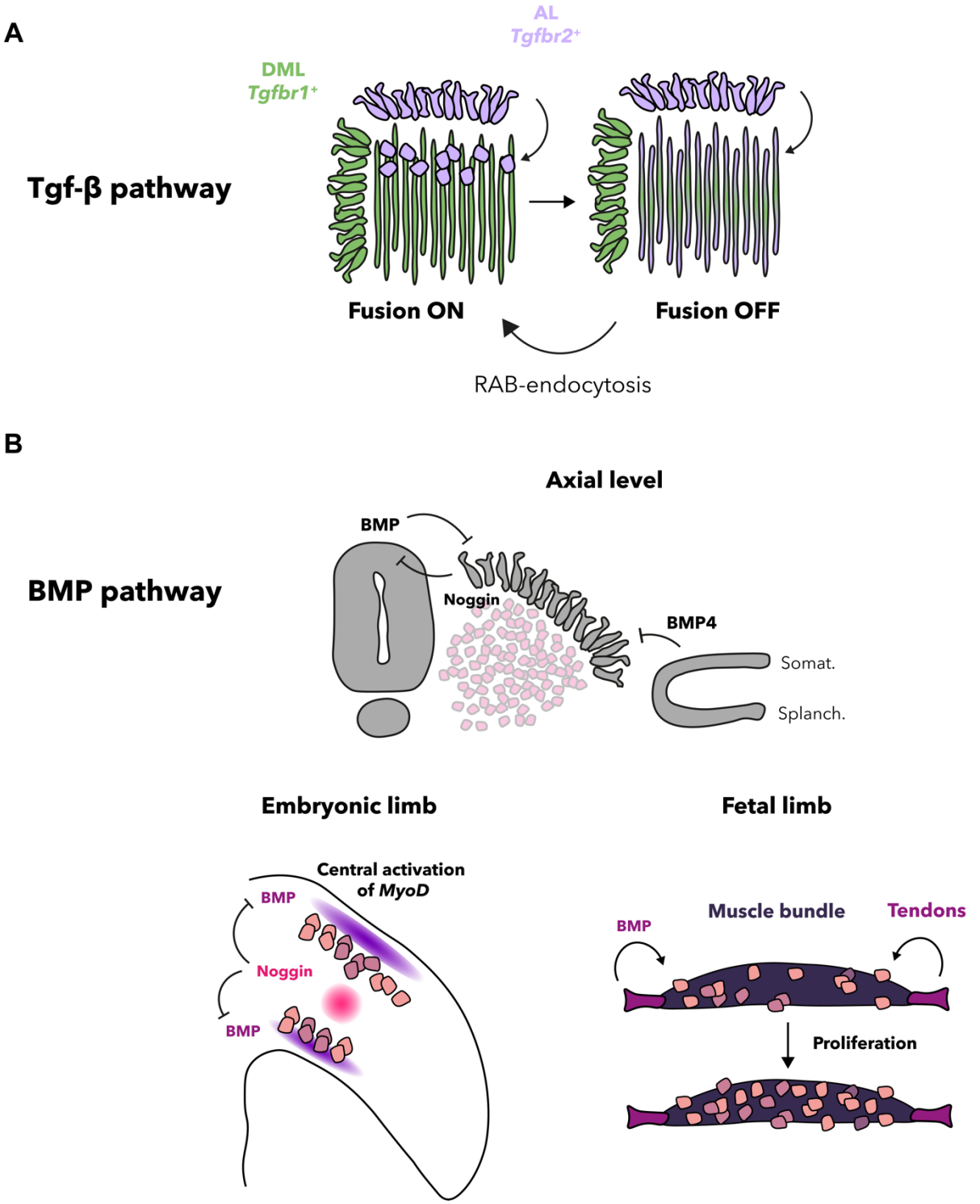

Figure 9. Signaling pathway regulating myogenic development. *(A) Fusion of myoblasts from the DML with the AL or the PL (not represented) lead to the formation of a functional TGF- heterodimeric receptors and inhibit fusion, a RAB-mediated endocytosis reset the system and allow a new round of fusion. (B) BMP either from the lateral plate mesoderm or from the roof of the neural tube inhibits myogenesis in the dermomyotome lip. Noggin expression from the DML allow the rapid entry of the DML in the myogenic lineage. At the limb level, BMP from the ectoderm or the surrounding mesenchyme inhibits myogenesis, this effect is counteracted by the central expression of Noggin, resulting in a central expression of MyoD. At fetal stages, BMP from the tendons promote the proliferation of myoblasts.*

The central expression of Noggin therefore seems essential to counteract the inhibitory effect of BMP and ensure an adapted spatio-temporal activation of limb myogenesis. Later during fetal life, BPM signaling is activated in a subset of muscle progenitors, preferentially located at the tip of muscle bundles, at the interface between muscle and tendon. At this stage, BMP secreted from the tendons

promotes the proliferation of *Pax7*$^{+}$ muscle progenitors specifically at the myotendinous junction (H. Wang et al., 2010).

Limb Myogenesis and Wnt signaling

As said hereinabove, the intrinsic and extrinsic factors regulating the entry in the myogenic lineage within the somite, as well as the early migration of muscle progenitors have been well characterized. The late events regulating the growth of the muscle during fetal stages have also gain a lot of interest in the recent years. However, the early events following the entry of myogenic progenitors inside the limb bud have not been elucidated so far. Regarding the Wnt signaling pathway several ligands, secreted inhibitor, or intracellular effectors are expressed within the limb bud (Ladher et al., 2000; Loganathan et al., 2005) and it has been independently proposed that the Wnt/TCF-LEF pathway might be an **inhibitor** (1), an **activator** (2) or **dispensable** (3) regarding limb myogenesis.

(1) *The msh homeobox 1,* ***Msx1****,* is expressed in *Pax3*$^{+}$ limb myoblasts during their migration and antagonizes the myogenic activity of *Pax3* (Bendall et al., 1999). Molecularly, Miller et al. found that the Wnt signaling effector TCF4 is able to bind regulatory elements in the proximal enhancer of *Msx1* to activates its expression and therefore **block *MyoD* activation** (Miller et al., 2007).

(2) ***Wnt6*** is expressed in the ectodermal cells of all the limb bud and therefore surrounds all the limb mesenchyme (Loganathan et al., 2005). By experimentally removing a portion of ectoderm, Geetha-Loganathan et al. demonstrated that the expression of both *Pax3* and *Myf5* was dependent on epidermis-derived signals and that their expression could be rescued by the injection of WNT6-secreting cells (Geetha-Loganathan et al., 2005). Still, they did not observe any rescue of *MyoD*, while later makers of myogenesis were restored (*MyoG*, MyHC). They argue that WNT6 promote the so-called Myf5-dependant / MyoD-independent myogenic pathway. As shown above, *Myf5* and *MyoD* can compensate between each other, therefore it is highly probable that another unknown ectodermal factor was essential for *MyoD* activation and that simply WNT6 was required for *Myf5* which is sufficient to drive myogenesis alone. Moreover, at these stages, muscle progenitors represent only a tiny fraction of all the mesenchymal cells within the limb and therefore the ectopic WNT6 could act on others cell types and influences myogenesis in an indirect manner. Finally, their analysis was only based on wholemount colorimetric hybridization *in situ* that could not allow to determine if the genes expression was restored by increasing the transcription of *Myf5* in the pre-existing cells, by boosting their proliferation or maybe by recruiting new myoblasts from the adjacent hypaxial dermomyotome. Retroviral infections of limb bud with the Secreted frizzled related protein 2, ***Sfrp2***, a Wnt inhibitor, impair the myogenic differentiation, however, these results could not be just attributed to a cell-autonomous effect of Wnt signaling in myogenic cells, as the whole limb bud was transfected and inhibition of Wnt signaling might have dampen the development of others tissues and therefore retard the overall appendage development (Anakwe et al., 2003). In addition, the time between the infection and the analysis was considerable (6 days), leading to difficult interpretations

(3) Other studies point toward a scenario where Wnt signaling would be totally **dispensable for early limb myogenesis**. Using chicken embryo manipulations Abu-Elgmad et al. demonstrated that implantation of bead soaked into the Wnt inhibitor, DKK1, does not have any effect on the expression of *Myf5* or *MyoD* and that misexpression of a dominant-negative form of the transcriptional effector of the TCF/LEF pathway *Lef1* has no effect on the expression of *MyoD* and *MyoG*. The same results were found for myogenesis within the branchial arch, while in the epaxial domain the TCF/LEF pathway seems essential to foster myogenesis (Abu-Elmagd, 2010). Similar conclusions were drawn by Huncheston et al. in

mice, where deleting the two allele of the β-catenin does not seem to impact the ability of early myoblasts to activate *MyoD*, even though early *MyoD*$^{+}$ limb myoblasts are positive for a transcriptional TCF/LEF reporter (Hutcheson et al., 2009). Using *Pax7*^{CRE} mice, to activate or knock-out the β-catenin only in the fetal muscle progenitors, they propose that the overall quantity of slow myosin myofiber was positively regulated by the β-catenin (Hutcheson et al., 2009).

Out of these four studies, the more convincing model would be that, even activated in early limb myoblasts, Wnt-TCF/LEF signaling seems to be dispensable for early myogenic specification (i.e. activation of *Myf5*, *MyoD*) but required only later at fetal stages.

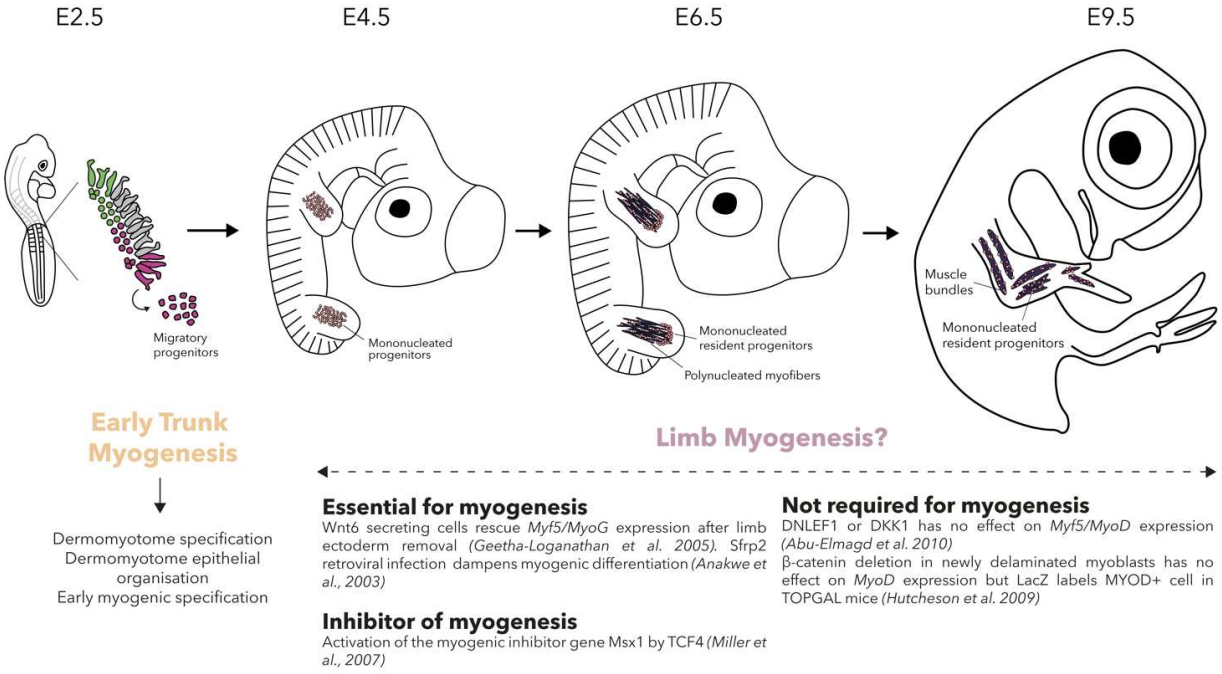

Figure 10. Role of Wnt signaling during limb myogenesis

Development of Sclerotome-Derived Tissues

Bone derivatives

Bones of the vertebrate skeleton provide attachment sites for muscles, tendons and ligaments, enabling locomotion. Bone formation during embryogenesis can occur via two distinct processes: **intramembranous** or **endochondral ossification**. Both start with condensations of high cellular density that outline the shape and size of the future bones. Intramembranous ossification begins with the condensation of mesenchymal populations that directly differentiate into **osteoblasts** to form the bone. The flat bones of the body, including the **skull, mandible, maxilla and clavicle**, are generated by intramembranous ossification. By contrast, endochondral ossification is an intricate process characterized by the development of bone through a **cartilage intermediate**. During endochondral ossification, the cells in the middle of the mesenchymal condensations develop into cartilage precursors, the chondrocytes, which begin to secrete cartilage matrix. The replacement of cartilage with mineralized tissue in endochondral bones is a complex process, triggered by the differentiation of proliferating **chondrocytes** in the center of cartilage anlage into a non-proliferative hypertrophic state. This is followed by the invasion of osteoblast progenitors, osteoclasts, blood vessels, endothelial and hematopoietic cells into the hypertrophic cartilage. When the hypertrophic cartilage

is resorbed, the incoming osteoblast progenitors differentiate into trabecular bone-forming osteoblasts, and hematopoietic and endothelial cells establish bone marrow in what becomes the primary ossification center. Endochondral bone formation occurs in the skull base and the **posterior part of the skull, the appendicular and axial skeleton** (see Berendsen and Olsen, 2015; Salhotra et al., 2020 for a detailed review of bone development).

Vertebrae Anatomy

The axial skeleton of vertebrates, **the vertebral column**, is the defining feature of the whole clade and comprises a **segmented** and **repeated** series of individual bones, the **vertebrae**. Vertebrae possess two fundamental parts: the **vertebral body**, or centrum, at the ventral side, which envelops the embryonic **notochord** to provide axial mechanical strength, and the **vertebral arch** which provides articulation and anchorage for ribs and epaxial muscles. Together, these two structures enclose the **vertebral foramen** that contains the spinal cord. The vertebral arch is formed by a pair of **pedicles** and a most dorsal pair of **laminae** and contains a total of seven processes, four small **articular process**, two **transverse process** and one **spinous process** in the medial position (Draga and Scaal, 2024). Vertebrae are often regrouped into different categories based on their morphology and position along the A-P axis: **cervical**, **thoracic** (bearing ribs), **lumbar**, **sacral** and **coccygeal** or **caudal** depending on the species (Romer and Parsons, 1986). The number of vertebrae of each category is specific to each species and regulated mainly by Hox genes. Some general rules can be applied. For instance, **mammals** always have **7 cervical vertebrae**. Nevertheless, this rule is broken within two mammalian clades with slow metabolic rates, sloth and manatee, with three-toed sloths (*Bradypus tridactylus*) usually having eight or nine cervical vertebrae and two-toed sloths (*Choloepus*) and manatees (*Trichechus*) only five or six (Varela-Lasheras et al., 2011). Moreover, abnormal additional cervical vertebrae have a higher rate of appearance in primates with low metabolic rate compared to high metabolic ones, leading several authors to the conclusion that a slower metabolic rate relaxes the pressure of selection on skeletal abnormalities, that *in fine*, leads to a diversification of the axial skeletal pattern (Galis et al., 2022; Varela-Lasheras et al., 2021). The case of cervical vertebrae in dinosaurs is not the same. Birds can display a **great variety** of cervical vertebrae, ranging from around 10 in some parrots to 14 in the chicken and even 23 in the swan, the actual record being hold by an extinct plesiosaur with 76 cervical vertebrae (Böhmer et al., 2019). Interestingly, the increase of cervical vertebrae number is associated with a diminution in the relative size of the cervical vertebrae, correlating what has been found in snakes, where the increase of somite number was associated with a higher somitogenesis rate, but also a smaller relative somite size (Böhmer et al., 2019; Gomez et al., 2008a). Whether bird embryos with a huge number of cervical vertebrae use the same developmental mechanism is unknown. Vertebrae can also fuse together to form larger structure, such as the **sacrum** in mammals or the **synsacrum** and **pygostyle** in birds. All birds have a series of vertebrae adjacent to the ilium that are fused together, forming a bone called the **synsacrum**, moreover they also display several fused terminal caudal vertebrae named the **pygostyle**, a situation also present in tailless primates with the appearance of the **coccyx** (tail bone). Some birds have a third series of fused vertebrae, the **notarium**, defined as any group of thoracic vertebrae that are fused to each other but not to the synsacrum (Bui and Larsson, 2021). A fully fused notarium has evolved independently at least twelve times in passerines (James, 2009), suggesting a strong tendency in birds to fuse their vertebrae. The developmental mechanisms of vertebrae fusion in amniotes have been only poorly described and remain completely mysterious.

Early Sclerotome Development

Embryologically, each vertebra comes from the ventral part of the somite that undergo an EMT to form a **mesenchymal pool** of cell named the **sclerotome**. The induction of sclerotome development is described above. Sclerotomal cells are recognized by the expression of the paired box transcription factor ***Pax1*** and ***Pax9***. In the chicken embryo, even though somite III is still epithelial,

Pax1 is already expressed in the ventral region, prefiguring the sclerotome (Draga and Scaal, 2024). In somite V-VI, the mesenchymal *Pax1*$^{+}$ sclerotome is clearly visible (Draga and Scaal, 2024). This is true for most somites, except in the occipital region where somites IV to VIII simultaneously compartmentalize and activate *Pax1* (Maschner et al., 2016). Soon after its specification, the sclerotome is then divided into different sub-compartments that will, in the end, correspond to different structures of the vertebra (Draga and Scaal, 2024). The mediolateral and dorsoventral polarity of the sclerotome is dependent on inductive signals from surrounding tissues and are not established before stage III somite. On the contrary, the anteroposterior, or craniocaudal polarity of the sclerotome is already determined at the PSM stage, as it is tightly intertwined with somitogenesis (Aoyama and Asamoto, 2000).

Cranio-caudal Polarity

The craniocaudal segmentation of the sclerotome has been morphologically described in the 19th century as the sclerotome exhibit a thin cleft between its cranial and caudal part, names the **von Ebner's fissure** (Ebner 1888). The caudal sclerotome half shows higher cell density than the cranial half, which is due to a higher rate of proliferation. This polarity is mediated by several regulators including the bHLH transcription factor ***Mesp2*** which specifies the cranial part of the somite and repress the caudal identity, whereas the homeobox transcription factor ***Uncx4.1*** specifies caudal identity (Neidhardt et al., 1997; Sasaki et al., 2011; Schrägle et al., 2004; Takahashi et al., 2007). Later the von Ebner fissure maintenance is mediated by the T-box transcription factor ***Tbx18***, which is expressed in the cranial somite half together with *Uncx4.1* expressed in the caudal somite half (Bussen et al., 2004). Moreover, transcriptomic analyses found out that several hundred of genes are differentially expressed between cranial and caudal sclerotome, with no function associated yet (Hughes et al., 2009). This segregation along the anteroposterior axis has important consequences on the development of the vertebra. Indeed, each vertebra do not only derive from one somite but is the product of two adjacent half sclerotomes. More precisely, one vertebra originates from the fusion of the caudal part of a defined somite and the cranial part of the somite positioned just posteriorly. Both Analysis of peanut agglutin staining, lineage tracing with lipophilic dye or quail-chick chimeras have confirmed this process, named **resegmentation** (Aoyama and Asamoto, 2000, 1988; Bagnall et al., 1989; Huang et al., 1996; R. Huang et al., 2000). Recently, Ward et al. proposed a resegmentation-shift model where the resegmentation *per se* is also accompanied by a shift of the sclerotome along the AP axis (Ward et al., 2017). The resegmentation is observed from the cervical to lumbosacral domain and, until recently was thought to be a specific feature of tetrapods, as graft of eGFP^{+} somite in axolotl pinpoint toward a conserved mechanisms in Lissamphibia and amniotes (Piekarski and Olsson, 2014; Ward et al., 2017). This assumption was also based on the fact that in teleost fishes the resegmentation is less apparent, with cells from adjacent somite halves undergoing substantial mixing, resulting in vertebrae without clear lineage-restricted compartment (Morin-Kensicki et al., 2002). However, a recent study using DiO and DiI lineage tracing in the little skate, a cartilaginous fish, demonstrated that both trunk and tail vertebrae derived from two adjacent somites, proving that the resegmentation is an ancestral feature of axial gnathostome skeleton (Criswell and Gillis, 2020). The craniocaudal polarity of the sclerotome does not just have important consequences for the sclerotome-derivatives but also is essential to set the periodicity of the **segmentation of the spinal nerves**. As said before, the caudal-half exhibit higher cell density while the cranial half is composed of a loose mesenchyme. The caudal-half also express several neuro-repellent genes such as the *Semaphorin3a* and *EphrinB* that dictate the migration of the neural crest, forming the dorsal root ganglia, only in the permissive cranial sclerotome (Krull et al., 1997; Rickmann et al., 1985; Wang and Anderson, 1997). Moreover, the mechanically loose constitution of the cranial-half favors the ingression of motoneuron axons specifically in this region instead of the caudal one (Schaeffer et al., 2022).

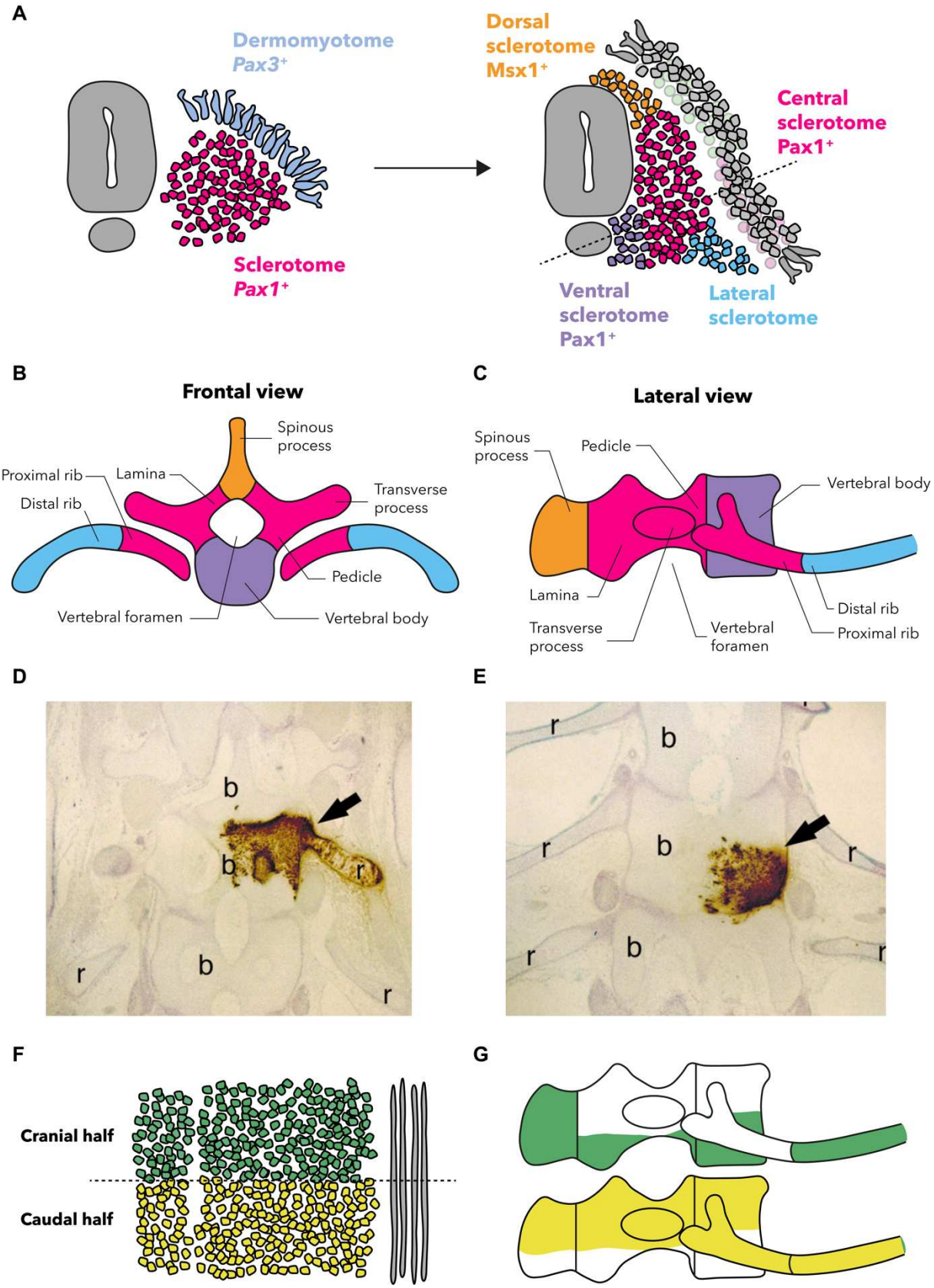

Figure 11. Vertebra development. *(A) Expansion of the early sclerotome into the different sclerotomal sub-compartment. (B,C) Anatomy of the vertebrae and the contribution of each sclerotomal sub-compartment. (D,E) Quail-chick graft of a sclerotome caudal half (D) or a sclerotome cranial half (E), (from Aoyama and Asamoto, 2000). (F) Dorsal view of an early sclerotome with the cranial and caudal half. (G) Contribution of the two sclerotomal halves to two adjacent vertebrae.*

The Ventral Sclerotome

Even though the ventral sclerotome is only a small fraction of all the sclerotome at early stages, it contributes to the entirety of the vertebral body (Draga and Scaal, 2024). The ventral sclerotome is composed of the cells of the medioventral part, located nearby to notochord. These cells **migrate medially** toward the notochord and **massively proliferate** to give rise to the **vertebral body** (Wilting et al., 1994). This proliferation is essential to procure enough cells that will fuse with their contralateral counterparts to form the vertebral body. This process is dependent on *Pax1* expression (Furumoto et al., 1999). Regarding the resegmentation, each sclerotomal half contributes equally to the vertebral body (Aoyama and Asamoto, 2000; R. Huang et al., 2000). In addition to providing chondrocytes and osteoblast for the vertebral body, the ventral sclerotome also gives rise to the ***annulus fibrosous*** of the **intervertebral disks**, the soft ***nucleus pulposus*** coming from the **notochord**.

The Central Sclerotome

The central sclerotomal cells represent the largest subpopulation of the early sclerotome. These cells essentially differentiate *in situ* without previous migration and give rise to the **pedicle** of the vertebral arch, the **transverse process** and the **proximal rib**. Like the ventral sclerotome, the development of the central sclerotomal derivatives requires Shh signaling from the notochord/floor plate complex and *Pax1* activity (Chiang et al., 1996; Dietrich and Gruss, 1995; Wallin et al., 1994). Quail-chick chimeras have shown that the skeletal derivatives of the central sclerotome mainly arise from the **caudal half** of the sclerotome (Aoyama and Asamoto, 2000; R. Huang et al., 2000). The loose mesenchyme in the cranial half of the central sclerotome makes no major contribution to skeletal structures but provides a suitable environment for dorsal root ganglia and spinal nerve development (described above). However, it has been proposed that the cells from the cranial-half can differentiate into neural-associated conjunctive tissues, such as the **endo-** and **perineurium**, without no founded experimental proof.

Arthrotome

Two adjacent vertebrae are connected by **intervertebral joints** and the **intervertebral discs**. The intervertebral joints (also called **zygapophysial joints**) are synovial joints between the posterior articular process of one vertebra and the anterior articular process of the posterior vertebra. These joints allow the spine to bend and twist, while at the same time limiting movement. The **intervertebral discs** link two adjacent vertebrae through the vertebral bodies. In mammals, each disc is composed of an external ***annulus fibrosus***, which surrounds the internal ***nucleus pulposus***. The internal *nucleus pulposus* is derived from the **notochord**. The newly formed somite consists of an outer spherical epithelial structure of cells with a central lumen, the **somitocoele**. The somitocoele is filled with *Pax1/9*$^{+}$ mesenchymal cells that have remained mesenchymal from their PSM stage to somitogenesis (Huang et al., 1996). Using quail-chick chimeras Huang et al. traced their developmental fate and found that they accumulate in the **anterior most** part of the **caudal half** of the sclerotome, lining along the von Ebner's fissure. At later stages they incorporate into the ribs, where they undergo resegmentation, including the **costovertebral joints** and into the vertebrae at level of the **zygapophyseal joint** but also into the ***annulus fibrosus*** of the intervertebral disks. Excision of the somitocoele cells does not lead to obvious vertebrae segmentation default, however when replaced by a neutral bead, the formation of the zygapophysial joint was systematically blocked and intervertebral disk often failed to form (Mittapalli et al., 2005). The participation of somitocoele cells to several joint and articular compartment has lead some authors to regroup those cells under the name of **arthrotome** (Mittapalli et al., 2005). At the cellular level, after immigration into the perinotochordal space, the *Pax1*$^{+}$ sclerotomal cells temporarily continue to proliferate to completely ensheathe the notochord. This cellular sheath is initially not segmented, but uniform along the craniocaudal extent of the notochord. In zones representing the prospective vertebral bodies, *Pax1*

expression is downregulated to enable chondrogenesis, while *Pax1* expression is maintained in the zones representing the *anulus fibrosus* of the prospective intervertebral disks. In the intervertebral disk anlagen, the notochord persists and expands into separated lentiform discs, which eventually give rise to the *nucleus pulposus*, while it disappears at the level of the vertebral body anlagen (see (Williams et al., 2019 for a detailled review).

The Dorsal Sclerotome

The dorsal sclerotome gives rise to the **dorsal lamina** of the vertebral arch and the **spinous process**. This implies that the sclerotomal cells migrate from their original position in the dorso-medial compartment, dorsal to the neural tube, where they unite with the corresponding cells from the contralateral side of the embryo. The dorsal sclerotome does not express *Pax1/9* (Draga and Scaal, 2024). It depends on **BMP4** signaling from the dorsal neural tube, which suppresses *Pax1* and induces the homeobox transcription factors ***Msx1*** and ***Msx2*** in the migratory dorsal sclerotomal cells during the pre-cartilaginous stages of differentiation (Monsoro-Burq et al., 1996; Watanabe and Le Douarin, 1996). In contrast, **SHH** from the notochord/floor plate complex antagonizes *Msx1/2* expression, thus limiting their expression to the dorso-medially located sclerotomal cells. Regarding resegmentation, the spinous process has been shown to originate from both the cranial and caudal halves, however, it is not clear if cells from two segments respect a sharp boundary between them or if the cranial sclerotome is able to colonize the anterior most part of the spinous process (Aoyama and Asamoto, 2000; R. Huang et al., 2000). In addition to give rise to skeletal tissue, the dorsal part of the sclerotome also provides the spinal cord with **meningeal precursors**. Quail-chick chimeras have shown that the neural tube does not provides any cell of the meninges and that the medial portion of the sclerotome was at the origin of spinal meninges (Bagnall et al., 1989; Christ et al., 2007b; Halata et al., 1990). However, these results are not entirely clear and would need complementary investigations with modern tools.

The Lateral Sclerotome and Rib Formation

The lateral sclerotome gives rise to the **distal part of the ribs**. Like the dorsal sclerotome, the lateral sclerotome develops **independently** of notochordal/floor plate Shh signaling and does not express *Pax1/9* (Draga and Scaal, 2024). In contrast, it is specified by **BMP4** signaling from the LPM, which induces expression of ***Sim1*** in both lateral sclerotome and lateral dermomyotome cells (Pourquié et al., 1996). In the sclerotome, *Sim1* is expressed for a short time while it persists longer in the dermomyotome and its derivatives, where it marks the epaxial–hypaxial boundary. The development of ribs will be more precisely described in the next section.

Rib Anatomy

The thoracic body wall of a typical amniote is characterized by the existence of **ribs**. Ribs are lateral extensions of the vertebrae that span the ventrolateral extent of the body wall and form the thoracic **rib cage**, which hosts the heart and the lungs. They form most of the thoracic skeleton of amniotes except for narrow mid-dorsal and mid-ventral strips, which are formed by the vertebral column and the sternum, respectively. They are interconnected by **intercostal muscles**, which enable movements of the ribs and the rib cage as a whole. The dynamic rib cage allows inspiration and expiration of the lungs and participates in locomotion. Anatomically, the ribs can be divided into two major parts: the **proximal** and **distal rib**. The proximal rib, articulates with the vertebra via two **articular processes**, the **capitulum** and the **tuberculum** (Romer and Parsons, 1986). The distal rib is composed of the two different parts, the **vertebral rib**, more medial and the **sternal rib** at the distal end, eventually articulating with the **sternum**. In the archetypal amniote body plan, these two bones are separated by a cartilaginous intermediate portion, that has been lost in birds and mammals (Scaal, 2021). Mammals, also exhibit reduced sternal ribs, being composed only of cartilage (Scaal, 2021). Birds and reptiles display a supplementary process on the vertebral ribs, named the **uncinate**

process that forms a long protrusion and articulate to the caudal rib by **syndesmosis**. Ribs can be classified according to their connection with the sternum: **true ribs** and **false ribs** are attached **directly** or **indirectly** to the sternum, respectively, while **floating ribs** do not contact the sternum at all and end freely in the muscular body wall. Birds and mammals have true, false and floating ribs, whereas snakes only have floating ones (Scaal, 2021).

Rib Development

As for others non-vertebrae axial bones, the **embryonic origin** of the ribs has been a long-standing **debate**. While being traced back to the somites by most of the authors using carbon labelled particles , X-ray irradiation, or quail-chick chimeras, and even to the **medio-lateral part of the somite**, the dermomyotomal or sclerotomal origin of the ribs has been debated since the early 00s (Chevallier, 1975; Olivera-Martinez et al., 2000; Pinot, 1969; Seno, 1961). Kato and Aoyama suggested that the proximal part of the rib comes from the sclerotome while both intercostal muscles and the distal ribs were from **dermomyotomal origin** (Kato and Aoyama, 1998). Using the same technique, Huang et al., demonstrated that all parts of the rib emanate from the **sclerotome**. A few years later, Evans used *LacZ* retroviral transfection in the chicken embryo to precisely map the origin of each part of the rib (Evans, 2003). His results clearly indicate that the sclerotome of all thoracic somites (19- to 26 in the chicken) contributes to both the proximal and distal elements of the ribs. Moreover, he confirmed the results obtained with quail-chick chimeras, that only the central sclerotome gives rise to the proximal part of the rib, while the lateral sclerotome, and not the lateral dermomyotome, is the embryonic origin of the distal rib. These injections also demonstrated that ribs are subject to **resegmenation**. Injections of somites 20 to 25 result in the labelling of two adjacent ribs, while somite 19 and 26 injections give rise to only one rib. The proximal rib only derives from the **caudal half** of the most cranial somite, but the vertebral and sternal ribs are composed of both the caudal and cranial halves of two adjacent somites. However, only the vertebral rib displays an evident resegmentation, as cells forming the sternal rib mix together and do not segregate according to their cranio-caudal origin.

The confusion for the sclerotomal vs. dermomyotomal origin of the rib might found its origin in **three different reasons:**

(1) Classical embryology experiments rely mainly on the ability of the experimenter to manipulate different embryonic territories. While numerous tissues form clear boundaries between them, such as for instance the neural tube and the somites, it is not always the case, especially for mesenchymal somite sub-compartments. Indeed, Evans shown that retroviral injection of lateral thoracic dermomyotome specifically labels the hypaxial muscles but also shown that targeting the interface between the lateral sclerotome and dermomyotome leads to a labelling of both rib and hypaxial muscle, demonstrating that these two tissues are physically **tightly associated** and that grafting of somite sub-compartments might not always lead to pure grafted populations (Evans, 2003).

(2) While specifically being markers of the dermomyotome, both ***Pax3*** and ***Myf5*** null mutants exhibit severe **rib development defects** (Braun et al., 1992; Dickman, et al., 1999; Wood et al., 2020). However, at earlier stages *Pax3* is strongly expressed in the PSM and $Myf5^{CRE}$ has shown to label the sclerotome, in addition to dermomyotome derivatives, probably due to a transient activation of the *Myf5* locus in the paraxial mesoderm (Gensch et al., 2008). These earlier expressions of both *Pax3* and *Myf5* therefore complicate the analysis of the mutant mice and cannot allow to conclude on a sclerotomal or a dermomyotomal origin for the ribs, as these genes might affect the development of all paraxial mesoderm.

(3) Careful anatomical analysis of rib musculo-skeletal development in wholemount chicken embryos has shown that the intercostal muscles anlagen develop in advance of rib anlagen, thus, as it were, paving the way for the following sclerotomal (Khabyuk et al., 2022). Indeed, the proximal ribs, as vertebrae, mainly rely on SHH from the notochord/floor plate while the development of the distal part of the rib required **FGF8** and **PDGF** from the myotome (Huang et al., 2003a; Soriano, 1997; Tallquist et al., 2000). Collectively, these data support the conclusion that defects observed in *Pax3* and various *Myf5* null mutant are **secondary effects** of myotome disruption, leading to a severe delay of rib formation. Interestingly, Wood et al. confirmed this close interaction by removing late differentiated muscle cells using either a Myo^{iCre} or HAS-CRE line coupled with a $R26^{GDTA}$ and showed that muscle-rib interactions are important beyond early stage to properly pattern the distal element of the rib (Wood et al., 2020). If molecular signaling still exist between the late myotome and rib anlagen is unknow. Moreover, mechanical cues coming from the attachment and contraction of intercostal muscles on the rib might also play a significant role. These active roles for muscle cells on the formation and patterning of skeletal component seems to be quite unique to the trunk, indeed, the current view is that muscle cells are passive and that the final patterning is dictated by the surrounding cell types (see sections below). However, most of these studies have been performed in the limb bud that, while containing muscle cells coming from the somites, exhibit a completely different anatomical organization (see sections below and Sefton and Kardon, 2019). Further investigation on the interplay between trunk muscles and their environment during musculo-skeletal patterning might shed the light on a more instructive role for myogenic cells than previously thought.

The Chelonian Rib Cage Development

Turtles exhibit a very derivative thorax anatomy compared to other amniotes (Romer and Parsons, 1986). Their shell is composed of a dorsal carapace and a ventral plastron that encloses the shoulder and pelvic girdles. Unlike the ribs of other amniotes, the turtle ribs grows laterally and hypertrophies to form the costal plate of the carapace while the neural plate is formed from hypertrophied vertebrae (Hirasawa et al., 2013). By a mechanism that remain to be identified, the turtle rib anlagen never invades the body wall and relocates **above the scapula** (Nagashima et al., 2009). This reorganization is associated with several muscle attachments modifications, as for instance the m. *latissimus dorsi* links the humerus with the dorsal carapace instead of attaching to the vertebrae (Nagashima et al., 2009). Turtle embryos equivalent to E5.5 chicken embryo exhibit a longitudinal ridge on the flank, at the level of the lateral somitic frontier called the **carapacial ridge** (CR). The CR comprises the condensation of undifferentiated mesenchyme underlying a thickened epidermis and thus histologically resembles to the apical ectodermal ridge of the limb bud (Burke, 1989). Dil labeling in the Chinese soft-shelled turtle embryo, confirmed that the dense mesenchyme of this structure is formed by **dermomyotome-derived dermis** (Nagashima et al., 2007). Removal or ectopic implantation of the CR regulates the medio-lateral patterning of the turtle rib and therefore has been proposed to act as a **signaling center** to regulate carapace development. However, CR manipulation experiments failed to perturb the dorsoventral translocation of the ribs. Suggesting a two-step mechanism in which the dorsoventral shifting of vertebrae is first regulated independently from the CR that, in a second time, regulates the medio-lateral patterning of the turtle ribs (Nagashima et al., 2007).

Occipital Bone Development

In human, the occipital bone is a cranial **dermal bone** that composed the main part of the **base of the skull**. It has a curved and trapezoidal shape. The occipital bone contains a large opening at its base which is called the **foramen magnum** and allow the passage of the spinal cord. The human

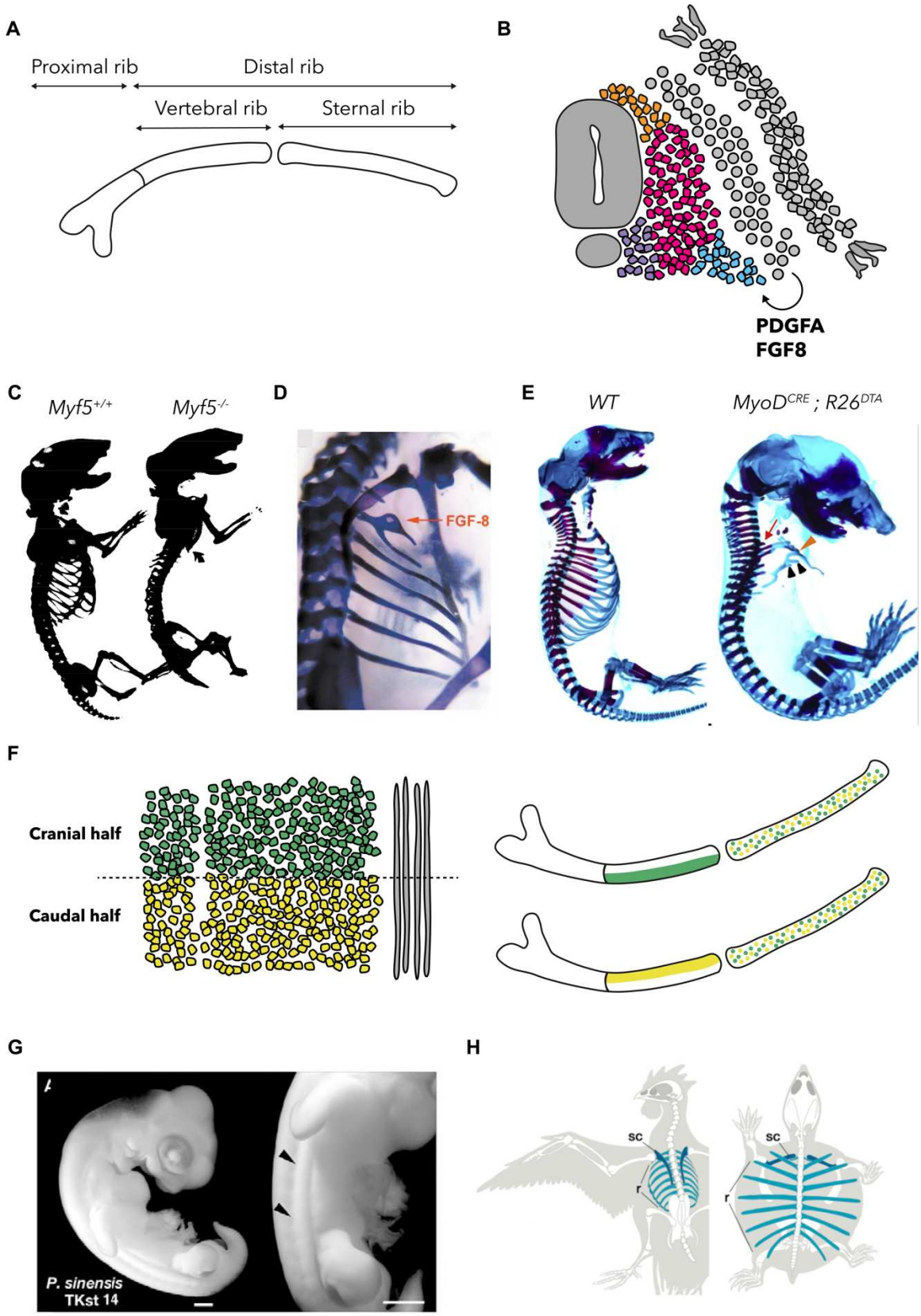

Figure 12. Rib development. *(A) General rib anatomy (B) Influence of the lateral myotome on the lateral sclerotome development. (C) Skeletal preparation showing defects of rib development in Myf5$^{-/-}$ mice (from Braun et al., 1992). (D) Induction of a thicker rib following FGF8 bead implantation in chicken embryo (from Huang et al., 2003). (E) Rib developmental defect following muscle lineage ablation (from Wood et al., 2020). (F) Resegmentation of the proximal and distal rib. (G) Carapacial ridge development in P. sinensis (turtle) embryo (from Nagashima et al. 2007). (H) Anatomy of rib and scapula in birds and turtles (from Kuratani et al., 2011).*

occipital bone, like that of most other mammals, is ontogenetically and functionally unique when compared to other bones of the cranium. It is one of the first bones of the skull to develop and is anatomically composed of four different parts surrounding the foramen magnum: the **squamous**, **basilar**, and two **lateral/condylar** parts (Romer and Parsons, 1986). The squamous, or **supraoccipital** part is the main part of the bone, curved and situated above the foramen magnum, the **basioccipital**, or basilar part, extends away from the foramen magnum under the skull and the two lateral parts, also named the **exoccipital** or the condylar parts, lay down on each side of the foramen magnum and on their ventral sides they exhibit two protuberances, the **occipital condyles**, that articulate with the superior facet of the atlas.

Due to its amenability, all the studies made to decipher embryonic contribution of the occipital somite to the skull were done chicken embryos using **quail-chick chimeras**. Occipital somites in the chicken are **somites 1-5** (Couly et al., 1993; Ruijin Huang et al., 2000b). The cranial most vertebrae are the **atlas** and **axis** (C1 and C2 respectively) and are tightly associated as a process from the axis, called the **dens**, penetrates the atlas to articulate the two vertebrae. The atlas and axis are therefore derived from the caudal half of the 5th sclerotome/cranial half of the 6th sclerotome and the caudal half of the 6th sclerotome/cranial half of the 7th sclerotome, respectively, with the tip of the dens axis being derived from the 5th somite (Ruijin Huang et al., 2000b). However, there is a debate about the precise contribution of each somite to the different part of the occipital bone. Couly et al. proposed that somites give rise to the basio- and exo-ccipital parts but not to the supra-occipital bone and that the first somite partially generates the *pars canalicularis* of the otic capsule (Couly et al., 1993). Besides, Huang et al., propose a model where somites one and two form stripes of cells in the basioccipital, exoccipital and supraoccipital, somites three to five give rise to the subsequent caudal parts of the basioccipital and exoccipital and somite five forms the first motion segment including the occipital condyle, the cranial part of the atlas and the tip of the dens axis (Huang et al., 1997; Ruijin Huang et al., 2000b). However, the few studies that have been down cannot allow a to draw a clear picture of the contribution of each somite to the occipital bone. Instead of relying on serial section, graft of single somite coupled with 3D imaging might help resolved the complexity of this mechanisms. Moreover, others experiment with somitic-specific or sclerotomal-specific drivers should be performed in mice. Finally, there is still a piece of mystery in how and when during evolution the contribution of somite to the skull emerged. Indeed, Augier described an evolutionary scenario in which agnates skull, called the **archiskull**, does not contain any somite derivatives, while the skull of Lissamphibia and jawed fishes, named the **paleoskull**, incorporates three somites, finally, the so-called **neoskull** of amniotes have incorporated five somites, completely including the hypoglossal nerve into the skull (Augier, 1931; see Maddin et al., 2020 for a detailled review). Nonetheles, a *bona fide* lineage tracing experiment is still missing to prove the contribution of the first three somites in Lissamphibia and jawed fishes. This could be achieved by somites grafting using transgenic axolotl or optogenetic labeling of single somite in the zebrafish. Moreover, no molecular mechanisms have been identified that would regulate specifically the destiny of somites into the occipital bone.

Tenogenic Derivatives

With bones and muscles, **tendons** are one of the main components of the musculoskeletal system. They are indispensable to transmit the force generated by the muscles to the bones and allow body movement. Tendon is a specialized **connective tissue** displaying a specific spatial organization of **type I collagen fibrils** that are organized parallel to the tendon axis. Collagen fibril assembly occurs mostly during fetal stages, while collagen fibril growth and maturation occurs at postnatal stages. This maturation is accompanied by a dramatic change of tendon mechanical properties. Tendons are qualified as hypocellular connectives tissues with the vast majority of the tissue being composed of **ECM** secreted by a few cellular residents, the **tenocytes**. These cells display an elongated shape and reside between the collagen fibers. As for muscle tissue and acto-myosin fibrils, the tendons

tissular organization can be subdivided into different anatomical scales. Collagen molecules assemble together successively forming collagen fibrils, collagen fibers, collagen bundles or fascicles and the tendon unit. Parallel collagen fascicles are separated by the **endotenon**, a loose connective tissue that also contains fibroblasts as well as **blood vessels** and **nerves**. The whole tendon is surrounded by the **epitenon** and then by a synovial sheath, the **paratenon**, composed of collagen fibers organized in a perpendicular direction to those of the tendon *per se*. The tendons are attached to the muscle via the **myotendinous junction**, which consists in interdigitation of the plasma membrane of both tendons and muscle fibers. At the molecular level collagen fibrils produced by tendon cells bind to laminin or integrins present at the level of sarcolemma and produced by muscle cells. On the other side, the junction between tendon and bone is called the **enthesis**. Depending on the anatomical location, both fibrous and fibrocartilaginous enthesis exist. At the cellular level, the enthesis comprise successive cellular layers of tenocytes, uncalcified fibrocartilage cells, calcified fibrocartilage cells and osteocytes, which create a direct connection between the soft tendon and the calcified bone (see Bobzin et al., 2021; Gaut and Duprez, 2016 for a detailled review). It is noteworthy to precise that the classical muscle-tendon-bone system might varies in the body as some tendon can be found attaching two muscle bundles together such as in the *m. digastricus* of the human jaw, the *m. rectus abdominis* muscle, or in the *m. biventer cervicis* in the neck of birds, muscles can even directly be attached the muscle to the dermis, such as the *m. panniculus carnosus* in mammals or directly to the sclera of the eyeball for the extraocular muscles (Böhmer et al., 2020; Romer and Parsons, 1986; Schünke et al., 2021). At the embryological level, even functional similar, tendons at different body location **do not derive from the same embryonic tissue.** Tendons in the head derive from the **neural crest cells**, limb tendons from the **lateral plate mesoderm**, while axial tendons come from the **somites** (Brent et al., 2003; Chevallier et al., 1977; Grenier et al., 2009). As linking the head and the trunk, the musculo-skeletal system of the neck exhibits a complex mismatch of embryonic origin for muscles and tendons, but generally, embryonic origin of neck tendons match that of the bone to which they attach (Heude et al., 2018, see below for a detailled discussion).

Axial Tendon Development

At the molecular level, the major regulator in tendon differentiation is the bHLH transcription factor **Scleraxis (*Scx*)**. As soon as around E4.5 in the chicken embryo, or E10.5 in the mouse, *Scx* transcripts can be observed at both the axial and limb level (Brent et al., 2003; Schweitzer et al., 2001). Within the limb bud it seems to be expressed in mesenchymal progenitors without no visible pattern while, at the same stage, in the trunk, *Scx* is expressed in an alternate periodic pattern with the myogenic progenitors. At later stages, *Scx* mRNA are detected in all tendons of the limb and the trunk (Brent et al., 2003; Schweitzer et al., 2001). Using both transgenic mice bearing an allele composed of the coding sequence of the *eGFP* in the first exon of the *Scx* locus (***ScxGFP* mice**), and quail-chick chimeras, it has been demonstrated that *Scx* gene also labels tendons of the tail and the face (Grenier et al., 2009; Pryce et al., 2007). Thus, these experiments demonstrated that *Scx* labels both **tenogenic precursors** and **mature tendons**. Its expression in a periodic pattern in the trunk has led to the creation of a novel somitic compartment, the **syndetome** (Brent et al., 2003). In detail the syndetome is defined as a sub-compartment of the sclerotome, by the expression of *Scx* at the anterior and posterior border of the dorsal sclerotome, flanking the developing. This organization therefore reflects the final organization of **intervertebral segmented epaxial muscles**, attaching to two adjacent vertebrae via tendons coming from the anterior and posterior part of two adjacent somites. Establishment of this specific patterned of Scx^{+} syndetome is dependent on **myotomal FGF signaling**, via FGF8 (Brent et al., 2003; Brent and Tabin, 2004). The entire sclerotome is competent to express *Scx* in response to FGF signaling. However, upon *Fgf8* secretion from the myotome, the anterior and posterior dermomyotome start to express two ETS transcription factor ***Pea3*** and ***Erm***, which are both target and transcriptional effector of the FGF signaling pathway.

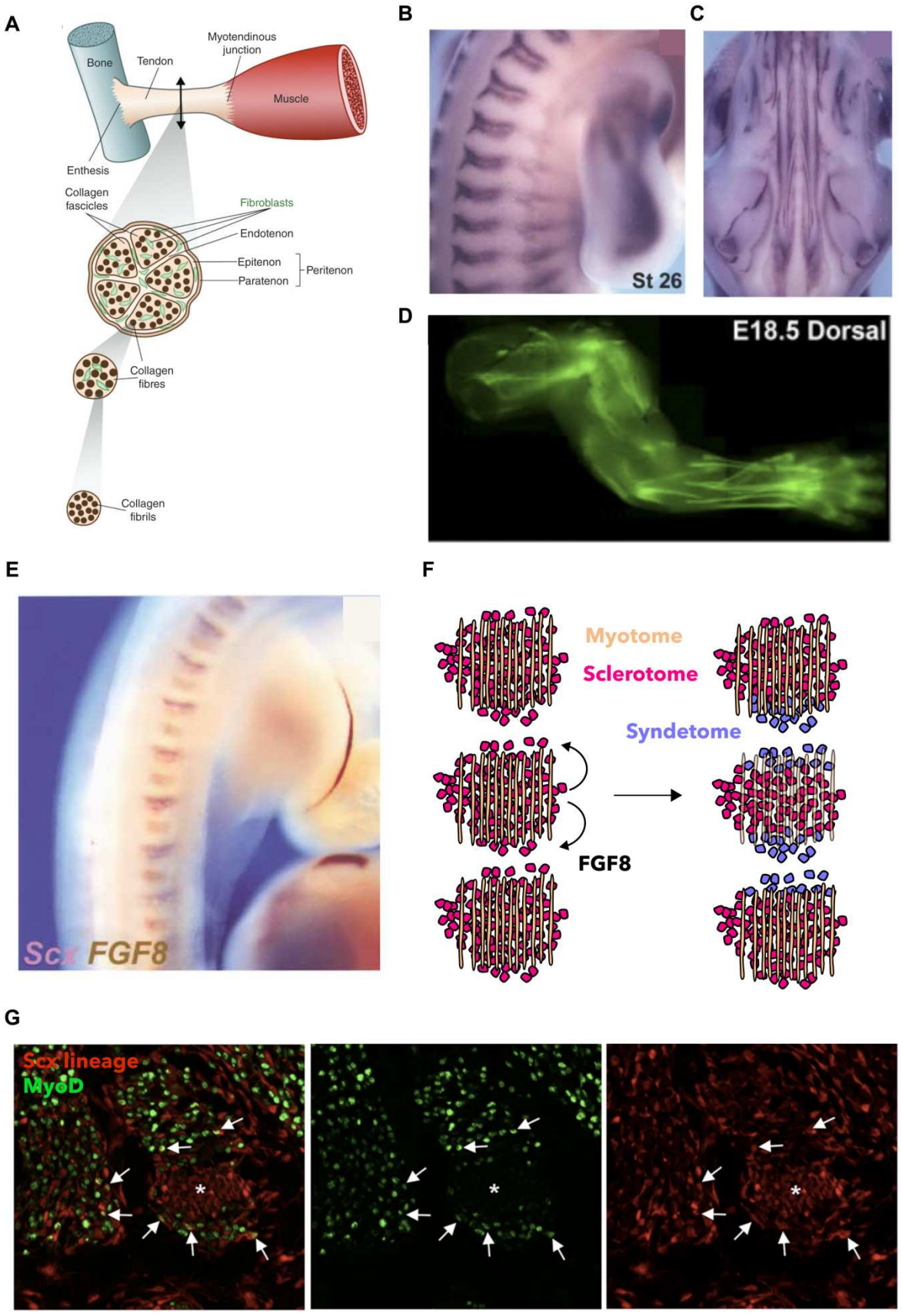

Figure 13. Tendon development. *(A) Tendon organization (from Gaut and Duprez, 2016). (B) Scleraxis expression in trunk and limb bud of chicken embryo (from Brent et al., 2003). (C) Scleraxis expression in chicken fetus back muscles (from Brent et al., 2003). (D) Limb from Scx^{eGFP} transgenic mice (from Pryce et al., 2007). (E) Alternate expression of Scx and myotomal Fgf8 In chicken embryo. (G) Limb section of transgenic mice labelled with the Scx lineage and MyoD, showing doubly myogenic cells from the Scx lineage (from Esteves de Lima et al. 2021).*

Once these two domains of expression have been established, further FGF signaling triggers the activation of *Pea3* and *Erm* which, in turn, foster the transcription of *Scx*, leading to the specific expression of *Scx* in the antero-posterior border of the sclerotome (Brent and Tabin, 2004). This mechanism, as the intricate link between hypaxial myotome and ribs development, show again how important the myotome is to organize the development and patterning of the axial musculoskeletal system. Interestingly, when examined, *Scx*$^{-/-}$ mice do not exhibit defect in all tendons (Murchison et al., 2007). The **long-range tendons** of the trunk and limbs and intermuscular tendon are either missing or severely deficient, while **short-range anchoring tendons** in the back and limbs appear normal. Importantly, the ability of tendon to connect muscle to skeleton is not impaired in the absence of *Scx*, as the Scx$^{-/-}$ mutant is viable after birth, despite limited mobility due to disruption of these long tendons (Murchison et al., 2007). This demonstrates two things (1) that tendon development can be initiated without *Scx* and (2) that short and long tendons do not relies on the same morphogenetic mechanisms.

(1) Regarding the molecular role of *Scx* in tenogenic differentiation it has been shown that *Scx* can positively activates ***Col1a1***, however its expression is maintained in numerous tendons in *Scx*$^{-/-}$ mice, suggesting redundant function with other transcription factors (Murchison et al., 2007). In addition, *Scx* can positively activates ***Tenomodulin*** *(Tnmd)*, a transmembranal glycoprotein maker of late tendons (Shukunami et al., 2018, 2006). Two others transcription factors are involved in tenogenic development, the first one is **Early Growth Response 1 (*Egr1*)**, a Zinc finger transcription factor. *Egfr1* is sufficient for the expression of *Scx*, *Tnmd* and tendon-associated collagen *in vivo* in the chicken embryo (Lejard et al., 2011). Moreover, Egr1 mice display defect in tendons formation and mechanical weakness (Guerquin et al., 2013). The homeobox **Mohawk (Mkx)** has also been implicated in tendon differentiation. *Mkx*$^{-/-}$ mice exhibit smaller tendons at postnatal stages, fetuses display a reduced expression of *Tnmd* and *Col1a* (Kimura et al., 2011; Liu et al., 2010). *Mkx* is expressed in early somitic progenitors not only giving rise to tendons but also to muscles, cartilages and bones. *Scx* and *Mkx* expression in developing tendons appear to be normal in *Mkx*$^{-/-}$ and *Scx*$^{-/-}$ mutant mice, respectively, suggesting that *Scx* and *Mkx* act in different genetic cascades during tendon development (Guerquin et al., 2013; Lejard et al., 2011). In addition, *Mkx* expression is not modified in *Egr1*$^{-/-}$ mice (Guerquin et al., 2013). Therefore, the respective role of these three transcription factors, and their potential interactions with each other remains elusive and a complete picture of the tenogenic commitment remain to be drawn.

(2) Using genetic lineage tracing and loss of function, Ronen Schweitzer lab demonstrated that *Scx* is not required in the development of short, anchoring tendons (Huang et al., 2019; Murchison et al., 2007). Moreover, they demonstrated that *Scx*$^{-/-}$ mice exhibit a default in **tendon cell recruitment** essential for **tendon elongation**. This mechanism can be put in parallel of myogenesis where myoblasts first need to elongate to form differentiated myoblasts and then fuse with surrounding myoblasts to elongate and form long polynucleated myofibers. Therefore, long tendons formations seems to be a bi-phasic system, where *Scx* expression is essential only in the second phase, suggesting that, at least two, different gene regulatory networks successively co-exist within tendon progenitors cells (Huang et al., 2019). If one tendon population derivates from one other and how they might be regulated by two different gene regulatory networks remains to be studied.

Limb Tendon Development

In the limb tenogenic precursors do not emanate from the somite but come from the lateral plate mesoderm. In the limb, *Scx* expression is dependent of **BMP signaling** as retroviral infections with BMP4 retrovirus or grafting of beads coated with BMP4 leads to a severe downregulation of *Scx* (Schweitzer et al., 2001). Therefore, limb tendons differentiation seems to be dependent on the BMP-

inhibitor **Noggin** which expression mirror the one of tenogenic precursors. The **TGF-β** signaling is also required in E10.5 mouse limb for *Scx* activation (Havis et al., 2014). If *Scx* expression in the limb bud, *in vivo*, also relies on **FGF signaling** is not known, even though it negatively regulates *Scx* in mouse limb explant (Havis et al., 2014). Contrary to what have been proposed in the trunk, the development of limb tendon is independent of muscle development during early stages, but around E12.5 in mice the limb tenogenesis is considered as muscle dependent. Even though the current view for limb musculoskeletal is that myogenic cell originates from the somite and tenogenic cell from the LPM, this textbook view has been currently challenging by several studies. Using mice lineage tracing, co-culture, scRNA-seq, quail-chick chimeras and *in ovo* electroporation, both Esteves de Lima et al. and Yaseen et al. recently proposed that a sub population of **myonuclei at the myotendinous junction are of LPM origin** (Esteves De Lima et al., 2021a; Yaseen et al., 2021). These nuclei derived from mesenchymal progenitors with a dual fibro-myogenic identity. Surprisingly, they can turn-on myogenic factor before fusing to a myofiber, demonstrating that these nuclei are not incorporated in the polynucleated myofiber randomly. Moreover, once fused these particular nuclei conserved their mixed identity as for instance only myonuclei from the LPM are able to express ***LoxL3***, an enzyme essential for the MTJ formation and attachment. This minor contribution of LPM-derived myonuclei at the MTJ has therefore been proposed to be regulated by **BPM signaling** and therefore creates a boundary of fibroblast-derived myonuclei at the MTJ that control limb muscle patterning. If the same mechanism happens in the epaxial or hypaxial domain in the trunk is unknow. As most of hypaxial muscles developed with a connective tissue deriving from the LPM, one could hypothesize that the same kind of mechanism is happening, however as the embryonic origin of the connective tissue of the epaxial musculature is still blurry it is difficult to extrapolate these results in this compartment. Conversely, a recent population of migrating cells derived from the somite has been shown to contribute to a plethora of normally LPM-derived tissues inside the limb, including tendons (Arostegui et al., 2022). These cells emanate from the sclerotome and express ***Hic1***. They therefore constitute a pool of migrating cells coming from the somite and colonizing the growing limb bud. In addition to tenocytes, they have been shown to differentiate into chondrocytes, pericytes, muscle-associated and dermal fibroblasts as well as endo- and perineurium. However, no differential function for cells coming from the somites or the LPM has been proposed. Thus, these three studies challenge the textbook view of somite-LPM relationship in limb formation and further raise the question of the lineage relationship of these various cell type in the trunk.

Non-Muscular Dermomyotome Derivatives

Endothelial Cells, Pericytes and Vascular Smooth Muscle Cells Development

During embryonic development, **endothelial cells** (ECs) assemble into a tree-like tubular network of **blood vessels** that eventually permits the transport of fluids, nutrients, circulating cells, hormones and gasses to almost all tissues throughout the vertebrate body. Once mature, the vasculature consists of an elaborate hierarchical system of **arteries**, **arterioles**, **capillaries**, **venules** and **veins** that promotes the circulation of oxygenated blood between the heart, lungs (or gills) and target tissues. All blood vessels are composed of an inner layer of endothelial cells and an immediately adjacent layer of **pericytes**. Pericytes are indispensable for the formation of mature blood vessels, and they also mediate capillary vasoconstriction and secrete specialized extracellular matrices for microvessels. In addition to endothelial and pericytic components, larger blood vessels also possess one or more concentric layers of **vascular smooth muscle cells (vSMCs)** responsible for the vasoconstriction. These two types of cells are often called mural cells. Mural cells endow vessels with viscoelastic and vasomotor properties and assist ECs in acquiring specialized functions in different environments, being therefore responsible for endothelial organ specificity.

Regarding their formation in the embryo, blood vessels can form via two types of mechanisms:
(1) vasculogenesis and **(2) angiogenesis**

(1) The formation of *de novo* blood vessels in the embryo is called **vasculogenesis** and involves the differentiation, migration and coalescence of endothelial progenitors, named **angioblasts**, to form a primordial vascular network (Herbert and Stainier, 2011). Immediately following vasculogenic blood vessel assembly, ECs undergo specification into either **arterial** or **venous** fate in response to a combination of genetic factors and mechanical haemodynamic stimuli. During early embryonic development angioblasts acquire arterial or venous fate and coalesce to form either the **dorsal aorta** or the **cardinal vein**, the two first major embryonic vessels in vertebrate embryo. Aside from this process, angioblasts also aggregate to form blood island, which fuse to form a primitive interlaced network of arterial or venous plexi (Herbert and Stainier, 2011).

(2) In contrast, **angiogenesis** is the proliferation and migration of endothelial cells as **sprouts** from preformed vessels to form new vessels. Following their vasculogenic assembly, angiogenic remodeling of the dorsal aorta, cardinal vein and vascular plexi creates a complex hierarchical network of arteries, arterioles, capillary beds, venules and veins throughout the embryo. This complex network is then completed with the subsequent recruitment of mural cells (pericytes and vSMCs) that stabilize nascent vessel and promotes their maturation. Finally, sprouting of the **lymphatic endothelial cells (LECs)** from venous vessel, a process called **lymphangiogenesis**, complete the scheme by creating a connextion between the lymph and the blood system (Herbert and Stainier, 2011).

Development of Trunk Endothelial Cells

No matter the body location, ECs always derived from **mesodermal structures**. In the trunk, quail-chick chimeras experiment have demonstrated that endothelial cells originate from two different mesodermal lineages : one from the **splanchnopleure** of the lateral plate mesoderm, which give rise to endothelial cell of the **visceral organ**, the other one coming from the **somites**, colonizes the somatopleural mesoderm and gives the vasculature of the **back**, **body wall** and **limbs** (Pardanaud et al., 1996; Wilting et al., 1995). At E3 in the chicken embryo, vessels surrounding the neural tube, intersomitic arteries, cardinal veins, kidney vasculature, body wall and limb bud vessels are somite-derived (Pardanaud et al., 1996; Pouget et al., 2006). Anatomically, grafting of different part of the somite has shown that the **entirety of the epithelial somite can gives rise to ECs** and that the different part of the somite populate the corresponding region of the embryo (Wilting et al., 1995). Angioblasts from the ventral halves of somites preferentially populate ventrolateral vessels such as the cardinal vein and vessels of the mesonephros, while the ones from the dorsomedial somite give rise to vessels of the dermis of the back and those from the dorsolateral somite quadrant mainly form the vessels of the ventrolateral body and limb. Wilting et al. pinpointed that the distribution of the angioblasts from the dorsal part of the somite is remarkably similar to the one of muscle cells (lateral somite forming the vasculature and the hypaxial musculature of the body wall while the medial somite forms the epaxial musculature and axial vasculature). This conjoint development has been particularly studies in the lateral part of the somite, regarding limb vasculature and muscle development (see above). However, a precise developmental roadmap between myogenic and angiogenic progenitors in the trunk remains to be precise, especially considering that both the presumptive territory for the dermomyotome and the sclerotome can give rise to ECs. The only exception to this precise angiogenic blueprint is the **dorsal aorta** that displays a **chimeric** and complementary pattern from lateral and paraxial mesoderm. Around E8 in the mouse, or E1.5 in the chicken, the initial structure of the dorsal aorta is present as **two tubes** extending under the neural tube and notochord, along the anteroposterior axis of the embryo. At this stage, the two aortae **only derived from the splanchnopleure** (Pouget et al., 2006). Fusion of the tubes, in the central region of the trunk, takes place progressively towards the extremities, to give the single midline dorsal aorta.

Immediately before fusion of the two vessels, the two aortae are of chimeric origin, the **roof and sides originate from the somites**, whereas the **floor remains of splanchnopleure origin** (Pouget et al., 2006). Immediately before the fusion of the two primitive aortae, a population of cells derived from the dorsolateral quadrant of the somite colonize their dorsal part to replace the initial roof by **somite-derived ECs**. After that, the cell of the splanchnopleure-derived floor of the aorta start to downregulate endothelial markers and acquires **hematopoietic features**, budding hematopoietic stem cells into the aortic lumen, while at the same time, the somite-derived ECs keeps colonizing the whole aorta. This capacity of ECs to form HSCs conferred the term of **haemogenic endothelium** to the splanchnopleure-derived ECs, while the somite-derived ECs are not haemogenic. At early stage the aorta is therefore composed of splanchnopleure -derived ECs, with haemogenic capacities, while this bipotent capacity fades away quickly with the colonization of somite-derived ECs. However, a recent study demonstrated that, both in mouse and chicken, ECs of the limb, that emanate from the somite, can contribute to the formation of HSPCs during late fetal/young adult stages, breaking the dogma that only the splanchnopleure-derived ECs could contribute to a haemogenic endothelium (Yvernogeau et al., 2019). This study therefore adds a complete array of hematopoietic cell types that derived from the somites.

Development of Limb Endothelial Cells

ECs of the limb derived from the somites (Kardon et al., 2002; Pardanaud et al., 1996; Wilting et al., 1995). Shortly after somite formation, around E2 in the chicken or E9 in mouse, at the level of the limb, the lateral portion of the somites turn on ***Vegfr2*** expression, a marker of angioblasts, and *Vegfr2*$^{+}$ cells start to **migrate distally** to invade the growing limb bud (Nimmagadda et al., 2004; Tozer et al., 2007). This emigration of ECs takes place approximatively 12h before the one of the myoblasts (Tozer et al., 2007; Yvernogeau et al., 2012). As *Vegfr2* is co-expressed with *Pax3* in the lateral part of the somite, it has been proposed that the somite might be the place where **bipotent myogenic-angiogenic** progenitors could exists. Indeed, works on mice from Margaret Buckingham lab showed that a subtitle equilibrium exists in the somite between *Pax3* and another transcription factors, ***Foxc2***. These two genes exhibit a reciprocal inhibition and upon stimulation by **Notch signaling**, *Fox2c* expression increases and downregulates *Pax3*, which *in fine* leads to the activation of *Pecam1*, a marker of ECs (Lagha et al., 2009; Mayeuf-Louchart et al., 2014). Complementary studies using mouse-chick chimeras have clarified the timing of existence of these bipotent progenitors and confirmed that as soon as ECs exists the somites, they completely shut down *Pax3* expression, demonstrating that bipotential progenitors only exist in the dermomyotome, for a short period of time (Yvernogeau et al., 2012). However, how Notch signaling can regulate this cell fate during such a short period of time remains a mystery. Several hypotheses could be inferred, such as the passage of a Notch-ligand^{+} population of cells nearby that would trigger the differentiation of ECs or maybe an intrinsic mechanism whereby cells express a Notch ligand and/or receptor only at a particular moment. At the anatomical level, single somite grafting has revealed two major concepts. First, as for myogenic cells, **somites 16 to 21** contribute to forelimb angiogenic cells in the chicken, and ECs coming from the more anterior somites are found in the most anterior region of the forelimb and *vice versa* for the posterior one (Huang et al., 2003b). However, when analyzing the relative dispersion of ECs regarding myogenic cells, Huang et al. did not find a clear correlation between myogenic and angiogenic cells distribution. For instance, ECs derived from the graft are capable to invade muscle bundles devoid of graft-derived muscle cells, while some muscles composed of grafted cells do not have only endothelial cells derived from the host (Huang et al., 2003b). Even though muscles and vasculature follow the same rule of antero-posterior confinement, these discrepancies are not surprising considering the dramatic different 3D morphogenetic road taken by these two tissues. Moreover, Yvernogeau et al. have shown that when myoblasts start to migrate distally, the angioblasts have already differentiated in the early limb bud to form a vascularized network (around E3 in the chicken), myogenic cells start to organize into bundles several days after (around E7 in the chicken).

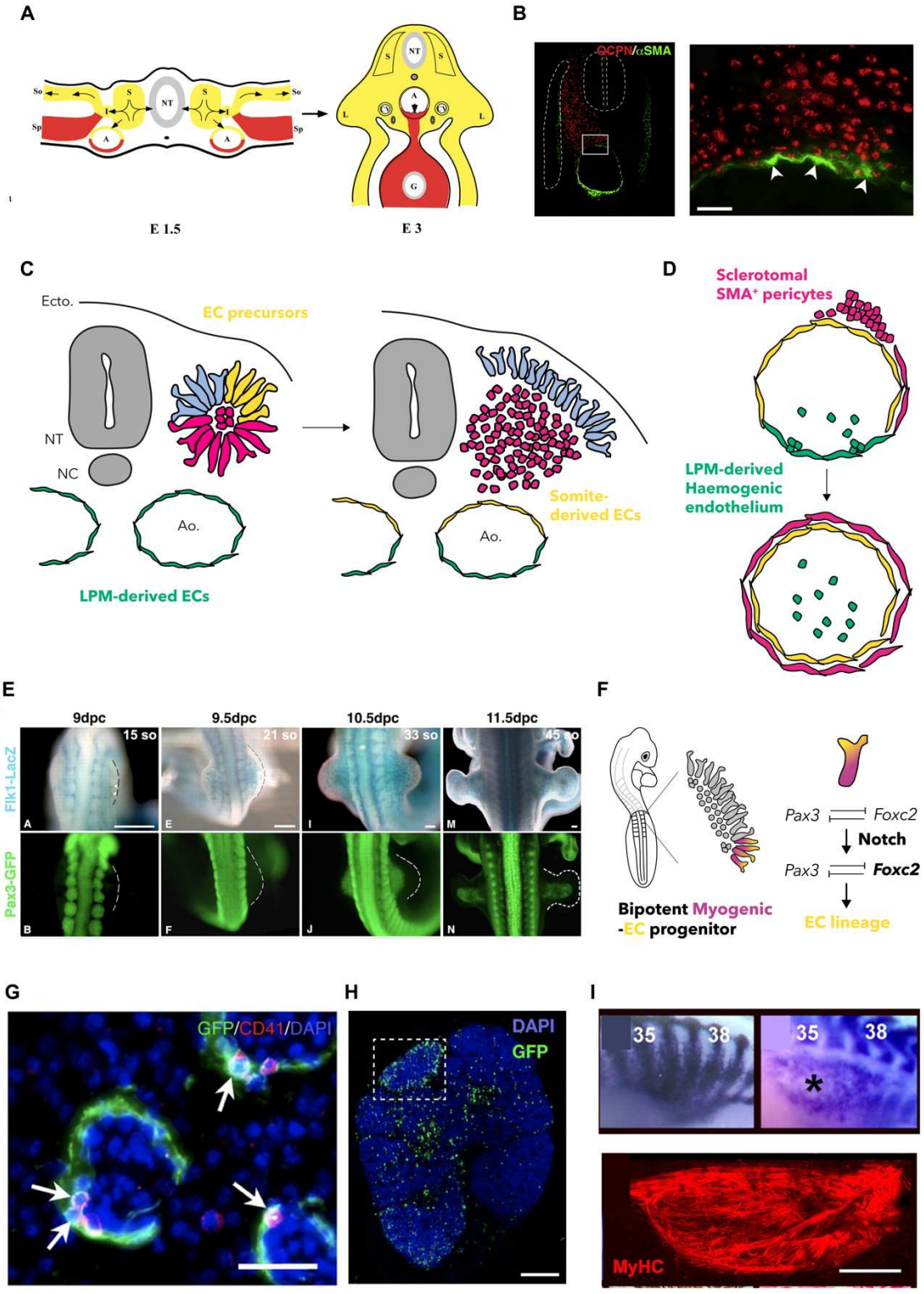

Figure 14. Endothelial lineage from the somites. *(A) Differential contribution of the LPM and somites to ECs of the body. Somite give rise to ECs of somitic and somatopleure-derived tissues while the splanchonopleure generate the ECs associated with the viscera. The dorsal aorta is of mixed origin (from Paradanaud et al., 1996) (B) Quail-chick chimeras showing the contributionof the sclerotome to the SMA⁺ cells of the aorta (C) Dual origin of the dorsal aorta by splanchopleure-derived ECs and somitic-derived ECs. (D) Colonization of the dorsal aorta by sclerotomal-derived SMA⁺ pericytes. (E) Differential colonization of the limb bud by ECs and myogenic precursors showing in mice illustrated by the Flk1-LacZ and the Pax3-eGFP transgenic mice (from Yvernogeau et al., 2012). (F) Bipotent myogenic-EC progenitors cell fate determination in the VLL. (G) eGFP⁺ CD41⁺ hematopoietic stem cells in limb bone marrow following graft of eGFP⁺ paraxial mesoderm in chicken. (H) Colonization of the thymus by paraxial mesoderm-derived cells in the same experiment than (G) (From Yvernogeau et al. 2018). (I) MyoD in situ hybridization of chicken embryo at the level of the 35 somites showing the development of the MyoD⁺ / MyHC⁺ lymph heart from the dermomyotome (From Valasek et al. 2007)*

With such a delay between the formation of these two tissues, and taking into account the extensive growth of the limb bud between this period, it is non-surprising to observe small discrepancies regarding the AP distribution of each somite-derivatives within the limb (Yvernogeau et al., 2012).

Development of vSMCs and Pericytes

Contrary to blood vessels that originate from mesoderm no matter the body location, **pericytes and associated vSMCs can emanate from different tissues according to the body location**. In the forebrain, face, neck and the truncus arteriosus, they derived from the cephalic neural crest cells (Etchevers et al., 2001; Jiang et al., 2000). In the heart region, aside generating cells from the cardiac septum, cardiac neural crest cells also contribute to the vSMCs of the proximal cardiac artery, whereas vSMCs of the coronary veins and arteries originate from the myocardium and epicardium respectively (Bergwerff et al., 1998; Etchevers et al., 2001; Pouget et al., 2008). For the trunk mural cells, quail chick chimeras have shown that the **somites give rise to mural cells of all the back, body wall and limbs**, while the **visceral mural cells**, as for the ECs, **do not come from the somites** (Pouget et al., 2008). Pouget et al. proposed that as somite-derived ECs and mural cell follow the same rule, *i.e.* that they do not migrate into the viscera, viscera-associated mural cells and thus provided by another embryonic tissue, probably the splanchnopleure mesoderm, but this remains to be proved. Moreover, both these authors and Wiegreffe et al. propose a mechanism whereby vSMC of the aorta derived from *Pax1*$^{+}$*/Foxc2*$^{+}$ cells provided by the **sclerotome** (Pouget et al., 2008; Wiegreffe et al., 2007). Opposite works on mice have proposed a dermomyotomal origin for vSMCs of the aorta (Esner et al., 2006). These authors used a Pax3^{eGFP} reporter mice as a specific marker of dermomyotomal cell, however *Pax3* is strongly expressed in the PSM, therefore leading to a labelling of all the somitic sub-compartment. Moreover, they used a retrospective clonal analysis, using a *nlaacZ* reporter gene targeted to the *α-cardiac actin* gene. This system is completely silent, however upon rare intragenic recombination, it can lead to the expression of a functional LacZ gene by a clone. Thus, all the β-gal^{+} cells are supposed to have the same clonal origin. Esner et al. found cells labelled both in the hypaxial domain of the dermomyotome and in the mural cell of the aorta, leading to the conclusion that they share a common dermomyotomal origin. This result could also be attributed to timing problems due to very early recombination events prior to the compartmentalization of the paraxial mesoderm in mice carrying *nlaacZ*-reporter or true differences between birds and mammals. A mouse carrying an allele of *Pax3* or *Pax7* gene driving an inducible CRE recombinase with a gene reporter could solve this question.

Lymphangiogenesis

The **lymphatic system** is a vital component of the circulatory system and plays a crucial role in maintaining fluid homeostasis, lipid absorption and creating a connected network of vessels for immune cells throughout the body. Comprising a vast network of lymphatic vessels, this intricate lymphatic system is a conduit for the transportation of lymph fluid, immune cells, and various macromolecules. Lymphatic vessels are lined with **lymphatic endothelial cells (LECs)**. Lymphatic vessels development involves **lymphangiogenesis** and **lymphvasculogenesis**. Lymphangiogenesis, *i.e.* sprouting from preexisting lymphatic vessels/embryonic veins to form new lymphatic vessels, is the main developmental mechanism underlying the formation and expansion of lymphatic networks in an embryo. The development of the lymphatic vascular system starts considerably later than the blood vascular system. In the chick, the first blood vessels can be seen after 1 day of incubation whereas morphological evidence for LECs is present around E5. In the mouse, blood vessels development starts at E7.5 and the anlagen of the lymphatic vessels can be seen in the jugular region at E9.5 (Wilting et al., 2006). Using quail-chick chimeras, seminal works by Wilting et al. have delineated the embryonic origin of limb LEC to the **somites** (Wilting et al., 2000). For trunks LECs however, the picture seems more complexed. Both mice and chick experiments have shown that **lymphatic vessels of the trunk have a mixed origin** (Stone and Stainier, 2019; Wilting

et al., 2006). For instance, study done in avian embryos proposed that the deep part of the jugular lymph sac seems to be derived from a non-somitic part of the jugular veins whereas the superficial parts develop by integration of lymphangioblasts from the somites (Wilting et al., 2006). The authors suggested that the jugular vein might not be of paraxial mesoderm origin but from cranial mesodermal origin. The issue with these experiments is that they have been performed in the neck region which is a particular developmental junction between the head and trunk. Organs developing in this region often exhibits a complex embryonic origin that might complicate clear conclusion (Heude et al., 2018). Grafting experiment should be performed in other location (*i.e.* in the thoracic region) where it would be easier to draw precise conclusion. Nonetheless, grating of lateral plate mesoderm never labelled LECs in the studied region. A more recent study in mice, using a conditional deletion of ***Prox1***, an essential gene for lymphatic vessel development, into the ***Pax3*** **lineage** a maker of the paraxial mesoderm, demonstrated that the expression of *Prox1* in paraxial mesoderm-derivatives is essential for the development of lymphatic vasculature (Stone and Stainier, 2019). Furthermore, using lineage tracing strategies with the same *Pax3* driver they identified that the paraxial mesoderm gives rise to ECs of the most dorsal part of the cardinal veins, the other part deriving from the splanchnopleure of the lateral plate mesoderm, and that **only these somitic-ECs can transdifferentiate from the cardinal vein to generate LECs of the cardiopulmonary system, liver, meningeal, subcutaneous and dermal lymphatic vessels** (Pardanaud et al., 1996; Rosenquist, 1971; Stone and Stainier, 2019). Finally, using a *Myf5* driver they also demonstrate that some lymphatic vessels of the head seem to share a common origin with muscle of the face. Other body locations, such as the intestine and its associated mesentery harbor lymphatic vessels derived from the haemogenic endothelium, while the second heart field gives rise to LECs of the ventral surface of the heart and the cervicothoracic region of the dermis (see Jafree et al., 2021 for a detailled review). Altogether these data suggest a complex multi-tissular origin for the lymphatic system.

The Lymph Heart

One less known organ of the lymphatic system is the **lymph heart**. Avian embryos have one pair of lymph hearts on either side of the first free tail vertebrae, situated caudally to the pelvic bones. However, in the chick, the lymph hearts are functional only *in ovo*. They return the lymph from the extraembryonic membranes, and they partially degenerate after hatching. In some birds, *e.g.* duck and emu, the lymph assists copulatory organ erection of male adults and lymph hearts function postnatally to return lymph from the lymphatic erectile phallus to the venous system (Valasek et al., 2007). Unlike birds, amphibians have several pairs of lymph hearts along the vertebral column which remain functional into adult life. **Mammals do not have lymph hearts** as their extra-embryonic membranes and placenta are drained by uterine circulation. Propulsion of lymph in adult mammals is achieved by smooth muscles in lymph collectors, contraction of adjacent skeletal muscles and through the action of respiratory pressure changes (Valasek et al., 2007). Around E5 in the chicken, *Prox1*$^{+}$ cell clusters can be detected in the lateral part of the embryo tail (Wilting et al., 2006). By E10 in the chicken embryo, the lymph heart is detectable underneath the skin, as an oblong ***MyoD***$^{+}$ structure ventral to the *m. levator caudae* and posterior to the *m. lateralis caudae*, expanding from the 12th lumbo-sacral to the 3rd coccygeal vertebra (Valasek et al., 2007). Valasek et al. further shown that the embryonic lymph heart originates from the **hypaxial dermomyotome** of somite 34 to 41 in the chicken embryo. Moreover, they say, but did not show, that the E10 lymph heart was positive for transcripts of *Pax7* and *Myf5*, suggesting a mechanism similar to muscle development, where the anlage of a muscle bundle segregates from the others and is fullfill of resident progenitors to allow its growth during later stages. However, contrary to a classical muscle bundle, the lymph heart anlage seems to be also populated by ***Prox1***$^{+}$ **lymphangioblasts** from early stages (Wilting et al., 2006). Indeed, pre-hatching lymph hearts are composed of both **smooth** and **striated muscle cells**, if both cellular types originate from the somites or not, how they are related one to others and how they interact within the lymph heart anlage remains unexplored.

Dermis Development

The vertebrates skin forms an external body envelope that sets the limits between the organism and its external environment. Anatomically, the skin is composed of two main tissues, the **epidermis**, a keratinized epithelium derived from the ectoderm and an **underlying mesenchyme**, the **dermis**, derived from **various embryonic origin according to its anatomical location**. Two main types of dermis are present in birds and mammals at the onset of skin morphogenesis: a superficial dense dermis, (overlying a deep sparse dermis) characteristic of future feather or hair fields, named the **pteryla** in birds, versus a superficial loose dermis in future bare skin regions, named the **apteria** in birds. Cells of the dense superficial dermis form regular pattern of cell condensations which represent the future **dermal papillae**. Those dermal condensations interact with the epidermis to form cutaneous appendages according to the species. Using quail-chick somite transplantations in the 70's, Annick Mauger was able to demonstrate that in the dorsal region, **dermal progenitors emanate from the somite**, while their origins can be traced down to the **lateral plate mesoderm in the ventral domain** (Mauger, 1972). Nearly 30 years after, Olivera-Martinez et al., using the same approach, delineated the origin of back dermis to the medial-most part of the somite (Olivera-Martinez et al., 2000). As said hereinabove, the dermomyotome is separated into three major domains along the medio-lateral axis, the most medial, the **DML**, being characterized by the expression of ***Wnt11*** and the most **lateral one** by ***Sim1*** expression, while the **central dermomyotome** is marked by ***En1***. DML-derived dermal cells are the first to delaminate (around E3 in the chicken) and migrate extensively toward the midline of the embryo (Morosan-Puopolo et al., 2014; Olivera-Martinez et al., 2002). On the contrary *En1*$^{+}$ cells undergo EMT from E4 in chicken / E10.5 in the mouse but do not extensively migrate medially and remain in a latero-dorsal position (Atit et al., 2006; Olivera-Martinez et al., 2002). Interestingly, even though the dense dermis of the back derived only from the medial part of the somite, the *Sim1*$^{+}$ lateral domain is also able to give rise to trunk dermal cells (Olivera-Martinez et al., 2004). These cells form a loose dermis and are located at the frontier between the dorsal and ventral domains. It has been proposed that they will form a narrow skin region that will remain almost apteric in the adult bird. Therefore, only the medial part of the somite seems to be able to generate dense dermis that can formed feathers, while the lateral most part is not able to do it. More lineage tracing of the lateral part of the dermomyotome, for example using long term electroporation of the VLL, coupled with wholemount analysis would be needed to depict the detailed contribution of the lateral dermomyotome to the dermis.

DML-derived Dermis formation

Molecularly **WNT1** protein coming **from the dorsal neural tube** is essential for the expression of *Wnt11* in DML cells. Following neural tube removal, grafts of WNT1-producing cells can restore *Wnt11* expression in DML and normal dermis formation. Nonetheless, even though *Wnt11* is involved in orientation of epaxial myofiber, its rescued expression with WNT1-producting cells is not sufficient to trigger myogenic commitment, while, strikingly, is sufficient to trigger the formation of a dense dorsal dermis (Olivera-Martinez et al., 2004). RNAi-mediated loss of function of *Wnt11,* in the chicken embryos, and examination of *Wnt11*$^{-/-}$ mice embryos have confirmed these results (Morosan-Puopolo et al., 2014; Olivera-Martinez et al., 2004). At around E3 in the chicken embryo, *Wnt11* expression perdures in dermal progenitors migrating toward the midline of the embryo and one day later (E4) its expression is detected in all the sub-ectodermal mesenchyme while it gradually starts to be undetectable in the DML (around E5 in chicken or E11.5 in the mouse). As said hereinabove, *Wnt11* expression in the DML at early stages is dependent on neural tube derived WNT1, but medio-lateral rotation of somites has shown that this expression rapidly become independent from any signal from the neural tube (Olivera-Martinez et al., 2004). It has been shown that WNT1 protein instead of being secreted freely in the mesenchyme between the neural tube and DML, is loaded onto the neural crest cells that, while migrating nearby the DML-cell provide them with WNT1 ligand. DML-cells are therefore exposed to WNT1 protein only during the timeframe of NCC migration and it not surprising that its expression depend on the neural signal only for a short-period of time (Serralbo and Marcelle,

2014). However, a complete framework of both the transcriptional regulation of *Wnt11* itself and its activity on other gene transcription remain missing, especially knowing that *Wnt11* RNAi downregulation trigger a downregulation of *Dermo1* and an upregulation of *Pax3 (Morosan-Puopolo et al., 2014)*. Further investigations are needed to determine which signaling pathway triggers these differential regulations. To date, only one study, traced back the origin of medial dermal cells from the DML using eGFP electroporation, but embryos were analyzed at early stages. It would be interesting to determine to which extend DML-derived dermal cells migrate medially and if some of these cells are capable to cross to midline to invade the other side of the embryos. Moreover, it would be also important to determine to which extent dermal progenitors from a single somite migrate, or not, along the A-P axis of the embryo or if they remain confined to their segment of origin. Finally, the cellular diversity and the differentiation pathway(s) taken by these cells have not been investigated.

Central Dermomyotome-derived Dermis formation

Using both DiI labelling in the chicken and genetic lineage tracing experiment with $En1^{CRE}$; *Rosa-floxed Stop-LacZ* reporter mice, the central dermomyotome has been shown to contribute to the dense dermis of the back (Atit et al., 2006; Olivera-Martinez et al., 2004). Expression pattern of *En1* in the chick suggests that $En1^{+}$ cells do not migrate that far from the central region of the dermomyotome and contribute locally to the dermis of the back (Olivera-Martinez et al., 2002). Genetic studies in mice however have shown that *En1*-derivatives are more widespread than what has been thought by looking at gene expression in the chicken embryo and that they can contribute to dermis on the entire medio-lateral axis of the back (Atit et al., 2006). This might represent a fundamental discrepancy between mammals and birds, or, that the putative map predicted via gene expression in the chicken is obsolete. To clarify the respective medio-lateral contribution of both the DML and the central dermomyotome, lineage tracing experiments should be performed in avian embryos, either with grafting or electroporation technique. If the distribution of dermal derivative from these two domains highly overlapped each other it would therefore suggest that while exhibiting differential expression of *Wnt11* and *En1,* the cells DML and the central dermomyotome, contribute equivalently to the formation of the back dermis. Ablation and cells grafting expression have shown that *En1* expression is also dependent on **SHH** coming from the **floor plate and the notochord**, **WNT1** from the **dorsal neural tube** and **ectodermal WNT6** (Cheng et al., 2004). However, it is not known if a similar mechanism of WNT1-loaded NCC is at the root of this regulation in the central dermomyotome but, conceivable regarding the distant between the two structures and knowing that NCC migrate also dorsally, between the epidermis and the dermomyotome to form melanocytes. On the contrary, the same study has shown that **BMP4** from the lateral plate mesoderm is essential to confined $En1^{+}$ domain to the more medial part of the dermomyotome.

Dermo1/Twist2 Regulation

Dermo1, or often named ***Twist2***, is a **bHLH transcription factor** (Gong and Li, 2002; Li et al., 1995). *Dermo1* expression in the sub-ectodermal mesenchyme is detected from E4 in the chicken and E10.5 in the mouse in a somite-related metameric pattern. Around E7 in the chicken it expression in the skin is strong in the mesenchyme of the nascent feather buds, the dermal papillae, underneath the ectodermal placodes, but weak in interbud skin (Li et al., 1995; Scaal et al., 2001). In the mouse, from E13.5 its expression is also strong in the dermis of the trunk, especially in hair follicles (Li et al., 1995). Molecularly, *Dermo1* function as a **transcriptional repressor** on others myogenic bHLH (*MyoD/Mef2C*), therefore negatively regulating the myogenic program (Gong and Li, 2002). Forced expression of *Dermo1*, via RCAS viruses, in apteric regions of the chicken embryo leads to the formation of dense dermis and formation of feathers (Hornik et al., 2005). Thus, *Dermo1* can be considered as a **master regulator of dermis development**. Nonetheless, little is known about the regulation of *Dermo1* expression, and especially its relationship with *En1* and/or *Wnt11*. In reporter

mice for **TCF/LEF signaling** at E11.5 cells of the sub-ectodermal mesenchyme in the trunk respond to TCF/LEF signaling and gain and loss of function of β-catenin specifically in *En1*$^{+}$ cells, have suggested that TCF/LEF signaling is necessary and sufficient for a proper *Dermo1* expression. However, these experiments have two majors issues: **(1)** the TCF/LEF reporter used is a combination of a minimal promoter with 6 TCF/LEF binding sites controlling the expression of a *LacZ* gene reporter, however, β-galactosidase protein harbor a half-life of nearly 48 hours, therefore it is not clear if the β-gal^{+} cells in the surrounding mesenchyme are actually responding to TCF/LEF signaling or if they have had respond while they were in the dermomyotome/somite (Barzilai-Tutsch et al., 2022; Rios et al., 2010). **(2)** Wnt TCF/LEF signaling is highly involved in PSM specification, somite patterning and epithelial maintenance of the dermomyotome (see sections above), conclusions on a specific role on the dermis lineage might be taken cautiously giving the early activation of the driver used. Moreover, conflicting results have been observed, whether or not TCF/LEF signaling positively regulate axial myogenesis (Atit et al., 2006; Tajbakhsh et al., 1998). Thus, even with genetic tools, it is hard to draw conclusion on the precise role of Wnt/TCF-LEF signaling in this region as it is associated with many early processes (see section above). Using novel transcriptional reporter tools and/or others way to inhibits specifically the TCF/LEF signaling in the dermis lineage might resolved these questions. Aside these works, nearly no other efforts were done to understand the molecular regulation of *Dermo1*/*Twist2*, especially regarding its role on the specification of dermal cells and/or its position in dermal lineage. Recent studies using single-nuclei transcriptomics identified a cluster of cells characterized by *Emx2* expression that express both markers of dermal cell and brown adipocytes precursors. Unfortunately, the focus of the paper was not dermal development *per se* (Jun et al., 2023; Rao et al., 2023). These datasets might represent an unprecedent opportunity to re-investigate the lineage commitment of dermomyotome cells towards dermis.

Dermis and Muscle-Connective Tissue (MCT) Developmental Relationship

Muscles are not only composed of myogenic cell. Several others cell types are found within the muscle mesenchyme including **fibroblast cells** (referred as **muscle-connective tissue, MCT**) and tendon cells. In between the skin (epidermis and dermis) and the muscle bundles there is a tissue called the **hypodermis** that link the whole musculoskeletal system to the skin, and that is not part of the skin *per se*. Inside the muscle bundles, MCT is composed of different fibroblasts layers, the **epimysium**, **perimysium** and **endomysium** that surround individual muscles, muscle fiber bundles and muscle fibers, respectively (Sefton and Kardon, 2019). In the hypaxial-abaxial musculature, both **MCT and tendon found their origin in the lateral plate mesoderm**, while myogenic cells emanate from the somites. A recent work from Hirsinger at al. delineated the molecular hierarchy between all these cells types in the growing limb and established different markers for each one of the MCT population (Hirsinger et al., 2024). In the epaxial region, however, the picture is not that clear. Tendons of the epaxial muscles derived from the a sub-compartment of the sclerotome, the **syndetome** (Brent et al., 2003). While tendon-associated cell (epi- and peritenon) also derived from the syndetome is unknown. As dermis emanate from the dermomyotome it would be tempting to hypothesis that also the hypodermis derived from dermomyotome, however this remain to be tested. Finally, the endo-, peri- and epimysium of the epaxial muscles have not been clearly traced. There is some partial evidence that somite can generate MCT in quail/chick grafting, but as for the hypodermis it would be tempting to hypothesize that they come from the dermomyotome. A recent scRNA studies identified a cluster of *Cdh4*$^{+}$/*Ngfr*$^{+}$ muscle-associated fibroblast developmentally close to *Cdh4*$^{+}$ brown fat precursor (another derivative of dermomyotome, see below) (Jun et al., 2023). However, analysis of *ScxGFP* mice, a marker of the syndetome, has revealed labelling of cells

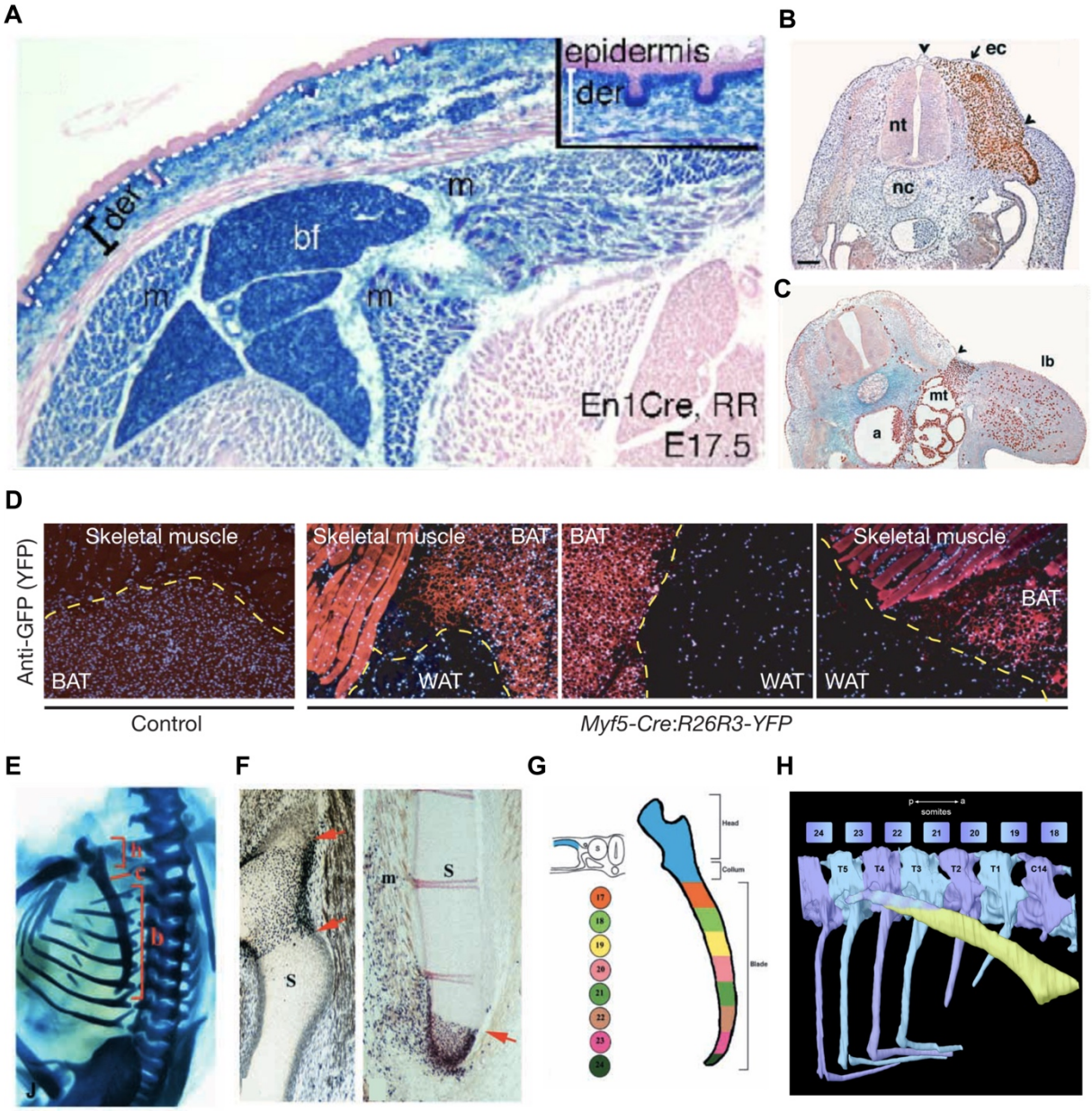

Figure 15. Development of others non-myogenic dermomyotome derivatives. *(A) Lineage tracing of the En1+ central dermomyotome cells in transgenic mice showing the labelling of muscles, brown fat and dermis (from Atit et al. 2006). (B,C) Quail chick chimeras in which either the medial (B) or the lateral (C) part of the somite has been grafted. The medial part form most of the dorsal dermal mesenchyme while the lateral form only a few dermal cells confined to the most ventro-lateral part of the trunk. (D) Lineage tracing of Myf5+ cells in transgenic mice, showing the labelling of both the skeletal muscle and the brown adipose tissue (from Seale et al. 2008). (E) Skeletal preparation of a chicken embryo showing the scapula with the scapula head (h) and the scapula blade (b). (F) Graft of somite 21 and 24, respectively, showing the segmented contribution of a somite to the scapula blade. (G) Model proposed by Huang et al. 2000, for the somite contribution to the scapula blade (E-G from Huang et al. 2000). (H) Model of somitic contribution to the scapula blade proposed by Shearman et al. 2011.*

intertwined with epaxial muscle bundles during fetal development, suggesting a mixed origin for MCT in epaxial muscles (Deries et al., 2010). Nonetheless, the precise nature of these cells remain elusive and could be just *bona fide* tenogenic cells precursors, as epaxial muscles harbor intertwined myogenic and tenogenic cells due to their multiple attachments to the axial skeleton. Further investigations using transplantations and electroporations of chicken somite sub-compartment coupled to mouse transgenic, single-cell technology and fluorescent-RNA in situ would be necessary to infer a precise blueprint of somite-derived fibroblasts and determine which sub-compartment generates which MCTs and tendon-associated fibroblasts.

Adipose Tissue Development

In mammals, two classes of adipocytes co-exist the **white adipose tissue (WAT) and the brown adipose tissue (BAT).** While white adipocytes store and release energy as fatty acids in reaction to systemic needs, brown adipocytes generate **heat** by burning substrates such as fatty acids and glucose in response to various stimuli. This phenomenon is referred to as **adaptive non-shivering thermogenesis**. **The uncoupling protein 1, UCP1**, is specifically expressed in brown adipocytes and is the major component of the BAT thermogenic activity (Wang and Seale, 2016). When activated, UCP1 catalyzes the leak of protons across the mitochondrial membrane, which uncouples oxidative respiration from ATP synthesis. The resulting energy, derived from substrate oxidation, is dissipated as heat. UCP1 expression and a high number of mitochondria can be observed in WAT following cold exposure for instance. These adipocytes are called "**beige**" or "**brite**" (brown-in-white adipocyte) and appear as cluster of UCP1-expressing adipocytes within WAT (Wang et al., 2014; Wang and Seale, 2016). Such properties allow a fine tuning between thermogenesis and energy storage according to environmental and physiological circumstances. As most of the lineage tracing experiment of somite derivatives have been performed in avian embryos with quail-chick chimeras, the mammalian-specificity of brown and beige adipose tissues has rendered their identification dependent on the development of mouse genetics. Using transgenic lines carrying a CRE reporter under the *En1*$^{+}$ or *Pax7*$^{+}$ endogenous promoter, studies from the mid 2000 has narrowed the interscapular and cervical brown fat (**iBAT** and **cBAT**, respectively) origin to **dermomyotome** (Atit et al., 2006; Lepper and Fan, 2010). Moreover, the brown fat and muscle development are even more intermingled as ***Myf5^{CRE}* reporter** label both tissues. However, is it crucial to note that while the *Myf5* reporter (a marker of all the dermomyotome derivatives), and the *Pax3* or *Meox1* reporters (marker of all the somitic derivatives) label the entirety of adipose cells of the iBAT, *En1* and *Pax7* drivers do not (around 50% in the Pax7 reporter) (Sanchez-Gurmaches and Guertin, 2014; Sebo et al., 2018). These lineage tracing experiment therefore suggest a general dermomyotomal origin instead of just being restricted to the central *En1*$^{+}$ domain. Interestingly, several genes that have been identified as necessary for BAT development, ***Ebf2*** and ***Prmd16*** are able to reprogram myogenic cells into brown adipose cells, and conversely their downregulation in adipocytes favors the transcription of muscle specific genes, confirming the tight relationship between these two lineages (Seale et al., 2008; Wang et al., 2014). It is only recently with the apparition of single cell transcriptomics that the full developmental trajectory of the iBAT has been fully elucidated. Patrick Seal's and Olivier Pourquié's laboratories identified ***Gata6* as a marker for adipocytes progenitors** during development (Jun et al., 2023; Rao et al., 2023) . They revealed that pre-adipocytes start to appear around E13.5/E14.5 in mice and are marked by the expression of *Gata6*. Temporally, *Gata6* seems essential to drive the transition of *Ebf2*$^{+}$/*Cdh4*$^{+}$ adipocyte into pre-adipocytes. Interestingly, *Gata6* is also expressed in a population of fibroblasts marked by the expression of ***Dpp4*** and developmentally related to pre-adipocytes. These fibroblasts constitute the **connective tissue** surrounding iBAT lobes.

It is important to emphasis that **BAT origin throughout the body is not homogenous**. While some dorsal deposits are fully derived from the dermomyotome, such as the iBAT, some others are only partially labelled by the *Myf5* or *Pax3* reporter, while some more ventral deposits are completely devoid of cell from the paraxial mesoderm and derived from the LPM (Sanchez-Gurmaches et al., 2016; Sanchez-Gurmaches and Guertin, 2014; Sebo et al., 2018). Furthermore, *Myf5*-lineage cells are also able to generate WAT in some regions of the trunk. LPM, NCC, and cranial mesoderm can also generate BAT, in the ventral region and at the face/neck interface respectively (Fu et al., 2019; Huang et al., 2023; Sebo et al., 2018). Altogether, these studies suggest that the developmental origin of WAT and BAT is quite heterogeneous throughout the body and might have evolved several times in different cell lineages.

Scapula Development

The **scapula**, or **shoulder blade**, is a bone located in the dorsolateral region of the thorax and is a central component of the shoulder girdle. In general, the scapula has a **triangular shape** and consists medially of a large, flat, thin plane known as the **blade**, which is divided dorsally into the supraspinatus and infraspinatus fossae by a bony spine. More laterally are found the acromion and coracoid process along the glenoid fossa and altogether they from the **scapula head and neck** (Young et al., 2019). In human the **humerus** inserts into the glenoid process of the scapula and forms the glenohumeral joint while the acromioclavicular joint articulates the acromion process of the scapula with the **clavicle** (Schünke et al., 2021). However, the scapula connects the axial skeleton only through muscle connections. The *m. rhomboideus* and the *m. levator scapulae* link the scapula to the **axial skeleton**, the *m. serratus anterior* and *m. pectoralis minor* to the **ribs** and the *mm. deltoid*, *coracobrachialis*, *infraspinatus*, *supraspinatus*, *teres major* and *minor* and the long portion of the *m. triceps brachii*, to the **humerus** (Schünke et al., 2021). Being at the interplay between trunk and limb elements the scapula has therefore a particular role and has been considered by certain authors to act like a bug **sesamoid bone** connecting the LPM-derived forelimb with the somitic axial structures. Scapula morphology varies a lot among tetrapods, essentially according to their locomotion mode. If in humans it has a triangular shape, chicken scapula, for instance, exhibits a narrower, blade-like posterior region that extends caudally. As described above, the axial skeleton is derived from the somite whereas the appendicular skeleton emanates from the somatopleura of the lateral plate mesoderm. The scapula being at the interplay between these two systems, its embryonic origin has always been debated. In a pioneer work from the mid 70's, Alain Chevallier mapped the origin of the scapula anlage to the somite and not from the somatopleure (Chevallier, 1977). However, at the beginning of the century, Huang et al. refined this discovery by finding that only the most posterior part of the scapula, the **scapula blade**, is in fact derived from the **somite** (Ruijin Huang et al., 2000a). The most anterior part, the scapula head and neck, being derived from the **somatopleura**. Moreover, by using grafting of somite sub-compartments they demonstrated that the **dermomyotome** was the only source of ossifying cells for the scapula blade. With single somite grafting they map the final position of cell derived from a defined somite into the scapula blade. This last experiment shown that each somite contributes to a specific part of the scapula blade corresponding to their original position along the antero-posterior axis. These results were confirmed in mice using a *Pax3* reporter, however, these results would need to be re-examined using dermomyotome-specific drivers as *Pax3* is expressed in all the PSM and in neural crest cells precursors (Valasek et al., 2010). Recently, using 3D reconstruction of serial sections, Shearman et al. refined those results by demonstrating that most of the chicken scapula is derived from the LPM and that only approximatively one third of the most distal part of the scapula blade was somite-derived (Shearman et al., 2011). This dual origin can be associated with the **primaxial/abaxial** concept, where the **lateral somitic frontier** separates the scapula blade at its two third. Nonetheless, the chondrogenic capacity of the dermomyotome is still not fully understood. Following its first study, Ruijin Huang laboratory demonstrated that the all dermomyotome was competent to contribute to the scapula blade, however, once the dermomyotome has undergone its EMT, only the hypaxial domain can be chondrogenic (B. Wang et al., 2010). This competence seems to be under the control of local ectodermal tissue and BMP4 from the LPM (Ehehalt et al., 2004; Wang et al., 2005). Again, a clear developmental trajectory for these dermomyotomal-derived chondrocytes remains to be investigated.

Late Muscle Development and Patterning

Muscle Anatomy and Evolution

Muscles account for approximatively for **30 to 50% of all vertebrate body mass** (Romer and Parsons, 1986). They support many critical functions such as locomotion, feeding, breathing, communication or postural support. Polynucleated myofibers generated during development are arranged at the macroscopic scales in different **muscle bundles** (also called fascicles) that are enveloped into a sheet of connective tissue called a **perimysium**. Each one of these muscle bundles have its own innervation, originate and insert at stereotypical sites in all the individual of the same species. The patterning of these different muscles is established during late embryonic/early fetal development in amniotes. In this section I will briefly overview the evolution of the muscle morphology in the vertebrate phylogenic tree, and especially the amniotes, and by emphasizing on the epaxial/hypaxial - primaxial/abaxial concepts especially regarding the various origin of muscles of the body and their MCTs. Then I will describe the morphogenetics mechanisms regulating the spatial arrangement of muscle bundles. I will also discuss the anatomical and molecular basis of the current view of the concept of primary and secondary myogenesis.

Evolutionary Context of the Epaxial/Hypaxial Concept

As aforementioned, the main anatomical differences in vertebrates can be traced back to the epaxial / hypaxial distinction. One of the most basal representant of **chordates**, the **cephalochordate amphioxus**, relies on side-to-side undulation to move in the water, this movement is also found in most of aquatic and semi-aquatic vertebrates (Romer and Parsons, 1986). This primitive mode of locomotion is presumed to be the ancestral type of movements of the last common ancestor of all chordates. In amphioxus these side-to-side undulations are assured by segmented structures along the AP axis, called the **myomeres**. The myomeres are separated by collagenous **myosepta** that are laterally continuous with the sub-epidermal collagen layer and medially to the collagenous layers ensheathing the axially located notochord and nerve cord (Mansfield et al., 2015; Romer and Parsons, 1986). Successive contraction of opposite myomeres contract sequentially the body wall and, as the generated force is transmitted to the notochord via axial connective tissues, allow undulatory movements of swimming. In cephalochordates the myomeres are present all along the axis of the body (Mansfield et al., 2015; Romer and Parsons, 1986). One myomere basically represents the derivatives of one somite that has kept their metamerism. The paraphyletic group of **Agnatans**, lampreys and hagfish, is the most basal group to exhibit a distinction between the epaxial and hypaxial musculature. Lamprey axial musculature is also organized in chevron-shaped myomeres and but exhibit a differential innervation regarding their dorso-ventral organization (Fetcho, 1987). As mentioned above, the hypaxial musculature of tetrapods comprised the body wall, limb, and hypoglossal (or hypobranchial in aquatic species) musculature. As lampreys and hagfishes do not possess any pectoral or pelvic fins and their “body wall” musculature resemble the epaxial one. Nonetheless, molecular markers of the hypaxial domain are already expressed in the ventrolateral region of the myotome and, at the level of the head, ***Lbx1*$^{+}$** muscle progenitors contribute to the formation of the hypoglossal musculature (Kusakabe et al., 2011). In gnathostomes, the functional separation of epaxial and hypaxial muscles became more obvious with the appearance of a **horizontal septum** of connective tissue between these two muscle groups. The apparition of a clear boundary between hypaxial and epaxial muscles coincides also with the development of paired

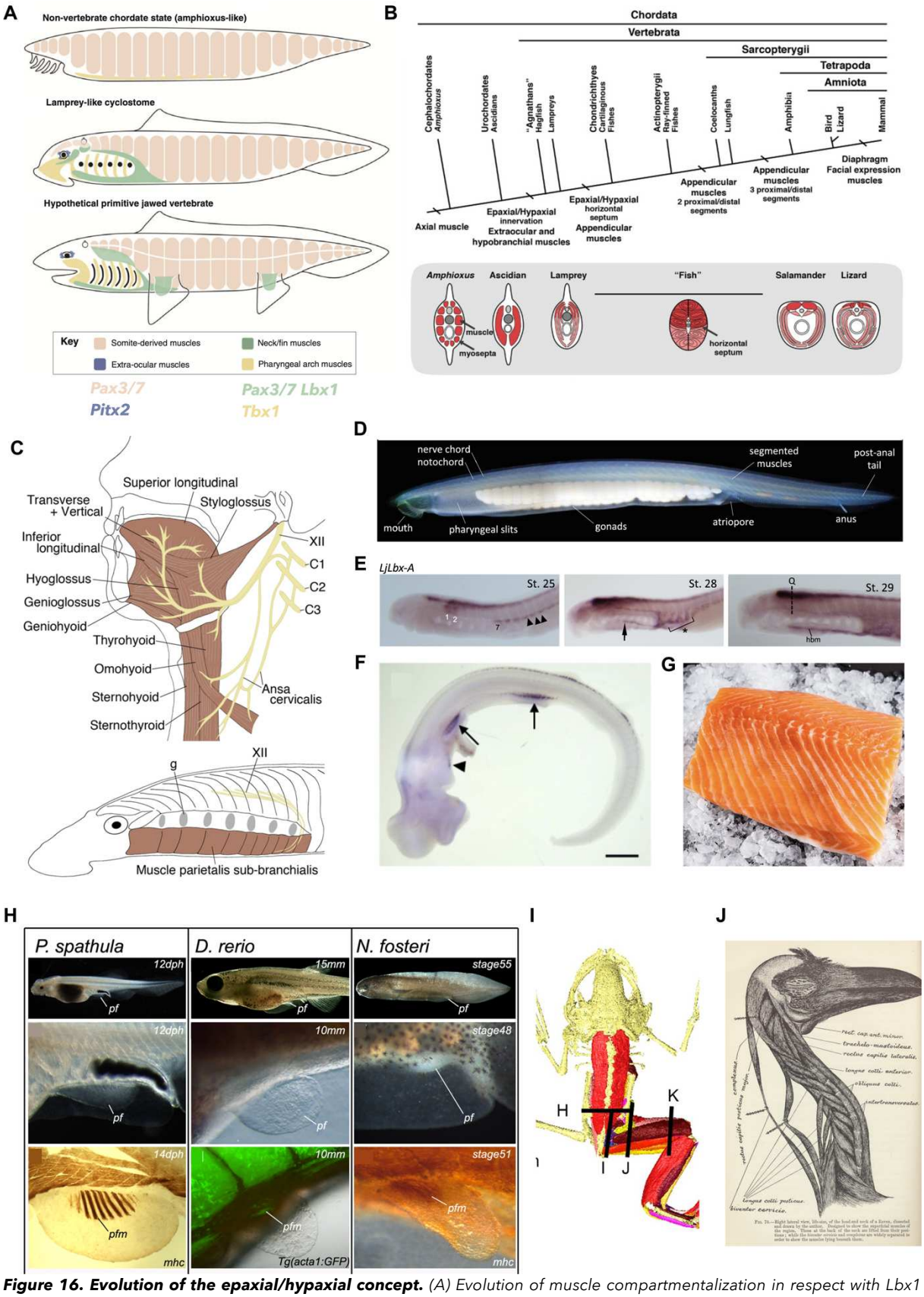

Figure 16. Evolution of the epaxial/hypaxial concept. *(A) Evolution of muscle compartmentalization in respect with Lbx1 expression (from Sambasivan et al., 2011). (B) Phylogentic tree depicting the principal muscular innovation during chordates evolution (From Sefton et al. 2019). (C) Hypoglossal / hypobranchial muscle anatomy and homology between human and lamprey (Kusakabe et al. 2020). (D) Anatomy of amphioxus, a cephalochordate, showing the segmented myomeres. (E) Expression of the lamprey homologue of Lbx1, expressed in the lateral most part of the dermomyotome (arrowheads) and in migratory muscle progenitors (arrow) forming the hypobranchial musculature (Kusakabe et al. 2011). (F) Expression of Lbx1 in*

shark embryos, the arrow indicated the fin buds while the arrowhead indicates the migrating hypobranchial muscle progenitors (Kusakabe et al. 2020). (G) A filet of salmon showing the metamerism of all the axial musculatures, each myomeres (orange) being separated by the next one by a myoseptum (white). (H) Colonization of the fin bud by myogenic cells in sharks (P. spathula), an actinopetrygians fish (D. rerio) or a sarcopterygians fish (N. fosteri) (from Cole et al. 2011). (I) Apparent non-metameric longissimus dorsi in an amphibian (Porro et al 2017). (J) Unmetamerized muscles in the neck of a raven (from Shufeldt, 1890).

pectoral and pelvic appendages (Romer and Parsons, 1986). Moreover, ***En1*** is expressed is the center of the developing muscle blocks in all gnathostomes, demarcates the site of the future epaxial-hypaxial demarcation and is essential to drive the differential innervation of these two compartments (Ahmed et al., 2017). In amniotes, at the level of limbs and in the occipital/neck region, the lateral part of the dermomyotome delaminates to generate fully **migratory muscle progenitors (MMPs)**, while at the interlimb levels, the lateral dermomyotome extend laterally by keeping its epithelial structure (Khabyuk et al., 2022; Pu et al., 2013). It was thought that the same kind of mechanisms of **lateral extension** of the lateral dermomyotome was used by the most basal gnathostomes to populate the fin with muscle progenitors. However, recent analyses in shark embryos demonstrated that hypobranchial and fin muscles are formed by a dermomyotomal ***Lbx1*$^+$** population that de-epithelializes, accumulates shortly after the de-epithelialization and finally invades the pectoral fin bud as compact cell aggregates to form the muscle of the fin (Okamoto et al., 2017). In amniotes however, the muscle progenitors completely delaminate and move freely within the somatopleura-derived mesenchyme, even though the A-P identity is somehow kept (see below). Interestingly, sarcopterygian fishes exhibit an **hybrid process** with first the detachment of an epithelial mass from the dermomyotome that, buds individual progenitors into the limb bud (Hirasawa and Kuratani, 2018). Even though the hypaxial domain of teleost fishes gives rise to various shape of muscle at the occipital and fin level, the inter-fins hypaxial domain and the epaxial domain all along the AP axis, remain segmented as myomeres, as in amphioxus. This organization is described as conserved in Lissamphibia where the epaxial musculature is formed by a succession of small muscle units named the ***muscle truncii*** *(Romer and Parsons, 1986)* . Nonetheless, no specific regionalization is observed along the AP axis. However, most of the anatomical description available are done on the axolotls, which in neotenic and therefore might have kept some juvenile features. Besides, some authors have proposed that anurans managed to break this metamerism in their epaxial musculature by forming two long muscle bundles on each side of the spinal cord, named ***mm. longissimus dorsi*** (Collings and Richards, 2019). In amniotes the complexification of epaxial musculature becomes more evident and epaxial muscles **do not remain metameric**. Laterally, a thin sheet of muscle, the ***m. iliocostalis***, extend downward on the flank, external to the ventral muscles and attached laterally to the ribs. A long muscle, the ***m. longissimus dorsi***, lies above the transverse processes of the vertebrae and the most medial muscle group composed of several small muscles is often referred as ***m. transversospinalis***. These three muscles groups are in fact composed of a plethora of muscle bundles tightly associated with multiple attachment point and represent an hypothetical nomenclature which of course exhibit a lot of variation according to the amniote subgroup (Romer and Parsons, 1986; Schünke et al., 2021).

Limb Muscles

Limb Muscle Anatomy

With the apparition and evolution of the paired fins into limbs, the muscular pattern of vertebrate appendages has undergone a lot of complexifications. Fin musculatures exhibit a simple organization where **two opposed little masses of muscles** are usually discernable. The dorsal muscle mass serves primarily to elevate or extend the fin, while the ventral one to depress of adduct it. In teleosts, the muscle architecture is kept simple but can be constituted of several muscle bundles connecting the pectoral girdle to bony rays, such as in the perch (Winterbottom, 1973). Some teleosts harbor a more complex anatomy with a more distinct proximal and distal part, such as in the mudskippers fish that is able to live temporally in open air on the ground (Winterbottom, 1973). This

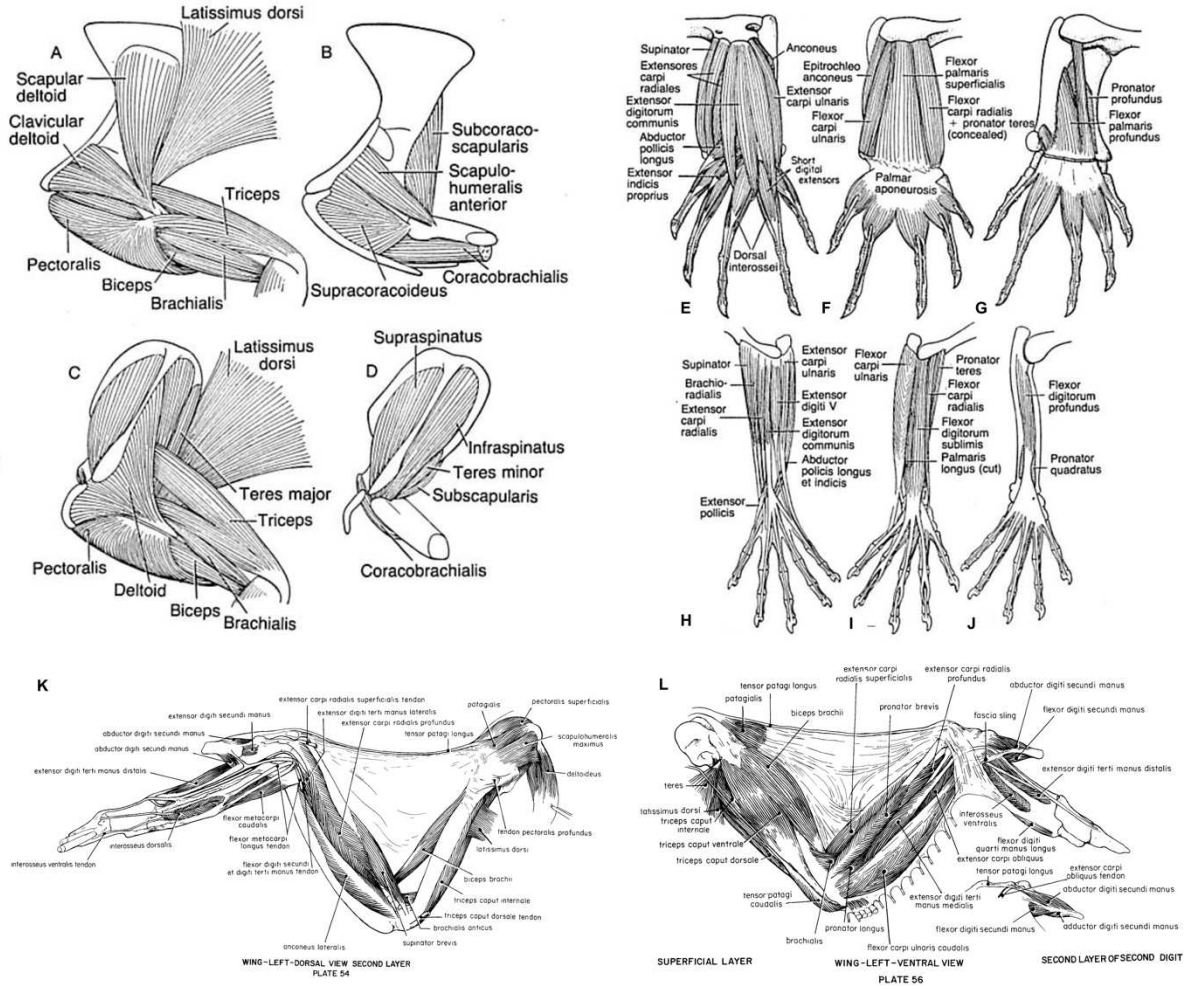

Figure 17. Comparative anatomy of the amniote forelimb. *(A,B) Shoulder and upper arm muscle in the lizard. (C,D) Shoulder and upper arm muscles in the opossum. (E-G) Muscles of the forearm and hand in the lizard. (H-J) Muscle of the forearm and hand in the opossum. (E) and (H) are views of the extensor surface, (F) and (I) are superficial and deeper, (G) and (J) dissections of the flexor aspect. (K,L) Muscles of a turkey wing, dorsal view (K) and ventral view (L).*

proximo-distal separation is even more evident in sarcopterygians fishes such as in lungfish where the distal and proximal part form two distinct units that can be link to homologous muscle bundles in tetrapods (Diogo et al., 2016). The transition from water-to-land was accompanied by a dramatic increase in the number of appendicular muscle bundles, not only the complexity of the most proximal bundles increases but the apparition of the wrist, and more generally the autopod, have led to a new array of distal muscles. The general blueprint in most tetrapods is therefore organized into four different muscles units, **autopodial**, **zeugopodial**, **stylopodial** and several muscles at the junction between the limb and the axial structures, that composed the **pectoral** or **pelvic girdle**. Several dorsal muscles attach to the humerus near its head and are responsible for much of the movement of that bone. Superficially, most of tetrapods exhibit a fan shaped dorsal muscles, the ***m. latissimus dorsi***, connecting the humerus with the axial skeleton and the **m. *deltoideus***, often in two parts, connecting the humerus with the clavicle and the scapula. In mammals and birds, the *m. latissimus dorsi* is split in other muscles bundles, known as the ***m. teres major*** and ***m. subscapularis***. In reptiles a small deep muscle arises from the outer surface of the scapula, the ***m. scapulo humeralis anterior***, which is homolog to the ***m. teres minor*** of mammals. Finally, reptiles possess another muscle, the ***m. supracoracoideus***, linking the humerus to the scapula, that have been moved upward in mammals and now form the ***m. supra- and infraspinatus***. The dorsal surface of the humerus is

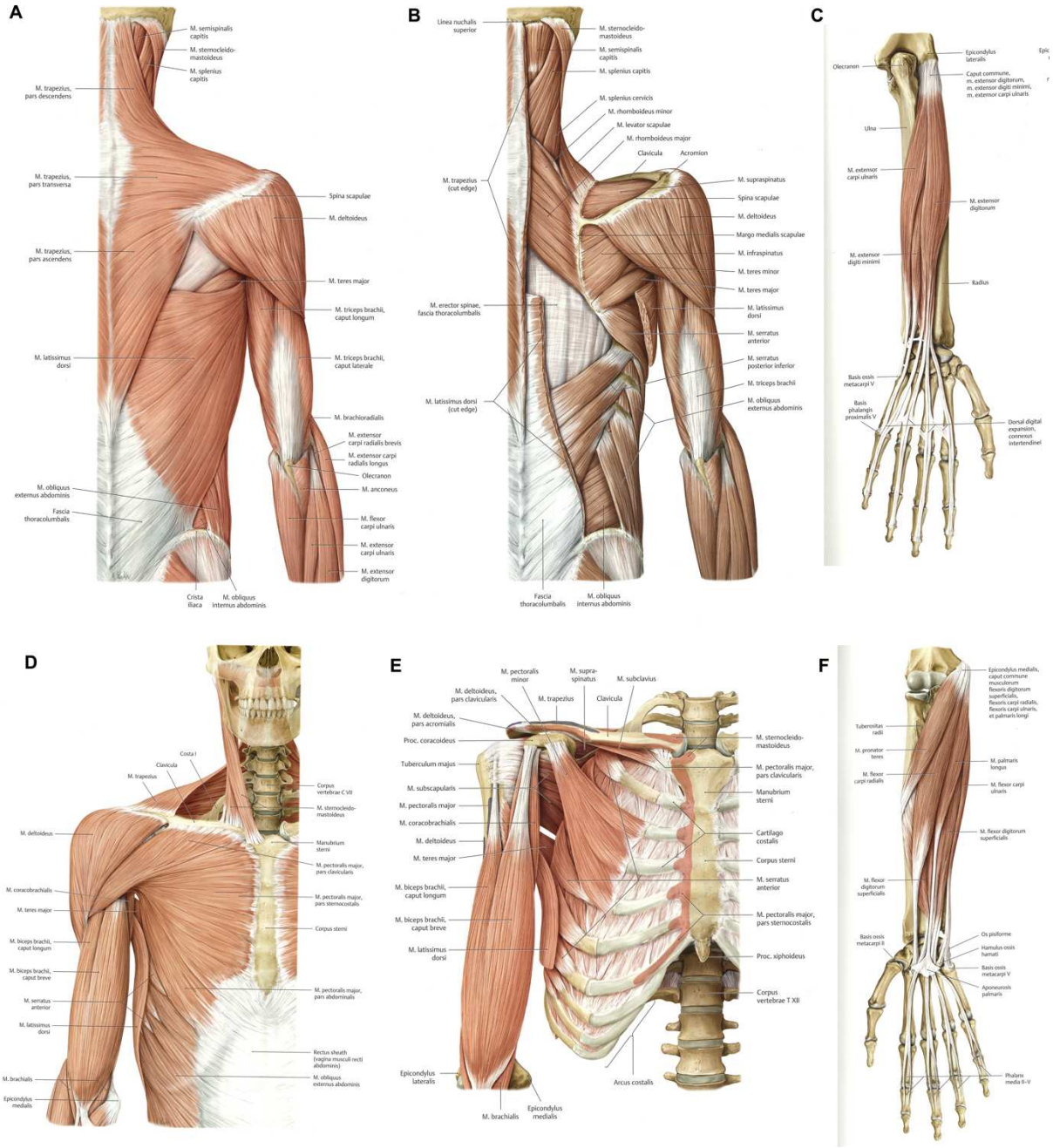

Figure 18. Human limb and pectoral girdle anatomy. *(A,B) Dorsal view of the pectoral girdle anatomy, first layer (A), second layer (B). (C) Anatomy of the dorsal portion of the forearm. (D,E) Ventral view of the pectoral girdle anatomy, first layer (A), second layer (B). (F) Anatomy of the ventral portion of the forearm. (From Schuenke et al., 2021)*

covered by the ***m. triceps brachii***, which arises from the humerus and the scapula and attachs distally to the ulna. On the ventral side of the shoulder, the most important muscle in size is the ***m. pectoralis*** that spread far back over the sternum and ribs and inserts onto the humerus and clavicle. The coracobrachialis attaches the humerus to the scapula. Besides, two main muscle groups are responsible for the flexion of the forearm, the ***m. biceps brachii***, and the ***m. brachialis*** that connect the scapula to the radius and the ulna, respectively. These muscles are present in a similar fashion in most of the tetrapods. Muscles of the zeugopod (forearm) and autopod (hand) are usually divided into two main categories, **extensor** and **flexor**. In reptiles, extensor and flexor muscles are found at both the zeugopodial and autopodial levels, while in mammals the dorsal part of the autopod is devoid of muscle, the extension of autopodial bones is therefore executed by tendon originated

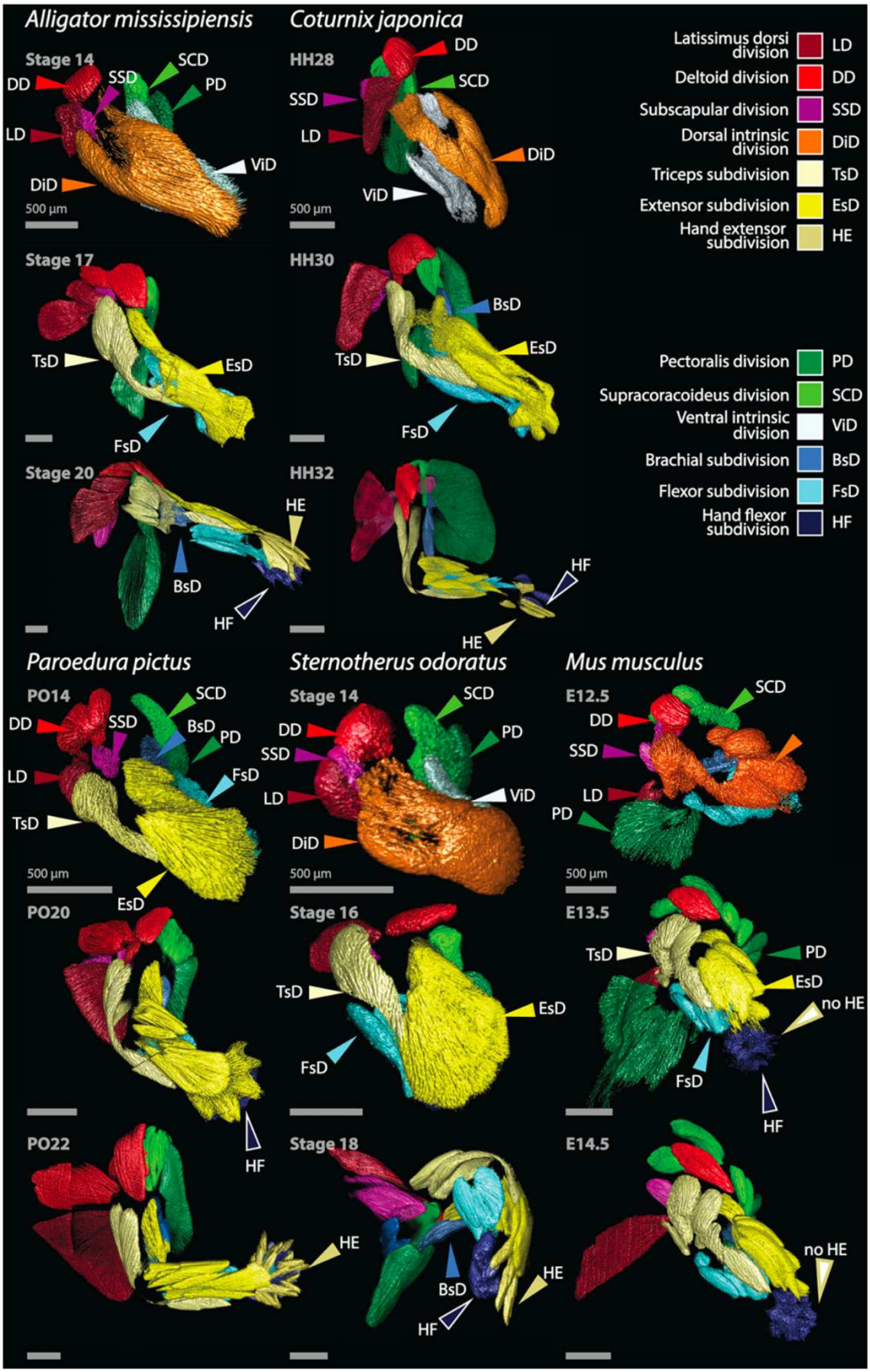

Figure 19. Stereotypical early cleavage pattern of the forelimb musculature in amniote embryos. *In all species studied, the Dorsal and Ventral muscle masses cleave into the same distinct anatomical units, originating the individual muscles of the arm. The only exception to this sequence and arrangement of divisions seems to be the failure to develop of the Hand extensor subdivision (HE) in therian mammals (only the mouse is shown). (From Smith-Paredes et al., 2022). Alligator mississipiensis: alligator ; Coturnix japonica: quail ; Paroedura pictus: gecko ; Sternotherus odoratus: turtle ; Mus musculus: mouse.*

from extensor of the forearm. The muscle anatomy of the tetrapod hindlimb is based on the same principle but will not be described here. As said above, even if limbs have adopted specialized structures in different tetrapod clades, the overall blueprint remains the same, especially during development. Smith-Paredes et al. have analyzed the muscle limb bud development of birds, crocodilians, lizards, chelonian and mammals embryos and concluded that **the splitting of muscles during embryonic development in tetrapod relies on the same pattern** (Smith-Paredes et al., 2022). The derivatives anatomy of bird forelimb results from slight early topological modifications that are exaggerated during late ontogeny and mammals, while conservative in their cleavage pattern, differ drastically from the ancestral amniote musculoskeletal organization at later stages, especially regarding the dorsal autopodial musculature.

Genetics of Limb Muscle Patterning

In tetrapods the anterior and posterior appendages, named the **forelimb** and **hindlimb**, respectively, exhibit different organization regarding the musculoskeletal system, one of the best examples being the specialized forelimb of birds for flight. Early specification of forelimb and hindlimb identity begins in the limb fields prior to the limb bud formation. Even if the position of limb along the AP axis varies in different species, their position is constant with respect of the *Hox* code. For instance, the pectoral fins / forelimbs are found at the most anterior expression region of ***Hoxc6***, the position of the first thoracic vertebra. ***Tbx5*** is transcribed in limb field of the forelimb, while ***Islet1***, ***Tbx4*** and ***Pitx1*** are expressed in the presumptive hindlimbs (Gilbert, 2014). Downstream of the regulatory function of these transcription factors is ***Fgf10***, the primary inducer for limb bud formation (Gilbert, 2014). If induced in the flank of the embryo, depending on the region of expression of *Tbx5* and *Tbx4*, the ectopically induced limb bud will adopt a forelimb or hindlimb identity. However, when induced at the junction of the two domains, the most anterior part of the limb will have a forelimb identity while the most posterior part will have a hindlimb identity (Gilbert, 2014). Nonetheless, how these genes are able to induce one or the other identity is not understood. Even though the axial determination of the limb bud is set early; somites have shown to be quite plastic regarding their contribution to the limb. Swapping of the orientation of limb PSM or heterotopic grafting of neck or flank PSM into limb territory paraxial mesoderm have shown that any myoblasts can penetrate the forelimb mesenchyme when placed at the corresponding level (Alvares et al., 2003; Lance-Jones, 1988a). This result is in sharp contrast with what have been found regarding the regional identity of axial sclerotomal structure, where the axial identity is determined before the formation of somite, as a heterotopic graft of thoracic PSM into the cervical level lead to the formation of ectopic ribs in the neck (Kieny et al., 1972). This capacity of forming limb muscle is based upon the competency of a somite to activate *Lbx1*. As said hereinabove, the activation of *Lbx1* depends on both extrinsic signal from the LPM and intrinsic cues, the *Hox* code. However, the limb mesenchyme, thanks to a strong presence of FGF signaling, can induce *Lbx1* in flank somites that are normally not able to produce MMPs (Alvares et al., 2003)

Using single somite transplantation, Beresford precisely determine that the **somite 16 to 21** in the chicken were contributing to the forelimb while Cynthia Lance-Jones mapped the origin of hindlimb muscles to the **somite 26 to 33** (Beresford, 1983; Lance-Jones, 1988b). Regarding the AP contribution of single somite to various limb muscles, both in the forelimb and in the hindlimb, each somite contributes to the corresponding muscle bundles along the AP axis and only the more central somites (18-19 for the forelimb and 27-31 in the hindlimb) contribute to all the muscles along the proximo distal axis, the most anterior and posterior somites were limitated only to the more proximal muscles (Rees et al., 2003; Zhi et al., 1996). Moreover, no perfect matches were found between a particular somite and a particular muscle. Migrating limb myoblasts mix along the AP axis, **one somite can contribute to several muscle bundles and conversely, one muscle bundles can be formed by myoblasts from several somites**. Thus, migratory limb myoblasts seem quite plastic

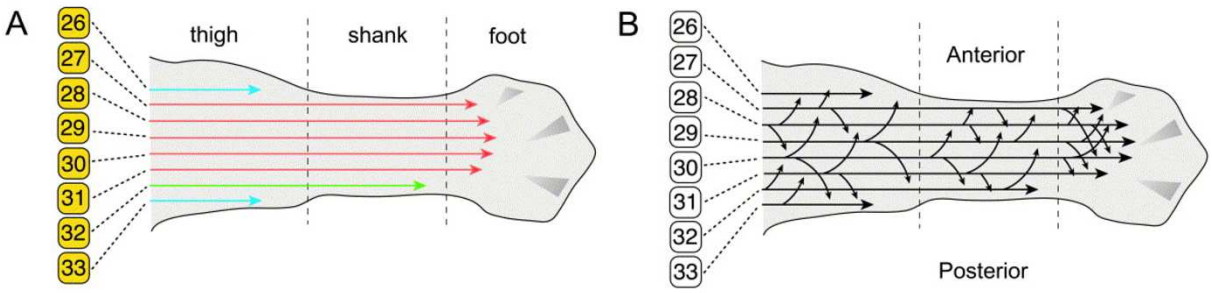

Figure 20. Contribution of individual somites to the forelimb musculature. *(A) Progenitor emanating from the somites 26 to 33 colonize the growing limb bud. Only the most central somites contribute to all the muscle bundles along the proximo-distal axis of the limb. The most anterior and posterior somites being restricted to the most proximal limb muscle bundles. (B) Muscle progenitors mix along the AP axis of the limb with the most distal part being where muscle progenitors intertwined the most (from Rees et al. 2003).*

regarding the late muscle patterning, a characteristic that has been probably in favor of a great diversification and complexification of limb musculature. As aforementioned, while conserving the early cleavage pattern of muscle mass during early development, the mammalian limb musculature exhibits some derivative characteristic, such as the complete absence of dorsal muscle in the autopod and most distal part of the zeugopod (Romer and Parsons, 1986). Indeed, around E14.5 in mouse, development the ***m. flexor digitorum*** are positioned as *bona fide* muscle bundles within the dorsal part of the autopod, while later during prenatal stages, it is relocalized to the zeugopod via **tendon anchorage and muscle contraction** (Huang et al., 2013). More generally, the tendons/tenogenic cell does not seems to be required for the early patterning of the forelimb muscle, however, mice in which the *Scx*$^{+}$ lineage has been depleted exhibit several defects of late muscle patterning and attachments, demonstrating that the **interaction between the tenogenic and myogenic compartment** is essential to correctly shape the 3D architecture of the adult limb musculature (Ono et al., 2023). In addition, during the last decades, more and more evidence has emerged that non-myogenic cell have an important role on the muscle patterning, even at early stages, to instruct a correct muscle splitting. These non-myogenic cells have been regrouped under the term of **muscle-connective tissue (MCTs)**. They mainly originate from the LPM and composed around 90% of all the cells during early stage of limb development (Esteves De Lima et al., 2021a). Early experiment in chick demonstrated that **MCT form a muscle-like pattern even in the absence of myogenic cell** and even that they can organize non-muscle cells to form muscle-like structures (Grim and Wachtler, 1991; Jacob and Christ, 1980). Replacement of hindlimb LPM by flank LPM causes the development of flank muscles, these results with the others heterotopic experiments described above, demonstrated that **the formation and patterning of limb musculature is quite plastic and is mainly under the influence of the somatopleura** (Alvares et al., 2003; Jacob and Christ, 1980). ***Tcf4*** was identified as specifically expressed in MCT of the limb in a muscle pattern, but not into myogenic cells, and viral infection of *Tcf4* in in chick limb non-muscle mesoderm led to induction of ectopic muscle while disruption of *Tcf4* led to muscle mis-patterning (Kardon et al., 2003). Others transcription factors are expressed in MCTs and/or more generally in non-myogenic cells of the limb bud (bones, synovial joint, tendons) and are involved in muscle patterning, such as ***Tbx3***, ***Tbx4/Tbx5***, the Odd skipped-related 1, ***Osr1***, and members of the Hox family, ***Hoxa11*** and ***Hoxd11*** (Sefton and Kardon, 2019). Genetic deletion of *Tbx4* and *Tbx5* induce a mis-patterning of hindlimb and forelimb muscles and tendons, respectively, without disrupting skeletal development (Hasson et al., 2010). During development, *Hoxa11* is expressed is MCTs, tendons and perichondrium (fibrous connective tissue of the cartilage) but not in mature myofibers, chondrocytes and osteoblasts. Both tendons and muscle patterning are disrupted in *Hoxa11/Hoxd11* double mutants (Swinehart et al., 2013). However, *Hoxa11* is expressed at early stages within migrating muscle progenitors (around E4.5 in chicken and E10.5 in mice) and have been shown to regulate their proximo-distal migration, therefore, the effects observed in the double *Hoxa11/Hoxd11* mutant

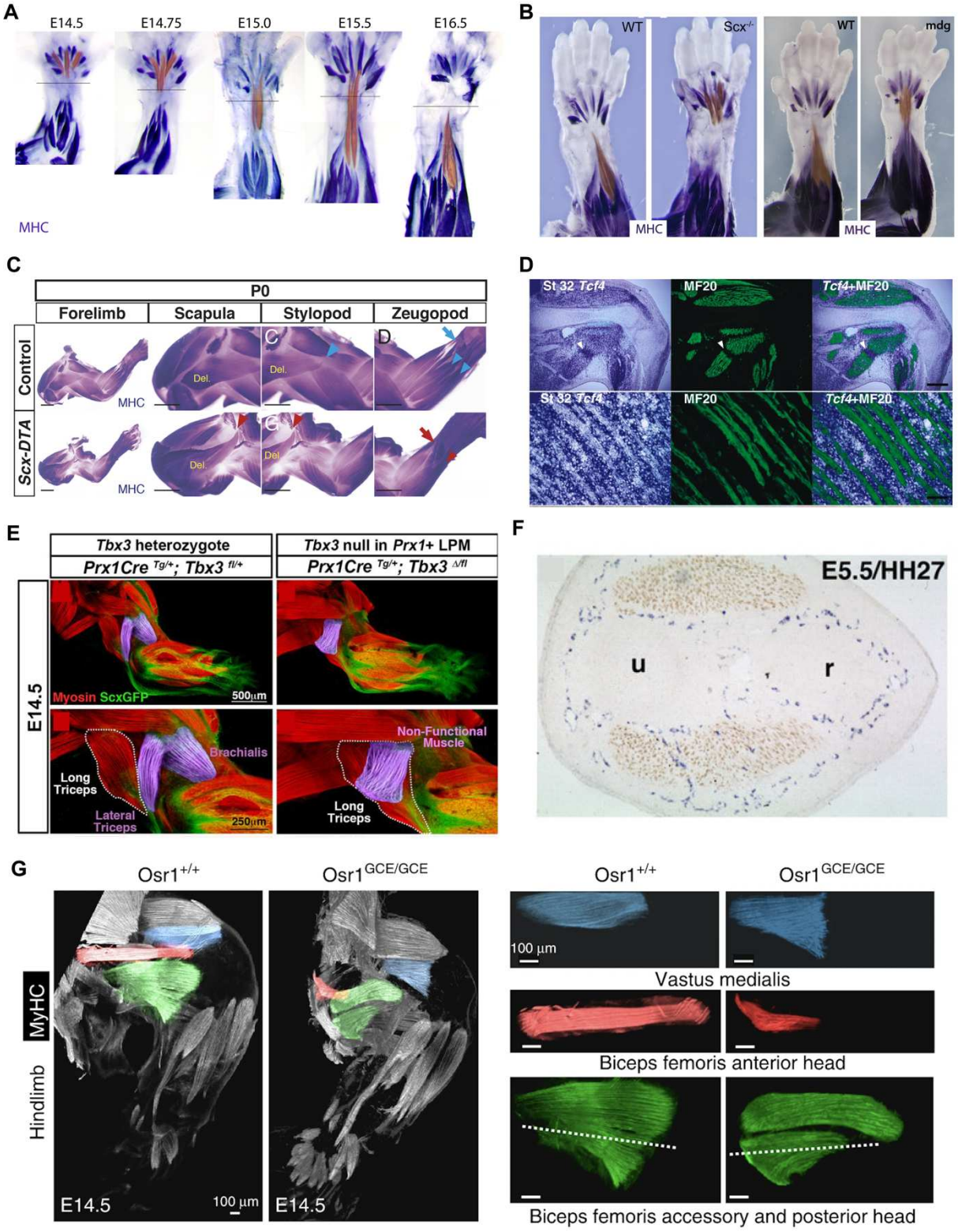

Figure 21. Regulation of muscle limb patterning by muscle-connective tissue. *(A) Reposition of the m. flexor digitorum in the hindlimb of the mouse. (B) m. flexor digitorum repositioning is dependent on the tendon and muscle contraction (A-B, from Huang et al., 2013). (C) Deletion of the Scx lineage causes several defects in stylopod and zeugopod forelimb muscles (from Ono et al. 2023). (D) Expression of Tcf4 in chicken embryo hindlimb, showing their expression in a muscle-like pattern but that do not correlate with the muscle fiber staining. (E) Deletion of Tbx3 in the Prx1 lineage (lateral plate mesoderm) showing non-cell autonomous defects in the muscle patterning (from Colosanto et al., 2016). (F) Section of a chicken embryo forelimb showing the muscles mass (brown) with the endothelial cells (purple) at the muscle splitting sites (from Tozer et al., 2007). (G) Non-cell autonomous muscle patterning defects in the Osr1 mutant (from Vallecillo-Garcia et al., 2017).*

might be due to both cell-autonomous and non-cell autonomous effect on myogenic cells (Asfour et al., 2023). On the contrary *Osr1* is not expressed in muscle progenitors but only expressed in non-myogenic cells whose expression overlap with *Tcf4*. At later stages they form a cell population that are tightly associated with muscle cells and called **fibro-adipogenic progenitors (FAPs)**. These cells are resident fibroblasts of the muscle and upon injury, for instance, they rapidly expand and favor myogenesis. Knockout of *Osr1* during development leads to several defect in limb muscle patterning by impairing the secretion of muscle connective tissue ECM proteins and chemokines from the MCTs (Vallecillo-García et al., 2017). *Tbx3* is expressed in the anterior and posterior MCT, posterior bones and a subset of bone eminences. Mice mutant for *Tbx3* in the lateral plate mesoderm lineage lack the lateral portion of the *m. triceps brachii* and the *m. brachialis*, leading to severe defects in adult locomotion (Colasanto et al., 2016). **Altogether, these studies highlight how the development of the myogenic lineage is under the influence of MCTs, bone and tendons development**. Muscle patterning is also tightly link to another paraxial-mesoderm derivatives, the endothelial lineage. As said above, these migrate early in the developing limb, before any myogenic cell have left the somites (Tozer et al., 2007; Yvernogeau et al., 2012). In the chick limb bud, **endothelial cells are detected in the future zones of muscle cleavage, delineating the cleavage pattern of muscle masses** (Tozer et al., 2007). Overexpression of *VegfA* demonstrated that ectopic blood vessels inhibit muscle formation while promoting connective tissue formation, via **PGDF signaling** that fosters the formation of ECM and attracts MCTs at muscle splitting sites (Tozer et al., 2007). Besides, even if it is known that **developmental cell death** participates in the elimination of interdigit mesenchyme this process has been investigated only recently regarding muscle patterning. Cell death is involved in the formation of the muscle of the hindlimb autopod in avian embryos, a process that seems to been mediated by RA signaling (Rodriguez-Guzman et al., 2007). Moreover, using live imaging of hindlimb explants, a recent study identified that a massive cell death event was at the root of the separation of the initial hindlimb muscle anlage into autopodial and zeugopodial muscles masses. Interestingly, this massive cell death was minorly done via apoptosis but majorly through **ferroptosis**, a cell death mechanism accompanied by a large amount of iron accumulation and lipid peroxidation (Co et al., 2024). It would be interesting to discriminate if this iron-dependent cell death pathway is involved in other muscular patterning context.

In most tetrapods, hypaxial musculature have tend to adopt a complicated muscle architecture, especially at the level of the pectoral and pelvic girdle. For instance, the ***m. latissimus dorsi*** and the ***m. rhomboideus*** as being attached to the vertebrae are located above the epaxial muscle bulk. Quail-chick chimeras have confirmed that the this two muscles originate from the lateral part of the somite, confirming their hypaxial identity (Saberi et al., 2017). However, MCTs and tendons seems to be of epaxial origin in its most medial part, as for others muscle in the neck/pectoral region, whose MCTs origin depend on the insertion of the muscles (Heude et al., 2018; Saberi et al., 2017). This complex pattern of MCTs will be discussed in the following section. As for the early entry of MMPs in the limb bud, the later muscle patterning of the girdle relies on ***Sdf1/Cxcr4*** signaling. At around E5 in the chicken, ***Sdf1*** is strongly expressed in the proximal part of the limb, in the shoulder region, and attracts myoblasts that have already entered the limb bud to migrate back in the trunk (Masyuk et al., 2014; Valasek et al., 2011). Therefore, after a brief residential period in the limb bud, some of the myogenic precursors migrate out of the limb bud, back into the main body axis to form ventral and dorsal component of the pectoral girdle, this phenomenon has been called the **"in-and-out"** process. Interestingly, at the hindlimb level, muscle undergoing the "out" phase generate the cloacal muscles suggesting that it is a conserved mechanism that is at the roots of the diversification of hypaxial structures. One could argue that migrating into the limb bud is an effective way to lose the metameric pattern imposed by the somites and therefore might contribute to generate more diverse muscle bundles. It is noteworthy to note that other embryonic tissues contribute to articulate the limb with the axial skeleton, such as the ***m. cucullaris*** or ***m. trapezius*** in mammals that connect the occipital bone with the axial skeleton, the clavicle and the scapula. This muscle does not derive from

the somite but instead emanate from the unsegmented **cardiopharyngeal mesoderm** (described in the next sections). Other more specific cases also exist, such as in **bats**, where muscle progenitors from the **second branchial arch** invade the growing limb bud to form the ***m. occipito-policallis*** that connect the occipital bone with the wing skeletal element to ensure a proper flight (Tokita et al., 2012).

Axial Muscles

Axial Muscle Anatomy

Amniotes epaxial musculature of the back is generally composed of three distinct groups of muscle bundles, the ***m. transversospinalis***, the ***m. longissimus dorsi*** and the ***m. iliocostalis***, altogether often called the **erector spinae**. Each one of these groups of muscles are sometimes composed of different muscles groups with multiple attachment sites on the vertebrae and/or the ribs. These muscles are essential to straighten the back and maintain a stable posture. Some muscles bundles are short and articulate two adjacent vertebrae between them, such as the ***m. interspinales*** or the ***m. intertransversarii*** that link two spinous or transvers process between them, respectively (Schünke et al., 2021). These small muscles, with others, and the long ***m. spinalis*** are regrouped under the term of *m. transversospinalis*. Laterally, can be found the *m. longissimus dorsi* that spans the entirety of the back and be also into several domains depending on their position in the AP axis (*capitis*, *cervicis* and *thoracis*). The same nomenclature exists for the *m. spinalis and* the *m. iliocostalis*. Speaking of the m. iliocostalis, it is the most lateral muscle bundle of the erector spinae complex, and mainly insert on ribs. Most of the epaxial musculature exhibit multiple attachment points, with muscle fibers spanning several segments and shorter fiber attaching multiple vertebrae or ribs together. At the level of the neck, the epaxial musculature of human contains long muscles such as the ***m. splenius capitis*** or the ***m. complexus*** (also called *m. semispinalis capitis*) linking the occipital bone with cervical vertebrae, several small muscle bundles also link the occipital bone with the most anterior vertebrae (Schünke et al., 2021). The hypaxial part of the most anterior somites also form muscle of the ventral neck such as the ***m. longus colli*** and ***m. longus capitis***. The *m. longus capitis* link the transverse process of vertebrae with the basilar part of the occipital bone while the *m. longus colli* stops at the level of the atlas. Functionally, dorsal and hypaxial musculature of the neck coordinate head mobility and locomotion. At the limb level the hypaxial part of the dermomyotome gives rise to limb and pectoral/pelvic muscles (see section above), while at the interlimb level it generates the body wall muscles. In amniotes these muscles, with the aid of the ribs, are essential in land life to support the visceral organ of the abdominal cavity. Laterally, the body wall musculature is composed of three different layers, the external ***m. obliquus externus abdominis***, the intermediate, ***m. obliquus internus abdominis***, and the more internal ***m. transversus abdominis***. At the ventro-medial level, lay another layer of muscle with the fibers aligned in the AP axis and separated into 5 different quadrants by tendinous tissues, the ***m. rectus abdominis*** (Scaal, 2021; Schünke et al., 2021). At the thoracic level, the hypaxial domain generates a lot of muscle associated with the ribs, regrouped under the term of **intercostal muscles**. It is noteworthy that some ribs associated muscles, the ***mm. levatores costarum*** belong to the epaxial musculature. The epaxial musculature pattern is quite conserved in all amniotes, however, some exceptions exist. Amniotes with a long tail exhibit a metameric pattern composed of several dorsal and ventral small unit named ***muscle truncii***, reminding the segmental organization found in newt and fishes. In birds, their flight-specialized derivative anatomy has also modified the axial muscle patterning. As most of their thoracic vertebrae are fused together and therefore the back mobility is reduced, the axial musculature, while conserving the same general organization, has seen its volume reduced. Moreover, another group of epaxial muscles is present at most posterior level, involved in the movement of the tail, named the ***m. levator caudae***. Besides, as the number of cervical vertebrae is not fixed in birds, the avian neck tends to be longer than in other clades. One of the most impressive muscle adaptation resided in the cervical epaxial domain, where birds possess two really long muscles, the ***m. longus colli dorsalis***

and the ***m. biventer cervicis*** (Böhmer et al., 2020, 2019; Boumans et al., 2015; Kuroda, 1962). The *m. longus colli dorsalis* extend from the basis of the cervical domain to approximatively the middle of the neck while connecting with the axial skeleton at the multiple attachment points, whereas the *m. biventer cervicis* originates from the first thoracic vertebrae and inserts on the occipital bone.

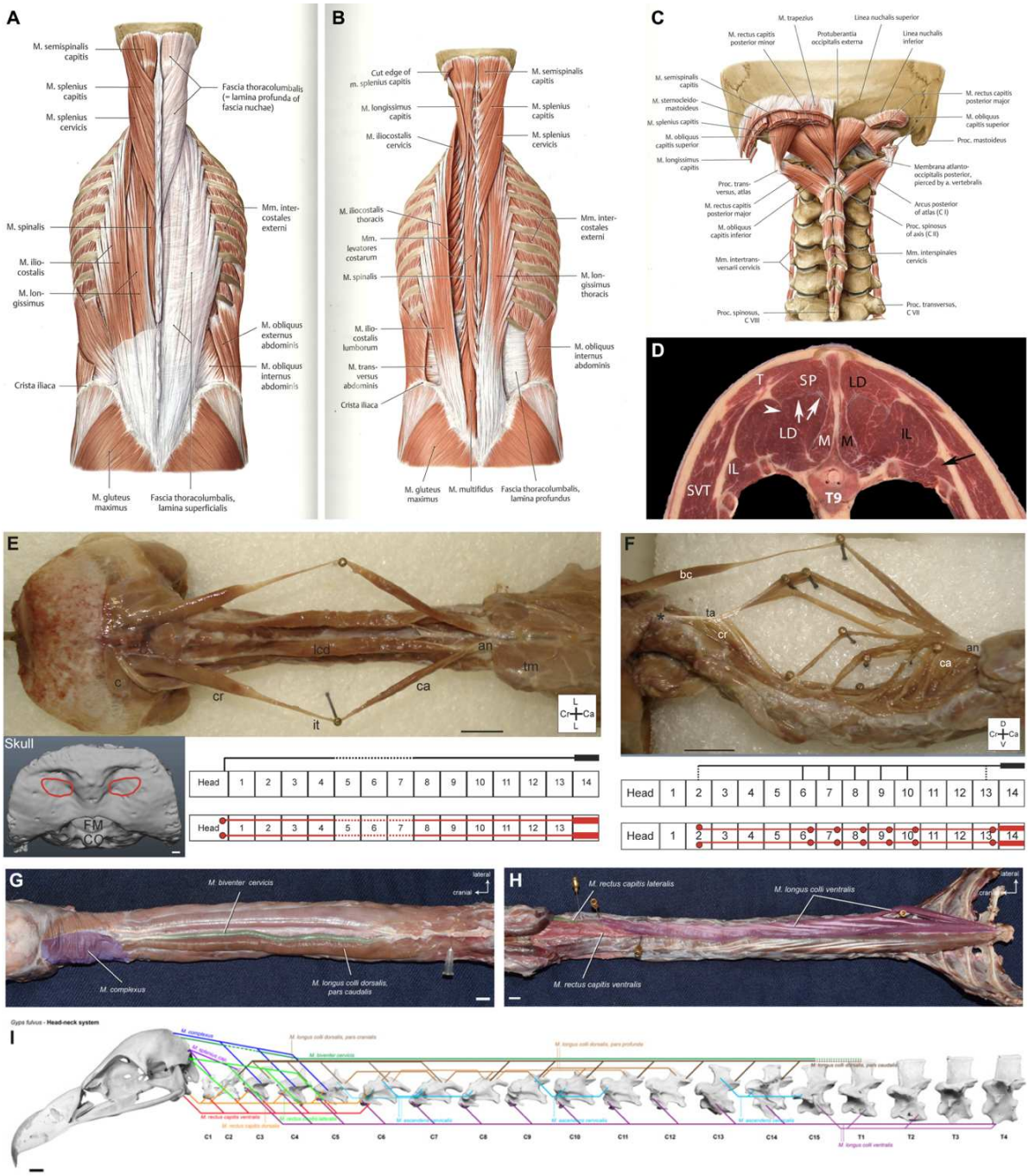

Figure 22. Epaxial muscle anatomy. *(A-B) Human anatomy of the erector spinae muscles (from Schuenke et al., 2021). (C) Small epaxial muscles in the occipital region, N.B. that the mm. intertransversarii and mm. interspinales are present at all vertebral level (from Schuenke et al. 2021). (D) Transverse section of the trunk of a horse, showing the three erector spinae muscles. IL: m. iliocostalis ; LD: m. longissimus dorsi ; SP: m. spinalis ; T : m. trapezius ; M : m. multifundus (a lumbar long muscle often grouped with the m. spinalis and others under the term of m. transversospinalis) (From Schultz et al., 2018). (E-F) Dorsal (E) and lateral (F) view the neck of an American barn owl showing the m. biventer cervicis (bc) that originate from the thoracic notarium, just posterior to the C14 and insert only in the occipital bone, with an intermediate tendon (intersection tendinae, it) in the middle separating the pars cranialis (cr) and the pars caudalis (ca). The lateral view shows the m. biventer cervicis but also the underlying m. longus colli dorsalis (lcd) composed of several muscle bundles attaching at several cervical vertebrae. (from Boumans et al., 2015). (G-H) Dissection of the neck of a vulture showing the different layers of muscles. (I) Schematization of the site of the origin and insertion of all the musculature of the neck in vultures (from Böhmer et al. 2020)*

Another important component of the amniote neck is the **infrahyoid musculature** that consist of several muscle bundles linking the sternum, the scapula, the hyoid bone and the thyroid cartilage of the larynx. These muscles, with the tongue muscles, constitute the **hypobranchial/hypoglossal musculature** and are derived from a population of **hypaxial MMPs from the most anterior somites**. The differential contribution of the hypaxial domain of the most anterior somite either to the cervical vertebrae muscles or the hypoglossal musculature is not well described. As the anatomy of the axial muscles is composed of several layers with multiple attachment points, the establishment of this pattern and the mechanism beyond that are not well known.

Cranial Muscles

Anatomy of Cranial Muscles

Except for the tongue musculature, the anterior most muscles of the neck and all the muscle of the face **do not derive from the somites**. **Extra-ocular muscles (EOMs)** emanate from the **pre-chordal mesoderm** while others cranial muscles come from the **cardiopharyngeal mesoderm (CPM)** within the **pharyngeal arches (PA)**. Pharyngeal arches are paired structures on each side of embryos, at the level of the pharynx. Each arch consists of a core of mesoderm and neural crest mesenchyme and the inside of the pharyngeal apparatus is lined with endoderm that forms infoldings or pouches between the arches, while the outside is covered by ectodermal tissues that form the outer pharyngeal clefts (or grooves). Thus, each arch contains all the various embryonic tissue found in an embryo and function as a separate functional unit to generate the various tissues of the head region. Regarding the musculo-skeletal system the mesoderm generate the skeletal muscles while in each arch **neural crest develops into bone, cartilage, and/or connective tissue**. The first pharyngeal arch is often called the **mandibular arch** and contribute mainly to **masticatory muscles**, the second one is often called the **hyoid arch** and is at the root of **facial expression muscles**, more posterior arches contribute to **laryngeal and pharyngeal musculature** and the **cucullaris-derived muscles** (**trapezius** and **sternocleidomastoid** in mammals). All these muscles are regrouped under the term of **branchiomeric muscles**. While of the most of the branchiomeric muscles are involved in food intake, respiration and vocalization with the hypoglossal musculature, the cucullaris-derived muscle participates in the stabilization and the articulation of the neck. The skeletal muscles of the mammalian **esophagus** also originate from the CPM (Comai et al., 2019).

Developmental Genetic of Cranial Muscles

Branchiomeric muscles and EOMs **do not develop with the same genetic network** than the epaxial and hypaxial muscles. *In fine*, they also rely on the same set of MRFs than the one of the trunk, *i.e. Myf5*, *MyoD*, *Mrf4*, and *MyoG*, however, the upstream regulators are completely different. *Pax3* is not involved at all and *Pax7* is only activated later during fetal development, when it marks the reserve cell population of myogenic progenitors. Although all branchiomeric muscles share a common embryonic origin, the upstream factors involved in each pharyngeal arch may vary. The craniopharyngeal mesoderm specifies dependently of ***Tbx1*** and ***Isl1*** and shares a clonal origin with the cell forming the second heart field, a second wave of cardiac differentiation. In *Tbx1*-null embryos, the first pharyngeal arch is hypoplastic and posterior pharyngeal arches do not form, resulting in variable penetrant defects of masticatory muscles and absence of muscles derived from more posterior arches (Kelly et al., 2004). Only the double mutant for *Tbx1* and *Myf5* exhibit a complete loss of the 1st PA muscles (Sambasivan et al., 2009). In addition, *Mrf4* is dispensable for pharyngeal muscle progenitor fate, therefore *Tbx1* and *Myf5* act synergistically for governing myogenesis at this location. Like *Pax3* in the body, *Tbx1* operates complementary to *Myf5* and acts genetically upstream of *MyoD* in the PA. Deletion of *Tbx1* does not impair EOMs muscles development (Kelly et al., 2004; Sambasivan et al., 2009). Regarding EOMs, ***Pitx2*** has been shown to be essential for their development (Zacharias et al., 2011). Moreover, *Pitx2* plays a pivotal role during the development of 1st PA, being upstream of *Tbx1*, *Tcf21* and *Msc* (see below), while it seems

to be dispensable for the 2nd branchial arch derivatives (Shih et al., 2007). Compared to trunk myogenesis, a common feature of PA and EOM founder cells is the epistatic relationship that exists between the MRFs: *MyoD* acts genetically downstream of *Tbx1* and *Myf5* in the PA, and downstream of *Myf5* and *Mrf4* in the EOMs, as opposed to the genetic compensation that exist between *Myf5* and *MyoD* in the trunk. *Tbx1* and *Pitx2* cross-regulate each other and might cooperate to activate the same target genes explaining the observation that PA myogenesis is observed occasionally in *Tbx1:Myf5* double mutant mice (Sambasivan et al., 2009). The development of esophagus muscle depends on *Tbx1* and *Isl1* alongside the **MET/HGF signaling** to drive the antero-posterior migration of muscle progenitor along the smooth muscle esophagus backbone (Comai et al., 2019; Gopalakrishnan et al., 2015). The bHLH transcription factors, ***Tcf21*** **(*Capsulin*)** and ***Msc*** **(*Musculin/MyoR*)**, were shown to act as upstream regulators of branchiomeric muscles development (Lu et al., 2002; Moncaut et al., 2012). In *Tcf21/Msc* double mutants, the *mm. masseter*, *pterygoid*, and *temporalis* were missing, while lower jaw muscles (*e.g.*, *m. anterior digastric* and *m. mylohyoid*) and EOM were not affected. The correct levels of expression of *Myf5* and *MyoD* in the 1st PA therefore result from activation by MSC and TCF21 through direct binding to specific enhancers (Moncaut et al., 2012). However, these two genes seem to be involved only in muscles derived from the first branchial arch, as they are not expressed in the EOM founder cells and the mouse mutant only exhibit default in muscle derived from the first pharyngeal arch. Similarly to what happens in the trunk and limb muscles, the **Six** gene family is essential for craniofacial muscles development as *Six1/Six2* mutants do not develop any EOMs, esophageal and branchiomeric muscles (Wurmser et al., 2023). Others transcription factors are expressed in some part of the cranial mesoderm and lineage tracing have revealed that they contribute to different cranial muscles. Lineage tracing of ***Isl1*** in mice have reveals that PA and cucullaris-derived muscles are labeled, however *Isl1* does not seems to label the entirety of the branchiomeric muscles, its precise role and position in the GNR remains to be determined (Heude et al., 2018; Nathan et al., 2008). ***Mesp1*** also labels branchiomeric muscles in addition to several epaxial and hypaxial muscle derivatives of the most anterior somites, suggesting **a mixed GNR regulating the formation of the somitic muscles of the neck**. Interestingly, *Isl1*^{CRE} also marks myogenic cells forming the *m. latissimus dorsi*, if *Isl1* is specifically expressed in some hypaxial muscle derivatives or if CPM participates to the formation of *m. latissimus dorsi* remains to be explored (Heude et al., 2018).

Cranial Muscle Patterning

Besides relying on a distinct set of GNR for their myogenic specification, branchiomeric muscles connective tissue originate from a different source compared with trunk ones. While the MCTs of the hypaxial domain originate from the LPM and the one of the epaxial domain, as it has been proposed, from the paraxial mesoderm, **the connective tissue of branchiomeric and tongue muscles mainly originate from the cranial neural crest cells (CNCCs)** (Evans and Noden, 2006; Noden, 1983; Ziermann et al., 2018). CNCC are dispensable for early muscle specification, however, they are regulating the patterning of head muscle (Rinon et al., 2007). Neural crest specific deletion of ***Pitx2*** via *Wnt1*^{Cre} demonstrated that *Pitx2* is required in neural crest to regulate the orientation of extraocular muscles regarding the optic cup (Evans and Gage, 2005). The transcription factors *Dlx5/6* were shown to be critical in non-skeletal neural crest cells for the development of the masseter muscle (Heude et al., 2010). Regarding the somite-derived muscles of the tongue, CNNCs are important for their migration and survival toward the tongue bud, via a cilia-dependent GLI processing (Millington) and their proliferation and differentiation via Tgf-β signaling (Hosokawa et al., 2007; Millington et al., 2017). Comparative studies using **interspecific grafts** have confirmed that the species-specific cranial muscle patterning information are encoded inside the CNCCs. Quails and ducks exhibit different cranial musculoskeletal organization related to their feeding habits. Transplantation of **quail cranial neural crest into a duck host** results in the production of quail-derived skeleton and MCT that transformed duck-derived muscles into quail-like shaped muscles (Tokita and Schneider, 2009). Neither the muscle specification nor differentiation were changed by

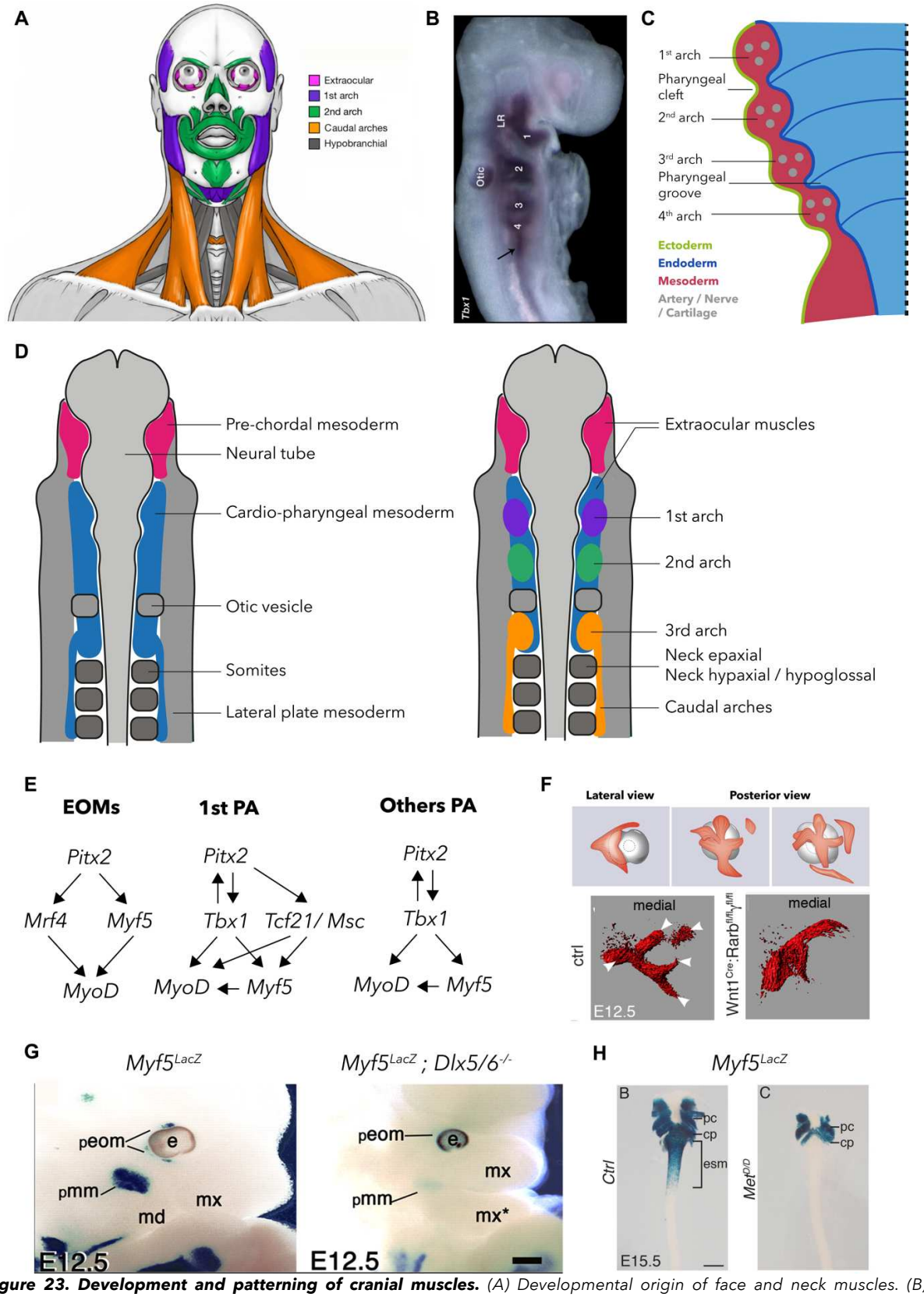

Figure 23. Development and patterning of cranial muscles. *(A) Developmental origin of face and neck muscles. (B) Pharyngeal arches (1,2,3 and 4) in chicken embryo seen by the expression of Tbx1 (from Ziermann et al., 2018). (C) Longitudinal section of pharyngeal arches showing their three-tissular origin. (D) Anatomical and developmental origin of head and neck muscles origin in the chicken embryo. (E) Genetic regulatory network of EOMs and pharyngeal-derived muscles. (F) 3D organization of EOMs in the mouse embryo. Deletion of retinoic acid receptor in neural crest-derived tissue induced muscle patterning defects (from Comai et al. 2020). (G) Defects in EOMs and masticatory muscles (mm) in mice deficient for Dlx5/6, a neural crest specific transcription factor (From Heude et al. 2010). (H) Defect in oesophagus muscularization in Met null embryos (from Comai et al 2019)*

these interspecific grafts, confirming that branchiomeric muscles specifies independently from the CNCCs but are highly dependent on their signals for their patterning. Moreover, by studying **parrot embryos**, that possess two additional jaw muscles compared to others birds, Tokita et al. found out that the migration of neural crest cell into the first PA is relatively more advanced in parrots than in Galliformes at equivalent stages, and that the expression patterns of several genes associated with the neural crest derived mesenchyme in parrots embryos highly diverge from the quail ones (Tokita, 2006; Tokita et al., 2013). Regarding EOMs patterning, the **eyeballs** has been shown to be the source of **retinoic acid (RA)** and endogenous local variations in the concentration of retinoids contribute to the establishment of tendon condensations and attachment sites that precede the initiation of muscle patterning (Comai et al., 2020).

While it is commonly admitted that majority of branchiomeric muscles and EOMs MCT emanate from the CNCCs, there are some exceptions to this rule. MCT of the EOMs exhibit two different origin depending on their location, with a gradient contribution of **CPM-derived MCT** toward the eyeball and an opposite gradient of **CNCC-derived MCT** from the eyeball (Grimaldi et al., 2022). The CPM can also gives rise to MCTs in CPM-derived muscles such as the laryngeal musculature and in somite-derived muscle such as the infrahyoid muscles (Adachi et al., 2020). In cranial muscles with no CNNC-derived MCTs the mesodermal cell where found to contribute to MCTs through a ***Myf5*$^{+}$ stage** (Grimaldi et al., 2022). Moreover, this was also the case in anterior most epaxial muscles. As *Myf5* drivers label several dermomyotome derivatives, it therefore demonstrates that some MCT can be generated by the dermomyotome, via a *Myf5*$^{+}$ bipotent stage. Nonetheless, the relative contribution of sclerotome and dermomyotome to the various MCTs remains to be identified. Regarding the MCTs of the neck region, only recently their precise origin in the neck and pectoral girdle region have been described. Using a plethora of genetic lineage tracing systems, Heude et al. proposed a scenario where **each muscle is composed of MCTs of the same origin as their attachment sites** (Heude et al., 2018). As for the EOMs, MCTs of the muscles of the neck exhibit a mixed identity, such as in the **cucullaris-derived muscles** (*m. trapezius* and *m. sternocleidomastoideus* in mammals), which originates from the most posterior PA and exhibit CNNC-derived MCT in their more anterior part, while having LPM-derived MCTs in their most posterior part. These findings bring some new pieces for the **primaxial/abaxial** concept. The predisposition of this concept was that muscles are solely composed of one or the other type of MCTs, however, as shown here depending on their attachment site the identity can be mixed as they might attach to two structures derived from different embryonic sources. Therefore, it seems that not a clear correlation can exist between the epaxial/hypaxial and primaxial/abaxial concept and that one should be careful when using these terms. In addition, some authors defined MCTs as only the fibroblasts associated with muscles cells while others also include all the tenogenic cells. Again, while the CNCCs can give rise to all these cell types, the blueprint is quite different in the epaxial domain, where the tenogenic cells derived from the sclerotome and the associated fibroblasts from the dermomyotome and/or the sclerotome, the continuum between these two embryonic origins and/or the overlapping cell types remains to be identified. Moreover, the role of MCTs in the patterning of epaxial muscles is completely unknown as our knowledge on their development paths and the late morphogenesis of epaxial muscles remain superficial.

During my Ph.D. I tackle this question by studying the late morphogenesis of epaxial muscles in chicken embryo mainly by using 3D light-sheet imaging and electroporations of single somite. These experiments showed that during early fetal life, myofibers and progenitors can break the impose metameric organization and elongate / shift over several segments. Furthermore, I showed that myogenic cells from two adjacent compartments do not fuse together until late fetal stages. Finally, I also investigated this process in other tetrapod species and confirmed that long epaxial muscles are a synapomorphy of all amniotes.

Primary and Secondary Myogenesis

Besides the molecular determination *per se* and the muscle patterning lays a third layer of complexity which is **the appearance of structurally and biochemically different myotubes during development**. These successive waves of myogenesis have been called the **primary and secondary myogenesis**. Examinations of transversal sections of muscle during fetal development have demonstrated that two types of myotubes exist during fetal life. Some myotubes are large and express both slow and fast myosin, while they are surrounded by numerous, less differentiated, smaller myotubes that only express fast myosin. (Kelly and Rubinstein, 1980). These two types of myotubes have been named **primary** and **secondary myotubes**, and are formed during primary myogenesis, *i.e.* during embryonic life, and secondary myogenesis, *i.e.* fetal life, respectively. A third wave of myogenesis have been referenced by some authors and corresponds to the post-natal myogenesis that is mainly driven by the growth of the pre-existing myofibers, as the number of myotubes within a defined muscle is fixed at birth in every amniotes (McMeekan, 1940; Meara, 1947; Montgomery, 1962; Smith, 1963; White et al., 2010). These different myotubes have been proposed to emanate from different myogenic progenitor populations during development, namely **the primary and secondary myoblasts** or alternatively **the embryonic and fetal myoblasts**. As mainly studied in the context of limb development, *in vitro* studies have shown that isolation of embryonic myoblasts from early limb buds, and fetal myoblasts from late limb muscles, exhibit drastic differences when cultivated *in vitro*. Embryonic myoblasts are more prone to differentiate and generate mononucleated myofibers, or myofibers with few nuclei, while fetal myoblasts have a higher rate of proliferation and form large, multinucleated myofibers (Biressi et al., 2007; Murphy and Kardon, 2011). In addition, these two populations **respond differentially to various drug treatments** (Biressi et al., 2007). Logically, these two types of progenitors also display different transcriptomes, with for instance, only the embryonic cells expressing *Hox* genes and therefore, being sensitive to patterning cues. The myotubes that they generate also exhibit differences in their **transcriptome**, as culture from embryonic myoblasts have higher level of slow myosin and troponin while cultures from fetal myoblasts have higher level of the fast isoforms (Biressi et al., 2007). Cellular analysis of cultures from both types of myoblasts have shown that only the primary myoblasts can generate both slow/fast and fast-only myotubes, while fetal myoblasts can only generate the second type (Miller and Stockdale, 1986; Vivarelli et al., 1988). This strongly suggest that the early limb contains all the capacity to form both primary and secondary myotubes, while later, fetal myoblasts can only produce secondary myotubes. These experiments raise two possibilities:

(1) That the embryonic myoblasts are highly potent regarding they capability of forming different myotubes, while during the late stages, the remaining fetal myoblasts lose this capacity of forming slow myotubes and only generate fast ones.
(2) That early embryonic myoblasts are composed of a heterogenous population of cells, one that can form slow primary myotubes, while the other is set aside to form the later fetal myoblasts and therefore the secondary fast myotubes.

One of the current best ways to label these two populations of myoblasts have come from genetic studies in mice, especially regarding the *Pax3* and *Pax7* genes. These studies in mice have shown that before E12.5, ***Pax3* reporter** labels all the fetal limb muscles and fetal progenitors while ***Pax7* reporter** only label a few myoblasts. However, at P0, both *Pax3* and *Pax7* lineage have contributed to all the myotubes of the limb. In addition, suppressing the *Pax3* lineage totally abolishes limb myogenesis, while suppressing the *Pax7* lineage only impairs the second wave of myogenesis, as $Pax7^{CRE}$/ $R26R^{DTA}$ mice exhibit smaller muscles nearly only composed of slow myotubes (Hutcheson et al., 2009). As *Pax3* is already expressed in the PSM and in the dermomyotome, it is not surprising that all the somitic derivatives would be label by the *Pax3* reporter, including the endothelia. Therefore, it is clear that both embryonic and fetal myoblasts share a common developmental history,

however, the temporal separation of the two lineages remain to be determined. Indeed, even though the differential expression of *Pax3* and *Pax7* is a useful tool to target these two different waves of myogenesis, these two markers might not be specific to the primary and secondary myogenesis, respectively. As just said just above, *Pax3* is expressed early in the dermomyotome while *Pax7* expression overlaps the first wave of myogenesis. Indeed, the current consensus about the determination of limb primary and secondary myogenesis is that the primary myogenesis takes place in between E10.5 and 12.5 in mice (E4.5 – E9.5 in the chicken) and that the secondary myogenesis takes place from E13.5/E14.5 (E9.5 in the chicken), when all the muscle bundles are individualized and properly innervated (Biressi et al., 2007; Messina et al., 2010; Murphy and Kardon, 2011). However, *Pax7* is expressed in limb myogenic cells from E11.5 in mice, and therefore overlap with the primary myogenesis (Relaix et al., 2004). In addition, in birds, where the primary and secondary myogenesis happen such as in mice, *Pax3* and *Pax7* are co-expressed at all steps of myogenesis and therefore, cannot be considered as major determinant of these two waves of myogenesis (Otto et al., 2006).

Besides these two genes, anatomical distinctions have been proposed, such as the formation of primary and secondary myotubes might relies on a **differential colonization** of the limb bud by successive wave of myoblasts (Van Swearingen and Lance-Jones, 1995). However, this study only looked at early stage of fetal development, when the slow myosin is not widely expressed in all the muscles bundles and therefore could be just due to a differential contribution of myoblasts to different muscle bundles. Nonetheless, this hypothesis could be re-investigated as it is completely not known how the myogenic progenitors behave during the colonization of the limb bud. Live-imaging technics, coupled with spatio-temporal labelling of subsets of myogenic cells could be informative. Thus, is it still not know is the early limb bud contain already two separated types of myoblasts that will segregate later or if only one stem population generates all the myogenic derivatives.

It noteworthy to mention that ***Nfix*** expression is enriched in *bona fide* secondary myoblasts during mice development and regulates positively the expression of fast isoforms whereas inhibits the expression of slow isoforms. However, *Nfix* does not seems to be specifically expressed in myoblasts, especially at younger stages and it is not known if it is expressed in some early myoblasts that will be set aside to become the secondary myoblasts (Gray et al., 2004). Therefore, even if it acts as a major switch of secondary myogenesis, *Nfix* does not seem to be useful to trace back the origin of primary myoblasts.

In the trunk, the current model is that cells from the dermomyotome borders form a primary myotome, in which the central dermomyotome delaminate to provide muscle resident progenitors. This hypothesis is supported by the fact that the early myotome is highly positive for *Myh7* (slow myosin) and that, in mice, the *Pax7*$^{+}$ cells are only provided by the central dermomyotome (Gros et al., 2005; Relaix et al., 2005, *Myh7* profile on GEISHA). Moreover, electroporation of the dermomyotome borders does not to label muscle resident progenitors and cells derived from the borders do not fuse with central dermomyotome-derived cells at early stages (Gros et al., 2005; Sieiro-Mosti et al., 2014). However, no long-term lineage tracing has been performed to confirmed that the central dermomyotome in fact generates only fast, secondary myotubes and that the dermomyotome borders do not generate satellite cells.

Interestingly, a third wave of myogenesis can be considered, often referred as the post-natal myogenesis. Recent scRNA-seq and scATAC-seq atlas of mouse skeletal muscle development at multiple stages of embryonic, fetal and postnatal life identified a differential mechanism whereby *MyoG* cooperates with *Klf5* and *Tead4* during embryonic stages to synergistically drives the expression of muscle genes, whereas in more mature myofibers the transcription factors *Maf* takes

over *MyoG* to drives a more mature, fast, phenotype. Moreover, *Maf* expression is positively regulated by muscle contraction through a calcium-dependent mechanism. Thus, this mechanism is really pronounced after P0 in mice (Dos Santos et al., 2023). Furthermore, even if the adult muscle stem cells, the satellite cells, are largely involved in muscle repair after injury or during exercise-induced hypertrophy, the muscle growth during the first month of life in mice seems to be highly dependent on non-muscle interstitial cells that can fused with pre-existing myotubes. *Twist2*$^{+}$ interstitial cells contribute to the formation of type II myotubes in mice and participate to muscle regeneration. In addition, interstitial cells expressing *Hoxa11*, largely contributes to the growth of muscle during the post-natal myogenesis (Flynn et al., 2023; Liu et al., 2017). The relative contribution of these heterologous cells with the *bona fide* satellite cells during the first month of life is not known.

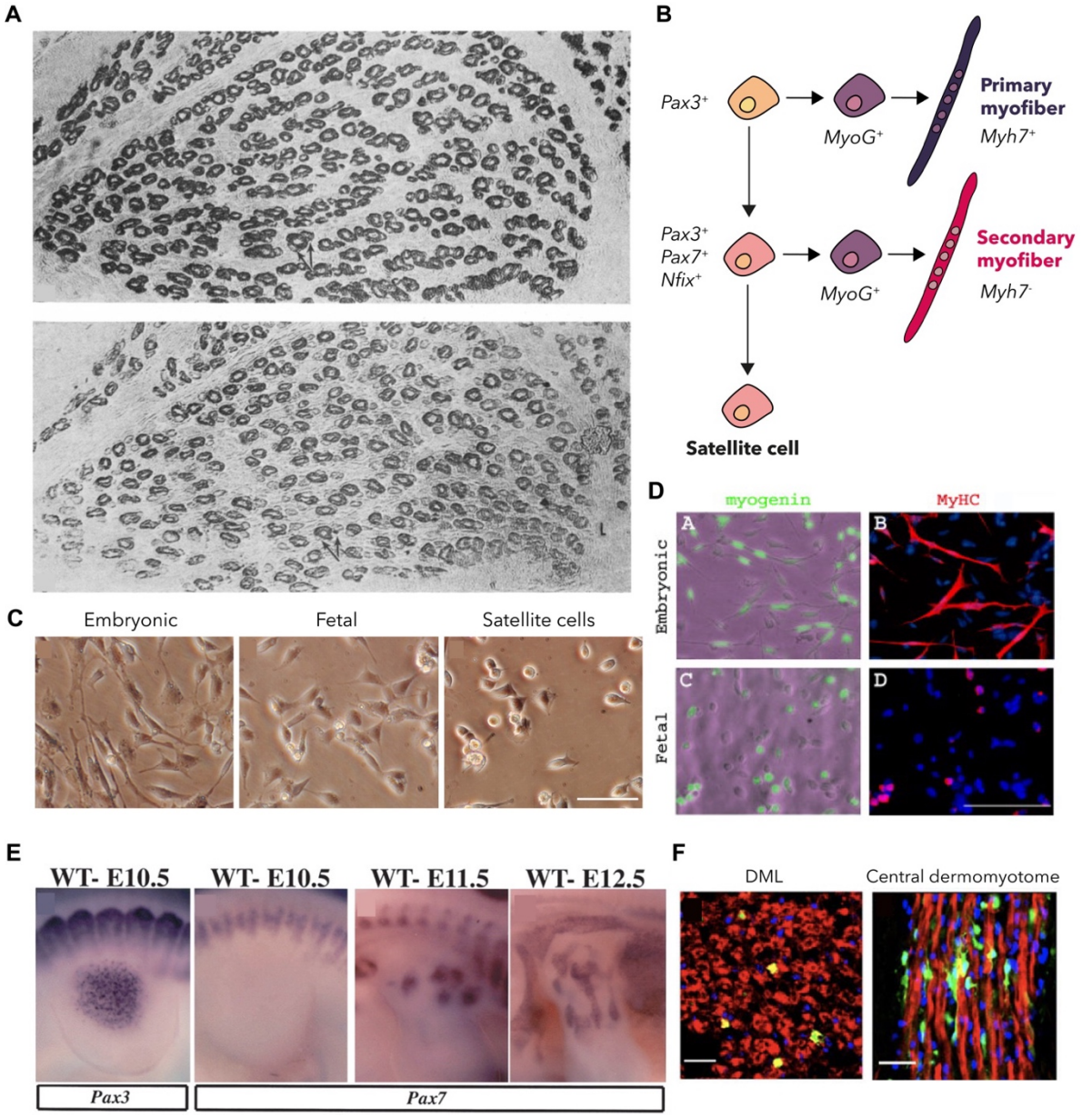

Figure 24. Primary and secondary myogenesis. *(A) Cross-section of a fetal rat EDL and immunostained with an antibody recognizing either a fast or a slow isoform of the MyHC (from Kelly and Rubinstein, 1980). (B) Schematic representation of the current view of the relationship between primary and secondary myoblasts/myofibers. (C) Morphological characteristics of embryonic, fetal and post-natal muscle progenitors extracted from mice limb bud (from Biressi et al 2007). (D) Expression of MyoG and MyHC in embryonic and fetal myoblasts after the same time in culture (from Biressi et al. 2007). (E) Expression of Pax3 and Pax7 in embryonic limb bud in mice embryos (from Relaix et al. 2004). (F) Electroporation of the DML with an eGFP showing a few muscle fibers labelled and not a single muscle progenitor, while electroporation of the central dermomyotome label plenty of Pax7*$^{+}$ *muscle progenitors (from Gros et al. 2005)*

During my Ph.D., by using a lineage tracing system to follow the destiny of limb myoblasts responding, or not, to TCF/LEF signaling I challenge this question and found out that the early limb bud contains two population of myoblasts that can be differentiated by their responsiveness to TCF/LEF signaling. In addition, only the TCF/LEF responding population give rise to primary, slow myofibers, while the other one generates late muscle progenitors and participates to the secondary myotubes formation. Moreover, I also investigated the functional role of Wnt/TCF-LEF signaling during these events and discovered that Wnt / TCF/LEF signaling regulates the transcription of genes involved in cellular migration, one of which being *Cxcr4*, a major regulator of Wnt signaling. These results are presented and discussed below.

Results

Implication of the TCF/LEF Signaling in the Primary and Secondary Myogenesis of the Limb

A new bright and highly destabilized TCF/LEF reporter

The Wnt/β-catenin pathway is a pleiotropic signaling module that is present in all metazoan and is involved in various process during development, regeneration or cancer. The so-called canonical Wnt signaling pathway always lead to the stabilization of the β-catenin that translocate into the nucleus and bind the transcription factor of the TCF/LEF family to activate the transcription of target genes (Clevers, 2006). The first reporter of the Wnt-TCF/LEF signaling, TOPFlash, was used *in vitro* and contained three TCF/LEF response elements upstream of a basal *c-fos* promoter driving the expression of the luciferase gene (Korinek et al., 1997). More sensitive TOPflash reporters were generated in *Drosophila* and zebrafish by increasing the number of TCF/LEF sites to 8, 12, and 16 (DasGupta et al., 2005; Veeman et al., 2003). In an attempt to detect Wnt signaling activity in mouse, three TCF/LEF binding sites were associated to *LacZ* and used to generate the TOPGAL mouse line (DasGupta and Fuchs, 1999), thus allowing the first analysis of Wnt responses in a vertebrate embryo. A significant increase in sensitivity was achieved by expanding the number of TCF/LEF binding sites to seven, in the BAT-gal mouse line (Maretto et al., 2003). Fluorescent reporter proteins (GFP or RFP and their variants) were also used in mouse and zebrafish (Ferrer-Vaquer et al., 2010; Moro et al., 2012). The main advantage of using either the β-galactosidase system or fluorescent proteins as reporters is their high stability: β-galactosidase half-life is reported to be up to 48 hr. ; that of GFP and RFP is about 24 hr., and fusion of GFP to an H2B nuclear localization signal further stabilizes the fluorescent label (Corish and Tyler-Smith, 1999; Foudi et al., 2009).

Such high stabilities lead to a considerable accumulation of reporter proteins in cells activating the pathway, thus facilitating their detection. However, significant drawbacks are an important lag-time between the activation of the pathway and the detection of the reporter and, conversely, the detection of signals in tissues where Wnt activity may have already ceased. This makes stable reporters largely unsuitable to detect rapid spatiotemporal changes of the activity of a pathway. Destabilized fluorescent reporters have been designed to alleviate this problem; however, shortening their half-life leads to dramatic fluorescence signal losses: for instance, d2GFP (half-life 2 hr), is 90% less fluorescent than its native GFP counterpart (He et al., 2019). Combining four TCF/LEF binding sites with a destabilized fluorescent reporter (d2eGFP, 2hr. half-life, Clontech) in zebrafish generated a transgenic line in which only intense activities of the pathway were detected through native fluorescence (Dorsky et al., 2002). Increasing the number of TCF/LEF binding sites to six (upstream of a minimal promoter, miniP, and d2EGFP) generated a fish line with four insertion sites, in which many of the known Wnt/β-catenin signaling-active sites were detected by native fluorescence, including through live imaging (Shimizu et al., 2012). While strategies described above are mainly based on enhancing transcriptional activity of Wnt TCF/LEF reporters, very little has been done to reinforce their translational efficiency. Sequence elements in the 5′ and 3′ untranslated regions of mRNAs play crucial roles in translation and well characterized elements derived from plant and viruses have been successfully used in heterologous systems (cell culture and *Drosophila*) to considerably increase reporter protein yields. These elements include a short 87 bp intervening sequence (IVS) from myosin heavy chain to facilitate mRNA export to the cytoplasm, a synthetic AT-rich 21 bp sequence (Syn21) to promote translational initiation, and a highly efficient p10 polyadenylation (polyA) signal from baculovirus. Here we generated a construct carrying 16 TCF/LEF repeats, upstream of a minimal promoter and a destabilized and nuclear form of the mVenus reporter gene and the three translational enhancers, IVS, Syn21 and p10 that we named 16TF-VNP.

To validate the physiological relevance of this construct we electroporated it in the neural of E2.5 chicken embryo and analyzed them one day after (Fig25.). It is known that Wnt TCF/LEF signaling is highly active in the roof of the neural tube and in neural crest cells. While the entirety of the neural tube along the DV axis was electroporated, only the roof of the NT and the migrating NCCs were positive for the reporter (Fig25. A). We next compared the percentage of electroporated TCF/LEF^{+}

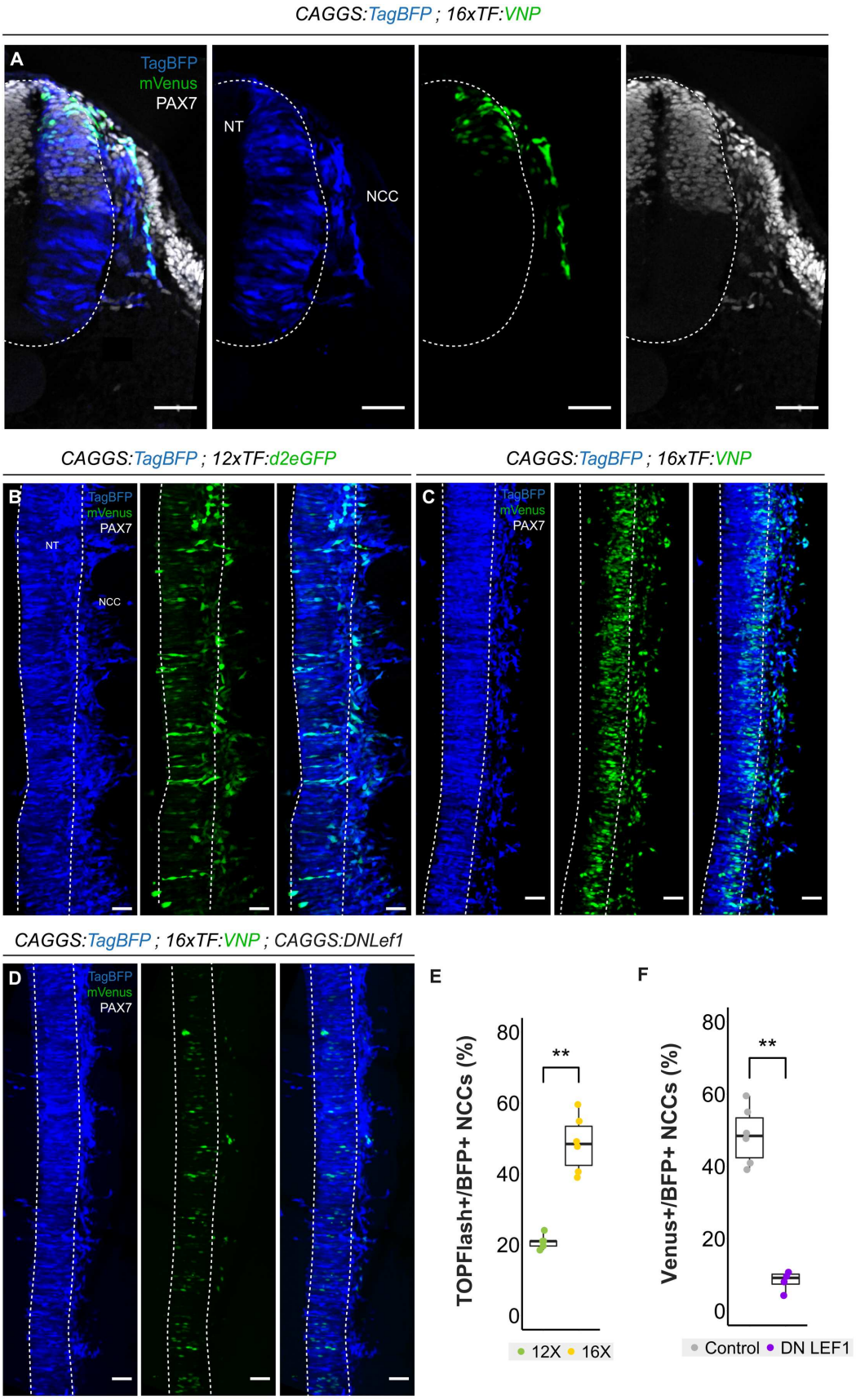

Figure 25. In vivo validation of the 16TF-VNP reporter. *(A) Transversal section of E3.5 neural tube electroporated with a ubiquitous TagBFP, the 16TF-VNP and stained for PAX7. (B-D) Dorsal view of confocal stack of E3.5 neural tube electroporated with a ubiquitous TagBFP and either the 12xTF-d2eGFP (B), the 16TF-VNP (C) or the 16TF-VNP with a dominant negative form of LEF1 (D). (E) Quantification of the percentage of TCF/LEF responding cells among the electroporated cells. (F) Quantification of the percentage of 16TF-VNP with or without the DNLEF1*

cells in three different conditions, by using a previously published reporter, with twelve TCF/LEF binding site upstream a destabilized eGFP (Fig25. A), our new 16TF-VNP reporter (Fig25. B) and the 16TF-VNP alongside a dominant-negative form of LEF1 (DnLef1, Fig25. D). Quantifications revealed that the percentage of TCF/LEF^{+} cells detected with the 16TF-VNP is two times higher compared to the previous reporter we had designed (Fig25. E) and that in presence of a TCF/LEF inhibition, the 16TF-VNP is nearly completely shut down (Fig25. F). Altogether these electroporations confirmed that the 16TF-VNP activity correspond to physiological zones of high Wnt TCF/LEF activity and that it can be downregulated when TCF/LEF is inhibited.

These results have been integrated into a publication that uses this construct to generate a new transgenic quail line: *Hila Barzilai-Tutsch, Valerie Morin,* ***Gauthier Toulouse****, Oleksandr Chernyavskiy, Stephen Firth, Christophe Marcelle, Olivier Serralbo (2022) Transgenic quails reveal dynamic TCF/β-catenin signaling during avian embryonic development doi:10.7554/eLife.72098*

TCF-LEF/β-catenin dependent signaling is restricted to early limb muscle development

We therefore used the 16TF-VNP reporter to monitor the TCF/LEF activity in limb myogenic cells. To target the muscle lineage of the developing wing in chicken embryos, we electroporated the lateral border (named the VLL) of forelimb somites (somites 17-21) in E2.5 embryos (Figure 26A). Since electroporation leads to the mosaic transfection of the targeted cell population, the reporter was co-electroporated with a ubiquitously expressed fluorescent marker to identify and analyze electroporated cells individually. We followed the activity of the 16TF-VNP reporter in the myogenic lineage throughout embryonic and fetal development. At E3, i.e. twelve hours after electroporation, the migration of progenitors emanating from the VLL has started (Fig26. C,D). At that stage, two distinct patterns of 16TF-VNP reporter activity were observed: a strong expression in a majority (66%) of electroporated epithelial cells located within the VLL and a weaker expression in a minority (21%) of migrating, electroporated cells exiting from the VLL (Fig26. C,K; Fig27. A,B). The expression of PAX7 in all (16TF-VNP^{+} and 16TF-VNP^{-}) electroporated migrating cells confirmed that these are bona fide muscle progenitors (Fig27. A). Half a day later, at E3.5, as all muscle progenitors have exited the VLL 37, 45% of electroporated muscle progenitors were strongly positive for the 16TF-VNP reporter (Fig26. E,K). During the following three days of development (E4.5 to E6.5) this proportion and level of expression remained relatively stable, in about 50 and 55% of electroporated cells (Fig26. F,G,H K). During this time period, 16TF-VNP^{+} cells were distributed among the 16TF-VNP^{-} cells, with an increasing tendency towards a localization at the distal end of the muscle masses (Fig26. F,G,H) . 16TF-VNP^{+} cells were evenly distributed along the dorso-ventral axis of muscles and were also present in the ventral muscle mass of the limb bud (Fig27. D,E,F). A sharp decrease in the reporter's activity was however observed on the next day, at E7.5, as 16TF-VNP^{+} cells became sparse and were confined mainly to the distal-most part of the muscle masses (Fig26. I, arrowheads).

We then performed long-term analyses of the reporter's activity. Embryos electroporated at E2.5 were analyzed on transversal and longitudinal sections of limbs collected at E9.5, E12.5, E14.5, E16.5 and E18.5. Despite a massive labeling of the muscle masses by the ubiquitously expressed electroporation marker, from E9.5 - E18.5, we did not detect any 16TF-VNP^{+} cells at any of the analyzed developmental stages (Fig26. J; Fig28. and Fig.29). These data demonstrate that TCF/LEF transcription in the muscle progenitor population is dynamic (see Fig26. 1L). An important feature of the reporter's activity is that it is observed in about 50% of electroporated muscle progenitors from E3.5 until E6.5. During that time period, muscle progenitors differentiate into many multinucleated muscle fibers, the first visible at around E5/E5.5 (Sieiro-Mosti et al., 2014). As muscle patterning progresses and distinct muscle bundles emerge, the reporter activity sharply drops and is kept silent until hatching.

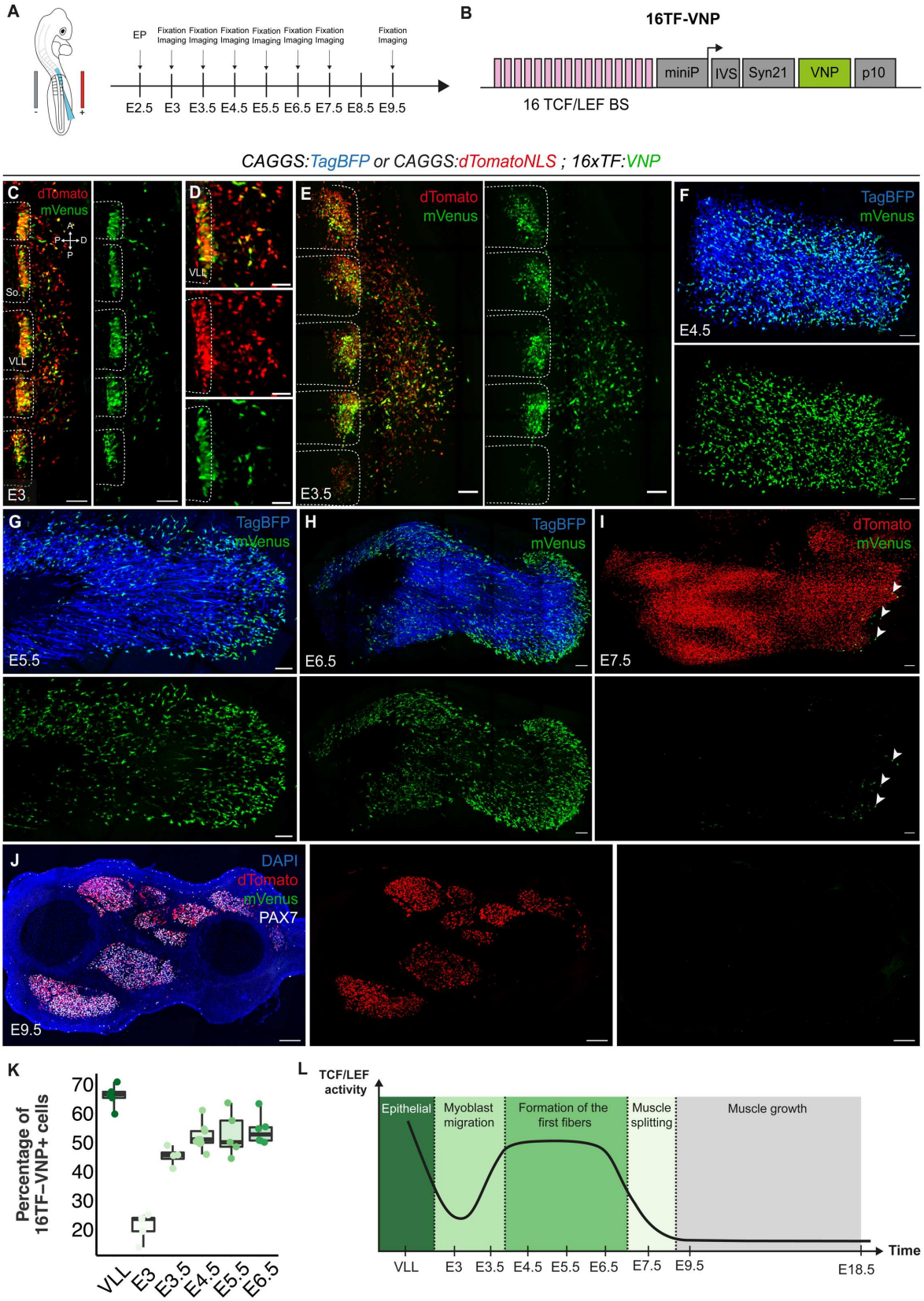

Figure 26. TCF-LEF/β-catenin dependent signaling is restricted to early limb muscle development. *(A) Brachial somites were electroporated at E2.5 and embryos were analyzed at indicated timepoints (B) Representation of the transcriptional reporter (16TF-VNP) used to monitor TCF/LEF/β-catenin dependent signaling. 16 TCF/LEF binding sites (BS) were placed upstream of a minimal promoter (miniP) driving the expression of a nuclear, destabilized Venus fluorescent protein (VNP), three translational enhancers were added*

(IVS, Syn21 and p10) to boost protein production. (C-E) Dorsal view of confocal stacks of brachial somites electroporated with a ubiquitously expressed dTomato and the 16TF-VNP, observed at E3 and E3.5. Somite borders are indicated by dotted lines, (D) is en enlargement of (C). (F-I) Dorsal views of confocal stacks of limb buds observed between E4.5 and E7.5, electroporated with either an ubiquitous TagBFP (F,G,H) or an ubiquitous nuclear dTomato (I), together with the 16TF-VNP. Arrowheads in (I) indicate the last remaining 16TF-VNP$^+$ cells present at E7.5. (J) Transversal section of E9.5 limb bud electroporated with an ubiquitous nuclear dTomato together with the 16TF-VNP. (K) Quantification of the percentage of 16TF-VNP$^+$ cells, between E3 and E6.5. VLL represents the progenitors within the epithelial VLL of the brachial somite, while E3 represent the migrating myoblasts. (L) Schematic representation of 16TF-VNP activity in the myogenic lineage during development. Scale bars: 100µm (C-F) or 200 µm (G-J)

TCF-LEF/β-catenin positive cells are PAX3$^+$/PAX7$^+$/MYF5$^+$/MYOD$^-$ muscle progenitors

We then investigated the myogenic differentiation state of 16TF-VNP$^+$ cells. As said above, during myogenesis, muscle progenitors sequentially express different transcription factors that correspond to different phases of myogenic commitment. In the mouse and chicken embryos, the proliferative muscle progenitor population comprises PAX7$^+$/MYF5$^-$ slow-dividing and PAX7$^+$/MYF5$^+$ fast-dividing cells (Picard and Marcelle, 2013). MYOD expression signals the exit of progenitors from cell cycle, and MYOG expression corresponds to terminally differentiated, pre-fusing muscle cells.

In birds, PAX7 and PAX3 proteins are co-expressed in limb myogenic progenitors, from the moment they exit the VLL and migrate into the limb mesenchyme. In fact, PAX3 and PAX7 co-expression persists in all limb myogenic progenitors throughout development, from E10.5 to E16.5, *i.e.* when progenitors assume satellite cell positions along the myofibers under the basal lamina. Therefore, all 16TF-VNP$^+$ and 16TF-VNP$^-$ progenitors present in the limb at E4.5 co-expressed PAX3 and PAX7 (Fig31.). To further characterize the molecular and proliferative signature of 16TF-VNP$^+$ cells in the limb bud, we performed immunostainings against PAX7, MYF5, MYOD and EdU. At E4.5, all muscle cells present in avian limb muscle masses are mononucleated and express PAX7 38. At this stage, we observed that, while MYF5 expression was widespread throughout the entire muscle progenitor population, MYOD expression was restricted to its central region (Fig30. A,B). We observed that all 16TF-VNP$^+$ cells (100%) expressed MYF5, while only 6% expressed MYOD (Fig30. A-F). At E6.5, many polynucleated MyHC$^+$ muscle fibers are present throughout the growing wing, and they are tightly intermingled with single-cell progenitors. Similar to E4.5, we observed at E6.5 that the vast majority of 16TF-VNP$^+$ cells (93%) co-expressed PAX7 and MYF5, but that the most (85%) 16TF-VNP$^+$ did not express MYOD (Fig30. G-J). At E7.5, even though very few progenitors were still found to express the reporter, all of them were PAX7$^+$ (Fig30. K). Even though we have previously shown that all PAX7$^+$/MYF5$^+$ progenitors are faster-dividing cells that PAX7$^+$/MYF5$^-$ progenitors, it was possible that the 16TF-VNP$^+$ and 16TF-VNP$^-$ subpopulations proliferated at different rates. However, labeling of embryos with EdU showed that both the negative and the positive populations displayed the same rate of proliferation (Fig32. A-C). Together, these experiments demonstrate that TCF-LEF/β-catenin dependent signaling is strictly restricted to a narrow time window of myogenesis, to a population of proliferating PAX3$^+$/PAX7$^+$/MYF5$^+$ progenitors. As soon as these progenitors progress further along the myogenic path, initiating MYOD expression, and exiting cell cycle, TCF-LEF/β-catenin dependent signaling is turned off.

TCF-Trace, a dynamic lineage tracing system to follow the fate of TCF-LEF/β-catenin$^+$ myogenic precursors

The 16TF-VNP reporter we engineered provides a snapshot of TCF-LEF/β-catenin dependent signaling at the time of analysis. It was however possible that limb muscle progenitors fluctuate between a 16TF-VNP$^+$ and a 16TF-VNP$^-$ state. To test this, we designed a reporter construct where

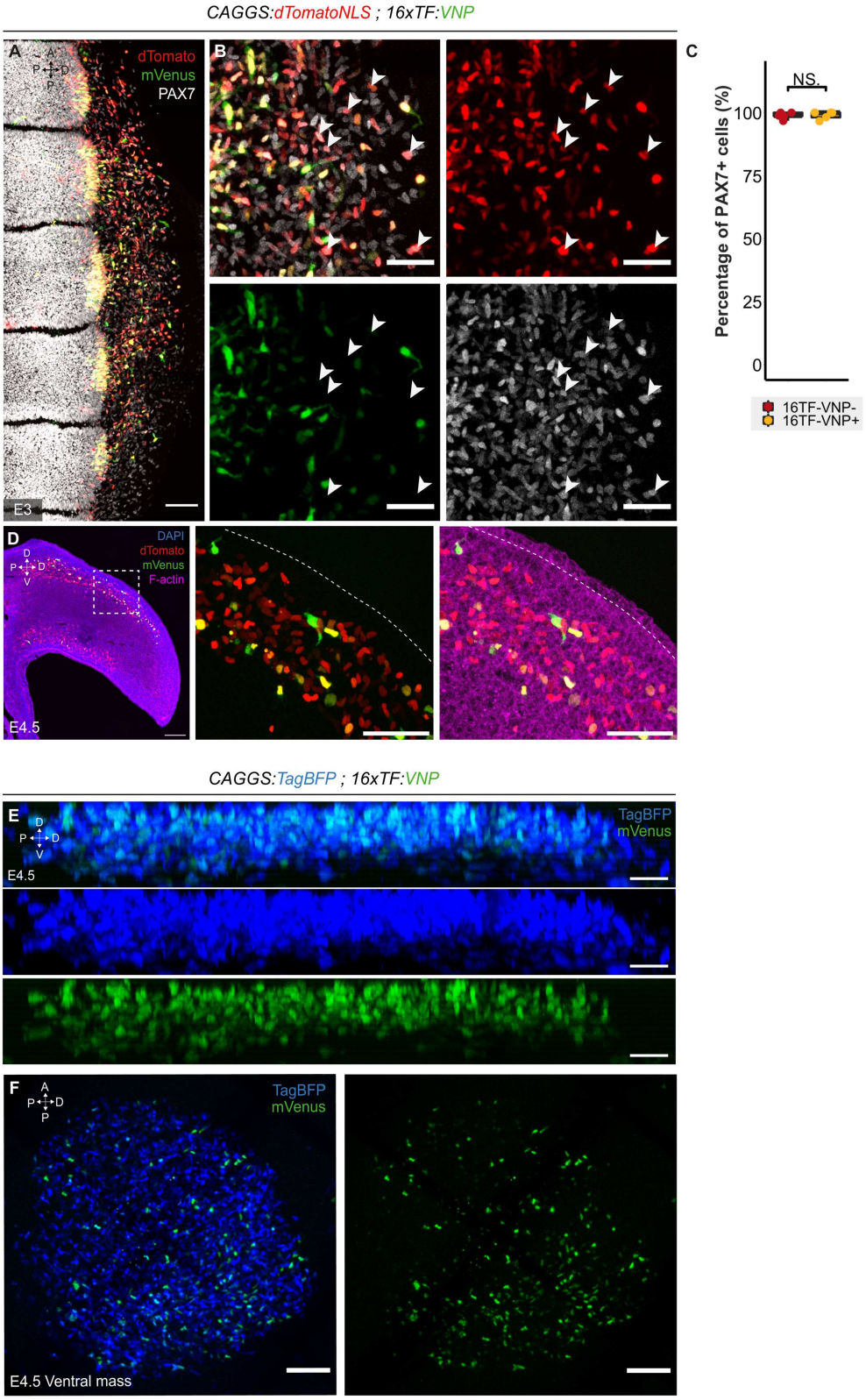

Figure 27. Early expression of the 16TF-VNP reporter in muscle progenitors. *(A,B) Dorsal view of a confocal stack of E3 brachial somites electroporated with an ubiquitous dTomato (in red), the 16TF-VNP reporter (in green) and stained for PAX7 (in grey). (B) is an enlargement of (A), arrowheads indicate electroporated cells that are 16TF-VNP⁻, but positive for PAX7. (C) Quantification of the percentage of PAX7⁺ cells that are 16TF-VNP⁻ and 16TF-VNP⁺. (D) Longitudinal section of E4.5 limb electroporated with a ubiquitous dTomato and the 16TF-VNP reporter. Dotted line indicates the junction between the dermis and the epidermis. (E) Longitudinal optical section of limb dorsal muscle mass electroporated with an ubiquitous TagBFP (in blue) and the 16TF-VNP reporter (in green). (F) Ventral view of a confocal stack of the ventral muscle mass of a E4.5 limb bud electroporated with a ubiquitous TagBFP and the 16TF-VNP reporter. Scale bars: 50µm (B), or 100µm (A, D-F)*

the destabilized nuclear Venus fluorescent protein was placed in tandem with a stable nuclear mCherry (half-life: about 18 hours) (Heng and Foo, 2022). This technique has been used in *Drosophilia* to test whether the activity of a promoter is fluctuating between an ON/OFF state (He et al., 2019). If the activity of the reporter was fluctuating, there would be more cells labeled with the stable mCherry than the destabilized mVenus. On the contrary if cells constantly respond to the signal, only double-positive cells should be observed. The construct was electroporated in the VLL at E2.5 and examined in the limb at E4.5. We observed a near-perfect (98%) correlation of mVenus and mCherry stainings, indicating that, within the time frame of the experiment, the reporter's activity does not fluctuate between a positive and negative state (Fig33.).

It therefore became important to investigate the long-term fate of myogenic progenitors that activate TCF-LEF/β-catenin dependent signaling. To address this, we developed a lineage tracing system using both Tet-On and Cre-Lox technologies (Fig34. A). This system aims to permanently label cells with dTomato fluorescence when they simultaneously experience TCF-LEF/β-catenin signaling and are exposed to doxycycline. The Tet-on technology is a well-established system of drug-induced gene activation, which displays low background and high induction rates. Combining this to the CRE-mediated excision of "Stop/PolyA" sequences placed upstream of a fluorescent protein should deliver a very sensitive system to permanently label myogenic progenitors. However, a significant drawback of the Tet-on system is that the rtTA protein is very stable, making it unsuitable for dynamic studies (Chassin et al., 2019) . We hypothesized that the rtTA protein could be destabilized, a process that should significantly enhances its utility for dynamic studies. We first engineered a rtTA construct where a PEST proteolytic signal was inserted at its N terminus (PEST-rtTA).

We used the electroporation technique to test these constructs in the dorsal region of the neural tube (Fig34. C), known to respond to TCF/LEF signaling. In the control experiment, we tested a native rtTA construct, where we observed that the addition of doxycycline to electroporated embryos led to a strong response, with many visible dTomato^{+} neural cells (Fig34. A,E). Expectedly, fusing PEST sequences to the rtTA construct led to a strong decrease in the efficiency of the response, with only few visible dTomato^{+} neural cells (Fig34. A,F,G). To address the reduced expression levels, we incorporated to the rtTA/PEST construct translation enhancer sequences (IVS/Syn21/p10; see above). The addition of translational enhancers to the rtTA-PEST sequence restored a labeling efficiency that was comparable to that observed with the original rtTA construct (Fig34. A,H,I). This suggests that the two-step strategy (destabilization/translation enhancement) generated a sensitive Tet-on system that responds to doxycycline exposure when TCF-LEF/β-catenin dependent signaling is active. The tracing system involves a succession of molecular steps (doxycycline-triggered activation of Cre expression, excision of Stop sequences and expression of the lineage tracing fluorescent protein). To evaluate the efficiency of the system to permanently label all cells experiencing TCF-LEF/β-catenin-dependent signaling, we substituted the 16TF promoter with a CAGGS ubiquitous promoter. This should theoretically lead to the activation of the tracing fluorescent protein in all electroporated cells upon doxycycline addition. The VLL of brachial somites were co-electroporated with this plasmid mix. Embryos were exposed to a doxycycline solution for two consecutive days and then analyzed one day later at E4.5 (Fig34. J). We observed that 98% of the electroporated cells, labeled by the expression of the constitutive mVenus protein, also expressed dTomato (Figure 3K-M). This near-perfect correlation between the expression of mVenus and dTomato suggests that, despite significant destabilization of the rtTA protein, and the many molecular steps required to activate the reporter, the doxycycline-mediated induction of dTomato fluorescence by the Tet-on/CRE system we designed is highly efficient. Furthermore, this experiment indicates that despite using multiple independent plasmids (five, including the transposase construct), all electroporated cells appear to have simultaneously incorporated them. This efficient and dynamic tool, that we named TCF-Trace, is the first molecular tool aimed at following the fate of

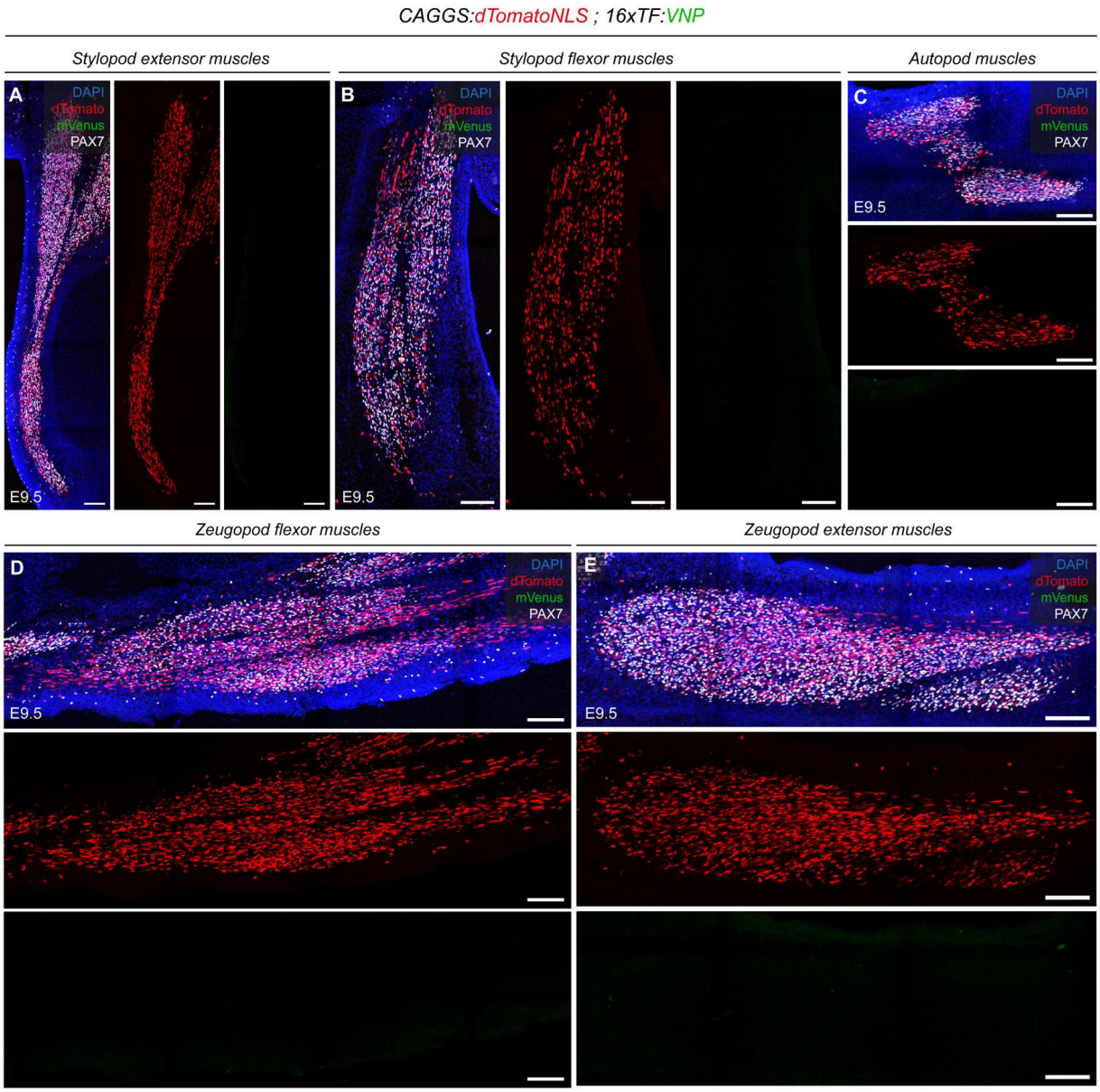

Figure 28. The 16TF-VNP reporter is not active in late embryonic muscle masses *(A-E) Longitudinal sections of E9.5 limb buds electroporated with a ubiquitous nuclear dTomato (in red), the 16TF-VNP reporter (in green) and stained for DAPI (in blue) and PAX7 in grey) at various anatomical locations along the limb proximo-distal axis. Scale bars: 100µm (A-E)*

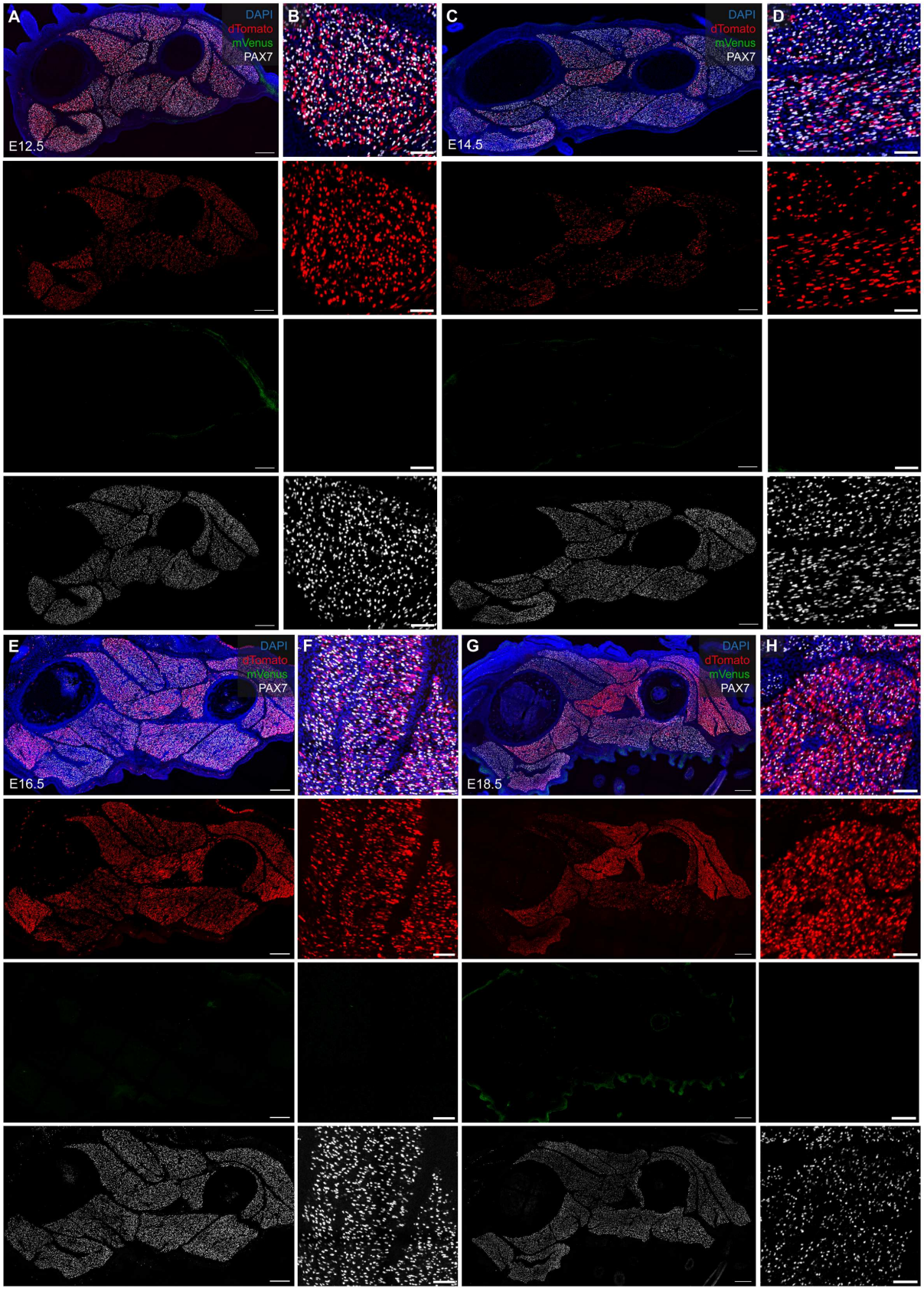

Figure 29. The 16TF-VNP reporter is not active in muscle masses in fetal stages. *(A-H) Transversal sections of E12.5 (A,B), E14.5 (C,D), E16.5 (E,F)) and E18.5 (G,H) limb buds electroporated with an ubiquitous nuclear dTomato (in red), the 16TF-VNP reporter (in green and stained for DAPI (in blue) and PAX7 (in grey). (B), (D), (F), (H) are enlargements of (A), (C), (E), (G) respectively. Each dot represents a limb bud. Scale bars: 50µm.*

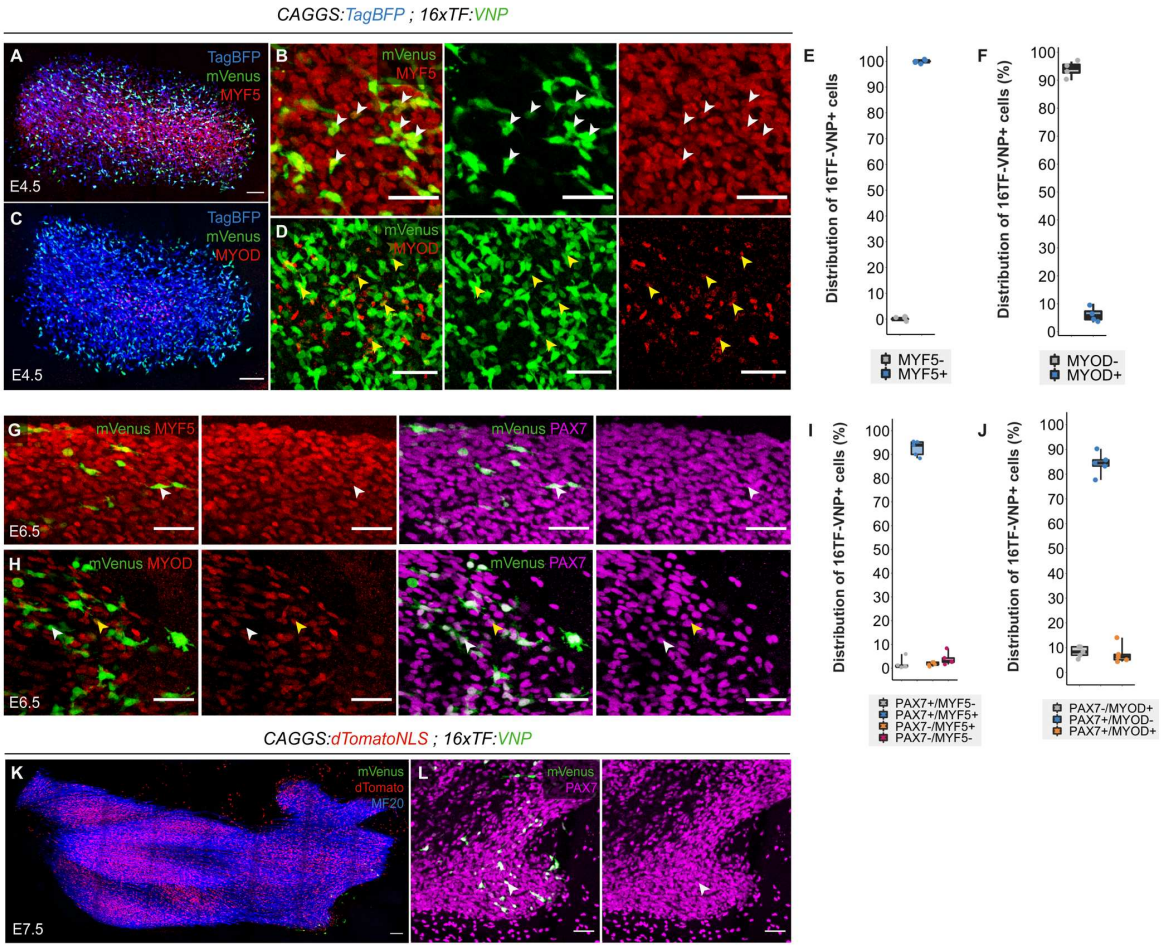

Figure 30. 16TF-VNP⁺ cells are early myogenic progenitors. *(A-D) Dorsal views of confocal stacks of E4.5 limb buds electroporated with an ubiquitous TagBFP, the 16TF-VNP reporter and stained for MYF5 (A,B) or MYOD (C,D). White arrowheads in (B) indicates 16TF-VNP⁺/MYF5⁺ cells; yellow arrowheads in (D) indicates some of the few 16TF-VNP⁺/MYOD⁺ observed (E,F). Quantification of the percentage of 16TF-VNP⁺ cells positive for MYF5 (E) and MYOD (F). (G,H) Dorsal view of confocal stacks of E6.5 limb buds electroporated with an ubiquitous TagBFP, the 16TF-VNP reporter and stained for PAX7 and MYF5 (G) or PAX7 and MYOD (H). The TagBFP channel is not represented. The white arrowheads indicate 16TF-VNP⁺/PAX7⁺/MYF5⁺ (G) cell and 16TF-VNP⁺/PAX7⁺/MYOD⁻ (H). The yellow arrowhead in (H) indicates a 16TF-VNP⁺/PAX7⁺/MYOD⁺ cell. (I,J) Quantification of the percentage of 16TF-VNP⁺ cells positive for PAX7 and MYF5 (I) or PAX7 and MYOD (J). (K,L) Dorsal view of confocal stacks of E7.5 limb buds electroporated with an ubiquitous nuclear dTomato, the 16TF-VNP reporter and stained for PAX7. The arrowhead indicates one of the few remaining 16TF-VNP⁺ cells that also expresses PAX7. (L) is an enlargement of (K). Scale bars: 50µm (G-H, L), 100µm (A-D), or 200 µm (K).*

cells experiencing temporary bursts of TCF-LEF/β-catenin-dependent signaling. We therefore proceeded to investigate the fate of myogenic precursor cells labeled by TCF-Trace.

Two distinct progenitor populations co-exist in early limb myogenesis

The TCF-Trace system displays accurate temporal labeling of targeted cells without significant lag from previous cell history. This temporal precision is crucial in our experimental design, as we electroporate VLL cells that display a high TCF-LEF/β-catenin-dependent activity at E2.5 (Figure 4A), an activity, likely linked to their epithelial state, that we do not intend to trace (Hutcheson et al., 2009). We therefore initiated the lineage fate of PAX7⁺/MYF5⁺ progenitors present in the limb from embryonic day 4.5 (E4.5). To do this, we electroporated the VLL of E2.5 brachial somites with a combination of the three plasmids described above, together with a ubiquitously expressed mVenus as an electroporation marker and the transposase plasmid. Subsequently, at E4.5, 5.5 and 6.5, doxycycline was added to developing embryos, aiming to label all progenitors activating TCF-LEF/β-catenin-dependent signaling during that time window. We analyzed the embryos at E7.5, at a time when the activity of the 16TF-VNP reporter is almost extinguished (see Fig26.). We tested for

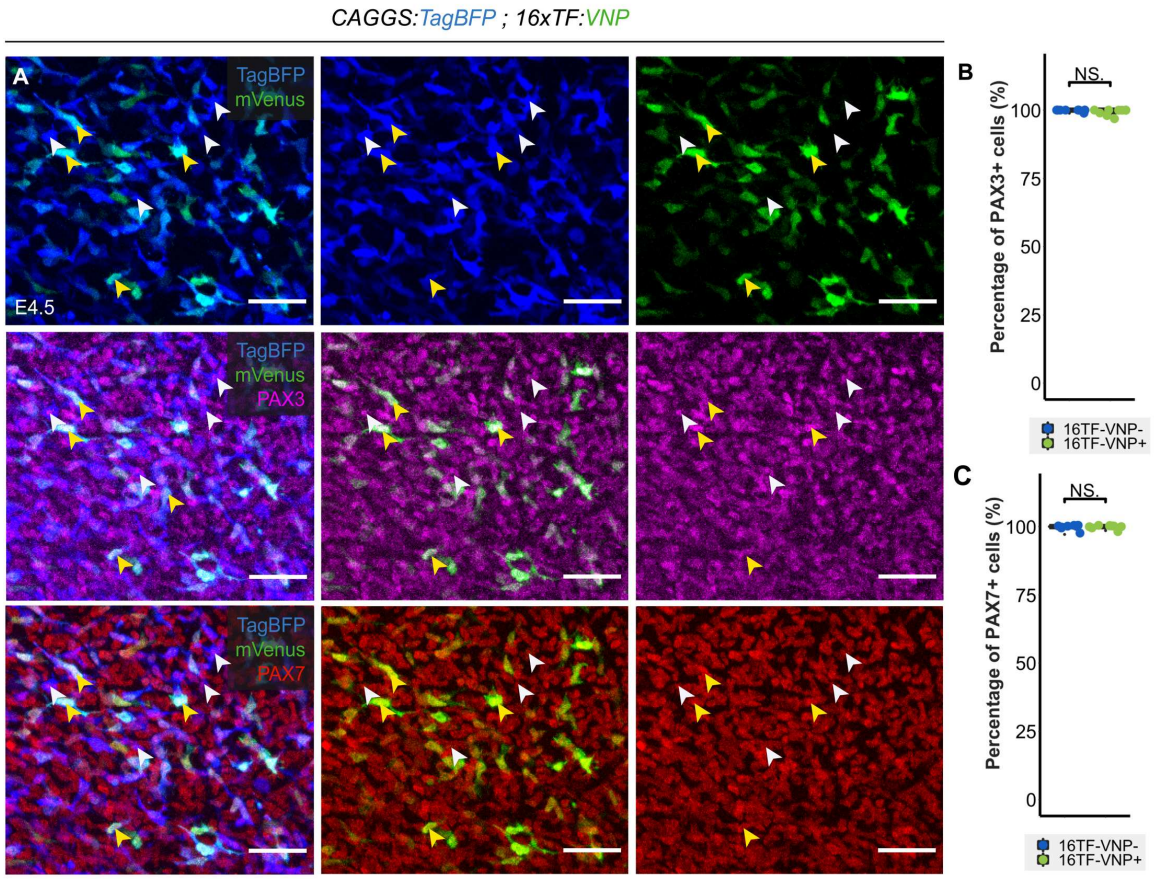

Figure 31. PAX3 and PAX7 do not discriminate between the TF16-VNP⁺ and 16TF-VNP⁻ cells *(A) Dorsal view of a confocal stack of a E4.5 limb bud electroporated with a ubiquitous TagBFP (in blue), the 16TF-VNP reporter (in green) and stained for PAX3 (in magenta) and PAX7 (in red). White arrowheads indicate 16TF-VNP⁻ cells, yellow arrowheads indicate 16TF-VNP⁺ cells. (B) Quantification of the percentage of PAX3⁺ cells within the 16TF-VNP⁻ and 16TF-VNP⁺ populations. (C) Quantification of the percentage of PAX7⁺ cells within the 16TF-VNP⁻ and 16TF-VNP⁺ populations. Each dot represents a limb bud. Scale bars: 50µm.*

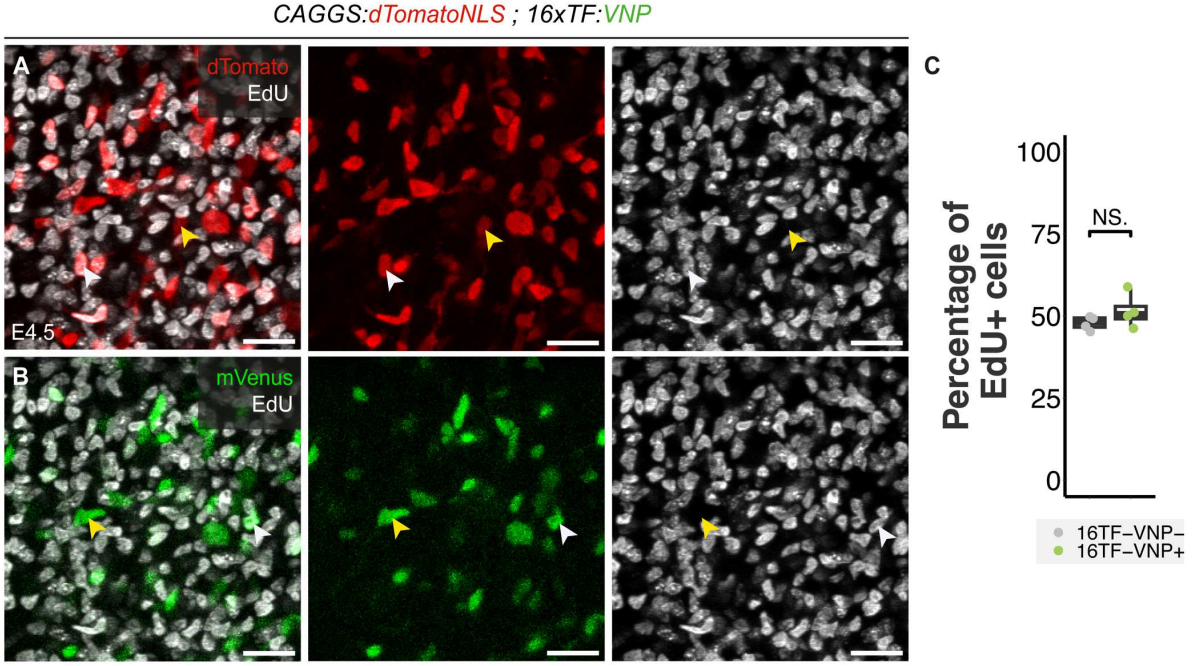

Figure 32. 16TF-VNP⁺ and 16TF-VNP⁻ progenitors proliferate at the same rate. *(A-B) Dorsal view of a confocal stack of E4.5 limb buds electroporated with a ubiquitous nuclear dTomato (in red), the 16TF-VNP reporter (in green) and labeled with EdU (in grey) to detect proliferating cells. White arrowheads indicate EdU⁺ cells; yellow arrowhead indicates EdU⁻ cells. (C) quantification of EdU⁺, 16TF-VNP⁺ or 16TF-VNP⁻ progenitors. Each dot represents a limb bud. Scale bar: 50µm*

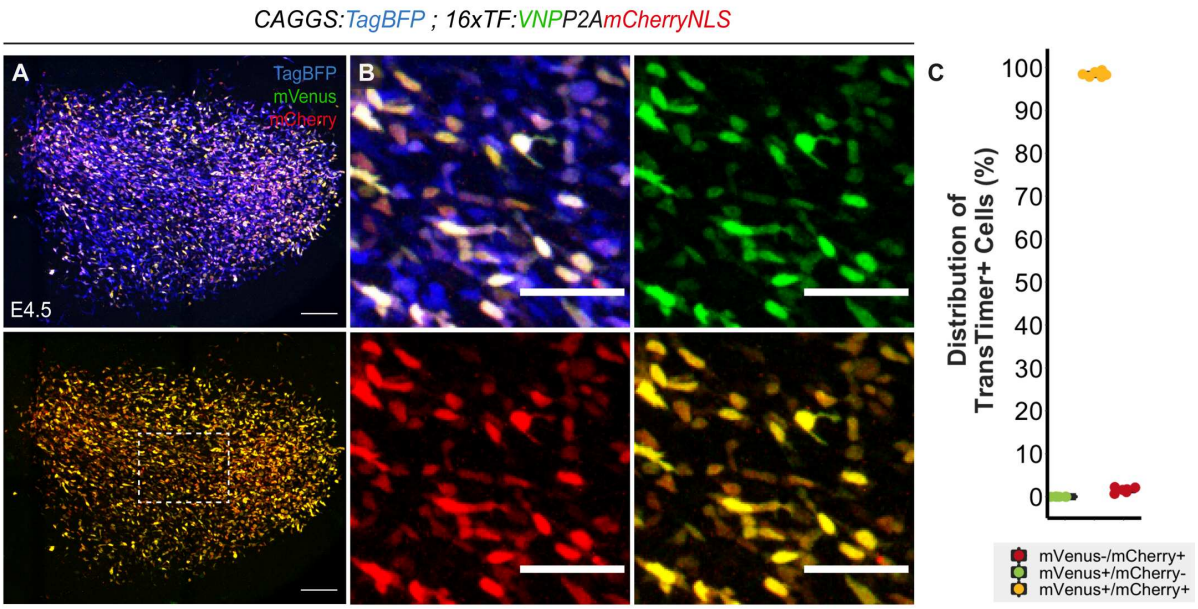

Figure 33. Pseudo-lineage of 16TF-VNP⁺ cells. *(A,B) Dorsal view of a confocal stack of E4.5 limb bud electroporated with a ubiquitous TagBFP (in blue) and the 16TF-VNP-P2A-mCherryNLS construct. The unstable VNP is detected in green; the stable mCherry is detected in red. (A) is an enlargement of (B). (C) Quantification (in percentage) of progenitors positive or negative for Venus and mCherry. Each dot represents a limb bud. Scale bars: 50µm (B) or 100µm (A)*

the expression of PAX7, Venus and Tomato proteins (Fig36. C). We observed numerous electroporated (green) myofibers containing dTomato⁺ nuclei (red), indicating a massive contribution of the TCF-LEF/β-catenin⁺ progenitors to myotube formation. Strikingly, this analysis unveiled an additional finding: a significant proportion (65-72%) of PAX7⁺, electroporated progenitors were not labeled by TCF-Trace. This was observed both in the proximal and distal region of the muscle masses (arrows in Fig36. D and quantifications in Fig36. E). As we showed the high sensitivity of the tracing system we designed, it is unlikely that the absence of label is due to a failure to detect and trace all TCF-LEF/β-catenin⁺ cells. Instead, it suggests the presence of a population of progenitors in the developing limb that never activate TCF-LEF/β-catenin signaling, co-existing with the TCF-Trace⁺ myofiber progenitor population.

TCF-LEF/β-catenin⁺ myogenic precursors differentiate into primary myotubes

To streamline myotube analyses, we engineered a second version of TCF-Trace, where a cytoplasmic forms of the fluorescent protein eGFP was used. This enabled straightforward identification of the entire myotube diameters on cross sections, thus facilitating more accurate quantifications. The electroporation tracer was a cytoplasmic form of dTomato driven by the myofiber-specific promoter (Myosin Light Chain: MLC) (Donoghue et al., 1988). A labeling protocol similar to the one utilized above was used, but embryos were analyzed at E9.5. On cross sections, we observed that nearly all (93%) electroporated myofibers (in red) were positive for eGFP (in green; Fig36. F,I). At E9.5 in chicken embryos, muscle bundles are clearly visible and only primary myotubes are present in muscle masses (Crow and Stockdale, 1986). Based on this temporal criterion, we therefore hypothesized that the TCF-LEF/β-catenin⁺ represent the precursors of primary myotubes. To confirm this, we proceeded with an immunostaining approach. As development progresses to fetal stages of development, slow and fast myosin expression is initiated in myotubes. It is widely accepted that all slow myosin-expressing myofibers are primary myotubes (Kelly and Rubinstein, 1980). Importantly, while all slow myosin-expressing myofibers are presumably primary myotubes, not all primary myotubes are slow myosin-positive, depending on the stage that is studies. We performed a survey of the slow myosin presence in the chicken embryo forelimb and found out that the, while the first

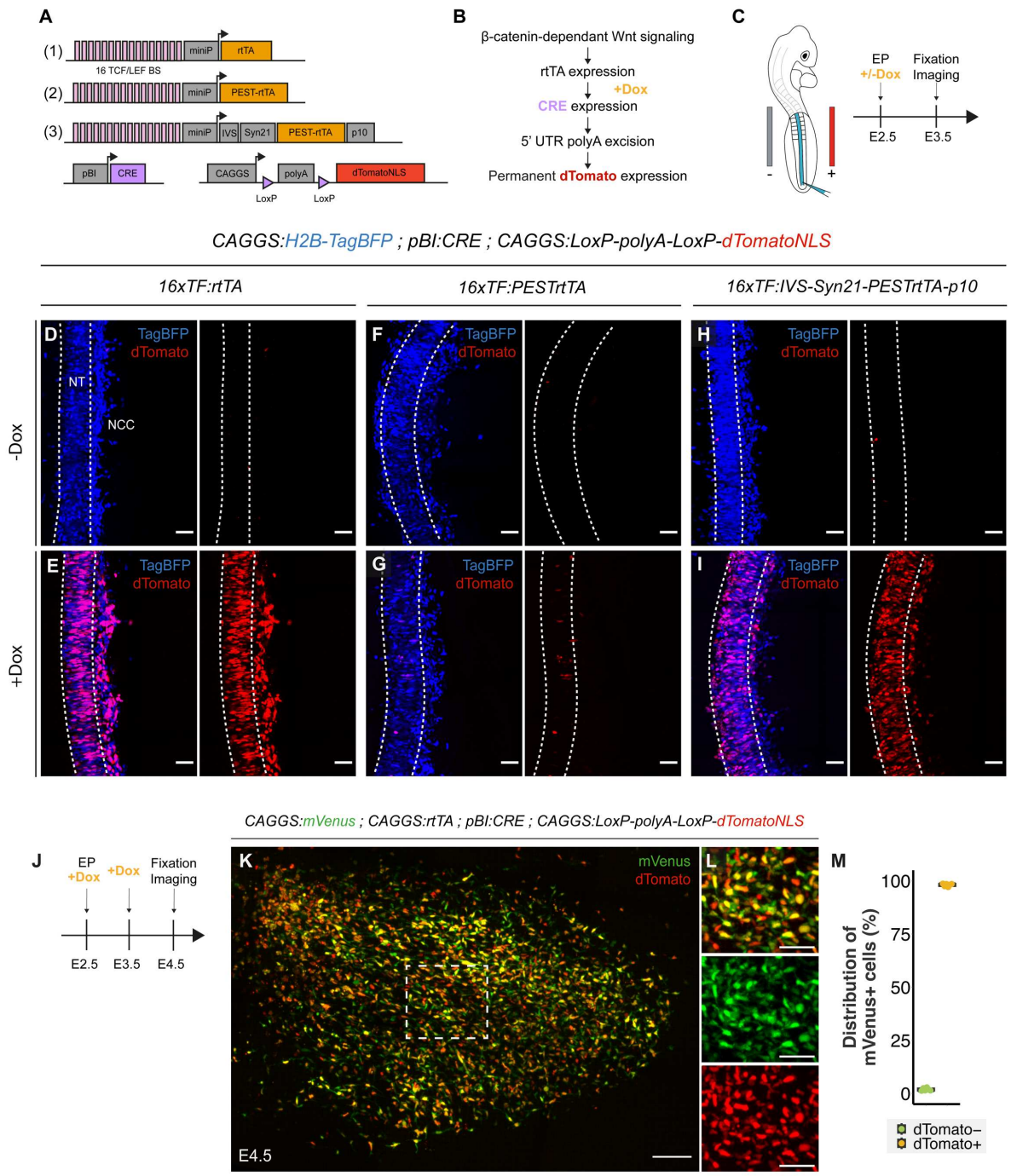

Figure 34. TCF-Trace, a tool to follow the fate of cells experiencing TCF-LEF/β-catenin dependent signaling. *(A,B) Schematics of the constructs tested. The three constructs comprise 16 TCF/LEF binding sites upstream of a minimal promoter driving the expression of a rtTA (1) or a rtTA fused with a PEST sequence at its N-terminal part (2) or a rtTA fused with a PEST sequence at its N-terminal part, flanked by translational enhancers (3). All constructs were co-electroporated with a plasmid containing a rtTA-dependent CRE recombinase and another containing a CRE-inducible nuclear dTomato. (C) Embryos were electroporated in the neural tube at E2.5, induced with doxycycline and analyzed one day later. (D-I) Dorsal view of confocal stacks of E3.5 neural tube (NT) electroporated with a ubiquitous H2B-TagBFP and the rtTA plasmid (D,E), the destabilized rtTA (F,G) or the destabilized and boosted rtTA (H,I). The dotted lines delineate the electroporated, right side of the neural tube. (J,K) Dorsal view of confocal stacks of E4.5 limb buds electroporated with an ubiquitous mVenus, an ubiquitous rtTA, the CRE and dTomato plasmids, doxycycline was added at E2.5 and E3.5. (L) Quantification of the percentage of dTomato^{+} cells within the mVenus^{+} population. Each dot represents a limb bud. Scale bars: 50μm (D-I, L) or 100μm (K).*

slow myotubes can be observed around E9.5, the slow primary myotubes are most distinguishable at E16.5, with fast-only surrounding smaller secondary myotubes. Moreover, this configuration was present in all the muscles of the limb (Fig35.). To investigate the biochemical signature of the TCF-LEF/β-catenin-derived myofibers at late embryonic stage, we performed a lineage tracing experiment similar to the one above but left the embryos to develop until stage E16.5 (Fig36. J). We observed that nearly all (98%) slow myosin-positive myotubes expressing the electroporation marker derived from the TCF-LEF/β-catenin^{+}-derived lineage (Fig36. J,K). Therefore, based on temporal and biochemical criteria, these experiments demonstrate that TCF-LEF/β-catenin^{+} progenitors present in the growing limb bud constitute the cellular origin of primary myotubes.

TCF-LEF/β-catenin- myogenic precursors differentiate into secondary myotubes and satellite cells.

We then wondered what the origin of secondary myotubes is. Secondary myotubes have been shown to appear after E9 in chicken, often surrounding primary myotubes. However, primary and secondary myotubes cannot be identified one from another based on biochemical characteristics. We followed the fate of TCF-Trace-positive and -negative progenitors, using the same protocol as in the previous experiment set, but left the embryos to develop until E12.5. In contrast to the analyses done at E9.5, we found that 21% of electroporated (red) myotubes were not labeled by the TCF-Trace system (green, Fig36. G,I). Often, we observed that dTomato-only myotubes were smaller than eGFP-positive myotubes and that they were located at their periphery, which are typical characteristics of secondary myotubes (Fig36. H, arrowheads). Therefore, based on temporal and morphological criteria, these experiments strongly suggest that TCF-LEF/β-catenin- progenitors present in the growing limb bud constitute the cellular origin of secondary myotubes. Interestingly, in a similar analysis done at E16.5, we observed a significant decrease in the proportion of TCF-Trace-negative myotubes, paralleled by an increase in the proportion of TCF-Trace positive myotubes (Fig36. I). During the E12.5-E16.5 time window, considerable growth of muscle masses and myofiber number takes place. It is possible that the shift in the proportions of TCF-Trace^{+} and TCF-Trace^{-} myotubes is due to a mixing between both lineages, either through myoblast to myofibers fusion or through fusion between myofibers.

Finally, we determined whether satellite cells originate from one, the other, or both progenitor populations. VLL cells of E2.5 brachial somites were electroporated with a combination of the three plasmids described above, together with a ubiquitously expressed H2B-Achilles as an electroporation marker and the transposase plasmid. At E4.5, E5.5 and E6.5, doxycycline was added to developing embryos. In birds and rodent, satellite cells are the only Pax7^{+} cells present in muscle masses in late fetal stages, just before hatching/birth 6,57–60. We explored whether Pax7^{+} cells present at E16.5 were labelled by the tracing system. We found that the vast majority (87%) of electroporated satellite cells present in limb muscle masses were TCF-Trace-negative, while a minority (13%) was positive (Fig36. L,M). This finding suggests that most satellite cells present in muscles at hatching derive from the TCF-LEF/β-catenin- progenitor population present in early limb buds, with a minor contribution originating from the TCF-LEF/β-catenin^{+} lineage.

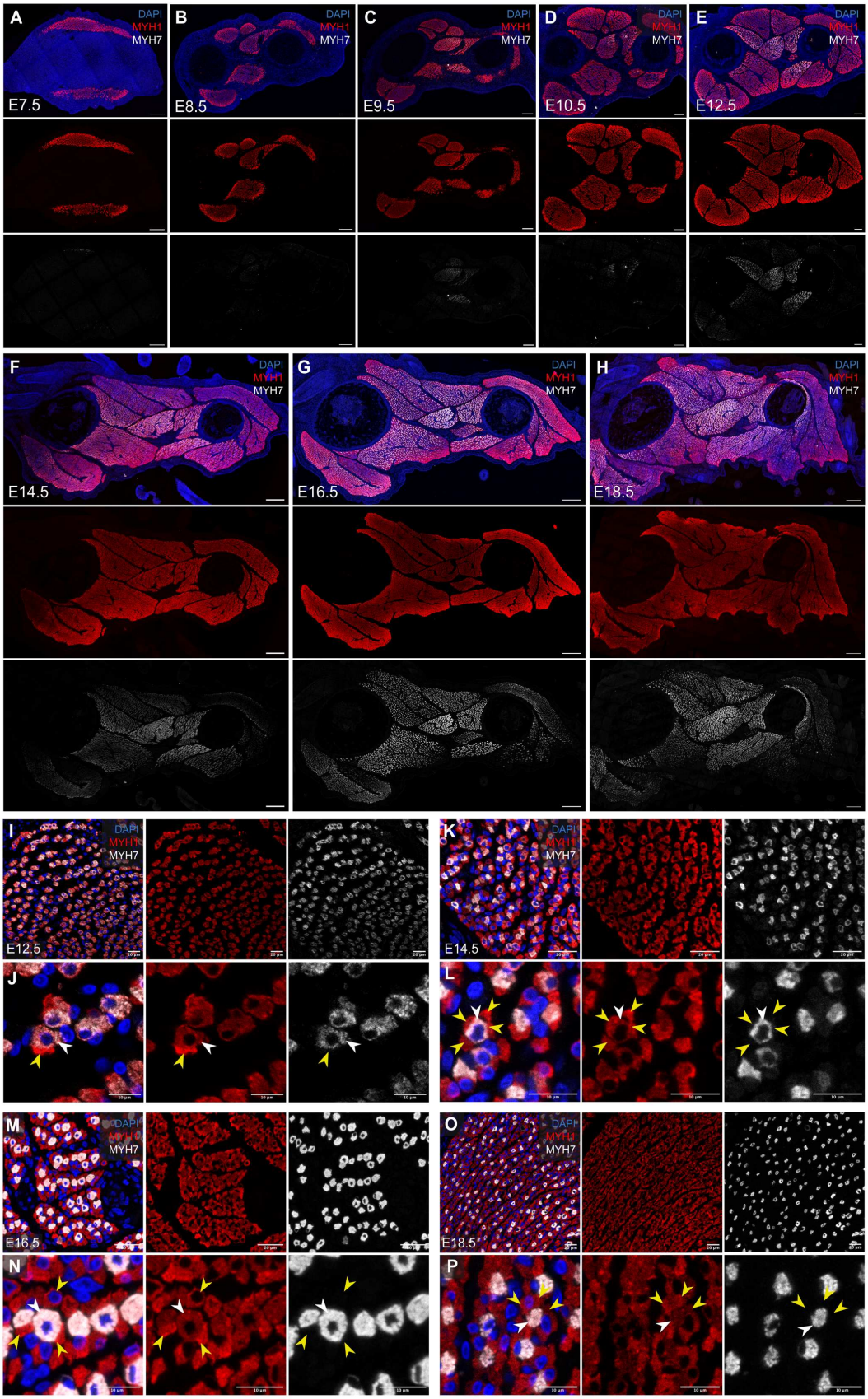

Figure 35. Expression of slow myosin throughout embryonic and fetal limb bud development. *(A-H) Transversal sections of whole limb bud from E7.5 to E18.5 stained for DAPI (in blue), MYH1 (Myosin Heavy Chain, in red) and MYH7 (Slow Myosin, in grey). (I-P) enlargements of limb bud muscles from E12.5 to E18.5 showing primary myotubes (MYH7^{+}, white arrowheads) surrounded by smaller presumably secondary myotubes (MYH7^{-}, yellow arrowheads). Scale bars: 10µm (J,L,N,P), 20µm (I,K,M,O) or 100µm (A-H).*

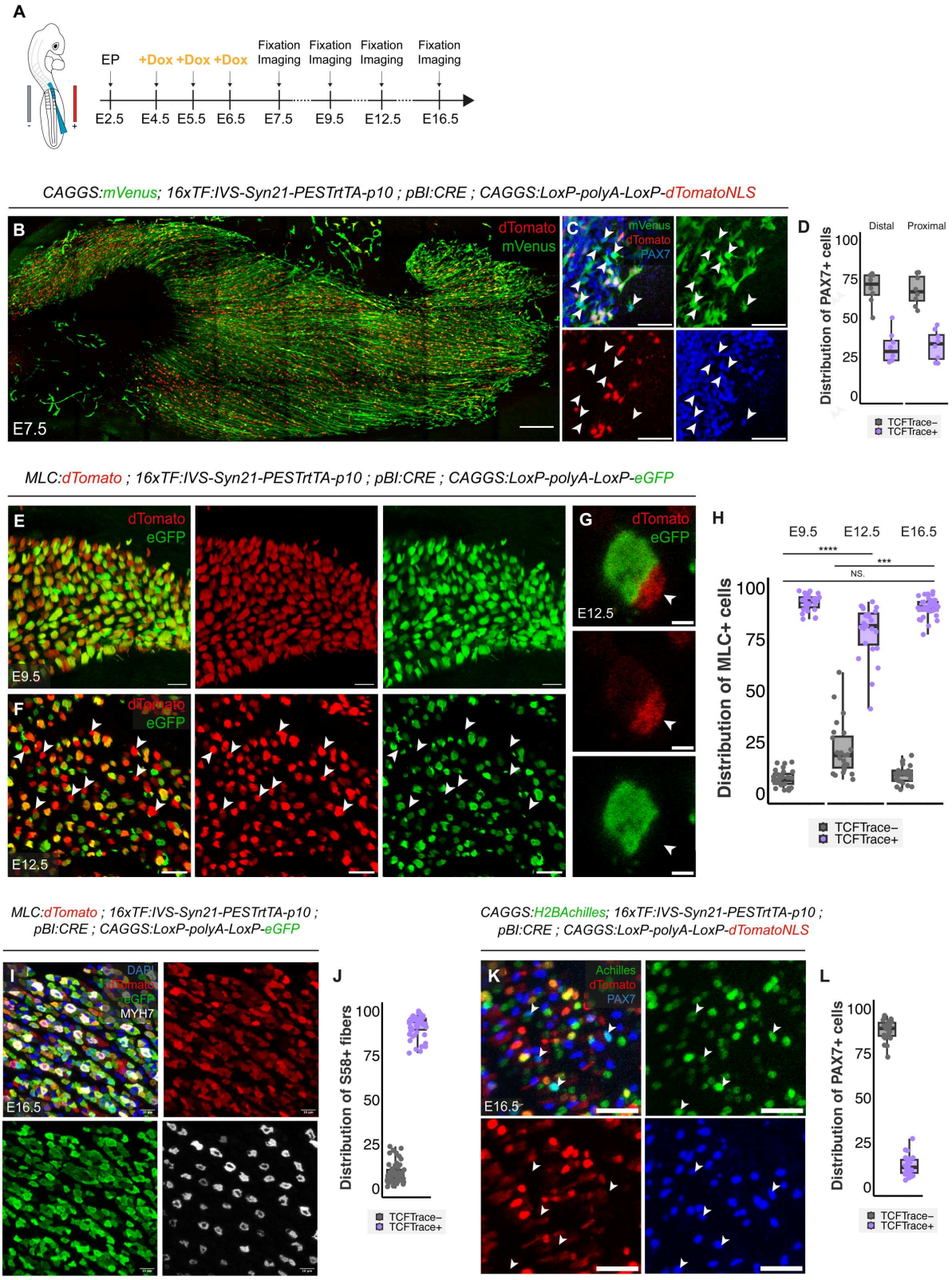

Figure 36. Lineage analysis of TCF-Trace⁺ and TCF-Trace⁻ populations. *(A,B) TCF-Trace was induced with doxycycline during the time period (E4.5-E6.5) in which muscle progenitors respond to TCF/LEF signaling. Brachial somites of E2.5 embryos were electroporated, TCF-Trace was induced 2-4 days later, and embryos were analyzed at various stages from E7.5 to E16.5. (C-D) Dorsal view of confocal stacks of E7.5 limb bud electroporated with a ubiquitous mVenus, the TCF-Trace lineage tool driving the expression of a nuclear dTomato and stained for PAX7. (D) is an enlargement of (C). (E) Quantification of the percentage of TCF-Trace⁻ or TCF-Trace⁺ cells in the PAX7⁺ electroporated population at E7.5 in the proximal and the distal part of the muscle mass. (F,G) Transverse sections of E9.5 (F) and E12.5 (G) limb buds electroporated with a myofiber-specific dTomato and the TCF-Trace lineage tool driving the expression of eGFP. (H) Representative example of a TCF-Trace⁺ myotube surrounded by a*

smaller TCF-Trace⁻ myotube (white arrowhead). (I) Quantification of the percentage of TCF-Trace⁻ and TCF-Trace⁺ myotubes in the MLC⁺ electroporated population. (J) Transverse sections of E16.5 limb buds electroporated with a myofiber-specific dTomato, the TCF-Trace lineage tool driving the expression of eGFP and stained for MYH7 (S58 antibody, recognizes slow myosin). (K) Quantification of the percentage of TCF-Trace⁻ or TCF-Trace⁺ myotubes in the S58⁺ electroporated myotubes. (L) Transverse sections of E16.5 limb buds electroporated with a nuclear Achilles, the TCF-Trace lineage tool driving the expression of a nuclear dTomato and stained for PAX7. (M) Quantification of the percentage of TCF-Trace⁻ or TCF-Trace⁺ cells in the PAX7⁺ electroporated population. Each dot represents a section, n=7 limbs. Scale bars: 10µm (J, L, H), 20µm (F,G), 50µm (D), or 200µm (C).

TCF/LEF signaling regulates the migration of primary myoblasts via Cxcr4

Knowing that TCF/LEF activity was a marker for primary myoblasts, we wondered its actual role during the early stages of limb muscle development. As said above, it has been independently proposed that the Wnt-TCF/LEF signaling might be an inhibitor, an activator or dispensable for the entry in the myogenic lineage (Abu-Elmagd, 2010; Anakwe et al., 2003; Geetha-Loganathan et al., 2005; Hutcheson et al., 2009; Miller et al., 2007). As most of the molecular tools used were not targeting only the myogenic progenitors or interfering with their epithelial status, by playing with the β-catenin, we decided to circumvent these issues by using a plasmid coding for a dominant-negative form of *Lef1*, a transcriptional effector of the TCF/LEF signaling pathway (Linker et al., 2005). We electroporated brachial somites with a nuclear dTomato as an electroporation marker alongside or not the plasmid coding for the dominant negative *Lef1*. While the control muscle masses exhibited a compact pear-shaped organization (Fig37. A), the one in which TCF/LEF signaling has been totally blocked shown two major defects (1) they were not as compacted as in the control, with cells losing their cohesivity and (2) a lot of myoblasts were accumulating at the proximal-most part of the limb (Fig37. B). These results were quantified by measuring the percentage of dispersion and the shifting of the mass center of the muscles masses (Fig37. C,D, see Materiel and Methods). Interestingly, these effect where neither associated with a lack of entry in the myogenic commitment, as survey by the correct expression of *Myf5* (Fig39. E-G), nor with their proliferative capacity (Fig39. A-D). To validate that TCF/LEF signaling was not involved in later stages of differentiation, we used the Tet-On system to engineer an inducible construct were the DnLef1 is co-expressed with a nuclear dTomato. We injected brachial somites and induced the system with doxycycline at E4.5 and E5.5 and analyzed the limb muscles masses at E6.5 (Fig39. G). While in the control condition, the muscle masses appeared normal, the one with the DNLef1 exhibited several clumps of cells in their most proximal part and a lack of myogenic cells at the distal most part of the limb. Furthermore, both non-induced and induced cells were exhibiting similar levels of the terminal differentiation marker, *MyoG*, demonstrating that Wnt-TCF/LEF is not required neither for the early and late myogenic differentiation and proliferative status but rather is essential to confer a proper migration and 3D organization to the embryonic muscle masses.

To gain some insight into the molecular mechanism regulated by the TCF/LEF signaling, we extracted myoblasts from limb buds electroporated with both a ubiquitous red fluorescent reporter and the 16TF-VNP and shorted them according to the red fluorescence. We next perform single-cell RNA-seq (scRNA-seq) on this enriched population of myoblasts (Fig37. E). By using unsupervised graph-based clustering and embedded cells with FFT-accelerated interpolation-based t-SNE (Flt-SNE) we found several clusters, including reb blood cells, macrophages, fibroblasts, endothelial cells and a biggest cluster of myogenic cells (Fig37. A). We next re-clustered the myogenic cells and found that muscle progenitors segregate into 6 different clusters, whose mainly represent proliferating (cluster 1 and 2), differentiating (cluster 0,3,4) and differentiated (cluster 5) myogenic cells (Fig37, F and Fig38. B, C). We next map the presence or absence of the transcripts from the two transgenes that we inserted into the chicken genome, the cells were grouped into two different groups, the dTomato⁺/mVenus⁻ (named dTomato⁺ only) corresponding to the myoblasts not responding to TCF/LEF and the dTomato⁺/mVenus⁺ that correspond to myoblasts actively responding to the TCF/LEF signaling. Interestingly, the dTomato⁺/mVenus⁺ cells were present in all the clusters in similar proportion than the dTomato⁺/mVenus⁻ expect for the cluster 5 (*MyoD*⁺/*MyoG*⁺) that

represents the differentiated myogenic cells, confirming that TCF/LEF responding cells are early muscle progenitors (*Myf5*$^{+}$/*MyoD*$^{-}$) (Fig37 G, H). By performing a differentially expressed gene analysis, we first confirmed that the dTomato^{+}/mVenus^{+} cells show higher level of expression of various Wnt receptors, co-receptors, transcriptional effectors and target genes than the dTomato^{+} only (Fig38. D). On the contrary, these cells were showing higher levels of secreted Wnt inhibitors (Fig38. D). Secondly, we found genes involved in migration/positional cue in the most differential genes for the dTomato^{+}/mVenus^{+} population, such as the actin remodeler, *Wasf3* and *Dcx*, which has been implicated in neuronal migration via microtubule, *Nedd9* that regulates the focal adhesion assembly, or the *Hox* gene family member *Hoxa11 (*Fig37. I*)*. More importantly, we identified *Cxcr4* as one of the major differentially expressed genes, which has been previously defined as a major regulator of limb myoblasts migration (Vasyutina et al., 2005). To test the link between TCF/LEF signaling and the expression of *Cxcr4*, we performed electroporation of the *DnLef1* construct and process the limb buds for HCR FISH in order to detect the expression of *Cxcr4* at the cellular level. In agreement with our hypothesis, the expression of *Cxcr4* was drastically reduced in PAX7^{+} electroporated myoblasts compared to their non-electroporated counterparts (Fig37. J-L). Altogether these results strongly suggest that the Wnt-TCF/LEF signaling is essential in a sub-population of primary myoblasts to drive the expression of genes involved in migration, including *Cxcr4*, and confirmed that the muscle progenitors at the origin of the primary myotubes are more sensitive to positional cue than their neighbors.

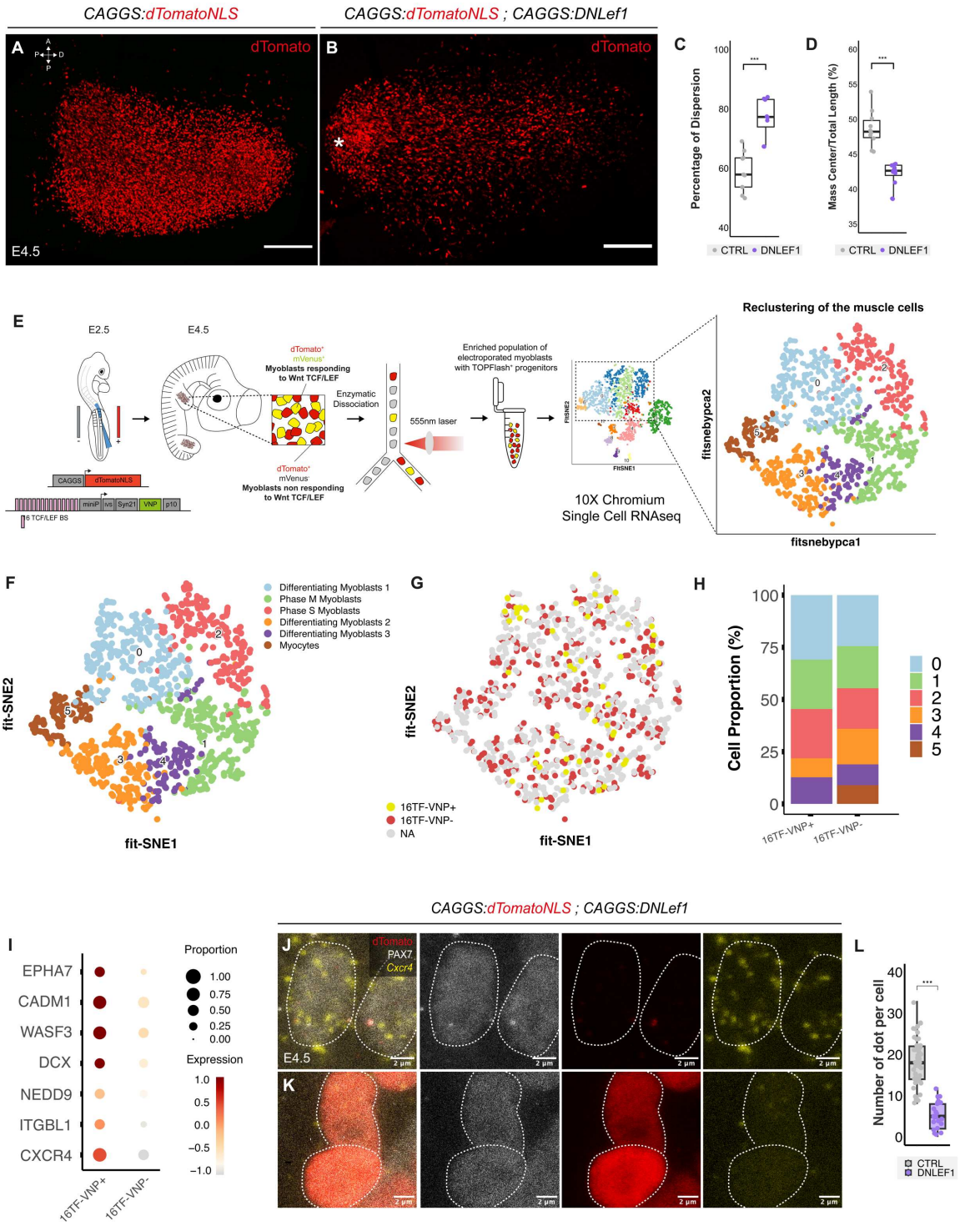

Figure 37. Functional role of TCF/LEF signaling in primary myoblasts *(A,B) Dorsal view of confocal stack of E4.5 limb bud electroporated with a ubiquitous dTomato with or without the DnLef1 plasmid, the asterisk in (B) indicate the accumulation of cell at the proximal-most level. (C-D) Quantification of the percentage of dispersion (C) or the shift of the mass center (D) of the muscle mass in the two conditions. (E) Experimental pipeline to perform the scRNA-seq on purified electroporated myoblasts. (F) Single-cell transcriptomic analysis showing the integrated Flt-SNE with the six clusters color-coded. (G) Single-cell transcriptomic analysis showing the presence of the dTomato⁺ only cells and the dTomato⁺/mVenus⁺ cells in the various clusters (H) Proportion of the dTomato⁺ only cells and the dTomato⁺/mVenus⁺ cells in the various clusters. (I) Bubble plot representing the genes involved in migration/positional cue positively differentially expressed in the dTomato⁺/mVenus⁺ compared to the dTomato⁺ only. (J,K) HCR FISH for Cxcr4 on limb bud electroporated with a ubiquitous nuclear dTomato and the DNLef1 plasmid, limbs were immunostained for PAX7 to compared electroporated (J) vs non-electroporated myoblasts (K). (L) Quantification of the number of dots for Cxcr4 in the two conditions, each dot represent a cell, n=4 limb buds. Scale bar represents 100µm (A,B).*

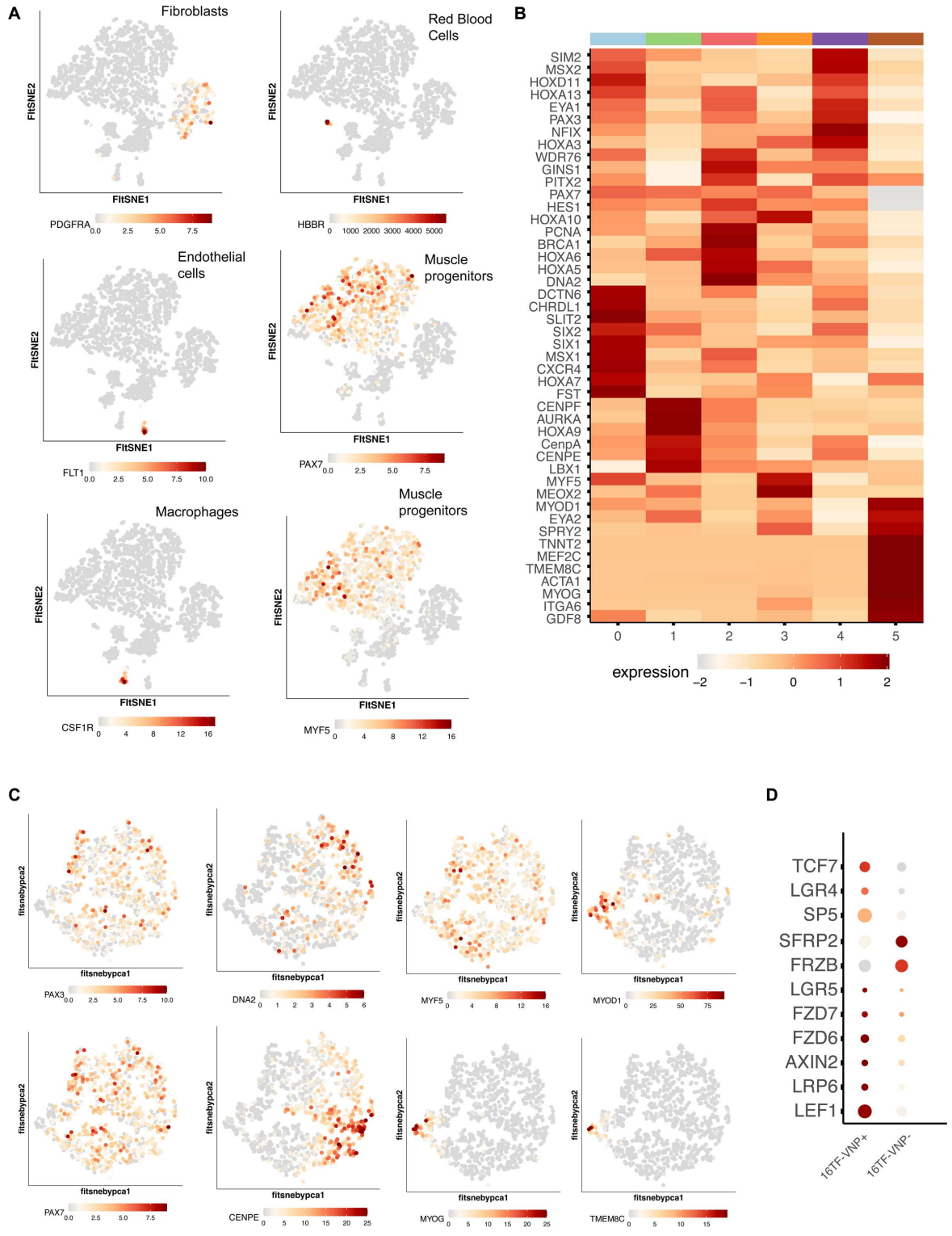

Figure 38. Single-cell transcriptomic analysis of sorted myoblasts. *(A) Expression of various markers for different cell lineages in raw dataset. (B) Heatmap showing the expression of some differentiated genes in the 6 myogenic clusters (C) Representation of some key genes in the myogenic clusters (D) Differential gene expression of Wnt-TCF/LEF related genes in the dTomato⁺ only and the dTomato⁺/mVenus⁺ population.*

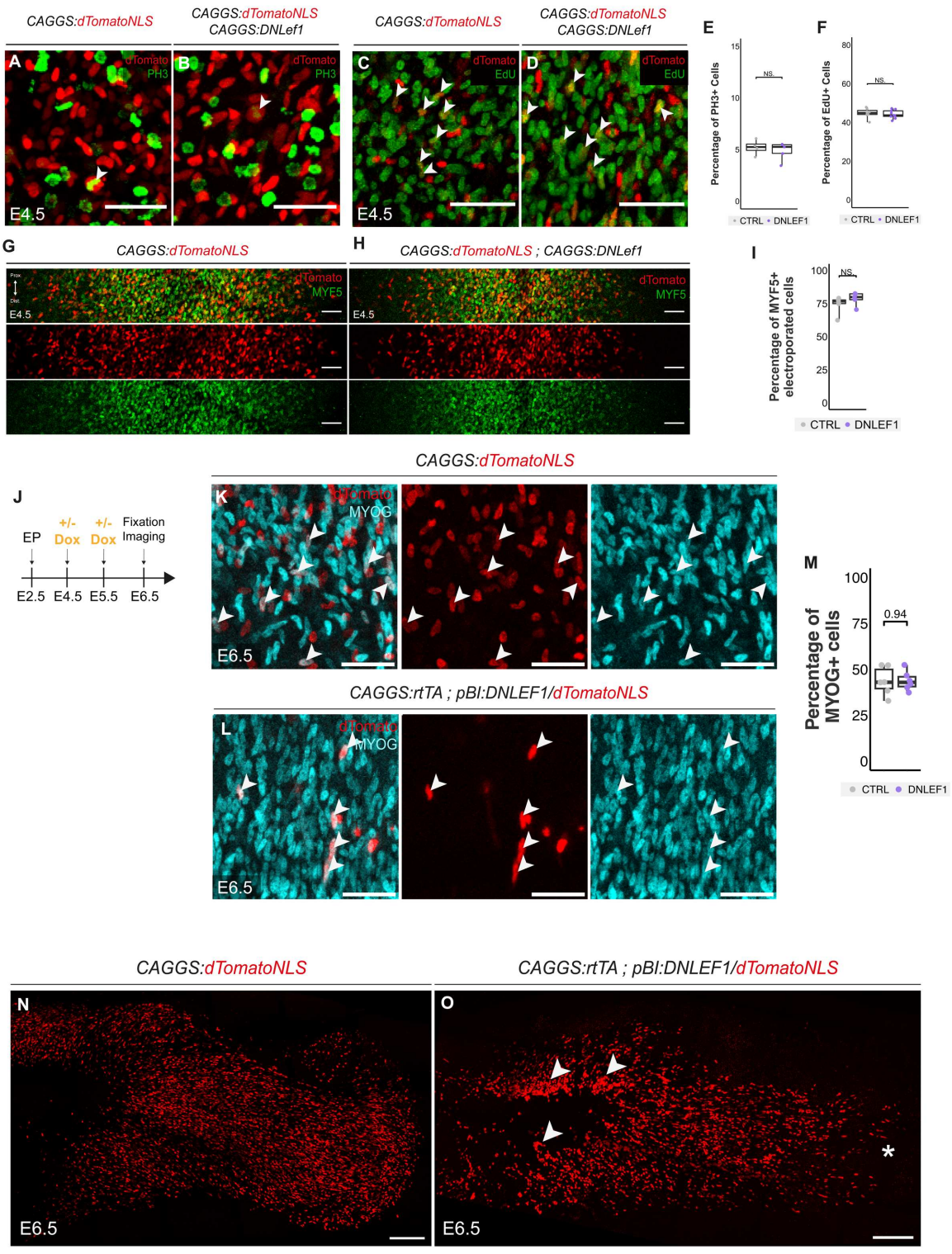

Figure 39. Functional analysis of the TCF/LEF signaling in limb myoblasts. *(A) Dorsal view of confocal stack of E4.5 limb bud electroporated with a ubiquitous nuclear dTomato with or without the DNLef1 plasmid and immunostained for the phosphor-histone H3 (PH3) (B) Dorsal view of confocal stack of E4.5 limb bud electroporated with a ubiquitous nuclear dTomato with or without the DnLef1 plasmid and exposed to EdU for 1h. (C,D) Quantification of the percentage of PH3⁺ and EdU⁺ cells in both conditions. (G) Brachial somites were electroporated at E2.5 with a ubiquitous nuclear dTomato or with a ubiquitous rTta alongside a plasmid with a bi-directional promoter driving the expression of a nuclear dTomato and the DNLef1 at the same time. Embryos were exposed to doxycycline at E4.5 and E5.5. (H,I) Dorsal view of confocal stack of E6.5 limb bud electroporated with a ubiquitous nuclear dTomato or the ubiquitous rtTA and the inducible nuclear dTomato and DNLef1. Arrowheads indicate the clumps of cell in the proximal-most part, while the asterisk indicates the depletion of myoblasts in the most distal part. (J-K) Enlargement of (H) and (I), respectively, and stained for MYOG. (K) Quantification of the percentage of MYOG⁺ cells in both conditions*

Results

Late Patterning of the Epaxial Musculature

Long epaxial muscle are present in the back and neck of birds

Detailed anatomical descriptions of epaxial anatomy of birds are quite sparse and mainly focused on the neck region. The first drawing of neck epaxial muscles can be traced back to 1890, by Shufeldt, who examined raven cadaver (Shufeldt, 1890). More recently, in the 60's, together with a turkey anatomical study by Harvey et al., a detailed overview of 11 orders of birds conveyed a more exhaustive view of the general pattern of bird neck musculature, including Galliformes, with the green pheasant and the domestic turkey as mentioned (Harvey et al., 1969; Kuroda, 1962) . This study by Nagahisa Kuroda confirmed that a general architecture tends to be conserved in all birds, but some particularities might exist, such as the *m. biventer cervicis* being completely absent in some clades, while being composed of only one long muscle bundle, without any medial tendon, in penguins. More recently, anatomical dissection coupled with CT scan imaging of the American barn owl and several species of vultures provided a more detailed comprehensive blueprint of the musculoskeletal origins and insertions of the neck epaxial musculature (Böhmer et al., 2020; Boumans et al., 2015). As no anatomical preparation of neck musculature was available for chicken, we undertook neck dissections of adult chicken to confirm if the general pattern of Galliformes was still present in *Gallus gallus*. In addition, we performed a detailed anatomical dissection of the back region of a chicken, which, to the best of our knowledge, was not available for any type of birds. Regarding the neck anatomy, the *m. biventer cervicis* was present, originating from the basis of the neck at the level of the first thoracic vertebrae and inserting at the occipital bone. The *m. biventer cervicis* of chicken is composed of two muscles bellies (the *pars caudalis* and the *pars cranialis*) linked by an intermediate tendon (*intersection tendinae*) such as in other birds. The *m. biventer cervicis* therefore span more than 15 vertebrae with the *pars caudalis* being extended over approximatively 7 vertebrae (Fig40. A, B, asterisks). Just under, lays another long muscle referred as the *m. longus colli dorsalis* which, contrary to the *m. biventer cervicis,* harbors a complex attachment pattern with several muscle bundles not completely separated from each other. Still, the *m. longus colli dorsalis pars caudalis* is composed of a long muscle bundle that span over approximatively the same length than the *m. biventer cervicis par caudalis* with three smaller muscle bundles being more and more short as they are more ventrally located (Fig40. A, B). Smaller muscles bundles could be also detected, such as the *mm. interspinales* and the *mm. intertransversarii* linking together two spinous or transvers processes, respectively (Fig40. A, B). On the lateral side of the neck, repeated small muscles, named the *mm. obliquotransversales*, are situated just above the transverses process and appear to be shifted from half a segment compared to the *mm. intertransversarii*, *i.e.* they are centered on the transverse process. Regarding the back anatomy, the first layer is mainly composed of muscle involved in limb movement, that are all hypaxial (except for the CPM-derived *m. trapezius*) but relocated at a dorsal location. The only epaxial muscle directly visible under the skin is the *m. levator caudae* that is situated at the most posterior part of the body, at the level of the pygostyle (Fig40. C). Removing of all the superficial layers revealed the deeper, epaxial musculature (Fig40. D, E). As most of the thoracic vertebrae of birds are fused together either as a notarium or the synsacrum, the thoracic skeleton of birds is quite rigid and concomitantly, the epaxial musculature is reduced compared to others quadruped amniotes. Still, several muscles bundles can be identified, such as the *m. longissimus dorsi* that is located more medially, and the *m. iliocostalis*, alternatively named *m. sacrolumbalis,* and separated into two different parts, a *pars cranialis* and a *pars caudalis*. Moreover, smaller muscles, named the *mm. levator costarum* can be detected in the medial part, associated with ribs. Altogether, this anatomical dissection confirmed that the neck musculature of chicken follows the general organization of birds and demonstrated that the deep back of chicken muscles is also composed of long epaxial muscles bundles

Late development of epaxial muscles in the chicken embryo

The late development of epaxial muscles is poorly known for several reasons: (1) As embryos get bigger with times, the classical imaging technics are not suited for such samples, thus our knowledge mainly relies on a few sections, not giving enough 3D information, (2) epaxial muscles get rapidly

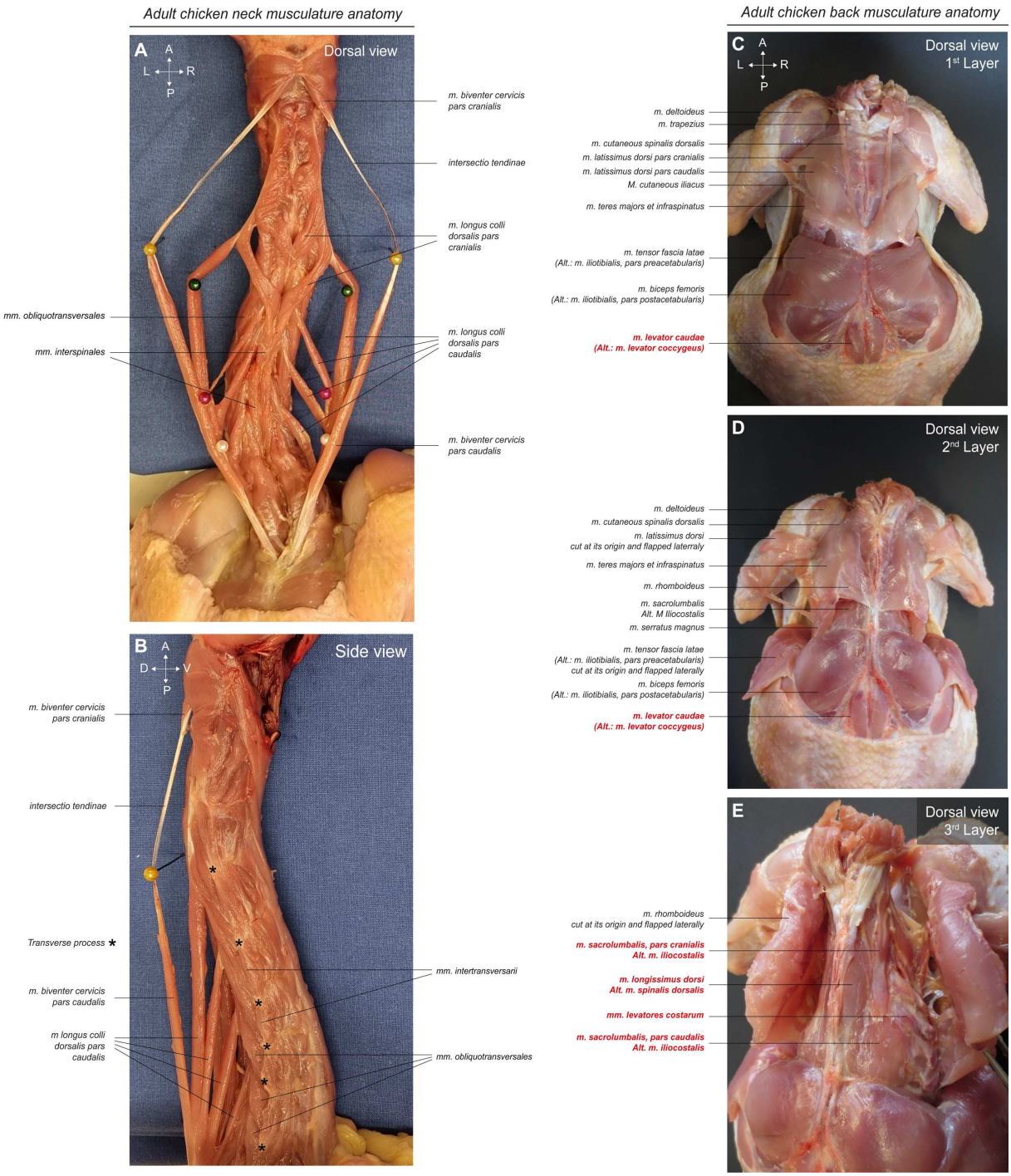

Figure 40. Chicken adult epaxial muscles anatomy. *(A) Dorsal view of neck epaxial muscles with the skin removed. The m. biventer cervicis and all the part of the m. longus colli dorsalis were separated by small pin for easier visualization. (B) Lateral view of the epaxial neck muscles, the transverse process of each vertebra is indicated by asterisk. (C-E) Dorsal view of back epaxial musculature with only the skin removed (C), with the m. latissimus dorsi and m. tensor fascia latae cut and flapped laterally (D) or the m. rhomboideus cut and flapped laterally (E), epaxial muscles are indicated in red.*

covered by limb-associated muscles and therefore become non accessible for imaging and (3) simply because nearly all the studies performed on muscle patterning were focusing either on limb or cranial muscle development. To circumvent these imaging problems, we performed whole-mount fluorescent immunostaining against Myosin Heavy Chain (MyHC), a specific marker of terminally differentiated myofibers, coupled with Ethyl cinnamate-based clearing (ECi). This chemical clearing homogenizes the refractive index of the sample, leading to a very high transparency of the embryonic tissues (Masselink and Tanaka, 2023). We then imaged the samples with light sheet fluorescence

microscopy (LSFM). LSFM is particularly appropriate for the imaging of large samples due to very fast-imaging speed, good spatial resolution, and high depth penetration (Huisken and Stainier, 2009; Wan et al., 2019). We imaged chicken embryos at different developmental stages from E5.5 to E8.5. At 5.5 days, the metameric organization of myotomes along the A-P axis of the embryo is still visible (Fig41. A,B). At this stage, however, we observed a few myofibers crossing somitic borders in the most anterior part of the embryo, at the neck level (Fig41. C, white arrowhead). At 6.5 days, in the neck the myofibers have started to loss their segmental organization, with the most medial part being still segmented, pre-figuring the pattern of *mm. interspinales* (Fig41, D). At the forelimb level myotomes have adopted a chevron-shape structure with each myotome recovering the anterior-one and being recovered by some fibers from the posterior one (Fig41. E). At E7.5 days, a long muscle mass extends all along the neck of the embryo with well-defined smaller segmented muscles at the medial level (Fig41. F,G). These two types of organization foreshadow the adult segregation of the long unmetamerized *m. biventer cervicis* and *m. longus colli dorsalis* on one side and the segmented *mm. interspinales* and *mm. intertransversarii* on the other side. Besides, in the trunk, the imbrication of the chevron-shaped myotomes is even more pronounced (Fig41. F). One day later, at E8.5, except in the more medial region, no apparent segmentation is visible, both in the neck and in the trunk. Separation of the muscle bundles starts becoming visible, outlining the late muscle patterning of the embryo (Fig41. I,J). These data show that the segmental organization is gradually lost, initially in the neck region, and rapidly progress posteriorly. This phenomenon is quite fast as it takes only three days from the first myofibers breaking the metamery until a complete apparent loss of segmentation.

Comparative development of epaxial muscles in tetrapods

Even though the epaxial muscles anatomy is well described in human and most mammals such as dogs and horses, for medical and veterinary purposes, the embryology of mammal epaxial muscles remains elusive (Schultz and Elbrønd, 2018; Schünke et al., 2021; Webster et al., 2014). Regarding reptiles, it has been proposed they display a typical amniotes epaxial muscle arrangements, separated into three distinct blocks, with a more or less segmented pattern (Romer and Parsons, 1986). However, a detailed anatomical preparation is hard to find, and developmental studies simply do not exist. Regarding Lissamphibia, general anatomical descriptions of urodeles point toward a conservation of the metameric situation at adult stages, however, most of these studies were performed in axolotls, which is a neotenic animal, *i.e.* that never undergoes metamorphosis and retain juvenile characters throughout its entire life (Liem, 2001). Seminal anatomical studies however suggest a metameric organization of the epaxial muscle in adult salamander, with no further details (Francis, 1934). Nevertheless, no proper dissections are available in the literature for adult axial musculature in metamorphic urodeles. Besides, regarding anurans, anatomy textbooks described the organization of their epaxial muscles as metameric with a *m. longissimus dorsi* composed of several smaller unites spanning the entirety of the back, while more recent studies using CT-scan reconstructions consider the *m. longissimus dorsi* as one and only long muscle (Collings and Richards, 2019; Noble, 1931). However, no cellular description allowing to evaluate the length of epaxial myofibers along the back of anurans are available to date. We therefore performed a survey of epaxial muscle general anatomy in tetrapod representant by examining the development of two non-avians amniotes, the lizard *Anolis sagrei* and the mouse, *Mus musculus*, as well as two Lissamphibia, one urodele, the newt *Pleurodeles waltl*, and one anuran, the African clawed frog, *Xenopus laevis*, at pre- and post-metamorphosis stages. As for the chicken embryos we performed whole-mount fluorescent immunostaining against MyHC, cleared the specimen in ECi and imaged them with a light sheet microscope. Examination of pre- and post-metamorphosis newts revealed that epaxial musculature is segmented all along the antero-posterior axis, from the neck to the end of the tail, at both stages, with the differences that post-metamorphic specimens exhibit a chevron-shaped organization of the non-tail *muscle truncii* that is comparable with the one found in adult fishes or in chicken embryo (Fig42. A-F). For *Xenopus laevis*, the analysis of the pre-metamorphic specimen confirmed the metameric organization of the larvae, with chevron-shaped like structures

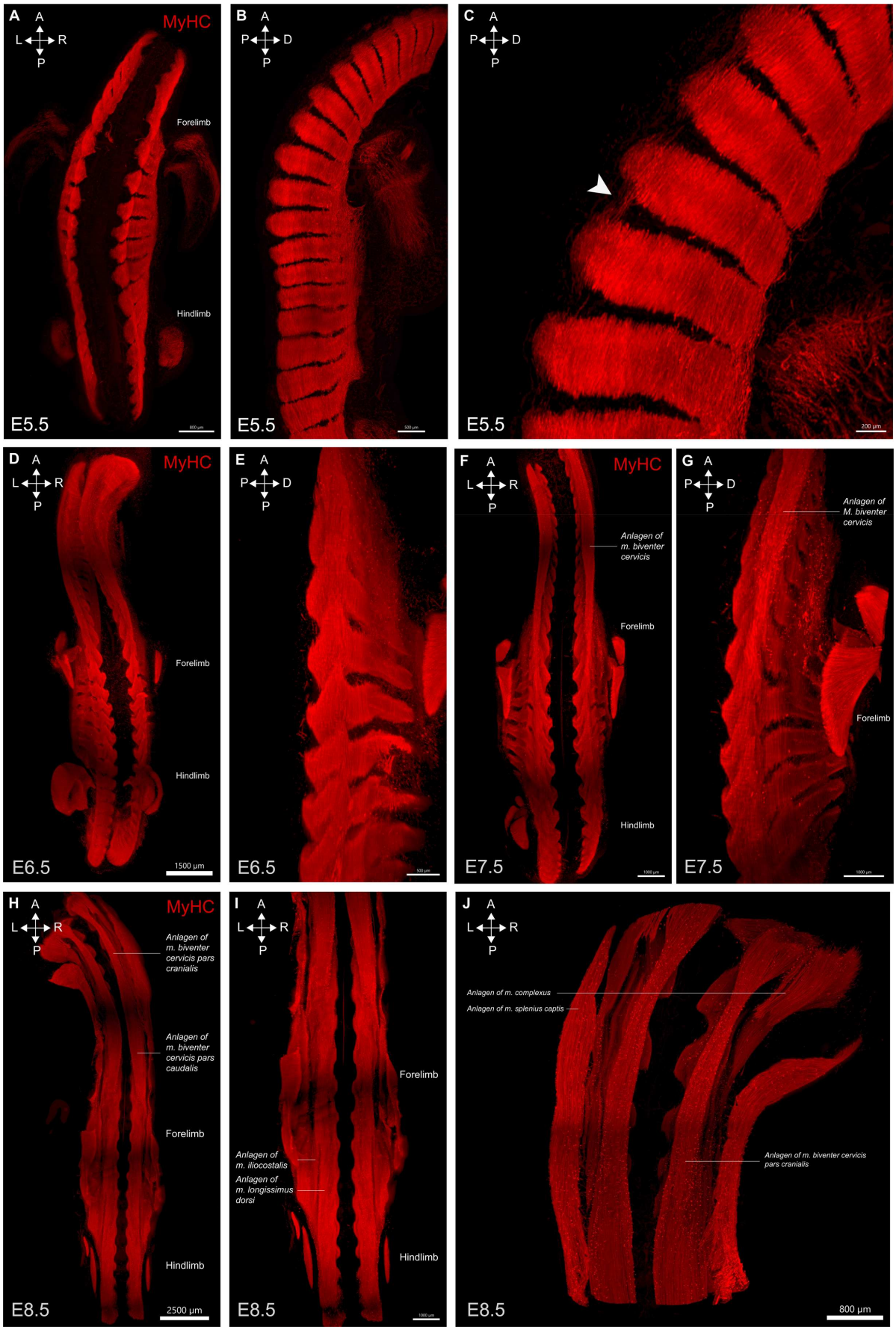

Figure 41. Late development of epaxial muscles in the chicken embryo. *All specimens were stained for myosin heavy chain (MyHC). (A-C) Light-sheet 3D reconstruction of a E5.5 chicken embryo, dorsal view (A), lateral view (B), (C) is an enlargement of (B) at the level of the forelimb, arrowhead indicates fiber breaking the metamery. (D-E) Light-sheet 3D reconstruction of a E6.5 chicken embryo, dorsal*

view (D), (E) is an enlargement of (D) at the level of the forelimb. (F-G) Light-sheet 3D reconstruction of a E7.5 chicken embryo, dorsal view (F), (G) is an enlargement of (F) at the level of the forelimb. (H-J) Light-sheet 3D reconstruction of a E8.5 chicken embryo, dorsal view (H), (I) is an enlargement of (H) at the level of the back and the basis of the neck, (J) is an enlargement of (H) at the level of the basis of the skull.

as it can be found in adult newt and fishes (Fig42. D,E). As reporter for other anurans, two long muscles, laying of each side the spinal cord can be observed in the back of *Xenopus laevis* froglet, however, small fibers can be detected, suggesting a metameric pattern also in adult (Fig42. F,G). To be sure of these wholemount observation we performed parasagittal sections of both adult species and stained them for MyHC and DAPI. Post-metamorphic newt exhibits small fibers being repeatedly separated at the level of each vertebra by non-myogenic interstitial cells (Fig42. H, I, arrowheads). For xenopus, the vertebrae were not visible, probably because the epaxial muscles are located just beneath the ectoderm while the vertebrae are deeper in the back. Still, we were able to confirm that the *m. longissimus dorsi* of *Xenopus laevis* is in fact composed of small fibers separated by non-myogenic interstitial cells. They form several *muscle truncii* highly overlayed between each other that give the macroscopic impression of one and only *m. longissimus dorsi* (Fig42. J,K, white arrowheads).

For *Anolis sagrei* early embryos, we observed that the transition for a complete metameric state to a re-organization of the myotome was happening between stage 4 and 6, which would correspond to E5 to E6 in the chicken (Fig43. A,B). More interestingly, unlike chicken embryo, the early myotomes were separated into three distinct compartments in a dorso-ventral way, which was more visible at stage 8 and 12, with the most dorsal one (or medial, depending on the orientation) being composed of both small, segmented muscles, and non-segmented muscle bundles, that could correspond to the *m. transversospinalis* of mammals (which is a general term englobing the small *mm. interspinales* and *intertransversarii* with longer non-segmented muscles). The second medial muscle bundle seem to pre-figure what could be called the *m. longissimus dorsi*, while the most lateral one seems to be the anlage of the *m. iliocostalis* (Fig43. E-G). More cranially, the anlagen of the *m. complexus* and *m. splenius capitis* can be observed (Fig43. H). Examination of mice embryos between E12.5 and E15.5 also revealed that the re-organization of the myotome was happening quite fast, in between E12.5 and E13.5 (Fig43. I,J). By E14.5 the cleavage between the unsegmented epaxial muscle mass and the more ventral rib-associated musculature is clearly visible (Fig43. K). By E15.5 the anlagen of the *m. transversospinalis*, *m. longissimus dorsi* and *m. iliocostalis* are recognizable. Altogether these comparative embryology analyses demonstrated that contrary to what is has been supposed with recent CT-scan data, all Lissamphibia possess a metameric epaxial musculature composed of juxtaposed *muscle truncii,* more or less overlapping each other depending on the clade. Besides, the three amniotes representant that we examined (chicken, lizard and mouse) altogether exhibit a re-arrangement of the myotome at equivalent embryonic stages, and all went to a chevron-shape like structure before forming the various epaxial muscle anlagen.

ECM remodeling is associated with epaxial muscle development

Extra-cellular matrix is highly involved in several step of myogenesis, from somite formation to the formation of the satellite cells niche (Bröhl et al., 2012; Thorsteinsdóttir et al., 2011). Regarding epaxial muscle, the re-organization of the myotomes around E13.5 in mice has already been associated with ECM remodeling, especially regarding tenascin, an extracellular matrix glycoprotein broadly expressed within developing connective tissues such as tendons (Deries et al., 2010). We therefore wondered if the same kind of mechanisms was happening in chicken embryos, with Tenascin and others ECM proteins. As a first insight, we performed 3D light sheet imaging of E5.5 and E6.5 chicken embryos immunostained for both MyHC and laminins. Laminins are one of the main components of the basal lamina and have already been shown to be associated with myotome formation at early stages (Thorsteinsdóttir et al., 2011). Concomitantly, at E5.5 the laminin staining

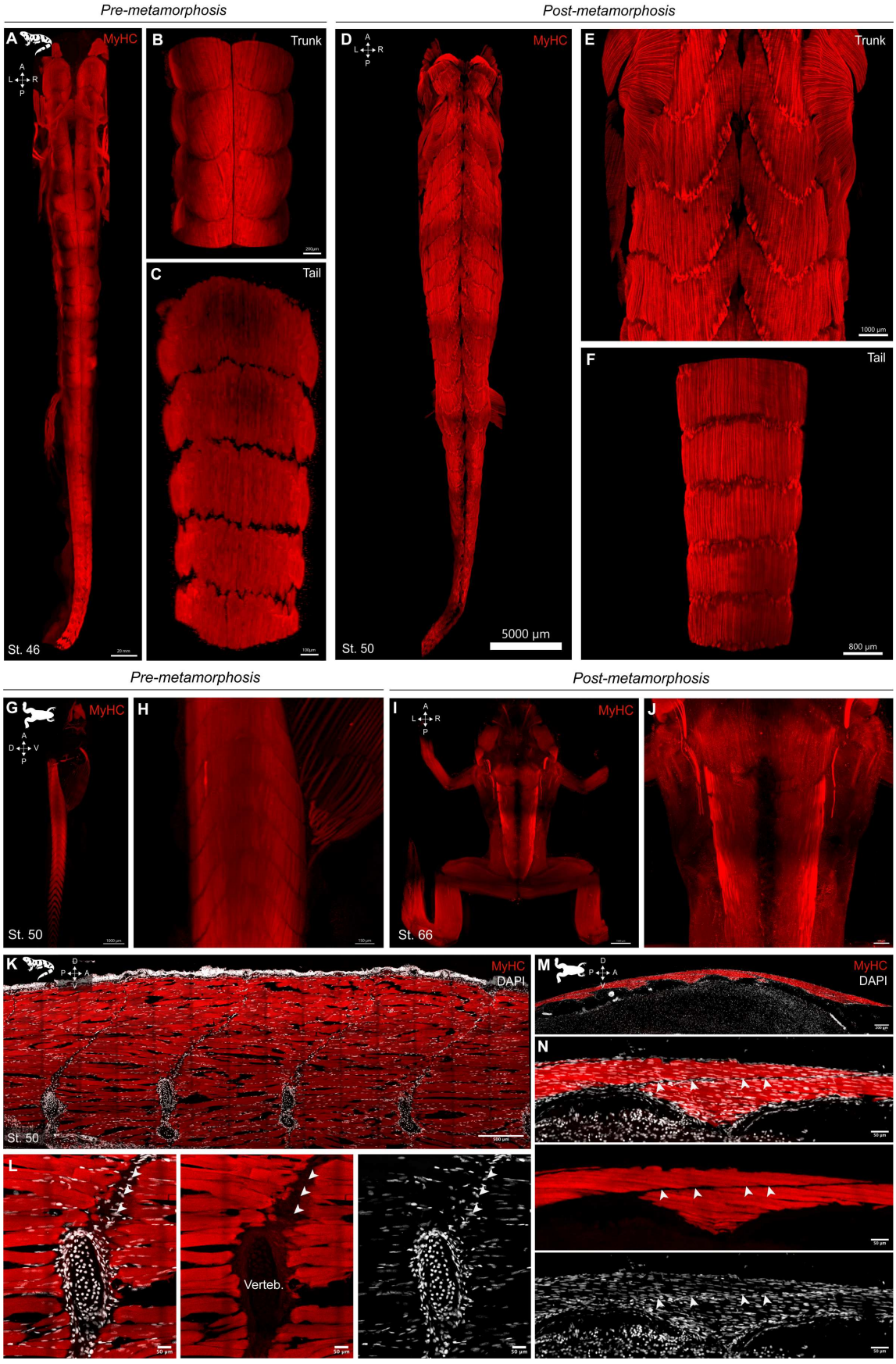

Figure 42. Epaxial muscle anatomy in Lissamphibia. *All specimens were stained for myosin heavy chain (MyHC) (A-C) Light-sheet 3D reconstruction of a stage 46 (pre-metamorphosis) specimen of Pleurodeles waltl, dorsal view, (B) and (C) are enlargements of (A) in the trunk and the tail region, respectively. (D-F) Light-sheet 3D reconstruction of a stage 50 (post-metamorphosis) specimen of Pleurodeles waltl, dorsal view, (E) and (F) are enlargements of (A) in the trunk and the tail region,*

respectively. (G,H) Light-sheet 3D reconstruction of a stage 50 (pre-metamorphosis) specimen of Xenopus laevis, lateral view, (H) is an enlargement of (G) in the branchial region. (I-J) Light-sheet 3D reconstruction of a stage 66 (post-metamorphosis) specimen of Xenopus laevis, dorsal view, (J) is an enlargement of (I) in the trunk region. (K,L) Longitudinal section of a stage 50 Pleurodeles waltl specimen and stained for MyHC and DAPI, (L) is an enlargement of (K) at the level of one vertebra (verteb.). (M,N) Longitudinal section of a stage 66 Xenopus laevis specimen and stained for Myosin heavy chain and DAPI, (N) is an enlargement of (M)

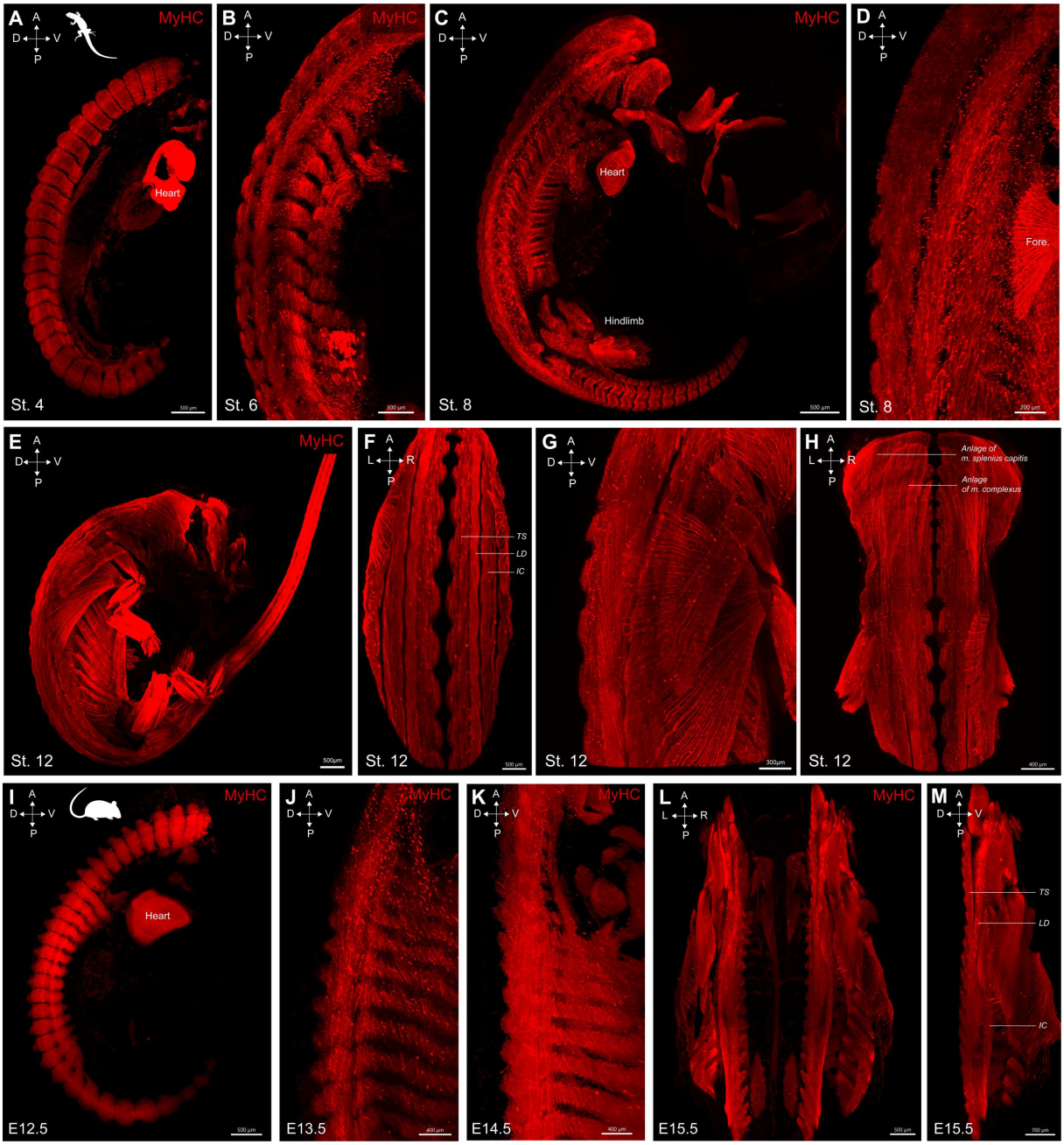

Figure 43. Epaxial muscle development in non-avian amniotes. *All specimens were stained for myosin heavy chain (MyHC). (A-H) Light-sheet 3D reconstruction of Anolis sagrei embryos from stage 4 to stage 12, (A) to (E) are lateral views, (F) is in enlargement of (E) at back level, dorsal view, (G) is an enlargement of (E) at the level of the forelimb, lateral view and (H) is an enlargement of (E) at the level of neck, dorsal view. (I-M) Light-sheet 3D reconstruction of Mus musculus embryos from E12.5 to E15.5, (I) to (K) are lateral views, (L) is a dorsal view, and (M) an enlargement of (L) from a dorso-medial view with the left side removed. TS: anlage of m. transversospinalis ; LD: anlage of muscle m. longissimus dorsi ; IC: anlage of m. iliocostalis*

appears to be a perfect negative of picture of the myotome, especially enriched at the junction between two adjacent myotomes (Fig44. A). This pattern is preserved one day later, in the most ventral part of the myotome, but at the dorso-medial level, where fibers have break the metamery, the laminins repartition appears more diffuse, and the previous well-defined borders of each myotome are not visible yet (Fig44. B). As several components of the muscle-associated ECM are also expressed in the surrounding epidermal and dermal tissues we switch back to parasagittal sections to more carefully inspect the distribution of two others ECM components, the fibronectin and the tenascin. We sectioned E6.5 chicken embryos longitudinally and compared locations where myotomes are still segmented with the anterior most, unsegmented myotomes. Not only for laminin but also for fibronectin and, as expected, tenascin, we observed a complete reorganization of these three ECM components following epaxial muscle unmetamerization (Fig44. C-F). These stainings therefore strongly suggest that an ECM remodeling is concomitant to epaxial muscle elongation, however if this phenomenon either is a cause, or a consequence to the first one remains to be determined.

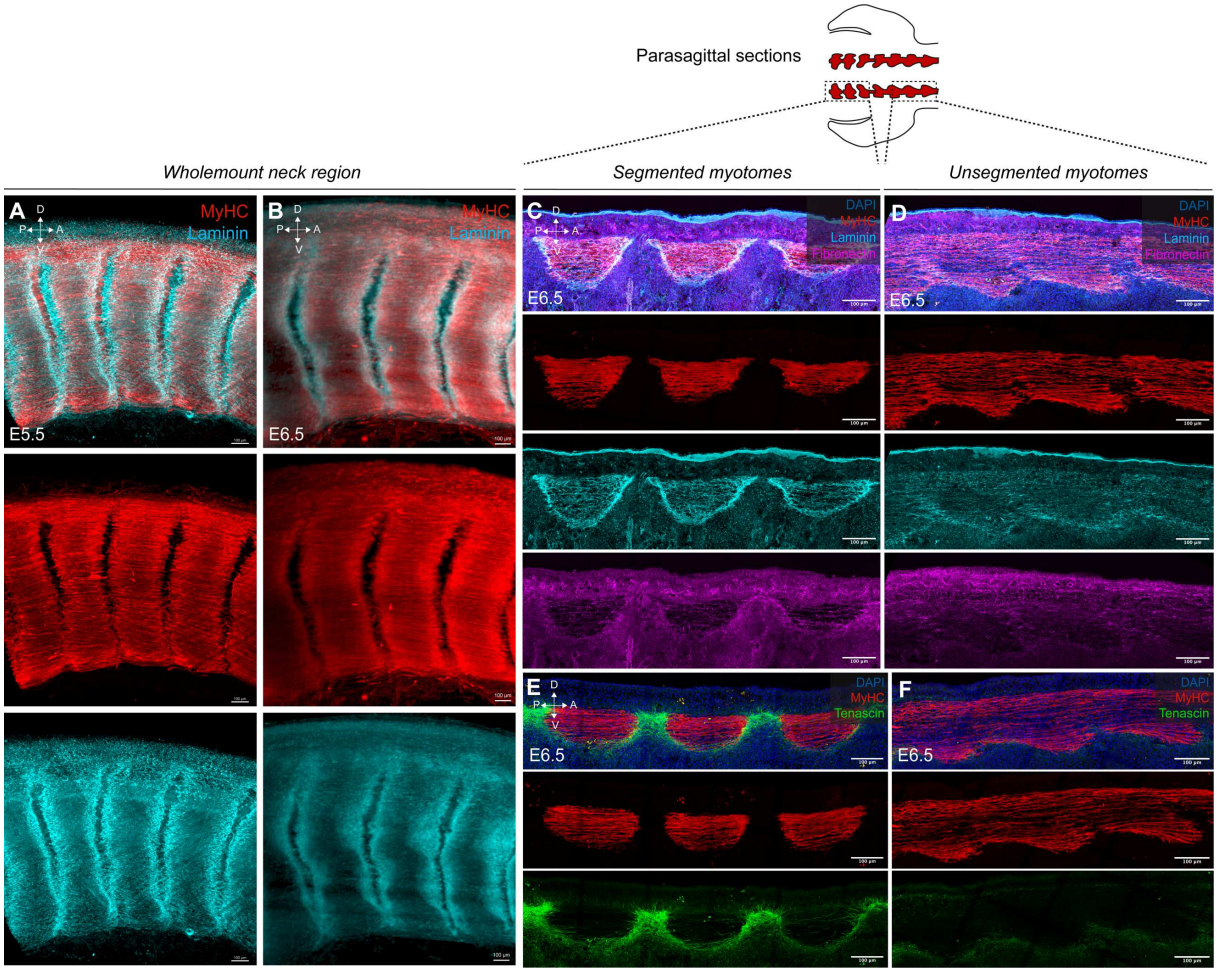

Figure 44. Extra-cellular matrix remodeling during metamery breaking. *(A-B) Light-sheet 3D reconstruction of a E5.5 (A) or E6.5 (B) chicken embryo stained for Myosin heavy chain and laminin at the level of the neck. (C-D) Parasagittal sections of E6.5 chicken embryo at a level where myotome are segmented (C,E) or not (D,F) and stained for Myosin heavy chain, laminin, fibronectin and tenascin.*

Fiber elongation and shifting during epaxial muscle development

Even though the MyHC staining is useful to detect the general re-arrangement of myofibers during late development of epaxial muscles, the high density of muscle fibers at these stages cannot allow us to study individual myofiber at a cellular resolution. To circumvent this, we adapt the somite electroporation technic to target the dorso-medial lip of only one somite with a plasmid coding for a

membranal-bound eGFP under the control of a myofiber specific promoter (*MLC:eGFP-CAAX*). We first electroporated the somite 15, in the cervical region and follow the fate of the myofibers coming from this segment at E6.5 and E8.5 (Fig45. A). At E6.5 days, while most of the myofibers are short and remain segmented in the ventral part of the myotome, in the most dorsal part we observed small myofibers shifting either anteriorly or posteriorly (Fig45. B, D). Moreover, myofibers start to elongate also in both antero-posterior direction, only in the dorsal most part of the myotome (Fig45. B, E). Two days, later, at E8.5 while a small part of the epaxial myotome remains segmented at its ventral most edge, most of the myotome have undergo dramatic changes and really long fibers (up to 1500µm) can be observed in nearly all the dorso-ventral axis of the myotome (Fig45. C, E). Logically, the mean myofibers length at E8.5 had increased by a factor of 2 compared to E6.5 (Fig45. F). Contrary to what happen in limb, the myofiber length in early trunk myotome is not correlated with nuclei gain, both in physiological context during the growth of the embryo, or when fusion is overstimulated via a TGF-β inhibition (Melendez et al., 2021; Sieiro-Mosti et al., 2014). To verify if the myofiber length was correlated with nuclei gain in the late epaxial myotome, we repeated the same experimental setup but used a plasmid that both label the membrane and the nuclei of myofiber with green and red fluorescent proteins, respectively (*MLC:eGFP-CAAX-IRES-NLS-mCherry*, Fig45. G). Interestingly, contrary to the early myotome, from E6.5 the myofibers length was highly correlated with the nuclei number, with myofiber of more 1500 µm bearing 34 nuclei for instance (Fig45. H-L). Altogether, these data suggest that from E6.5 the myotome undergoes dramatic morphogenetic events, whereby the myofibers first elongate in the dorsal most part of the myotome, but also shift both anteriorly and posteriorly. This results two days later in the elongation of nearly all the epaxial myotome, which is supported by the addition of new nuclei to the growing myofibers.

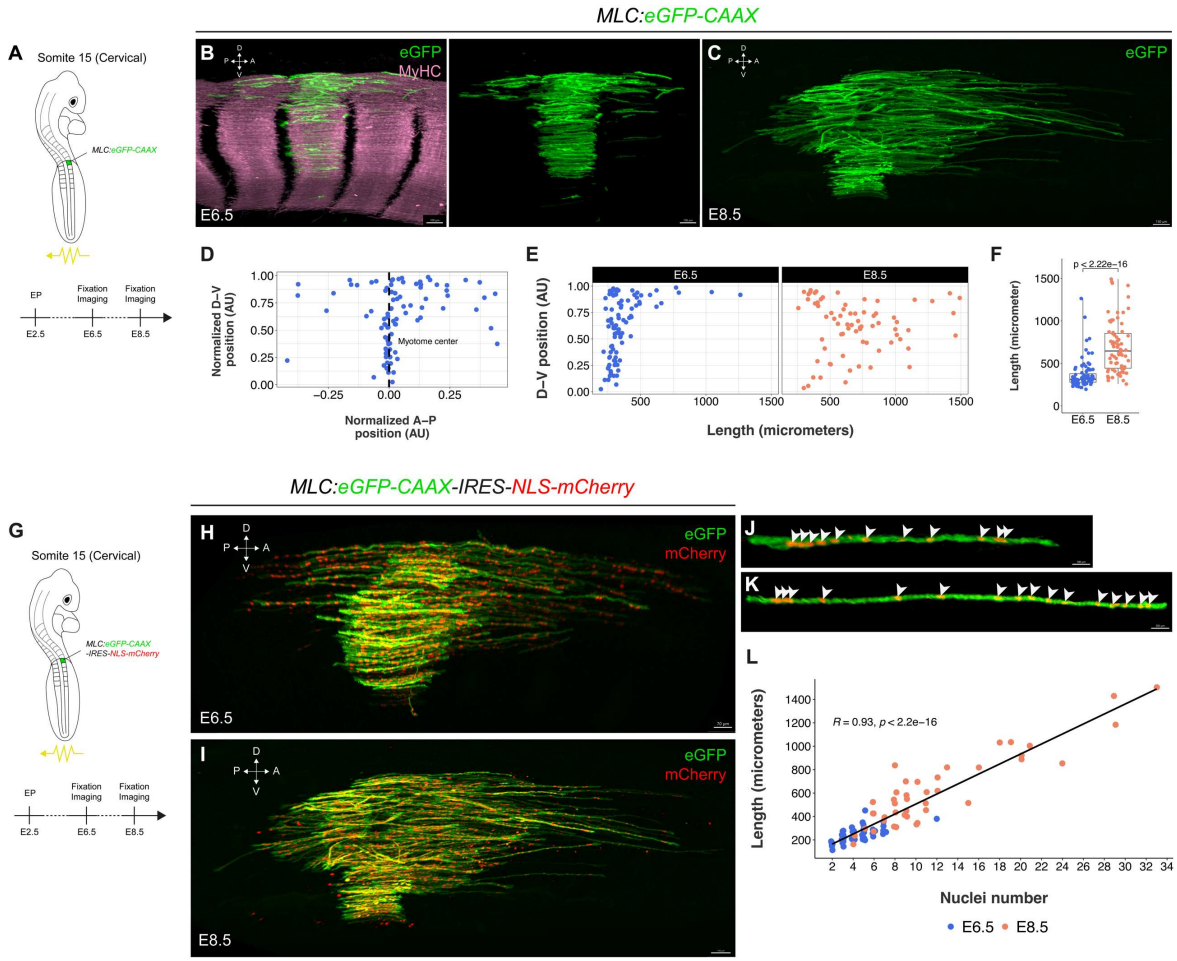

Figure 45. Fiber elongation and shifting during late epaxial muscle development. *(A) Somite 15 of chicken embryo was electroporated with a muscle-fiber specific plasmid driving the expression of a membrane-targeted eGFP (MLC:eGFP-CAAX),*

embryos were analyzed at E6.5 and E8.5. (B) Light-sheet 3D reconstruction of a E6.5 electroporated somite 15 and stained for MyHC. (C) Light-sheet 3D reconstruction of a E8.5 electroporated somite 15. (D) Quantification of the antero-posterior relative position of each fiber regarding the center of the myotome and according to their dorso-ventral position at E6.5. (E) Length of the myofibers according to their dorso-ventral position at E6.5 and E8.5. (F) Myofiber length increase between E6.5 and E8.5. (G) Somite 15 of chicken embryo was electroporated with a muscle-fiber specific plasmid driving the expression of a membrane-targeted eGFP and a nuclear mCherry (MLC:eGFP-CAAX-IRES-NLSmCherry), embryos were analyzed at E6.5 and E8.5 days. (H) Light-sheet 3D reconstruction of a E6.5 electroporated somite 15. (I) Light-sheet 3D reconstruction of a E8.5 electroporated somite 15. (J-K) Electroporated myofibers at E8.5 with different nuclei number. (L) Quantification of the fiber length according to the nuclei number, at E6.5 and E8.5.

Single somite-derivative contribute to different muscle bundles

Only one studies looked at the contribution of a single somite along the antero-posterior axis of the body, only in the neck and occipital region by using quail-chick chimeras. However, the study mainly focused on the occipital bone and even if they claimed that they observed myogenic cells away from the segment of origin, there was no quantification of that, as the analysis was performed on transversal sections. Moreover, the QCPN staining only permits to detect nuclei of quail origin and does not allow to precisely measure the length of a myofiber, in the case where they would have fuse with chicken myogenic cells (Ruijin Huang et al., 2000b). We decided to precise these results by looking at the muscular contribution of a single somite to the cervical or the thoracic domain by targeting either the somite 15 (cervical) or 23 (thoracic) and looked at their derivatives at late fetal stages (E14.5) (Fig46. A,H). Electroporation of the DML of somite 15 leads to a strong labelling of two major neck epaxial muscle anlagen, the *m. biventer cervicis* and the *m. longus colli dorsalis* (Fig46. B, C). Examination on the lateral side revealed that the eGFP was not present in a stripe of muscle in between the eGFP$^+$ *m. biventer cervicis* and the eGFP$^+$ part of the *m. longus colli dorsalis* (Fig46. C). This stripe of muscle is likely to be the most dorsal muscle bundle of the *m. longus colli dorsalis* (see Fig46. A,B), that therefore, does not seem to derive from the somite 15, which only participate in the formation of more ventral muscle bundles of the *m. longus colli dorsalis*. More ventral, on the lateral, side can also be identified several smaller muscles referred as *mm. obliquotransversales*, interestingly, the electroporated somite participated in the formation of three adjacent *mm. obliquotransversales*, the one of the segment of origin, the one just posterior and the one just anterior (Fig46. C). We then immunostained equivalent embryos at E14.5 or younger one, at E9.5, with an antibody detecting the collagen 2, a major constituent of the bone extracellular matrix, to visualize the underlying vertebrae. In order to locate the segment of origin, *i.e.* the putative place of the electroporated somite, we scan the more medial region to detect small fibers connecting two adjacent vertebrae, representing the anlage of one *m. interspinales* (Fig46. D, E, asterisk, see material et methods for a detailed explanation). We then quantify the number of segments on which the eGFP was found, with one vertebra as a unit (Fig46. F). Surprisingly, we found out that at E9.5 eGFP$^+$ myofibers can be found up to 6 or 7 vertebrae anterior to the segment of origin and 2 to 3 posteriorly (Fig46. F). This pattern was conserved five days later, at E14.5 with less variability (Fig46. E,F), even if the absolute length of the eGFP$^+$ domain has double in size (Fig46. G). While the myofibers participating to the formation of the *m. longus colli dorsalis* were found to be packed as well-defined muscle bundles by E14.5, the anterior part of the *m. biventer cervicis* seems to be less sharp, probably because this muscle is composed of two muscle bellies linked together by an intermediate tendon, contrary to the *m. longus colli dorsalis* that originates and inserts on bones. Still, much more eGFP$^+$ myofibers can be detected 7 vertebrae anterior to the segment of origin at E14.5 compared to E9.5 (Fig46. D,E). To validate that this phenomenon was happening all along the antero-posterior axis, we performed then the same experiment in the thoracic region by targeting the somite 23, at the interlimb level (Fig46. H). Surprisingly, we observed that the eGFP was found all along the epaxial musculature of the back of the embryo at E14.5, especially in the *m. longissimus dorsi* and the more lateral *m. iliocostalis* (Fig46. I). Moreover, the eGFP was also found in the most posterior epaxial muscle, the *m. levator caudae*, that appears to form a continuum with the *m. longissimus dorsi*, while at adult stage there are clearly separated by the pelvis. In addition, the eGFP was found more laterally

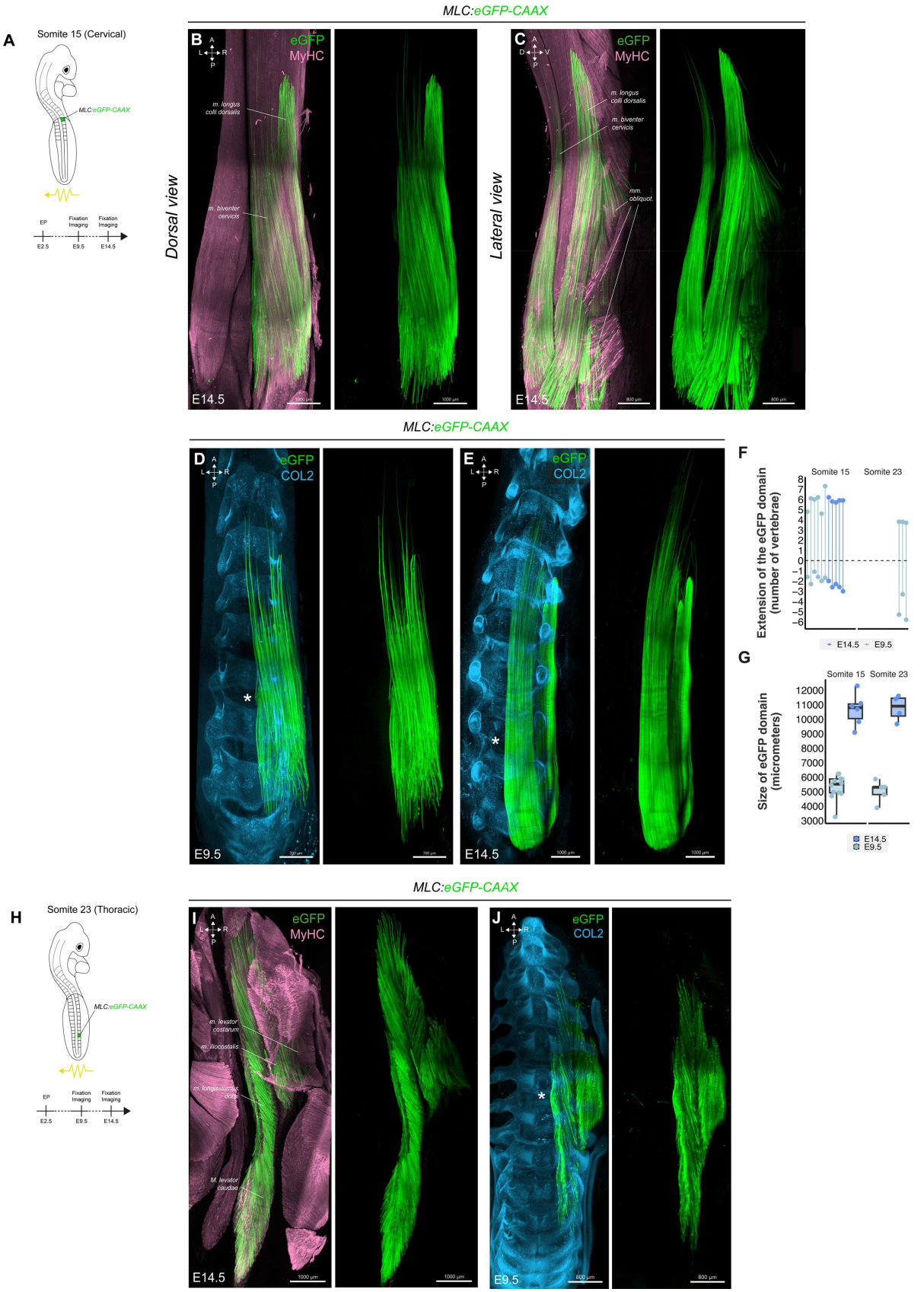

Figure 46. Contribution of a single somite myogenic derivative to adult epaxial musculature. *(A) The somite 15 of a chicken embryo was electroporated with a muscle-fiber specific plasmid driving the expression of a membrane-targeted eGFP (MLC:eGFP-CAAX), embryos were analyzed at E14.5. (B,C) Light-sheet 3D reconstruction of a E14.5 electroporated somite 15 and stained for MyHC, (B) dorsal view and (C) lateral view. (D-E) Light-sheet 3D reconstruction of a E9.5 (D) or E14.5 (E) electroporated somite 15 and stained for Collagen 2. (F) Quantification of the eGFP domain elongation in term of number of vertebrae. (G) Quantification of the absolute size of the eGFP domain. (H) The somite 23 of a chicken embryo was electroporated*

with a muscle-fiber specific plasmid driving the expression of a membrane-targeted eGFP (MLC:eGFP-CAAX), embryos were analyzed at E14.5. (I) Light-sheet 3D reconstruction of a E14.5 electroporated somite 23 and stained for MyHC, dorsal view. (J) Light-sheet 3D reconstruction of a E9.5 electroporated somite 23 and stained for Collagen 2. Asterisks in (D,E,J) indicate the segment of origin.

in a *m. levator costarum* at the level of the corresponding electroporated segment. The analysis of the collagen 2 staining revealed that the eGFP tends to spread nearly equivalently in the anterior and the posterior direction (4 to 5 vertebrae, Fig46. J). Altogether these analyses suggest that one somite can contribute to the formation of several muscle bundles, over great distance (up to 8 vertebrae). However, the mechanism of this, either by fiber extension or, by long distance migration of progenitors remains to be determined.

Myogenic cells coming from the DML are bona fide resident muscle progenitors that can give rise to satellite cells

After birth or hatching, muscle growth is mainly sustained by the addition of new myonuclei from muscle stem cells (the satellite cells) to pre-existing polynucleated myofiber. Satellite cells are the adult muscle stem cell, they express *Pax7* and are present under the basal lamina of each myotubes. In the trunk, these cells originate from the dermomyotome and, more particularly, the central dermomyotome (Gros et al., 2005). The current textbook model is that the different borders of the dermomyotome, including the dorsomedial lip (DML) will form a so-called "primary myotome" during early embryogenesis, while later, the central dermomyotome will invade this primary myotome with proliferating myoblasts that will sustain the growth of the myotome throughout embryonic and fetal life, while some of these resident muscle progenitors will be set aside to form the satellite cell pool. In this model only the central part of the dermomyotome is therefore capable to generate muscle progenitors ($PAX7^+$ cells) during late embryonic life and satellite cells ($PAX7^+$, under the basal lamina) at pre-hatching stages. Here, we challenge this view by using single-somite electroporation. We electroporated specifically the DML of E2.5 chicken embryo at both cervical and thoracic level (somite 15 and 23, respectively) with a plasmid coding for a nuclear Achilles fluorescent protein under the control of a ubiquitous promoter (*CAGGS:H2B-Achilles*) (Fig47. A, F). Three days after electroporation (E5.5), we observed a great number of $PAX7^+$ electroporated cells (Fig47. B, C, and G-H arrowheads). We next performed the same experiment but let the embryo grow until E18.5, two days before hatching, at a time where the satellite cells pool is recognizable thanks to the expression of *Pax7* and their location under the basal lamina. The cervical electroporated region was sectioned and immunostained for both PAX7 and the laminin, a marker of the muscle basal lamina. Again, we detected several electroporated cells positive for PAX7 and located under the basal lamina (Fig47. D,E and I,J, arrowheads). Altogether these results strongly demonstrate that the DML is able to generate not only myofiber that form the early myotome, but also, *bona fide* $PAX7^+$ resident muscle progenitors that will contribute to growth of the myotome and to the satellite cell pool. These results contradict the previous establish model and led us to investigate the cellular behavior of DML-derived muscle progenitors during epaxial muscle development.

Muscle progenitor from the DML migrate over long distance during late epaxial muscle development

As the MyHC staining only labelled nascent to fully mature myofibers, we used PAX7 as a reliable marker of muscle progenitors to study the behavior of muscle progenitors during late epaxial development. It is important to note that *Pax7* is also expressed in the roof of the neural tube and the migrating neural crest cells/melanocytes all around the embryo. We imaged wholemount chicken embryos from E5.5 to E7.5 and observed that at E5.5, even if the ventral part of the myotome is still segmented, $PAX7^+$ progenitors can be identified in between the dorsal part of adjacent myotomes, forming a bridge-like structure (Fig48., A). Furthermore, one and two days after we observed that the

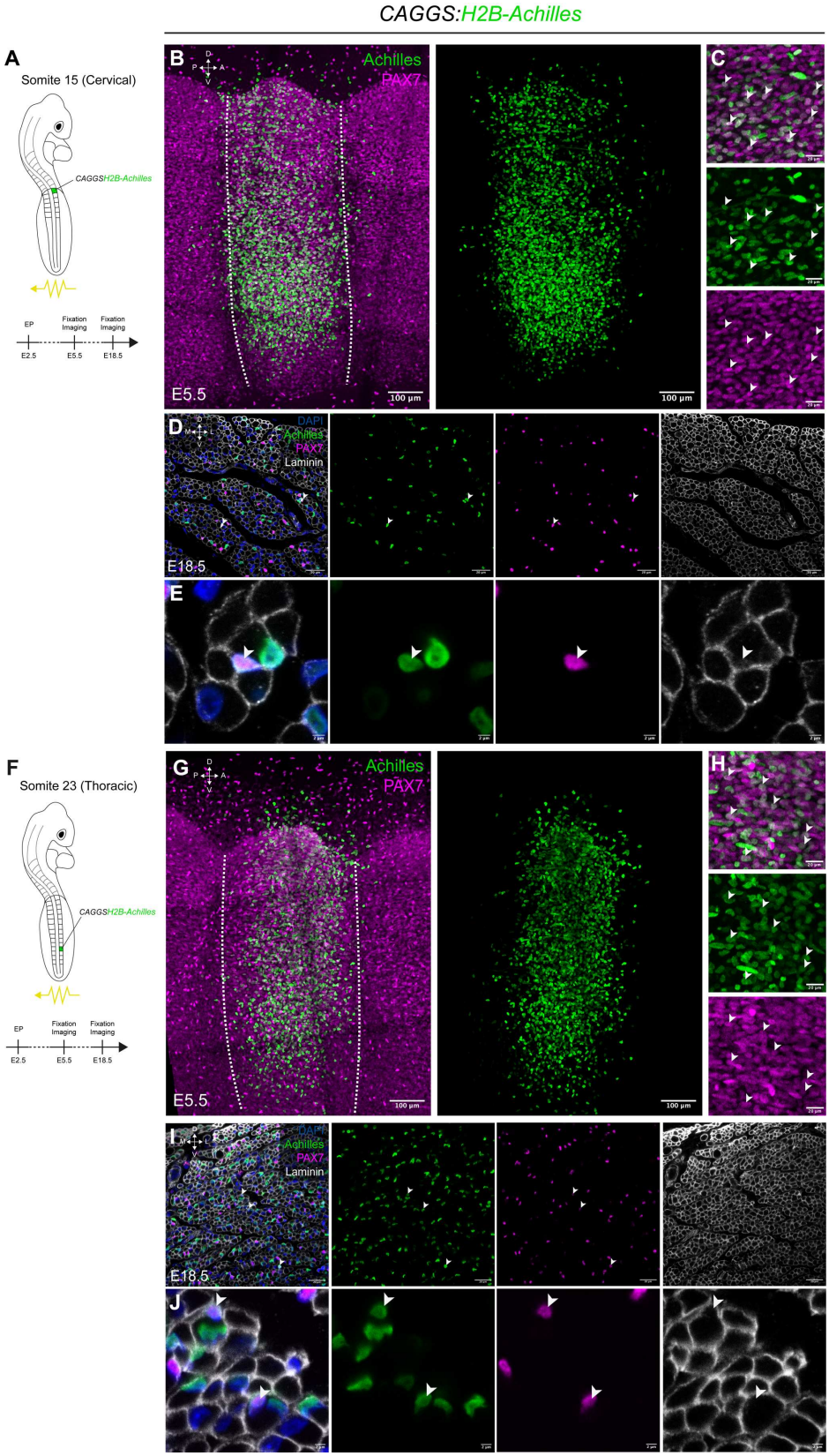

Figure 47. Contribution of DML-derived myogenic cells to the growth of epaxial muscle. *(A,F) The somite 15 (A) or 23 (F) of a chicken embryo was electroporated with a ubiquitous plasmid driving the expression of a nuclear enhanced green fluorescent protein (CAGGS:H2B-Achilles), embryos were analyzed at E5.5 and E18.5. (B,C,G,H) Medial view of a confocal stack an electroporated somite 15 (B,C) or somite 23 (G,H) and stained for PAX7, (C) and (H) are enlargements of (B) and (G), respectively. Arrowheads indicate PAX7⁺ electroporated cells. (D,E,I,J) Transversal sections of electroporated cervical (D,E) or thoracic (I,J) epaxial muscles and stained for PAX7 and laminin, (E) and (J) are enlargements of (D) and (I) respectively, white arrowheads indicate PAX7⁺ cells under the basal lamina.*

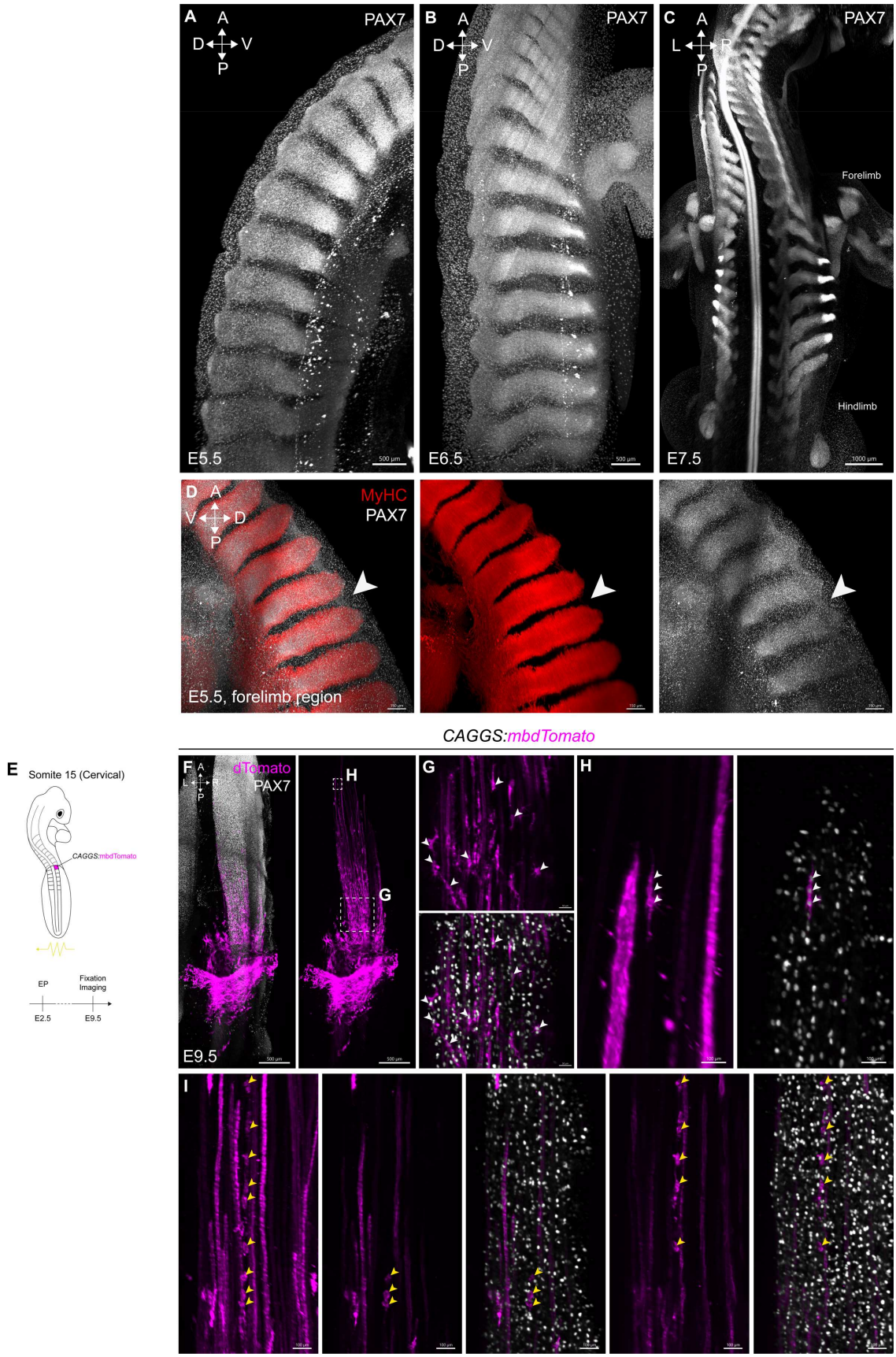

Figure 48. Muscle progenitors during late development of epaxial muscles in the chicken embryo. *(A) Light-sheet 3D reconstruction of a E5.5 chicken embryo stained for PAX7, lateral view at the forelimb level. (B) Light-sheet 3D reconstruction of a E6.5 chicken embryo stained for PAX7, lateral view at the forelimb level. (C) Light-sheet 3D reconstruction of a E7.5 chicken embryo stained for PAX7, dorsal view. (D) Light-sheet 3D reconstruction of a E5.5 chicken embryo stained for PAX7 and MyHC, lateral view, the arrowhead indicated muscle progenitor breaking the metamery one segment before the muscle fibers. (E)*

Somite 15 of chicken embryo was electroporated with a plasmid driving the expression of a ubiquitous membrane-targeted dTomato (CAGGS:mbdTomato), embryos were analyzed at E9.5. (F-H) Light-sheet 3D reconstruction of a E9.5 electroporated somite 15 and stained for PAX7, dorsal view. (H) and (G) are enlargement of (F). White arrowheads indicate PAX7$^+$ electroporated cells. (I) Enlargement of (F) showing aligned PAX7$^-$ cells along myofibers, yellow arrowheads.

myotomes labelled by PAX7 resemble the one observed with the MyHC immunostaining, with equivalent chevron-shaped like structures (Fig48. B,C). We co-immunostained E5.5 chicken embryo for both PAX7 and MyHC and found out that bridge of PAX7$^+$ cells was present one segment before the crossing myofibers (Fig48. D, white arrowhead), confirming that the muscle progenitors break the metamery just before the myofibers. To gain some insight into the cellular repartition of the muscle progenitors coming from a defined segment we electroporated the somite 15 with a membrane-bound dTomato under the control of a ubiquitous promoter and examined the embryos at E9.5. As medial dermomyotome cells give rise to both muscle and dermal lineage we co-immunostained the sample with PAX7, as PAX7 is downregulated upon the entry in the dermal lineage. Besides, the piece of dermis coming from the electroporated DML gave us information about the location of the segment of origin. Careful examination revealed that several muscle progenitors were located anterior to segment or origin (Fig48. F, G). More spectacularly, we detected some muscle progenitors clustering together really far away from the site of electroporation, at the tip of the most anterior myofibers (FigX. H), corresponding to approximately 6 or 7 vertebrae from the segment of origin. In the meantime, we spotted some electroporated PAX7$^-$ cells aligned along myofibers that could be differentiated muscle progenitors aligning to form *de novo* myofibers (Fig X. I, yellow arrowheads). Altogether, these observations provide strong proofs that the muscle progenitors from the DML can break the originally imposed metamery and, adopt a long-range migratory phenotype by travelling as far as 7 vertebrae from their segment of origin.

Alternate electroporation of somites to study the relative contribution of two adjacent myotome to epaxial musculature

Our previous experiments raised two main findings: (1) that myofibers from a defined segment elongate and/or shift antero-posteriorly to form long epaxial myofibers over several segments, via addition of myonuclei and (2) that muscle progenitors can migrate over long distance to break the metamery. Thus, two hypotheses are conceivable, either that myofibers from a defined segment elongate rapidly by addition of nuclei from their own myotome or that several segments participate to the formation of long myofibers by generating myogenic cells that fuse together. To determine between these two hypotheses, we set-up an experimental system where instead of electroporating a single somite, we electroporated two adjacent somites with two distinct plasmids, coding respectively for a membrane-bound eGFP and a membrane-bound dTomato (*MLC:eGFP-CAAX* and *MLC:mbdTomato*). We first validated this approach by analyzing the embryos one day after, at E3.5 when the myotome is still segmented, as seen with the MyHC staining (Fig49., A). Out of 18 embryos electroporated embryos we never detected eGFP$^+$/dTomato$^+$ cells, confirming that this technic allows a precise targeting of each myotome without any leakiness of the system. We then performed the same experiment but dissected the embryos at E6.5 when the myotomes have adopted a chevron-shape structure and myofibers start to break the metamery. At this stage however, even though it is clear the myofibers from a myotome are invaded the next one, we did not detect doubly labelled cells (Fig49., B). One day after, at E7.5 the two myotomes are even more intermingled, nonetheless, transversal optical sections, did not reveal any doubly labelled myofibers (Fig49. C,D). Two days after, at E9.5, we noticed that the longest myofibers in the anterior part of the electroporated domain, were only labelled by one of two fluorophores (Fig49., E,G), however, the picture does not seem that clear in the central and posterior zone, where myofibers are more intertwined (Fig49., F). Unfortunately, the resolution of the optical transversal sections on samples at this stage did not allow us to conclude if *bona fide* doubly labelled myofibers were present or not.

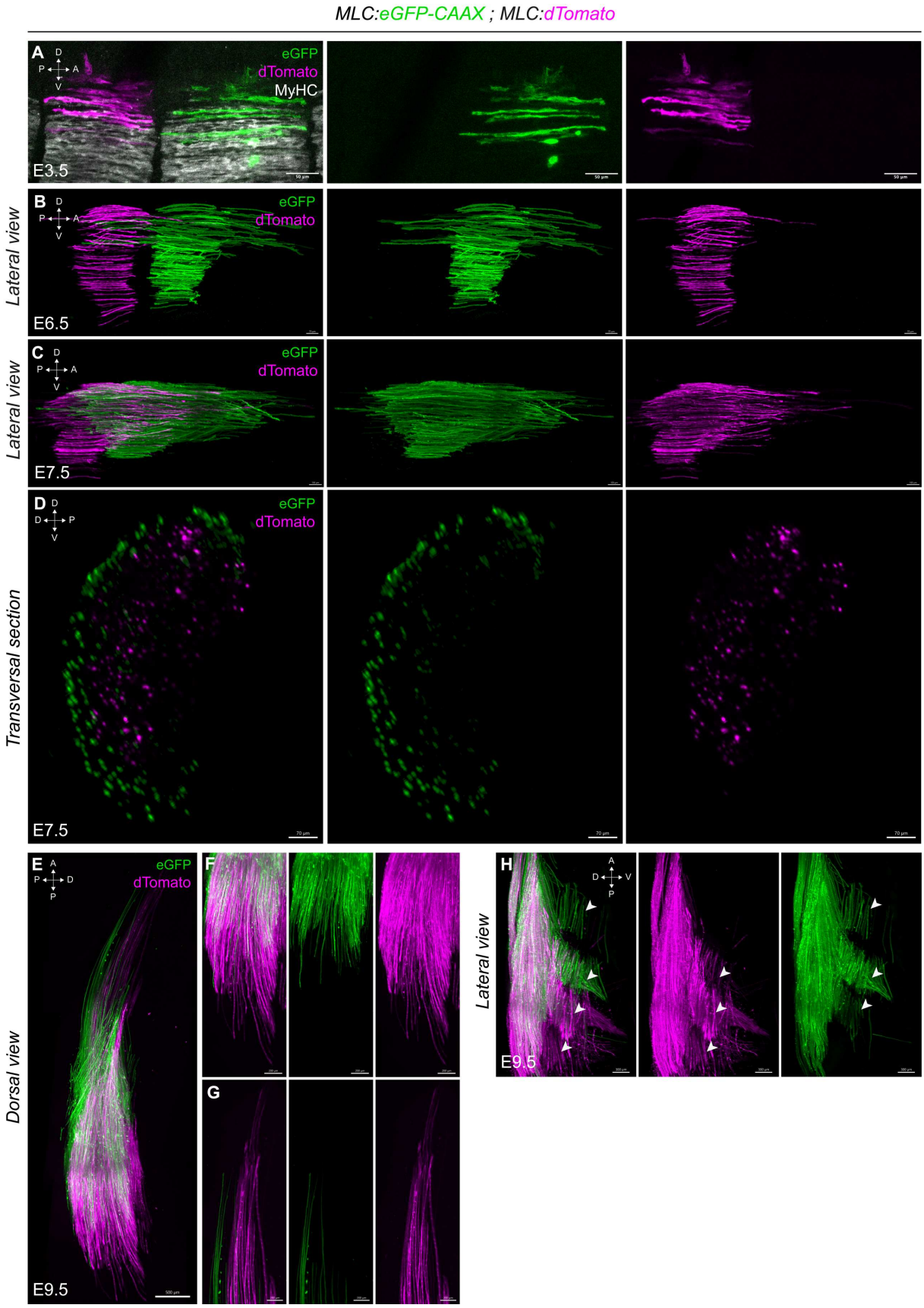

Figure 49. Alternate electroporation of chicken somites. *(A-C) Medial view of a confocal stack (A) or of a light-sheet 3D reconstruction of somite 15 and 16 electroporated with a muscle-fiber specific plasmid driving the expression of a membrane-targeted eGFP (MLC:eGFP-CAAX) or a membrane-targeted dTomato (MLC:mbdTomato), respectively. The most anterior somite was always electroporated with the MLC:eGFP-CAAX plasmid. Embryos were analyzed at E3.5 (A), E6.5 (B) or E7.5 (C). (D) Transversal optical section of (C) showing the clear distinction between the eGFP⁺ and dTomato⁺ myofibers. (E-H) Light-*

sheet 3D reconstruction of a E9.5 electroporated somite 15 and 16. (F) and (G) are enlargement of (E) showing the posterior and anterior part of the electroporated myofibers, respectively. Note that in (G) the long anterior myofibers are expressing only one or the other fluorescent protein. (H) Lateral view of (H) showing the mm. obliquotransversales anlagen (white arrowheads), note that one fluorescent protein is expressed in three successive mm. obliquotransversales anlagen.

We are currently performing cryosections on equivalent samples to determine if yes or no these events happen around E9.5. Still, our observations, (not shown here) indicates that at later stages, around E14.5, nearly all the electroporated domain is composed of doubly labelled myofibers, suggesting a progressive mechanism whereby cells from two adjacent myotomes gradually mix together. Nevertheless, 3D observations of the E9.5 samples confirmed that one myotome can contribute to the formation of three different *mm. obliquotransversales* and conversely, that one *mm. obliquotransversales* is formed by the myogenic cells from one segment, the one posterior and the one anterior. Again, we did not detect doubly labelled myofibers in these small lateral muscle anlagen, this needs the be confirmed with cryosections. Altogether these data suggest a mechanism in which first, myogenic cells shift (and elongate, for the myofibers) from their segment of origin, but do not fuse with adjacent myogenic cells until late stages.

Discussion

Implication of the TCF/LEF Signaling in the Primary and Secondary Myogenesis of the Limb

Firstly, our study resolves the longstanding question regarding the developmental origin of primary and secondary myotubes. It unequivocally demonstrates that these myotubes originate from two distinct myogenic progenitor populations co-existing early in the limb and distinguished by their TCF-LEF/β-catenin-dependent Wnt signaling activity. Previous contradictory observations suggested that embryonic and fetal myoblasts are two distinct precursor populations sequentially migrating into the limb bud (Van Swearingen and Lance-Jones, 1995). These discrepancies might be explained by the fact Van Swearingen and Lance-Jones' study focused on a relatively young limb buds (E8 in the tight, equivalent to E12.5 of the wing), when slow myosin begins to be expressed in specific muscle bundles (see Fig35.) This may simply reflect a differential contribution to muscle bundles between the first myoblasts to enter the limb bud and those that follow. Moreover, we never observed a differential distribution of 16TF-VNP^{+} and 16TF-VNP^{-} cells during early limb myoblast migration (between E3 and E4.5). The question of the differential colonization of the limb bud by myoblasts have never been properly addressed for limb and girdle musculature. Although some studies have shown that all the muscle progenitors of the limb and associated girdle are, at some point, inside the limb bud, before returning to the trunk (the In-and-Out mechanisms), it remains unknown if the girdle progenitors consist of a population of late-migrating cells that stay in the proximal part of the limb bud (Masyuk et al., 2014; Valasek et al., 2011, 2005). The same question could be posed for autopodial, zeugopodial and stylopodial muscles. For instance, whether muscle progenitors at the most distal tip of the muscle mass contribute exclusively to autopodial muscles remains unknown. These questions could be answered by electroporation of a CRE-inducible plasmid in chicken embryos, coupled with labeling different parts of the muscle mass, either by beads grafted with membrane-permeable CRE (TAT-CRE) or by optogenetics.

Our findings correlate with previous results, which demonstrated that embryonic limb myoblasts can generate both slow and fast colony while fetal progenitors only generate fast colonies when cultivated *in vitro* (Miller and Stockdale, 1986; Vivarelli et al., 1988). It is therefore likely that these embryonic cultures contain a heterogeneous population of cells (16TF-VNP^{+} and 16TF-VNP^{-}) capable of forming two different types of myofibers, while the fetal ones consist only of 16TF-VNP^{-} producing solely fast, secondary myotubes.

A surprising outcome of our studies is the identification of a shared origin for limb secondary myotubes and satellite cells. Although it is long established that all limb muscles, including its satellite cell component, originate from the VLL the developmental path that VLL cells follow to generate satellite cells, once they have migrated into the limb mesenchyme, had not been investigated (Schienda et al., 2006).

Our results also suggest that a different mechanism seems to control primary and secondary myogenesis in the trunk and the limb. As described in the introduction, the current textbook model of trunk primary and secondary myogenesis is that the dermomyotomal borders altogether generate a primary myotome, in which the central dermomyotome massively delaminates to provide resident progenitors that will form secondary myofibers and the satellite cells pool (Chal and Pourquié, 2017; Gros et al., 2005). In the limb, these two populations would correspond to the 16TF-VNP^{+} and 16TF-VNP^{-} myogenic cells, respectively. As trunk myogenesis occurs in a strict cellular and anatomical environment, capable of generating different myoblasts at different position and time, it is not surprising to that the limb bud, where the myogenesis happen in a less constrained mesenchymal

environment, has adopted a different, molecular, approach to distinguish between primary and secondary myoblasts. However, by studying the epaxial myogenesis, we also shown that the DML can produce satellite cells at pre-hatching stages, suggesting that the trunk primary and secondary myogenesis are not as clearly delineated as pretended in textbooks (see below for a discussion of the primary and secondary myogenesis in the trunk).

The analysis of the 16TF-VNP reporter expression throughout pre-natal life revealed two major insights: (1) that the response to TCF/LEF is completely shut down from the first sign of muscle splitting until hatching and (2) that the response to TCF/LEF before muscle splitting is restricted to an early stage of muscle differentiation, before the activation of *MyoD*. The absence of TCF/LEF activity in myoblasts during all fetal life proves that TCF/LEF is not physiologically required for driving the differentiation of resident muscle progenitors, contrary to what have been proposed (Geetha-Loganathan et al., 2005; Tajbakhsh et al., 1998). Besides, we also show, in accordance with results obtained in mice and chicken, that TCF/LEF signaling is dispensable for *Myf5* and *MyoD* expression in early limb myoblasts (Abu-Elmagd, 2010; Hutcheson et al., 2009). These results highlight the importance of always considering the effect of a signaling pathway *in vivo*, as even if exogenous addition of an activator or inhibitor might trigger observable phenotypes, it might not reflect physiological reality. The fact that TCF/LEF is restricted to only about 50% of early myoblasts, and for a short period, also demonstrate that its activity is very specific in space and time. This specificity could be explained by the possibility that all myoblasts are able to respond to TCF/LEF, but the ligand is available only to half of them. This hypothesis is unlikely, as we never managed to find out a spatial differential distribution between the two populations, as they seem to be intermingled in all the directions. Moreover, Wnt ligands are present throughout the limb mesenchyme and ectoderm, so it is not likely that the bioavailability of the ligand is responsible for this differential response (Loganathan et al., 2005). A more realistic hypothesis is that some myoblasts are refractory to Wnt-TCF/LEF signaling while others not. Interestingly, we observed an enrichment for some Wnt-TCF/LEF pathway components in 16TF-VNP$^+$ cells. Nonetheless, one cannot exclude the possibility that chromatin discrepancies could exist between all the limb myoblasts. scATAC-seq on electroporated limb buds could help answer these questions. The mechanisms for the differential expression of Wnt signaling component and/or a different chromatin landscape between the two population remain speculative and should be further investigated.

Lastly, we found that the 16TF-VNP$^+$ cells shown an enriched expression of several genes related to migration, one of which, *Cxcr4,* is known to be a master regulator of myoblasts migration during limb bud development. Through functional assay we also showed that Cxcr4 expression was downregulated by the expression of a dominant-negative form of LEF1. Moreover, we observed that *Hoxa11* was also enriched in the 16TF-VNP$^+$ cells, in accordance with previous studies showing that only early myoblasts have a Hox code. Here, we clarify, these results by demonstrating the embryonic myoblasts (16TF-VNP$^+$) over higher levels of *Hoxa11* transcripts. Furthermore, *Hoxa11* expression has been found to be essential for a correct patterning of muscle in mice (Asfour et al., 2023). In addition, *Cxcr4* was observed to be expressed only in a subset of myoblasts during their migration, which could correspond to the 16TF-VNP$^+$ myoblasts (Vasyutina et al., 2005).

The association of TCF/LEF with primary and secondary myogenesis has already been proposed by two studies. The first used culture of myoblasts exposed to various Wnt ligands and the number of slow or fast myotubes was evaluated, showing that while some Wnt ligands seem to promote the formation of slow myofibers, others foster the formation of fast myotubes. Then they overexpressed a natural secreted inhibitor of TCF/LEF, *Sfrp2*, in all the limb mesenchyme and claimed that primary myogenesis was affected (Anakwe et al., 2003). However, a significant number of slow myofibers were still present, and more importantly, pan-MyHC staining showed a dramatic decrease, suggesting an effect on myogenesis in general, rather than a slow-specific phenotype. However, no

quantifications at the cellular level were performed to evaluate this. Moreover, the global effect on myogenesis observed cannot be solely attributed to cell autonomous effects, as retroviral infection are non-tissue specific and non-myogenic cells represent the vast majority of all limb bud cells at the infection stage (Esteves De Lima et al., 2021a). A second study, in mice, demonstrated that a deletion of β-catenin in newly delaminated myoblast do not impair their differentiation, as we observed, but that deleting β-catenin in the *Pax7* lineage disrupts the establishment of a slow myofiber population (Hutcheson et al., 2009). The authors therefore proposed a model in which primary myoblasts (Pax3$^+$/ Pax7$^-$, in their model) are not sensitive to TCF/LEF, while the secondary myoblasts (Pax3$^+$/ Pax7$^+$, in their model) require TCF/LEF to form slow myofibers. This model proposes that Pax3$^+$/ Pax7$^-$ generate "embryonic myofibers" that are neither slow nor fast, while only the Pax3$^+$/ Pax7$^+$ myoblasts can generate both. It contradicts the current mainstream view of the primary and secondary myogenesis. As mentioned earlier, *Pax7* expression begins at embryonic stages, before the appearance of individualized muscles bundles. Therefore, deleting β-catenin in *Pax7*$^+$ myoblasts leads to a loss-of-function of TCF/LEF in actual embryonic myoblasts, and therefore primary myoblasts. These results align with our present study, associating TCF/LEF activity with the formation of primary myofibers during embryonic stages. Nonetheless, in our hands, the TCF/LEF signaling was activated at embryonic stages, days before the appearance of slow myofibers. Concomitantly, we did not detect a higher level of slow isoform in the 16TF-VNP$^+$ cells, as they are mononucleated early myoblasts (MYOD$^-$). Finally, the 16TF-VNP reporter was never activated during fetal myogenesis, pointing towards an activation of the slow-program independently of TCF/LEF.

Our current model would be therefore that when myoblasts emerge from the somites, some of them activate TCF/LEF and acquire higher levels of genes involved in migration and patterning. These cells will form the primary myoblasts population, responsible for the formation of the first myofibers and muscle bundles of the limb, while myoblasts not responding to TCF/LEF are set aside to form the secondary myofibers and the satellite cells pool.

Late Patterning of the Epaxial Musculature

As this project is currently ongoing, some evident experiments remain to be done. For the measurements of the expansion of the electroporated domain, the imaging and the quantification of electroporated somite 23 needs to be reconstructed and analyzed to have a complete overview of the mechanism both in the trunk and the neck. Regarding the alternate electroporations, cryosectionnings should be performed on electroporated somites 15/16 and 23/24 to confirm that at late stages (E14.5), mosaic myotubes (*i.e.* resulting from the fusion of myogenic cells from two adjacent somite) represent the major proportion of electroporated cells. Theses samples have been already electroporated and embedded for further sectioning. Besides, we re-performed the same king of electroporation around E9.5 to also analyze them by cryosectionning, as the resolution was not good enough with 3D imaging to pinpoint the exact timing of appearance of mosaic myofibers. If we detect such myofibers, it could signify that this process starts around E9.5 and progressively become more and more present as myogenesis progress. This means that at younger stages, around E7.5, while the myofibers from two adjacent myotome are intermingled, they grow only by the addition of nuclei from their own segment of origin. Next, around E9.5, as we shown, myoblasts start to migrate along the A-P axis, a process that could foster the appearance of mosaic myofibers.

By performing long term electroporation of the DML we proved that contrary to the dogma established for trunk myogenesis, the DML was able to provide the epaxial musculature with muscle resident progenitors and therefore, satellite cells. This invites to revisit the primary and secondary myogenesis of the epaxial compartment. It would be interesting to see if the emergence of mosaic myofibers has any concordance with the primary and secondary myogenesis. Indeed, contrary to what happen in the limb, the first fiber to be formed in the trunk are slow, *Myh7*$^+$ (*Myh7* gene profile

on GEISHA). However, the appearance of fast-only myofibers has never been explored in the trunk. It would be tempting to imagine that the first mosaic myofibers to appear could be in fact secondary myofibers (i.e. *Myh7*$^{-}$). However, our own observations seem to show that at late stages, all the electroporated cells are labelled by both fluorescent proteins, *i.e.* both primary and secondary myofibers. As said above, these represent only preliminary observations and careful analysis need to be conveyed to strongly support this statement. Still, if true, this would mean that the emergence of primary and secondary myofibers is not linked to the emergence of mosaic myofibers. Further investigations are needed in any case.

Most of the wholemount stainings with the MF20 antibody (targeting the MyHC of differentiated muscles fibers) or the eGFP/dTomato antibodies targeting electroporated myofibers (as the membrane-bound fluorescent proteins where under the control of the MLC promoter) often lead to small dots all around the samples (see Fig41. G,J and Fig43. C). Interestingly, these dots were not present in young embryos (E5.5) or late fetuses (E14.5), in both chicken and all the other species that we imaged. At first, we thought that these dots were non-specific immunostaining artefacts, however, increasing the washing period did not change anything. Moreover, the presence or absence of these dots were not correlated with the size of the sample, as for instance entire adult newts, or E14.5 trunk chicken fetuses (around 5cm) were devoid of these dots, while stage 8 of lizard embryos (a few millimeters) were full of them. A recent paper came out in Nature, showing the involvement of programmed cell death, mainly through ferroptosis, a lipid and iron-dependent cell death, in shaping the muscle of thigh in chicken (Co et al., 2024). They beautifully showed with live imaging that mature myofibers were undergoing cell death during late embryonic life, by forming small cellular debris, positive for MyHC and marker of ferroptosis. We are currently performing immunostainings of the epaxial musculature with these antibodies to determine if the same mechanisms are acting during axial muscle development.

From all the electroporations, something that was striking is that labelling of cervical somites never led to the labelling of thoracic muscles and vice-versa. This demonstrates that a strong dichotomy exists between these two compartments. While muscle progenitors are able to migrate over 7 vertebrae in their own domain, they never invade the other domain. Contiguous electroporation of the last cervical somite and the first thoracic one, could be done to determine if, in fact, a sharp boundary exists between these two domains. If this is the case, two possibilities could explain this phenomenon: (1) that muscle progenitors from the thoracic and the cervical compartments are molecularly different, for instance regarding their *Hox* genes signature that triggers a differential migratory behavior along the AP axis. One could imagine that the thoracic domain is filled with a soluble molecule that is chemoattractant for the thoracic progenitors and act as a chemorepellent for the cervical ones. A differential gene expression analysis of these two muscles progenitor could be informative. However, the exact timing of the experiment should be determined according to the results we are waiting for. (2) As the migration of the myogenic progenitors seems to begin around E9.5, when the organogenesis is well established, we could also suppose that the thoracic and the cervical compartments become more and more separated by different connective tissue, therefore segregating the two domains. (3) would be a mix of these two hypotheses.

Regarding the axial identity, it is not known if the epaxial muscles are determined by their instrinsic axial origin or are sensitive to their environment. Interestingly, this question was only studied for limb muscles, but it has never been addressed for the trunk or neck muscles, neither epaxial, nor hypaxial. This may be due to the complexity of shapes and insertion points that muscles adopt during development and the complexity to analyze this on sections. This must be compared to the relative simplicity of axial skeleton, vertebrae and ribs, for which these questions have been long addressed. Indeed, current evidences suggest that external cues from the developing connective tissue, tendons, vasculature and nerves provide information for the proper development of limb muscle

architecture (Kardon et al., 2003; Kieny et al., 1972; Sefton and Kardon, 2019; Tozer et al., 2007). Moreover, somites from any region along the antero-posterior embryonic axis can contribute to the formation of limb muscles, when grafted in the wing or leg regions of the embryo (Alvares et al., 2003). These experimental evidences suggest a high plasticity of limb muscle progenitors to the environmental cues they encounter during their differentiation. This sharply contrasts with observations made with another major derivatives of somites, the axial skeleton, whose final axial identity is determined even before somites form by the Hox code they express (Iimura et al., 2009; Kieny et al., 1972; Nowicki and Burke, 2000). Whether the patterning of epaxial muscles follows a developmental path similar to that of limb muscles, dependent upon environmental cues, or on the contrary is determined early, similar to the axial skeleton, was not investigated. The question is relevant, since epaxial muscles (as hypaxial, non- limb muscles) are evolutionary more primitive than limb muscles, which arose with terrestrial life. Likely due to their ancestral character, epaxial muscles are also generated through a morphogenic process that markedly differs to that of limb muscles. In limbs, the population of progenitors emanating from somites, initially evenly distributed within the limb mesenchyme, gradually becomes organized into the final muscle bundles constituting the limb musculature. In contrast, the morphogenesis of epaxial domain is based on two distinct steps, separated in time, which first generate the metameric units composed of individual myotomes that, in a second stage, reorganize into long back muscles. To answer this question, we will graft thoracic somites from a fluorescently labeled transgenic quail into the cervical region of a wild-type quail host (Moreau et al., 2019). As we characterized the different late muscle morphologies and elongation characteristics, it would be easy to compare the results obtained with heterologous and homologous grafts. This series of experiments should allow to determine if axial muscles patterning is set early in development, while somite are newly forms, or if it is plastic and sensitive to the local environment.

The integrated development of the epaxial musculoskeletal system, and more particularly of birds needs to be more studied, especially regarding the development of MCT and tendons. First, although the sclerotomal origin of the epaxial tendons is well-determined, some authors have shown that a fraction of epaxial MCT can emanate from the dermomyotome (*Myf5* lineage), while others have shown that the syndetome can also provide MCT (Brent et al., 2003; Deries et al., 2010; Grimaldi et al., 2022). The relative contribution of each one these somitic compartment should be studied, in both chicken and mice, to precise the embryonic origin of all the cellular component of the epaxial musculature. This could be done by grafting or electroporation in the chicken embryo and by using genetic lineage tracings in mouse. Moreover, as transgenic quails are more and more developing as a new transgenic model, the idea to merge these two approaches in a single organism might be of great help. Out of all of these, it could be interesting to determine if tenogenic and/or MCT in general can also migrate over a long distance along the AP axis or if they only contribute to the development of derivatives that remain segmented. Moreover, as the dermomyotome also generate dermal cells, the developmental path between *bona fide* dermal cells and the dermomyotomal MCT remains to be determined. Regarding the dermis, our electroporations suggest that dermal cells from a defined segment seems to remain segmented during late development. How some dermomyotome derivatives break the original segmentation, while other do not, represents an interesting question. Indeed, even though we observed a remodeling of the ECM concomitant with the appearance of the metamery breaking, the causality between these two events is unknown. Both integrins and cadherins are dynamically expressed during myotome formation (Bajanca et al., 2006, 2004; Esteves De Lima et al., 2021b; Horikawa and Takeichi, 2001). By disrupting N-cadherin in chicken embryos, Horikawa and Takeichi managed to trigger an early crossing of the myofibers, pointing toward an important role of cell-cell adhesion to regulate the timing of the loss of the metamery. It could be interesting to perform non-bias transcriptomic analysis to identify gene differentially regulated in pre- and post-crossing myofibers and/or in species that have long epaxial muscles versus the one that retain a form of metamery.

Finally, this study provides unique insights into the late patterning of bird neck musculature, a quite unique structure in amniotes. As the forelimbs of birds are devoted to flight, the musculoskeletal system of the neck has diverged from the stereotypical organization to provide more flexibility to the head and therefore, the beak (Böhmer et al., 2019). One of the most spectacular adaptations being the variable number of cervical vertebrae in each species of birds, but also the less well-known *m. biventer cervicis*. This muscle runs all along the neck, originating at the basis of the cervical domain and inserting in the occipital bone. This muscle also possesses an intermediate tendon separating the muscle into two different bellies. This organization is also found in some other muscles in various species, such as the *m. digastricus* in human. However, the developmental process at the origin of the formation of a tendinous tissue in between two muscle bellies is unknown, especially knowing that the length and position of the tendinous part varies between species, until completely disappearing in penguins (Kuroda, 1962). Comparative embryology of various species of birds could provide some hints on the developmental basis of these phenotypical discrepancies and could allow to gain some insight into the relationship between development, evolution and ecological adaptations.

Material and Methods

Animals

Fertile chicken eggs were acquired from the "Élevage Avicole du Grand Buisson" and were staged according to the day of incubation after laying (Embryonic day, E). Pregnant mice were bought from Charles River and stage according to the day post fertilization (Embryonic day, E). *Anolis sagrei* were obtained from a breeding colony at Georgie University, in Douglas Menke lab. Embryonic development of Anolis lizards typically takes place over a 30–33-day period, starting with internal fertilization. Early embryogenesis proceeds within the oviduct. *A. sagrei* embryos obtained from eggs that were collected after egg-laying were staged as described by Sanger et al. *Pleurodeles waltl* specimens used in this study were obtained from a breeding colony at Caltech University, in Marianne Bronner lab. The developmental stages were defined according to Shi, and Boucaut (Shi and Boucaut, 1995). *Xenopus laevis* specimens were provided by the TEFOR Paris-Saclay facility and staged according to Nieuwkoop and Faber (Gerhart and Kirschner, 2020).

Electroporation of chicken embryo

Chicken embryos were incubated at 37,5°C until E2.5 (HH16 or 52h) parallel to the ground. 3 to 4 ml of albumin were removed from the eggs before being windowed. A few drops of Ringer's solution containing penicillin/streptomycin were added onto the embryo before removing part of the extraembryonic membrane directly over the embryo to facilitate the injection. Indian ink diluted in the Ringer's solution was added above the embryo, in the yolk, to contrast and help visualizing all the embryonic structure. All electroporation were performed with a glass capillary and a mouth pipet. For neural tube electroporations, the DNA plasmid mix was injected into the neural tube and 3 pulses of 50V, 10ms and spaced by 10ms were applied directly to the embryo with a tungsten (-) and a platinum (+) electrode. The platinum electrodes were placed on the right of the embryo so only the right part of the neural tube was electroporated. For forelimb somites electroporations, somite 16 – 21 were injected with the DNA plasmid mix with a glass capillary and a mouth pipet. 3 pulses of 50V, 10ms and spaced by 10ms were applied directly to the embryo. The platinum electrode was placed on the right side of the embryo so only the lateral part of the somite was electroporated. For epaxial muscle electroporations, either somite 15, 16, 23 or 24 was injected from the side to ensure single-somite electroporation. 3 pulses of 60V, 10ms and spaced by 10ms were applied directly to the embryo. The platinum electrode was placed on the left side of the embryo so only the medial part of the somite was electroporated.

Plasmid constructs

DNA mixes were prepared extemporaneously by mixing 1 or 2 µl of DNA maxiprep concentrated at 7,5 µg/µl and mixed with 5 µl of a EP mix solution. H_2O was added until a final volume of 15 µl. For single somite electroporations, as a higher viscosity was needed, 10 µl of the carboxymethylcellulose solution were added instead of 5ul, the final volume was always 15 µl. The plasmids were therefore at a final concentration of 0,5 or 1 µg/µl. A ratio of 1:2 was conserved between the rtTA plasmid and the doxycycline inducible plasmid. Each region of interest in each plasmid is flanked by Tol2 sequences, and the CAGGS:Transposase plasmid was added to every mix, so all the plasmids were stably integrated into the genome of the chicken embryos.

EP mix solution:

- 25ml of CarboxyMethylCellulose 1% (C5013, Sigma)
- 3ml of MgCl2 50mM
- 15ml of PBS 10X
- 7ml of 20% FastGreen diluted in H_20 (F7252, Sigma)

Name	Function
CAGGS:Tranposase	Express a ubiquitous transpose
CAGGS:mTagBFP	Express a ubiquitous cytoplasmic blue fluorescent protein
CAGGS:mVenus	Express a ubiquitous cytoplasmic green fluorescent protein
CAGGS:dTomatoNLS	Express a ubiquitous nuclear red fluorescent protein
CAGGS:H2B-mTagBFP	Express a ubiquitous nuclear blue fluorescent protein
CAGGS:mbTomato	Express a ubiquitous membranal red fluorescent protein
MLC:dTomato	Express a myofiber-specific cytoplasmic red fluorescent protein
MLC:eGFPCAAX	Express a membranal myofiber-specific green fluorescent protein
MLC:mbTomato	Express a membranal myofiber-specific red fluorescent protein
12TF:d2eGFP	Express a destabilized and green fluorescent protein under the control of 12 TCF/LEF binding sites
16TF:VNP	Express a destabilized and nuclear green fluorescent protein under the control of 16 TCF/LEF binding sites and the three translational enhancers IVS, Syn21, p10
CAGGS:DnLef1	Express a ubiquitous dominant negative form of LEF1
16TF:VNP-P2A-mCherryNLS	Express a destabilized and nuclear green fluorescent protein and a stable nuclear red fluorescent protein at the same time under the control of 16 TCF/LEF binding sites and the three translational enhancers IVS, Syn21, p10
16TF:rtTA	Express a classical rtTA under the control of 16 TCF/LEF binding sites
16TF:d2rtTA	Express a destabilized rtTA under the control of 16 TCF/LEF binding sites
16TF:IVS-Syn21-d2rtTA-p10	Express a destabilized rtTA under the control of 16 TCF/LEF binding sites and the three translational enhancers IVS, Syn21, p10
pBI:CRE	Express a CRE recombinase under the control of a doxycycline-inducible promoter
CAGGS:flox-polyA-flox-dTomatoNLS	Express a ubiquitous nuclear red fluorescent protein only under the recombination by a CRE recombinase
CAGGS:flox-polyA-flox-eGFP	Express a ubiquitous cytoplasmic green fluorescent protein only under the recombination by a CRE recombinase
CAGGS:rtTA	Express a ubiquitous rtTA
pBI :dTomatoNLS/DnLef1	Express simultaneously a nuclear red fluorescent protein and a dominant negative form of LEF1 under the control of a doxycycline-inducible promoter

Wholemount immunostaining

Embryos from different species were dissected and fixed at various stages in 4% formaldehyde overnight at 4°C with agitation and then washed in PBS. For long term conservation of non-electroporated specimens, samples were progressively dehydrated in increasing concentrations of PBS/MetOH and kept at -20°C. The day of the immunostaining, samples were rehydrated in decreasing concentrations of PBS/MetOH. For electroporated chicken embryos after E9.5, the targeted region was grossly dissected before fixation and finely re-dissected after fixation. All the samples were then permeabilized and blocked in washing buffer (WB) composed of 0,2% BSA, 0,5% Triton X-100, 0,2% SDS in PBS at RT for several hours. The different samples were then process as described in the following table. As fixation can dampens the brightness of fluorescent proteins, electroporated embryos were stained for the various fluorescent proteins they express. As most samples were large, they were incubated with primary antibodies at RT for extended periods in WB containing 0,01% Thimerosal (Sigma) to prevent micro-organism growth.

Antibody	***References***	***Isotype***	***Concentration***
α-eGFP derivatives	A11120, Invitrogen	Mouse IgG2a	1/1000
α-eGFP derivatives	OSE00002W, Invitrogen	Rabbit	1/1000
α-DsRed derivatives	Ab62341, Abcam	Rabbit	1/1000
α-DsRed derivatives	600-401-379, Rockland	Rabbit	1/1000
α-DsRed derivatives	sc-101526, Santa Cruz	IgG1	1/1000
α-Tenascin	T3413, Sigma-Aldrich	Rat	1/200
α-Fibronetin	B3/D6, DSHB	IgG2a	1/200
α-Laminin	L9393, Sigma-Aldrich	Rabbit	1/200
α-MyHC	MF20, DSHB	IgG2b	1/10 (Wholemount) 1/5 (Sections)
α-PAX7	PAX7, DSHB	IgG1	1/10
α-MYH7	S58, DSHB	S58	1/5 (Sections)
α-MYF5	Bruce Paterson, Manceau et al. 2008	Rabbit	1/250
α-MYOD	Bruce Paterson, Manceau et al. 2008	Rabbit	1/250
α-Col2	II-II6B3, DSHB	IgG1	1/300

Species	***Stage***	***Fixation***	***Pre-treatment***	***Primary***	***Wash***	***Secondary***	***Wash***	***Imaging technic***
Gallus gallus	WM E3.5	1h RT	-	O/N 4°C	4x1h	O/N 4°C	4x1h	Confocal
	WM E4.5 – E7.5 limb bud	1h RT	-	O/N 4°C	4x1h	O/N 4°C	4x1h	Confocal
	Limb sections E4.5-E18.5	O/N 4°C	-	O/N 4°C	3x1h	2h RT	4x15min	Confocal
	Trunk sections E6.5 – E18.5	O/N 4°C	-	O/N 4°C	3x1h	2h RT	4x15min	Confocal
	WT WM E6.5-E8.5	O/N 4°C	3h day in 0,1% H_2O_2 in PBS	1 day RT	2 days	1 day RT	2 days	Light-sheet
	WT WM E9.5	O/N 4°C	Skin removal 3h day in 0,1% H_2O_2 in PBS	3 days RT	3 days	2 days RT	3 days	Light-sheet

	Electroporated WM E9.5-E18.5	O/N 4°C	Skin removal	3 days RT	3 days	2 days RT	3 days	Light-sheet
Anolis sagrei	WM St.6 – St.12	O/N 4°C	3h day in 0,1% H_2O_2 in PBS	1 day RT	2 days	1 day RT	2 days	Light-sheet
Mus musculus	E11.5 – E15.5	O/N 4°C	3h day in 0,1% H_2O_2 in PBS	1 day RT	2 days	1 day RT	2 days	Light-sheet
Xenopus laevis	WM	O/N 4°C	1 day in 0,5% H_2O_2 / 3% KOH in PBS	2 days RT	2 days	2 days RT	2 days	Light-sheet
	Trunk sections	O/N 4°C	-	O/N 4°C	4x1h	2h RT	4x15min	Confocal
Pleurodeles waltl	WM		1 day in 0,5% H_2O_2 / 3% KOH in PBS	2 days RT	2 days	2 days RT	2 days	Light-sheet
	Trunk sections		-	O/N 4°C	4x1h	2h RT	4x15min	Confocal

Doxycycline induction

Stock solution of doxycycline at a concentration of 20mg/ml in ddH2O was prepared in advance and stored at -20°C. A solution at 3,5 µl /ml was prepared by diluting the stock solution into sterile Ringer's solution on the day of the injection; 300µl of the solution was added per embryo.

EdU incorporation

50 µl of 10mM of EdU solution was added directly onto the embryo that was placed back in the incubator for 1h. Embryos were then dissected, fixed and immunostained as described above. Once immunostained, samples were pre-incubated in 250 µl of PBS with 1 µl of Alexa fluorophen for 1h at RT. Separately 150 µl of PBS was mixed with 100 µl of ascorbic acid at 0,5M and 2 µl of a 1M CuSO4 solution and added to the pre-incubated samples. Embryos were incubated overnight at 4°C with agitation, washed at least five times the following day and cleared into glycerol as described.

Cryosections

Electroporated embryos were dissected, and regions of interest were fixed in 4% formaldehyde at 4°C O/N. After being washed in PBS they were first incubated in 7,5% Sucrose/PBS for 2 hours and then in 15% Sucrose/PBS O/N at 4°C. Then, they were incubated in a solution of PBS 7.5% gelatin/15% sucrose solution for 2 hours to O/N at 42°C depending on the size of the embryo. Samples were embedded in molds and frozen in dry ice-cold 100% EtOH. 18-microns sections were

realized all along the interested region. Sections were dried at RT for 30 minutes; the gelatin was melted with 42°C PBS. Samples were permeabilized and saturated in a humidified chamber with 0,2% BSA, 0,1% Triton X-100 in PBS for 4 hours before being replaced with the primary antibody solution in the same buffer. The same antibodies were used as in the wholemount protocol. Sections were carefully washed 3 times for 1 hour, incubated with secondary antibodies for 2 hours at RT and washed 3 times for 15 minutes. Slides were mounted in Fluoromount™ (Invitrogen) and dry O/N at 4°C.

HCR RNA-FISH

The Cxcr4 probe was purchased from Molecular instrument. Electroporated limb bud were collected two days after electroporation, fixed in 4% paraformaldehyde for 1h at RT. Embryos were washed twice in PBS and dehydrated in growing concentration of MetOH/PBS (25%/50%/75%/100%). Embryos were stored at least one night at -20°C before being rehydrated in decreasing concentration of MetOH/PBS (75%/50%/25%/PBS) and post fixed for 20min in 4% PFA for 20min at RT. Limb bud where then washed twice in PBS for 5min, then once in a 1:1 solution of PBS/SSCT and finally once in SSCT. The embryos were pre-hybridized in 500 µL of hybridization buffer for 30 min at 37 °C (HCR™ Buffers, Molecular instruments). The pre-hybridization solution was replaced by the solution with the probes (2 pmol or 4 pmol in 500 µL hybridization buffer) and incubated overnight at 37 °C with shaking. After removal of the probe solution, samples were washed 4 times in 1 mL of washing buffer (HCR™ Buffers, Molecular instruments) for 15 min at 37 °C with shaking. Two 5 min washes in SSCT solution were made at RT. Next, the embryos were incubated in 500 µL of amplification buffer for 5 min at RT (HCR™ Buffers, Molecular instruments). The hairpins h1 and h2 (30 pmol 10 µL for 500 µL of buffer) were heated separately at 95 °C for 90 s, left at RT for 30 min minimum in the dark before being added in 500 µL of amplification buffer. The pre-amplification solution was replaced by the solution containing the amplifiers and incubated overnight in the dark at RT with gentle agitation. Amplifier solution was removed, and embryos were washed in SSCT at RT (2 × 5 min, 2 × 30 min, 1 × 5 min). They were post-fixed in 4% PFA for 20 min and washed twice in PBS. Samples were stored at 4 °C protected from light. Embryos were then stained as described above for the dTomato and PAX7, cleared in glycerol and imaged at the confocal.

Clearing

Wholemount samples for the light-sheet were washed in ultrapure water and dehydrated in growing concentration of H_2O/EtOH (25% / 50% / 75% / 2x 100%) for 2 hours each time at RT, before being incubated in Ethyl cinnamate (ECi) O/N at RT. Wholemount samples for the confocal were incubated in 50% glycerol/PBS and 80% glycerol/PBS for 2h each time and mounted in 80% glycerol in between the slide and the coverslip with pieces of adhesive tapes according to the size of the sample.

Confocal imaging

Sample where images were acquired with a Leica SP5 confocal microscope with either a 20x glycerol-immersion objective or a 40x-oil immersive objective. Images were acquired with a resolution of 1024x1024 pixels. The microscope was equipped with a resonant scanner; therefore, we used a line average of 8. The z-step was set to 1,5 µm. Confocal stacks were analyzed using Fiji and the cell counter plugin.

Analysis of DNLef1 phenotypes

Images of E4.5 control and DNLef1 limb bud were acquires in wholemount on the confocal as described above. 3D acquisitions were transformed into 2D images with a maximal projection in Fiji. For the percentage of dispersion, an oblong shape was drawn around the muscle mass to measure

its total area and then a threshold was set to measure the area of all the nuclei using the "analyze particles" function. The percentage of dispersion was calculated as follow:

$$Percentage\ of\ Dispersion = \frac{(Total\ Area\ -\ Sum\ of\ Particles\ Area)}{Total\ Area} \times 100$$

For the center of mass, a line was traced in the middle of the muscle mass, along the proximo-distal axis of the limb and the center of mass was measured using the "Measure" function. The center of mass is defined as the brightness-weighted average of the x and y coordinates of all pixels in the image or selection. Therefore, if the repartition of the fluorescence is homogeneous along the proximo-distal axis the center of mass should be around the middle of the region of interest. The center of mass was normalized by the total length of the muscle mass, therefore a value around 50 represent a homogeneous repartition.

$$Ratio = \frac{YM\ of\ Center\ of\ Mass}{Total\ Length\ of\ the\ Muscle\ Mass} \times 100$$

Light sheet imaging

Whole embryos being too large for usual confocal microscopy, they were imaged using an Ultramicroscope Blaze light sheet microscope (Miltenyi Biotec). The samples were mounted in the middle of the chamber, perpendicular to the light sheet and fluorescent illumination was collected from above. This microscope is equipped with 3 light sheets which come from both side of the chamber towards its center, providing a homogeneous illumination. We imaged the embryos using a 4X objective and added a zoom depending on the needs for each sample. All in all, we were able to obtain a total magnification of 2,4 to 10 times the original size of the samples. With three possible excitation wavelengths (488, 555, 647 um), we favored the far- red laser for imaging as it greatly limits the detection of autofluorescence from most the embryos, exept for mouse embryos that were imaged in the 555 channel. Moreover, we adjusted the shape of the light sheet depending on the sample characteristics. The width of the light sheet consists in adjusting the excited area of the sample to get the best ratio of intensity and homogeneity of illumination. Indeed, while a narrow light sheet has a higher intensity and penetrates the sample better, it can also create artefacts on the peripheral parts of the sample. Thus, the choice of light sheet width was adapted depending on the aim of the acquisitions, with specific areas deep in samples being illuminated with a narrow light sheet (i.e. electroporated fibers), and large samples being illuminated with a wider one (i.e. whole embryos). We then set the numerical aperture (NA) of the illumination. Modifications of the NA impact the thickness of the light sheet (in the z axis). Indeed, a higher NA creates a thin light sheet, which provides a higher z resolution. However, this also reduces the field of view (i.e. the area of horizontal focus) of the light sheet. Since large embryos require a large field of view, we used the dynamic horizontal focus function of the microscope to compensate for the loss of horizontal focus. To do so we defined a field of view comprising the whole region of interest of our samples, over which a series of images was taken horizontally (with the focus being adjusted for each step) and stitched. Altogether, these settings optimize both the x-y and z resolution.

Light sheet acquisition processing and analysis

SPIM images were processed using both Arivis Vision 4D (version 3.1.3, Arivis AG, Munich, Germany) and Imaris (version 10.0.1, Bitplane USA, Concord, MA, USA; RRID: SCR_007370).

(1) Basic image processing: Acquisitions carried out over several tiles were stitched using Arivis. They were first converted into a file format compatible with Arivis. Tiles were then aligned and stitched using the 'Tile Sorter' plugin. To be processed on the Imaris software, they were

exported as single tiff planes (which required for 16-bit images to be compressed into 8-bit images due to the exporter), and then converted into the Imaris file format. Brightness/contrast was adjusted, and irrelevant parts of the acquisitions were cropped using either clipping planes or surfaces, which allow for masking of manually defined regions.

(2) Fiber length: To measure fibers in electroporated somites, a surface was first created to improve their visualization (no proper separation of the objects was achieved). Measurement points were then placed over the length of each fiber that could be separated from the rest of the myotome. Additionally, an oblique slicer perpendicular to the myotome was used to check it was indeed an isolated fiber that was measured. A series of snapshots of a transversal view of the myotome was then taken with each measurement being color coded. The resulting series of RGB images was then processed in Fiji. We estimated the distance of fibers inside the myotome measuring their distance from the bottom of the myotome (in the dorso-ventral axis) and from its most lateral part (in the medio-lateral axis). This distance was then normalized depending on the total myotome's length.

(3) Position of the myofiber into the myotome: Myotomes were analyzed into Imaris and measurement point were added at each end of a myofibers. Snapshot were exporter into Fiji and the center of the myotome was arbitrary determined with the more ventral portion that is still segmented. The AP-shift of myofiber was determined by measuring the distance of the center of the myofiber to the center of the myotome. The same analysis was done to map the DV position of each myofiber.

(4) Extension along the AP axis: The absolute length of the eGFP domain was measured into Imaris by placing several measurement points along the eGFP domain. For the relative expansion of the eGFP domain according to the number of vertebrae we first identified the segment of origin of by looking at the *m. intertransversarii* that still harbor segmentation and therefore remain located in between the two transverse process of two adjacent vertebrae, because of the process of re-segmentation. Snapshots were export to Fiji with the measurement point at the origin. Each half-vertebra was counted as 0,5, with positive values in the anterior region and negative values in the posterior region.

Electroporated single cell isolation

E4.5 electroporated chicken embryos with a ubiquitous dTomato and the 16TF-VNP reporter were screen under a fluorescent binocular and electroporated limb buds were quickly dissected and incubated with 500 µl of pre-warmed Dispase (1,5mg/ml in DMEM / 10mM Hepes), pipette up and down 10 times and incubated 15min at 37°C. The sample was homogenized every 5min then 500 µl of pre-warmed Trypsin (0,05% in DMEM) was added to the tube, homogenized and incubated 3min at 37°C. Samples were then transferred into a 15ml falcon tube, and the reaction was stop with 10ml of Hanks buffer (for 100ml: 10ml of HBSS 10X, 250mg of BSA, 1ml of Hepes 1M, in sterile ddH_2O), homogenized and centrifugated 10min at 500g. The pellet was re-suspended in 4ml of Hanks buffer and filtered with a pre-humidified 40 µm sterile filter and re-centrifugated 10min at 500g. The final pellet was re-suspended into 250 µl of Hanks buffer and added to 250 µl of Hanks buffer in a pre-humidified FACS tube. For sorting, we added DAPI (1/1000) in the final Hanks buffer solution and prepare a sample containing non-electroporated tissues, and non-electroporated tissues stained with DAPI to calibrate the sorting. Cells were then sorting according to the dTomato fluorescence and collected into Hanks buffer. For the single-cell RNA-seq experiment, a total of 6 electroporated limb buds were pooled together in the same tube.

Statistical analyses

Plot and statistical analyses were done using R, with ggplot2 and ggsignif packages. Experiment with two different conditions were compared using Wilcoxon-Mann-Whitney test and experiment with three different conditions with Kruskal-Wallis test associated with Dunn-Bonferroni post-hoc test. NS represent a p-value>0.05, *** a p-value<0.001 and **** a p-value<0.0001

References

Abu-Elmagd, M., 2010. Wnt/Lef1 signaling acts via Pitx2 to regulate somite myogenesis. Developmental Biology 9.
Adachi, N., Bilio, M., Baldini, A., Kelly, R.G., 2020. Cardiopharyngeal mesoderm origins of musculoskeletal and connective tissues in the mammalian pharynx. Development 147, dev185256. https://doi.org/10.1242/dev.185256

Adhikari, A., Kim, W., Davie, J., 2021. Myogenin is required for assembly of the transcription machinery on muscle genes during skeletal muscle differentiation. PLoS ONE 16, e0245618. https://doi.org/10.1371/journal.pone.0245618
Ahmed, M.U., Cheng, L., Dietrich, S., 2006. Establishment of the epaxial–hypaxial boundary in the avian myotome. Developmental Dynamics 235, 1884–1894. https://doi.org/10.1002/dvdy.20832

Ahmed, M.U., Maurya, A.K., Cheng, L., Jorge, E.C., Schubert, F.R., Maire, P., Basson, M.A., Ingham, P.W., Dietrich, S., 2017. Engrailed controls epaxial-hypaxial muscle innervation and the establishment of vertebrate three-dimensional mobility. Developmental Biology 430, 90–104. https://doi.org/10.1016/j.ydbio.2017.08.011

Alvares, L.E., Schubert, F.R., Thorpe, C., Mootoosamy, R.C., Cheng, L., Parkyn, G., Lumsden, A., Dietrich, S., 2003. Intrinsic, Hox-Dependent Cues Determine the Fate of Skeletal Muscle Precursors. Developmental Cell 5, 379–390. https://doi.org/10.1016/S1534-5807(03)00263-6

Amthor, H., Christ, B., Weil, M., Patel, K., 1998. The importance of timing differentiation during limb muscle development. Current Biology 8, 642–652. https://doi.org/10.1016/S0960-9822(98)70251-9

Amthor, H., Otto, A., Vulin, A., Rochat, A., Dumonceaux, J., Garcia, L., Mouisel, E., Hourdé, C., Macharia, R., Friedrichs, M., Relaix, F., Zammit, P.S., Matsakas, A., Patel, K., Partridge, T., 2009. Muscle hypertrophy driven by myostatin blockade does not require stem/precursor-cell activity. Proc. Natl. Acad. Sci. U.S.A. 106, 7479–7484. https://doi.org/10.1073/pnas.0811129106

Anakwe, K., Robson, L., Hadley, J., Buxton, P., Church, V., Allen, S., Hartmann, C., Harfe, B., Nohno, T., Brown, A.M.C., Evans, D.J.R., Francis-West, P., 2003. Wnt signalling regulates myogenic differentiation in the developing avian wing. Development 130, 3503–3514.

Aoyama, H., Asamoto, K., 2000. The developmental fate of the rostral/caudal half of a somite for vertebra and rib formation: experimental con®rmation of the resegmentation theory using chick-quail chimeras. Mechanisms of Development.

Aoyama, H., Asamoto, K., 1988. Determination of somite cells: independence of cell differentiation and morphogenesis. Development 104, 15–28. https://doi.org/10.1242/dev.104.1.15

Arostegui, M., Scott, R.W., Böse, K., Underhill, T.M., 2022. Cellular taxonomy of Hic1+ mesenchymal progenitor derivatives in the limb: from embryo to adult. Nat Commun 13, 4989. https://doi.org/10.1038/s41467-022-32695-1

Asfour, H., Hirsinger, E., Rouco, R., Zarrouki, F., Hayashi, S., Swist, S., Braun, T., Patel, K., Relaix, F., Andrey, G., Stricker, S., Duprez, D., Stantzou, A., Amthor, H., 2023. Inhibitory SMAD6 interferes with BMP dependent generation of muscle progenitor cells and perturbs proximodistal pattern of murine limb muscles. Development dev.201504. https://doi.org/10.1242/dev.201504

Atit, R., Sgaier, S.K., Mohamed, O.A., Taketo, M.M., Dufort, D., Joyner, A.L., Niswander, L., Conlon, R.A., 2006. β-catenin activation is necessary and sufficient to specify the dorsal dermal fate in the mouse. Developmental Biology 296, 164–176. https://doi.org/10.1016/j.ydbio.2006.04.449

Augier, M., 1931. Squelette céphalique, 4ème édition. ed, Traité d'anatomie humaine. Masson, Paris.
Aulehla, A., Wiegraebe, W., Baubet, V., Wahl, M.B., Deng, C., Taketo, M., Lewandoski, M., Pourquié, O., 2008. A β-catenin gradient links the clock and wavefront systems in mouse embryo segmentation. Nat Cell Biol 10, 186–193. https://doi.org/10.1038/ncb1679

Babiuk, R.P., Zhang, W., Clugston, R., Allan, D.W., Greer, J.J., 2003. Embryological origins and development of the rat diaphragm. J of Comparative Neurology 455, 477–487. https://doi.org/10.1002/cne.10503

Bagnall, K.M., Higgins, S.J., Sanders, E.J., 1989. The contribution made by cells from a single somite to tissues within a body segment and assessment of their integration with similar cells from adjacent segments. Development 107, 931–943. https://doi.org/10.1242/dev.107.4.931

Bajanca, F., Luz, M., Duxson, M.J., Thorsteinsdóttir, S., 2004. Integrins in the mouse myotome: Developmental changes and

differences between the epaxial and hypaxial lineage. Developmental Dynamics 231, 402–415. https://doi.org/10.1002/dvdy.20136

Bajanca, F., Luz, M., Raymond, K., Martins, G.G., Sonnenberg, A., Tajbakhsh, S., Buckingham, M., Thorsteinsdóttir, S., 2006. Integrin α6β1-laminin interactions regulate early myotome formation in the mouse embryo. Development 133, 1635–1644. https://doi.org/10.1242/dev.02336

Barzilai-Tutsch, H., Morin, V., Toulouse, G., Chernyavskiy, O., Firth, S., Marcelle, C., Serralbo, O., 2022. Transgenic quails reveal dynamic TCF/β-catenin signaling during avian embryonic development. eLife 11, e72098. https://doi.org/10.7554/eLife.72098

Bendall, A.J., Ding, J., Hu, G., Shen, M.M., Abate-Shen, C., 1999. *Msx1* antagonizes the myogenic activity of *Pax3* in migrating limb muscle precursors. Development 126, 4965–4976. https://doi.org/10.1242/dev.126.22.4965

Berendsen, A.D., Olsen, B.R., 2015. Bone development. Bone 80, 14–18. https://doi.org/10.1016/j.bone.2015.04.035

Beresford, B., 1983. Brachial muscles in the chick embryo: the fate of individual somites. J Embryol Exp Morphol 77, 99–116.
Bergwerff, M., Verberne, M.E., DeRuiter, M.C., Poelmann, R.E., Gittenberger-de-Groot, A.C., 1998. Neural Crest Cell

Contribution to the Developing Circulatory System: Implications for Vascular Morphology? Circulation Research 82, 221–231. https://doi.org/10.1161/01.RES.82.2.221

Berkes, C.A., Tapscott, S.J., 2005. MyoD and the transcriptional control of myogenesis. Seminars in Cell & Developmental Biology 16, 585–595. https://doi.org/10.1016/j.semcdb.2005.07.006

Bi, P., Ramirez-Martinez, A., Li, H., Cannavino, J., McAnally, J.R., Shelton, J.M., Sánchez-Ortiz, E., Bassel-Duby, R., Olson, E.N., 2017. Control of muscle formation by the fusogenic micropeptide myomixer. Science 356, 323–327. https://doi.org/10.1126/science.aam9361

Biressi, S., Tagliafico, E., Lamorte, G., Monteverde, S., Tenedini, E., Roncaglia, E., Ferrari, Sergio, Ferrari, Stefano, Cusella-De Angelis, M.G., Tajbakhsh, S., Cossu, G., 2007. Intrinsic phenotypic diversity of embryonic and fetal myoblasts is revealed by genome-wide gene expression analysis on purified cells. Developmental Biology 304, 633–651. https://doi.org/10.1016/j.ydbio.2007.01.016

Bladt, F., Riethmacher, D., Isenmann, S., Aguzzi, A., Birchmeier, C., 1995. Essential role for the c-met receptor in the migration of myogenic precursor cells into the limb bud. Nature 376, 768–771. https://doi.org/10.1038/376768a0

Bober, E., Franz, T., Arnold, H.-H., Gruss, P., Tremblay, P., 1994. *Pax-3* is required for the development of limb muscles: a possible role for the migration of dermomyotomal muscle progenitor cells. Development 120, 603–612. https://doi.org/10.1242/dev.120.3.603

Bobzin, L., Roberts, R.R., Chen, H.-J., Crump, J.G., Merrill, A.E., 2021. Development and maintenance of tendons and ligaments. Development 148, dev186916. https://doi.org/10.1242/dev.186916

Böhmer, C., Plateau, O., Cornette, R., Abourachid, A., 2019. Correlated evolution of neck length and leg length in birds. R. Soc. open sci. 6, 181588. https://doi.org/10.1098/rsos.181588

Böhmer, C., Prevoteau, J., Duriez, O., Abourachid, A., 2020. Gulper, ripper and scrapper: anatomy of the neck in three species of vultures. J. Anat. 236, 701–723. https://doi.org/10.1111/joa.13129

Boumans, M.L.L.M., Krings, M., Wagner, H., 2015. Muscular Arrangement and Muscle Attachment Sites in the Cervical Region of the American Barn Owl (Tyto furcata pratincola). PLoS ONE 10, e0134272. https://doi.org/10.1371/journal.pone.0134272

Braun, T., Rudnicki, M.A., Arnold, H.-H., Jaenisch, R., 1992. Targeted inactivation of the muscle regulatory gene Myf-5 results in abnormal rib development and perinatal death. Cell 71, 369–382. https://doi.org/10.1016/0092-8674(92)90507-9

Brent, A.E., Schweitzer, R., Tabin, C.J., 2003. A Somitic Compartment of Tendon Progenitors. Cell 113, 235–248. https://doi.org/10.1016/S0092-8674(03)00268-X

Brent, A.E., Tabin, C.J., 2004. FGF acts directly on the somitic tendon progenitors through the Ets transcription factors *Pea3* and *Erm* to regulate scleraxis expression. Development 131, 3885–3896. https://doi.org/10.1242/dev.01275

Bröhl, D., Vasyutina, E., Czajkowski, M.T., Griger, J., Rassek, C., Rahn, H.-P., Purfürst, B., Wende, H., Birchmeier, C., 2012. Colonization of the Satellite Cell Niche by Skeletal Muscle Progenitor Cells Depends on Notch Signals. Developmental Cell

23, 469–481. https://doi.org/10.1016/j.devcel.2012.07.014

Bui, H.-N.N., Larsson, H.C.E., 2021. Development and evolution of regionalization within the avian axial column. Zoological Journal of the Linnean Society 191, 302–321. https://doi.org/10.1093/zoolinnean/zlaa038

Burke, A.C., 1989. Development of the turtle carapace: Implications for the evolution of a novel bauplan. Journal of Morphology 199, 363–378. https://doi.org/10.1002/jmor.1051990310

Burke, A.C., Nowicki, J.L., 2003. A New View of Patterning Domains in the Vertebrate Mesoderm. Developmental Cell 4, 159–165. https://doi.org/10.1016/S1534-5807(03)00033-9

Bussen, M., Petry, M., Schuster-Gossler, K., Leitges, M., Gossler, A., Kispert, A., 2004. The T-box transcription factor Tbx18 maintains the separation of anterior and posterior somite compartments. Genes Dev. 18, 1209–1221. https://doi.org/10.1101/gad.300104

Cao, Y., Kumar, R.M., Penn, B.H., Berkes, C.A., Kooperberg, C., Boyer, L.A., Young, R.A., Tapscott, S.J., 2006. Global and gene-specific analyses show distinct roles for Myod and Myog at a common set of promoters. EMBO J 25, 502–511. https://doi.org/10.1038/sj.emboj.7600958

Chal, J., Pourquié, O., 2017. Making muscle: skeletal myogenesis *in vivo* and *in vitro*. Development 144, 2104–2122. https://doi.org/10.1242/dev.151035

Chal, J., Pourquié, O., 2009. Patterning and Differentiation of the Vertebrate Spine.

Chassin, H., Müller, M., Tigges, M., Scheller, L., Lang, M., Fussenegger, M., 2019. A modular degron library for synthetic circuits in mammalian cells. Nat Commun 10, 2013. https://doi.org/10.1038/s41467-019-09974-5

Cheng, L., Alvares, L.E., Ahmed, M.U., El-Hanfy, A.S., Dietrich, S., 2004. The epaxial–hypaxial subdivision of the avian somite. Developmental Biology 274, 348–369. https://doi.org/10.1016/j.ydbio.2004.07.020

Chevallier, A., 1977. Origine des ceintures scapulaires et pelviennes chez l'embryon d'oiseau. Development 42, 275–292. https://doi.org/10.1242/dev.42.1.275

Chevallier, A., 1975. Rôle du mésoderme somitique dans le développement de la cage thoracique de l'embryon d'oiseau. I. Origine du segment sternal et mécanismes de la différenciation des côtes. Development 33, 291–311. https://doi.org/10.1242/dev.33.2.291

Chevallier, A., Kieny, M., Mauger, A., 1977. Limb-somite relationship: origin of the limb musculature. Development 41, 245–258. https://doi.org/10.1242/dev.41.1.245

Chiang, C., Litingtung, Y., Lee, E., Young, K.E., Corden, J.L., Westphal, H., Beachy, P.A., 1996. Cyclopia and defective axial patterning in mice lacking Sonic hedgehog gene function. Nature 383, 407–413. https://doi.org/10.1038/383407a0

Christ, B., Huang, R., Scaal, M., 2007a. Amniote somite derivatives. Developmental Dynamics 236, 2382–2396. https://doi.org/10.1002/dvdy.21189

Christ, B., Huang, R., Scaal, M., 2007b. Amniote somite derivatives. Dev. Dyn. 236, 2382–2396. https://doi.org/10.1002/dvdy.21189

Christ, B., Ordahl, C.P., 1995. Early stages of chick somite development. Anat Embryol 191, 381–396. https://doi.org/10.1007/BF00304424

Clevers, H., 2006. Wnt/β-Catenin Signaling in Development and Disease. Cell 127, 469–480. https://doi.org/10.1016/j.cell.2006.10.018

Co, H.K.C., Wu, C.-C., Lee, Y.-C., Chen, S., 2024. Emergence of large-scale cell death through ferroptotic trigger waves. Nature 631, 654–662. https://doi.org/10.1038/s41586-024-07623-6

Colasanto, M.P., Eyal, S., Mohassel, P., Bamshad, M., Bonnemann, C.G., Zelzer, E., Moon, A.M., Kardon, G., 2016. Development of a subset of forelimb muscles and their attachment sites requires the ulnar-mammary syndrome gene *Tbx3*. Disease Models & Mechanisms 9, 1257–1269. https://doi.org/10.1242/dmm.025874

Collings, A.J., Richards, C.T., 2019. Digital dissection of the pelvis and hindlimb of the red-legged running frog, *Phlyctimantis maculatus* , using Diffusible Iodine Contrast Enhanced computed microtomography (DICE *μ* CT). PeerJ 7, e7003.

https://doi.org/10.7717/peerj.7003

Comai, G., Heude, E., Mella, S., Paisant, S., Pala, F., Gallardo, M., Langa, F., Kardon, G., Gopalakrishnan, S., Tajbakhsh, S., 2019. A distinct cardiopharyngeal mesoderm genetic hierarchy establishes antero-posterior patterning of esophagus striated muscle. eLife 8, e47460. https://doi.org/10.7554/eLife.47460

Comai, G., Sambasivan, R., Gopalakrishnan, S., Tajbakhsh, S., 2014. Variations in the Efficiency of Lineage Marking and Ablation Confound Distinctions between Myogenic Cell Populations. Developmental Cell 31, 654–667. https://doi.org/10.1016/j.devcel.2014.11.005

Comai, G.E., Tesařová, M., Dupé, V., Rhinn, M., Vallecillo-García, P., Da Silva, F., Feret, B., Exelby, K., Dollé, P., Carlsson, L., Pryce, B., Spitz, F., Stricker, S., Zikmund, T., Kaiser, J., Briscoe, J., Schedl, A., Ghyselinck, N.B., Schweitzer, R., Tajbakhsh, S., 2020. Local retinoic acid signaling directs emergence of the extraocular muscle functional unit. PLoS Biol 18, e3000902. https://doi.org/10.1371/journal.pbio.3000902

Conerly, M.L., Yao, Z., Zhong, J.W., Groudine, M., Tapscott, S.J., 2016. Distinct Activities of Myf5 and MyoD Indicate Separate Roles in Skeletal Muscle Lineage Specification and Differentiation. Developmental Cell 36, 375–385. https://doi.org/10.1016/j.devcel.2016.01.021

Cooke, J., Zeeman, E.C., 1976. A clock and wavefront model for control of the number of repeated structures during animal morphogenesis. Journal of Theoretical Biology 58, 455–476. https://doi.org/10.1016/S0022-5193(76)80131-2

Corish, P., Tyler-Smith, C., 1999. Attenuation of green fluorescent protein half-life in mammalian cells. Protein Engineering, Design and Selection 12, 1035–1040. https://doi.org/10.1093/protein/12.12.1035

Correia, K.M., Conlon, R.A., 2000. Surface ectoderm is necessary for the morphogenesis of somites. Mechanisms of Development 91, 19–30. https://doi.org/10.1016/S0925-4773(99)00260-9

Couly, G.F., Coltey, P.M., Douarin, N.M.L., 1993. The triple origin of skull in higher vertebrates: a study in quail-chick chimeras. Development 117, 409–429. https://doi.org/10.1242/dev.117.2.409

Criswell, K.E., Gillis, J.A., 2020. Resegmentation is an ancestral feature of the gnathostome vertebral skeleton. eLife 9, e51696. https://doi.org/10.7554/eLife.51696

Crow, M.T., Stockdale, F.E., 1986. Myosin expression and specialization among the earliest muscle fibers of the developing avian limb. Developmental Biology 113, 238–254. https://doi.org/10.1016/0012-1606(86)90126-0

DasGupta, R., Fuchs, E., 1999. Multiple roles for activated LEF/TCF transcription complexes during hair follicle development and differentiation. Development 126, 4557–4568.

DasGupta, R., Kaykas, A., Moon, R.T., Perrimon, N., 2005. Functional genomic analysis of the Wnt-wingless signaling pathway. Science 308, 826–833. https://doi.org/10.1126/science.1109374

Davis, R.L., Weintraub, H., Lassar, A.B., 1987. Expression of a single transfected cDNA converts fibroblasts to myoblasts. Cell 51, 987–1000. https://doi.org/10.1016/0092-8674(87)90585-X

Delfini, M.-C., De La Celle, M., Gros, J., Serralbo, O., Marics, I., Seux, M., Scaal, M., Marcelle, C., 2009. The timing of emergence of muscle progenitors is controlled by an FGF/ERK/SNAIL1 pathway. Developmental Biology 333, 229–237. https://doi.org/10.1016/j.ydbio.2009.05.544

Delfini, M.-C., Hirsinger, E., Pourquié, O., Duprez, D., 2000. Delta 1-activated Notch inhibits muscle differentiation without affecting *Myf5* and *Pax3* expression in chick limb myogenesis. Development 127, 5213–5224. https://doi.org/10.1242/dev.127.23.5213

Dequéant, M.-L., Pourquié, O., 2008. Segmental patterning of the vertebrate embryonic axis. Nat Rev Genet 9, 370–382. https://doi.org/10.1038/nrg2320

Deries, M., Schweitzer, R., Duxson, M.J., 2010. Developmental fate of the mammalian myotome. Dev. Dyn. 239, 2898–2910. https://doi.org/10.1002/dvdy.22425

Diaz-Cuadros, M., Miettinen, T.P., Skinner, O.S., Sheedy, D., Díaz-García, C.M., Gapon, S., Hubaud, A., Yellen, G., Manalis, S.R., Oldham, W.M., Pourquié, O., 2023. Metabolic regulation of species-specific developmental rates. Nature 613, 550–557. https://doi.org/10.1038/s41586-022-05574-4

Dickman, E.D., Rogers, R., Conway, S.J., 1999. Abnormal skeletogenesis occurs coincident with increased apoptosis in theSplotch (Sp2H) mutant: Putative roles forPax3 andPDGFR? in rib patterning. Anat. Rec. 255, 353–361. https://doi.org/10.1002/(SICI)1097-0185(19990701)255:3<353::AID-AR11>3.0.CO;2-H

Dietrich, S., Abou-Rebyeh, F., Brohmann, H., Bladt, F., Sonnenberg-Riethmacher, E., Yamaai, T., Lumsden, A., Brand-Saberi, B., Birchmeier, C., 1999. The role of SF/HGF and c-Met in the development of skeletal muscle. Development 126, 1621–1629. https://doi.org/10.1242/dev.126.8.1621

Dietrich, S., Gruss, P., 1995. undulated Phenotypes Suggest a Role of Pax-1 for the Development of Vertebral and Extravertebral Structures. Developmental Biology 167, 529–548. https://doi.org/10.1006/dbio.1995.1047

Dietrich, S., Schubert, F.R., Gruss, P., 1993. Altered Pax gene expression in murine notochord mutants: the notochord is required to initiate and maintain ventral identity in the somite. Mechanisms of Development 44, 189–207. https://doi.org/10.1016/0925-4773(93)90067-8

Dietrich, S., Schubert, F.R., Healy, C., Sharpe, P.T., Lumsden, A., 1998. Specification of the hypaxial musculature. Development 125, 2235–2249. https://doi.org/10.1242/dev.125.12.2235

Dietrich, S., Schubert, F.R., Lumsden, A., 1997. Control of dorsoventral pattern in the chick paraxial mesoderm. Development 124, 3895–3908. https://doi.org/10.1242/dev.124.19.3895

Diogo, R., Johnston, P., Molnar, J.L., Esteve-Altava, B., 2016. Characteristic tetrapod musculoskeletal limb phenotype emerged more than 400 MYA in basal lobe-finned fishes. Sci Rep 6, 37592. https://doi.org/10.1038/srep37592

Dockter, J., Ordahl, C.P., 2000. Dorsoventral axis determination in the somite: a re-examination. Development 127, 2201–2206. https://doi.org/10.1242/dev.127.10.2201

Donoghue, M., Ernst, H., Wentworth, B., Nadal-Ginard, B., Rosenthal, N., 1988. A muscle-specific enhancer is located at the 3′ end of the myosin light-chain 1/3 gene locus. Genes & Development 2, 1779–1790. https://doi.org/10.1101/gad.2.12b.1779

Dorsky, R.I., Sheldahl, L.C., Moon, R.T., 2002. A transgenic Lef1/beta-catenin-dependent reporter is expressed in spatially restricted domains throughout zebrafish development. Dev. Biol. 241, 229–237. https://doi.org/10.1006/dbio.2001.0515

Dos Santos, M., Shah, A.M., Zhang, Y., Bezprozvannaya, S., Chen, K., Xu, L., Lin, W., McAnally, J.R., Bassel-Duby, R., Liu, N., Olson, E.N., 2023. Opposing gene regulatory programs governing myofiber development and maturation revealed at single nucleus resolution. Nat Commun 14, 4333. https://doi.org/10.1038/s41467-023-40073-8

Draga, M., Scaal, M., 2024. Building a vertebra: Development of the amniote sclerotome. Journal of Morphology 285, e21665. https://doi.org/10.1002/jmor.21665

Dubrulle, J., McGrew, M.J., Pourquié, O., 2001. FGF Signaling Controls Somite Boundary Position and Regulates Segmentation Clock Control of Spatiotemporal Hox Gene Activation. Cell 106, 219–232. https://doi.org/10.1016/S0092-8674(01)00437-8

Dunty, W.C., Biris, K.K., Chalamalasetty, R.B., Taketo, M.M., Lewandoski, M., Yamaguchi, T.P., 2008. Wnt3a/β-catenin signaling controls posterior body development by coordinating mesoderm formation and segmentation. Development 135, 85–94. https://doi.org/10.1242/dev.009266

Durland, J.L., Sferlazzo, M., Logan, M., Burke, A.C., 2008. Visualizing the lateral somitic frontier in the Prx1Cre transgenic mouse. Journal of Anatomy 212, 590–602. https://doi.org/10.1111/j.1469-7580.2008.00879.x

Ehehalt, F., Wang, B., Christ, B., Patel, K., Huang, R., 2004. Intrinsic cartilage-forming potential of dermomyotomal cells requires ectodermal signals for the development of the scapula blade. Anat Embryol 208. https://doi.org/10.1007/s00429-004-0415-0

Esner, M., Meilhac, S.M., Relaix, F., Nicolas, J.-F., Cossu, G., Buckingham, M.E., 2006. Smooth muscle of the dorsal aorta shares a common clonal origin with skeletal muscle of the myotome. Development 133, 737–749. https://doi.org/10.1242/dev.02226

Esteves De Lima, J., Blavet, C., Bonnin, M.-A., Hirsinger, E., Comai, G., Yvernogeau, L., Delfini, M.-C., Bellenger, L., Mella, S., Nassari, S., Robin, C., Schweitzer, R., Fournier-Thibault, C., Jaffredo, T., Tajbakhsh, S., Relaix, F., Duprez, D., 2021a. Unexpected contribution of fibroblasts to muscle lineage as a mechanism for limb muscle patterning. Nat Commun 12, 3851. https://doi.org/10.1038/s41467-021-24157-x

Esteves De Lima, J., Blavet, C., Bonnin, M.-A., Hirsinger, E., Havis, E., Relaix, F., Duprez, D., 2022. TMEM8C-mediated fusion is

regionalized and regulated by NOTCH signalling during foetal myogenesis. Development 149, dev199928. https://doi.org/10.1242/dev.199928

Esteves De Lima, J., Bonnin, M.-A., Birchmeier, C., Duprez, D., 2016. Muscle contraction is required to maintain the pool of muscle progenitors via YAP and NOTCH during fetal myogenesis. eLife 5, e15593. https://doi.org/10.7554/eLife.15593

Esteves De Lima, J., Bou Akar, R., Mansour, M., Rocancourt, D., Buckingham, M., Relaix, F., 2021b. M-Cadherin Is a PAX3 Target During Myotome Patterning. Front. Cell Dev. Biol. 9, 652652. https://doi.org/10.3389/fcell.2021.652652

Etchevers, H.C., Vincent, C., Douarin, N.M.L., F. Couly, G., 2001. The cephalic neural crest provides pericytes and smooth muscle cells to all blood vessels of the face and forebrain. Development 128, 1059–1068. https://doi.org/10.1242/dev.128.7.1059

Evans, A.L., Gage, P.J., 2005. Expression of the homeobox gene Pitx2 in neural crest is required for optic stalk and ocular anterior segment development. Human Molecular Genetics 14, 3347–3359. https://doi.org/10.1093/hmg/ddi365

Evans, D.J.R., 2003. Contribution of somitic cells to the avian ribs. Developmental Biology 256, 115–127. https://doi.org/10.1016/S0012-1606(02)00117-3

Evans, D.J.R., Noden, D.M., 2006. Spatial relations between avian craniofacial neural crest and paraxial mesoderm cells. Developmental Dynamics 235, 1310–1325. https://doi.org/10.1002/dvdy.20663

Ferrer-Vaquer, A., Piliszek, A., Tian, G., Aho, R.J., Dufort, D., Hadjantonakis, A.-K., 2010. A sensitive and bright single-cell resolution live imaging reporter of Wnt/ß-catenin signaling in the mouse. BMC Dev Biol 10, 121. https://doi.org/10.1186/1471-213X-10-121

Fetcho, J.R., 1987. A review of the organization and evolution of motoneurons innervating the axial musculature of vertebrates. Brain Research Reviews 12, 243–280. https://doi.org/10.1016/0165-0173(87)90001-4

Flynn, C.G.K., Ginkel, P.R.V., Hubert, K.A., Guo, Q., Hrycaj, S.M., McDermott, A.E., Madruga, A., Miller, A.P., Wellik, D.M., 2023. Hox11-expressing interstitial cells contribute to adult skeletal muscle at homeostasis. Development 150, dev201026. https://doi.org/10.1242/dev.201026

Foudi, A., Hochedlinger, K., Van Buren, D., Schindler, J.W., Jaenisch, R., Carey, V., Hock, H., 2009. Analysis of histone 2B-GFP retention reveals slowly cycling hematopoietic stem cells. Nat Biotechnol 27, 84–90. https://doi.org/10.1038/nbt.1517
Francis, E.T.B., 1934. The Anatomy of the Salamander. Clarendon Press.

Fu, M., Xu, L., Chen, X., Han, W., Ruan, C., Li, J., Cai, C., Ye, M., Gao, P., 2019. Neural Crest Cells Differentiate Into Brown Adipocytes and Contribute to Periaortic Arch Adipose Tissue Formation. ATVB 39, 1629–1644. https://doi.org/10.1161/ATVBAHA.119.312838

Furumoto, T., Miura, N., Akasaka, T., Mizutani-Koseki, Y., Sudo, H., Fukuda, K., Maekawa, M., Yuasa, S., Fu, Y., Moriya, H., Taniguchi, M., Imai, K., Dahl, E., Balling, R., Pavlova, M., Gossler, A., Koseki, H., 1999. Notochord-Dependent Expression of MFH1 and PAX1 Cooperates to Maintain the Proliferation of Sclerotome Cells during the Vertebral Column Development. Developmental Biology 210, 15–29. https://doi.org/10.1006/dbio.1999.9261

Galis, F., Van Dooren, T.J.M., Van Der Geer, A.A.E., 2022. Breaking the constraint on the number of cervical vertebrae in mammals: On homeotic transformations in lorises and pottos. Evolution and Development 24, 196–210. https://doi.org/10.1111/ede.12424

Gaut, L., Duprez, D., 2016. Tendon development and diseases. WIREs Developmental Biology 5, 5–23. https://doi.org/10.1002/wdev.201

Geetha-Loganathan, P., Nimmagadda, S., Pröls, F., Patel, K., Scaal, M., Huang, R., Christ, B., 2005. Ectodermal Wnt-6 promotes Myf5-dependent avian limb myogenesis. Dev. Biol. 288, 221–233. https://doi.org/10.1016/j.ydbio.2005.09.035

Gensch, N., Borchardt, T., Schneider, A., Riethmacher, D., Braun, T., 2008. Different autonomous myogenic cell populations revealed by ablation of Myf5-expressing cells during mouse embryogenesis. Development 135, 1597–1604. https://doi.org/10.1242/dev.019331

George, E.L., Georges-Labouesse, E.N., Patel-King, R.S., Rayburn, H., Hynes, R.O., 1993. Defects in mesoderm, neural tube and vascular development in mouse embryos lacking fibronectin. Development 119, 1079–1091. https://doi.org/10.1242/dev.119.4.1079

Georges-Labouesse, E.N., George, E.L., Rayburn, H., Hynes, R.O., 1996. Mesodermal development in mouse embryos mutant for fibronectin. Dev. Dyn. 207, 145–156. https://doi.org/10.1002/(SICI)1097-0177(199610)207:2<145::AID-AJA3>3.0.CO;2-H

Gerhart, J., Kirschner, M., 2020. Normal Table of Xenopus Laevis (Daudin): A Systematical and Chronological Survey of the Development from the Fertilized Egg Till the End of Metamorphosis, 1st ed. Garland Science. https://doi.org/10.1201/9781003064565

Gilbert, S.F., 2014. Developmental biology, 10th ed. ed. Sinauer associates, Inc. publishers, Sunderland (Mass.).

Giordani, J., Bajard, L., Demignon, J., Daubas, P., Buckingham, M., Maire, P., 2007. Six proteins regulate the activation of *Myf5* expression in embryonic mouse limbs. Proc. Natl. Acad. Sci. U.S.A. 104, 11310–11315. https://doi.org/10.1073/pnas.0611299104

Goh, K.L., Yang, J.T., Hynes, R.O., 1997. Mesodermal defects and cranial neural crest apoptosis in α5 integrin-null embryos. Development 124, 4309–4319. https://doi.org/10.1242/dev.124.21.4309

Gomez, C., Özbudak, E.M., Wunderlich, J., Baumann, D., Lewis, J., Pourquié, O., 2008. Control of segment number in vertebrate embryos. Nature 454, 335–339. https://doi.org/10.1038/nature07020

Gong, X.Q., Li, L., 2002. Dermo-1, a Multifunctional Basic Helix-Loop-Helix Protein, Represses MyoD Transactivation via the HLH Domain, MEF2 Interaction, and Chromatin Deacetylation. Journal of Biological Chemistry 277, 12310–12317. https://doi.org/10.1074/jbc.M110228200

Gopalakrishnan, S., Comai, G., Sambasivan, R., Francou, A., Kelly, R.G., Tajbakhsh, S., 2015. A Cranial Mesoderm Origin for Esophagus Striated Muscles. Developmental Cell 34, 694–704. https://doi.org/10.1016/j.devcel.2015.07.003

Goulding, M., Lumsden, A., Paquette, A.J., 1994. Regulation of *Pax-3* expression in the dermomyotome and its role in muscle development. Development 120, 957–971. https://doi.org/10.1242/dev.120.4.957

Gray, P.A., Fu, H., Luo, P., Zhao, Q., Yu, J., Ferrari, A., Tenzen, T., Yuk, D., Tsung, E.F., Cai, Z., Alberta, J.A., Cheng, L., Liu, Y., Stenman, J.M., Valerius, M.T., Billings, N., Kim, H.A., Greenberg, M.E., McMahon, A.P., Rowitch, D.H., Stiles, C.D., Ma, Q., 2004. Mouse Brain Organization Revealed Through Direct Genome-Scale TF Expression Analysis. Science 306, 2255–2257. https://doi.org/10.1126/science.1104935

Grenier, J., Teillet, M.-A., Grifone, R., Kelly, R.G., Duprez, D., 2009. Relationship between Neural Crest Cells and Cranial Mesoderm during Head Muscle Development. PLoS ONE 4, e4381. https://doi.org/10.1371/journal.pone.0004381

Grifone, R., Demignon, J., Giordani, J., Niro, C., Souil, E., Bertin, F., Laclef, C., Xu, P.-X., Maire, P., 2007. Eya1 and Eya2 proteins are required for hypaxial somitic myogenesis in the mouse embryo. Developmental Biology 302, 602–616. https://doi.org/10.1016/j.ydbio.2006.08.059

Grifone, R., Demignon, J., Houbron, C., Souil, E., Niro, C., Seller, M.J., Hamard, G., Maire, P., 2005. Six1 and Six4 homeoproteins are required for Pax3 and Mrf expression during myogenesis in the mouse embryo. Development 132, 2235–2249. https://doi.org/10.1242/dev.01773

Grim, M., Wachtler, F., 1991. Muscle morphogenesis in the absence of myogenic cells. Anat Embryol 183. https://doi.org/10.1007/BF00185836

Grimaldi, A., Comai, G., Mella, S., Tajbakhsh, S., 2022. Identification of bipotent progenitors that give rise to myogenic and connective tissues in mouse. eLife 11, e70235. https://doi.org/10.7554/eLife.70235

Gros, J., Manceau, M., Thomé, V., Marcelle, C., 2005. A common somitic origin for embryonic muscle progenitors and satellite cells. Nature 435, 954–958. https://doi.org/10.1038/nature03572

Gros, J., Scaal, M., Marcelle, C., 2004. A Two-Step Mechanism for Myotome Formation in Chick. Developmental Cell 6, 875–882. https://doi.org/10.1016/j.devcel.2004.05.006

Gros, J., Serralbo, O., Marcelle, C., 2009. WNT11 acts as a directional cue to organize the elongation of early muscle fibres. Nature 457, 589–593. https://doi.org/10.1038/nature07564

Gross, M.K., Moran-Rivard, L., Velasquez, T., Nakatsu, M.N., Jagla, K., Goulding, M., 2000. *Lbx1* is required for muscle precursor migration along a lateral pathway into the limb. Development 127, 413–424. https://doi.org/10.1242/dev.127.2.413

Guerquin, M.-J., Charvet, B., Nourissat, G., Havis, E., Ronsin, O., Bonnin, M.-A., Ruggiu, M., Olivera-Martinez, I., Robert, N., Lu,

Y., Kadler, K.E., Baumberger, T., Doursounian, L., Berenbaum, F., Duprez, D., 2013. Transcription factor EGR1 directs tendon differentiation and promotes tendon repair. J. Clin. Invest. 123, 3564–3576. https://doi.org/10.1172/JCI67521

Halata, Z., Grim, M., Christ, B., 1990. Origin of spinal cord meninges, sheaths of peripheral nerves, and cutaneous receptors including Merkel cells: An experimental and ultrastructural study with avian chimeras. Anat Embryol 182. https://doi.org/10.1007/BF00186459

Haldar, M., Karan, G., Tvrdik, P., Capecchi, M.R., 2008. Two cell lineages, myf5 and myf5-independent, participate in mouse skeletal myogenesis. Dev. Cell 14, 437–445. https://doi.org/10.1016/j.devcel.2008.01.002

Harvey, E.B., Kaiser, H.E., Rosenberg, L.E., 1969. ATLAS OF THE DOMESTIC TURKEY (MELEAGRIS GALLOPAVO). MYOLOGY AND OSTEOLOGY. (No. WASH--1123, 4811958). https://doi.org/10.2172/4811958

Hasson, P., DeLaurier, A., Bennett, M., Grigorieva, E., Naiche, L.A., Papaioannou, V.E., Mohun, T.J., Logan, M.P.O., 2010. Tbx4 and Tbx5 Acting in Connective Tissue Are Required for Limb Muscle and Tendon Patterning. Developmental Cell 18, 148–156. https://doi.org/10.1016/j.devcel.2009.11.013

Hasty, P., Bradley, A., Morris, J.H., Edmondson, D.G., Venuti, J.M., Olson, E.N., Klein, W.H., 1993. Muscle deficiency and neonatal death in mice with a targeted mutation in the myogenin gene. Nature 364, 501–506. https://doi.org/10.1038/364501a0

Havis, E., Bonnin, M.-A., Olivera-Martinez, I., Nazaret, N., Ruggiu, M., Weibel, J., Durand, C., Guerquin, M.-J., Bonod-Bidaud, C., Ruggiero, F., Schweitzer, R., Duprez, D., 2014. Transcriptomic analysis of mouse limb tendon cells during development. Development 141, 3683–3696. https://doi.org/10.1242/dev.108654

Havis, E., Coumailleau, P., Bonnet, A., Bismuth, K., Bonnin, M.-A., Johnson, R., Fan, C.-M., Relaix, F., Shi, D.-L., Duprez, D., 2012. Sim2 prevents entry into the myogenic program by repressing *MyoD* transcription during limb embryonic myogenesis. Development 139, 1910–1920. https://doi.org/10.1242/dev.072561

He, L., Binari, R., Huang, J., Falo-Sanjuan, J., Perrimon, N., 2019. In vivo study of gene expression with an enhanced dual-color fluorescent transcriptional timer [WWW Document]. eLife. https://doi.org/10.7554/eLife.46181

Heanue, T.A., Reshef, R., Davis, R.J., Mardon, G., Oliver, G., Tomarev, S., Lassar, A.B., Tabin, C.J., 1999. Synergistic regulation of vertebrate muscle development by Dach2, Eya2, and Six1, homologs of genes required for Drosophila eye formation. Genes & Development 13, 3231–3243. https://doi.org/10.1101/gad.13.24.3231

Heng, Y.C., Foo, J.L., 2022. Development of destabilized mCherry fluorescent proteins for applications in the model yeast Saccharomyces cerevisiae. Biotechnology Notes 3, 108–112. https://doi.org/10.1016/j.biotno.2022.12.001

Herbert, S.P., Stainier, D.Y.R., 2011. Molecular control of endothelial cell behaviour during blood vessel morphogenesis. Nat Rev Mol Cell Biol 12, 551–564. https://doi.org/10.1038/nrm3176

Hernández-Hernández, J.M., García-González, E.G., Brun, C.E., Rudnicki, M.A., 2017. The myogenic regulatory factors, determinants of muscle development, cell identity and regeneration. Seminars in Cell & Developmental Biology 72, 10–18. https://doi.org/10.1016/j.semcdb.2017.11.010

Heude, É., Bouhali, K., Kurihara, Y., Kurihara, H., Couly, G., Janvier, P., Levi, G., 2010. Jaw muscularization requires *Dlx* expression by cranial neural crest cells. Proc. Natl. Acad. Sci. U.S.A. 107, 11441–11446. https://doi.org/10.1073/pnas.1001582107

Heude, E., Tesarova, M., Sefton, E.M., Jullian, E., Adachi, N., Grimaldi, A., Zikmund, T., Kaiser, J., Kardon, G., Kelly, R.G., Tajbakhsh, S., 2018. Unique morphogenetic signatures define mammalian neck muscles and associated connective tissues. eLife 7, e40179. https://doi.org/10.7554/eLife.40179

Hirasawa, T., Kuratani, S., 2018. Evolution of the muscular system in tetrapod limbs. Zoological Lett 4, 27. https://doi.org/10.1186/s40851-018-0110-2

Hirasawa, T., Nagashima, H., Kuratani, S., 2013. The endoskeletal origin of the turtle carapace. Nat Commun 4, 2107. https://doi.org/10.1038/ncomms3107

Hirsinger, E., Blavet, C., Bonnin, M.-A., Bellenger, L., Gharsalli, T., Duprez, D., 2024. Limb connective tissue is organized in a continuum of promiscuous fibroblast identities during development. https://doi.org/10.1101/2024.03.18.585505

Hirsinger, E., Malapert, P., Dubrulle, J., Delfini, M.-C., Duprez, D., Henrique, D., Ish-Horowicz, D., Pourquié, O., 2001. Notch

signalling acts in postmitotic avian myogenic cells to control *MyoD* activation. Development 128, 107–116. https://doi.org/10.1242/dev.128.1.107

Hochreiter-Hufford, A.E., Lee, C.S., Kinchen, J.M., Sokolowski, J.D., Arandjelovic, S., Call, J.A., Klibanov, A.L., Yan, Z., Mandell, J.W., Ravichandran, K.S., 2013. Phosphatidylserine receptor BAI1 and apoptotic cells as new promoters of myoblast fusion. Nature 497, 263–267. https://doi.org/10.1038/nature12135

Horikawa, K., Takeichi, M., 2001. Requirement of the juxtamembrane domain of the cadherin cytoplasmic tail for morphogenetic cell rearrangement during myotome development. The Journal of Cell Biology 155, 1297–1306. https://doi.org/10.1083/jcb.200108156

Hornik, C., Krishan, K., Yusuf, F., Scaal, M., Brand-Saberi, B., 2005. cDermo-1 misexpression induces dense dermis, feathers, and scales. Developmental Biology 277, 42–50. https://doi.org/10.1016/j.ydbio.2004.08.050

Hosokawa, R., Urata, M., Han, J., Zehnaly, A., Bringas, P., Nonaka, K., Chai, Y., 2007. TGF-β mediated Msx2 expression controls occipital somites-derived caudal region of skull development. Developmental Biology 310, 140–153. https://doi.org/10.1016/j.ydbio.2007.07.038

Huang, A.H., Riordan, T.J., Wang, L., Eyal, S., Zelzer, E., Brigande, J.V., Schweitzer, R., 2013. Repositioning Forelimb Superficialis Muscles: Tendon Attachment and Muscle Activity Enable Active Relocation of Functional Myofibers. Developmental Cell 26, 544–551. https://doi.org/10.1016/j.devcel.2013.08.007

Huang, A.H., Watson, S.S., Wang, L., Baker, B., Akiyama, H., Brigande, J.V., Schweitzer, R., 2019. Requirement for Scleraxis in the recruitment of mesenchymal progenitors during embryonic tendon elongation. Development dev.182782. https://doi.org/10.1242/dev.182782

Huang, R., Stolte, D., Kurz, H., Ehehalt, F., Cann, G.M., Stockdale, F.E., Patel, K., Christ, B., 2003a. Ventral axial organs regulate expression of myotomal Fgf-8 that influences rib development. Developmental Biology 255, 30–47. https://doi.org/10.1016/S0012-1606(02)00051-9

Huang, R., Zhi, Q., Brand-Saberi, B., Christ, B., 2000. New experimental evidence for somite resegmentation. Anatomy and Embryology 202, 195–200. https://doi.org/10.1007/s004290000110

Huang, R., Zhi, Q., Christ, B., 2003b. The relationship between limb muscle and endothelial cells migrating from single somite. Anat Embryol 206, 283–289. https://doi.org/10.1007/s00429-002-0289-y

Huang, R., Zhi, Q., Izpisua-Belmonte, J.-C., Christ, B., Patel, K., 1999. Origin and development of the avian tongue muscles. Anatomy and Embryology 200, 137–152. https://doi.org/10.1007/s004290050268

Huang, R., Zhi, Q., Neubüser, A., Müller, T.S., Brand-Saberi, B., Christ, B., Wilting, J., 1996. Function of Somite and Somitocoele Cells in the Formation of the Vertebral Motion Segment in Avian Embryos. Cells Tissues Organs 155, 231–241. https://doi.org/10.1159/000147811

Huang, R., Zhi, Q., Ordahl, P., Christ, B., 1997. The fate of the first avian somite. Anatomy and Embryology 195, 435–449. https://doi.org/10.1007/s004290050063

Huang, Ruijin, Zhi, Q., Patel, K., Wilting, J., Christ, B., 2000a. Dual origin and segmental organisation of the avian scapula. Development 127, 3789–3794. https://doi.org/10.1242/dev.127.17.3789

Huang, Ruijin, Zhi, Q., Patel, K., Wilting, J., Christ, B., 2000b. Contribution of single somites to the skeleton and muscles of the occipital and cervical regions in avian embryos. Anatomy and Embryology 202, 375–383. https://doi.org/10.1007/s004290000131

Huang, Z., Gu, C., Zhang, Z., Arianti, R., Swaminathan, A., Tran, K., Battist, A., Kristóf, E., Ruan, H.-B., 2023. Supraclavicular brown adipocytes originate from Tbx1+ myoprogenitors. PLoS Biol 21, e3002413. https://doi.org/10.1371/journal.pbio.3002413

Hughes, D.S., Keynes, R.J., Tannahill, D., 2009. Extensive molecular differences between anterior- and posterior-half-sclerotomes underlie somite polarity and spinal nerve segmentation. BMC Dev Biol 9, 30. https://doi.org/10.1186/1471-213X-9-30

Huisken, J., Stainier, D.Y.R., 2009. Selective plane illumination microscopy techniques in developmental biology. Development 136, 1963–1975. https://doi.org/10.1242/dev.022426

Hutcheson, D.A., Zhao, J., Merrell, A., Haldar, M., Kardon, G., 2009. Embryonic and fetal limb myogenic cells are derived from developmentally distinct progenitors and have different requirements for beta-catenin. Genes Dev. 23, 997–1013. https://doi.org/10.1101/gad.1769009

Iimura, T., Denans, N., Pourquié, O., 2009. Chapter 7 Establishment of Hox Vertebral Identities in the Embryonic Spine Precursors, in: Current Topics in Developmental Biology. Elsevier, pp. 201–234. https://doi.org/10.1016/S0070-2153(09)88007-1

Jacob, H.J., Christ, B., 1980. On the Formation of Muscular Pattern in the Chick Limb, in: Merker, H.-J., Nau, H., Neubert, D. (Eds.), Teratology of the Limbs. De Gruyter, Berlin, Boston, pp. 89–98. https://doi.org/10.1515/9783110861082-012

Jafree, D.J., Long, D.A., Scambler, P.J., Ruhrberg, C., 2021. Mechanisms and cell lineages in lymphatic vascular development. Angiogenesis 24, 271–288. https://doi.org/10.1007/s10456-021-09784-8

James, H.F., 2009. Repeated Evolution of Fused Thoracic Vertebrae in Songbirds. The Auk 126, 862–872. https://doi.org/10.1525/auk.2009.08194

Jiang, X., Rowitch, D.H., Soriano, P., McMahon, A.P., Sucov, H.M., 2000. Fate of the mammalian cardiac neural crest. Development 127, 1607–1616. https://doi.org/10.1242/dev.127.8.1607

Jun, S., Angueira, A.R., Fein, E.C., Tan, J.M.E., Weller, A.H., Cheng, L., Batmanov, K., Ishibashi, J., Sakers, A.P., Stine, R.R., Seale, P., 2023. Control of murine brown adipocyte development by GATA6. Developmental Cell 58, 2195-2205.e5. https://doi.org/10.1016/j.devcel.2023.08.003

Kablar, B., Krastel, K., Tajbakhsh, S., Rudnicki, M.A., 2003. Myf5 and MyoD activation define independent myogenic compartments during embryonic development. Developmental Biology 258, 307–318. https://doi.org/10.1016/S0012-1606(03)00139-8

Kardon, G., Campbell, J.K., Tabin, C.J., 2002. Local Extrinsic Signals Determine Muscle and Endothelial Cell Fate and Patterning in the Vertebrate Limb. Developmental Cell 3, 533–545. https://doi.org/10.1016/S1534-5807(02)00291-5

Kardon, G., Harfe, B.D., Tabin, C.J., 2003. A Tcf4-Positive Mesodermal Population Provides a Prepattern for Vertebrate Limb Muscle Patterning. Developmental Cell 5, 937–944. https://doi.org/10.1016/S1534-5807(03)00360-5

Kassar-Duchossoy, L., Giacone, E., Gayraud-Morel, B., Jory, A., Gomès, D., Tajbakhsh, S., 2005. Pax3/Pax7 mark a novel population of primitive myogenic cells during development. Genes Dev. 19, 1426–1431. https://doi.org/10.1101/gad.345505

Kato, N., Aoyama, H., 1998. Dermomyotomal origin of the ribs as revealed by extirpation and transplantation experiments in chick and quail embryos. Development 125, 3437–3443. https://doi.org/10.1242/dev.125.17.3437

Kelly, A.M., Rubinstein, N.A., 1980. Why are fetal muscles slow? Nature 288, 266–269. https://doi.org/10.1038/288266a0

Kelly, R.G., Jerome-Majewska, L.A., Papaioannou, V.E., 2004. The del22q11.2 candidate gene Tbx1 regulates branchiomeric myogenesis. Human Molecular Genetics 13, 2829–2840. https://doi.org/10.1093/hmg/ddh304

Khabyuk, J., Pröls, F., Draga, M., Scaal, M., 2022. Development of ribs and intercostal muscles in the chicken embryo. Journal of Anatomy 241, 831–845. https://doi.org/10.1111/joa.13716

Kieny, M., Mauger, A., Sengel, P., 1972. Early regionalization of the somitic mesoderm as studied by the development of the axial skeleton of the chick embryo. Developmental Biology 28, 142–161. https://doi.org/10.1016/0012-1606(72)90133-9

Kimura, W., Machii, M., Xue, X., Sultana, N., Hikosaka, K., Sharkar, M.T.K., Uezato, T., Matsuda, M., Koseki, H., Miura, N., 2011. *Irxl1* mutant mice show reduced tendon differentiation and no patterning defects in musculoskeletal system development. Genesis 49, 2–9. https://doi.org/10.1002/dvg.20688

Korinek, V., Barker, N., Morin, P.J., Van Wichen, D., De Weger, R., Kinzler, K.W., Vogelstein, B., Clevers, H., 1997. Constitutive Transcriptional Activation by a β-Catenin-Tcf Complex in APC $^{-/-}$ Colon Carcinoma. Science 275, 1784–1787. https://doi.org/10.1126/science.275.5307.1784

Krull, C.E., Lansford, R., Gale, N.W., Collazo, A., Marcelle, C., Yancopoulos, G.D., Fraser, S.E., Bronner-Fraser, M., 1997. Interactions of Eph-related receptors and ligands confer rostrocaudal pattern to trunk neural crest migration. Current Biology 7, 571–580. https://doi.org/10.1016/S0960-9822(06)00256-9

Kuroda, N., 1962. On the cervical muscles of birds. Journal of the Yamashina Institute for Ornithology 3, 189–211.

https://doi.org/10.3312/jyio1952.3.189

Kusakabe, R., Kuraku, S., Kuratani, S., 2011. Expression and interaction of muscle-related genes in the lamprey imply the evolutionary scenario for vertebrate skeletal muscle, in association with the acquisition of the neck and fins. Developmental Biology 350, 217–227. https://doi.org/10.1016/j.ydbio.2010.10.029

Ladher, R.K., Church, V.L., Allen, S., Robson, L., Abdelfattah, A., Brown, N.A., Hattersley, G., Rosen, V., Luyten, F.P., Dale, L., Francis-West, P.H., 2000. Cloning and Expression of the Wnt Antagonists Sfrp-2 and Frzb during Chick Development. Developmental Biology 218, 183–198. https://doi.org/10.1006/dbio.1999.9586

Lagha, M., Brunelli, S., Messina, G., Cumano, A., Kume, T., Relaix, F., Buckingham, M.E., 2009. Pax3:Foxc2 Reciprocal Repression in the Somite Modulates Muscular versus Vascular Cell Fate Choice in Multipotent Progenitors. Developmental Cell 17, 892–899. https://doi.org/10.1016/j.devcel.2009.10.021

Lance-Jones, C., 1988a. The effect of somite manipulation on the development of motoneuron projection patterns in the embryonic chick hindlimb. Developmental Biology 126, 408–419. https://doi.org/10.1016/0012-1606(88)90150-9

Lance-Jones, C., 1988b. The somitic level of origin of embryonic chick hindlimb muscles. Developmental Biology 126, 394–407. https://doi.org/10.1016/0012-1606(88)90149-2

Lassar, A.B., Paterson, B.M., Weintraub, H., 1986. Transfection of a DNA locus that mediates the conversion of 10T12 fibroblasts to myoblasts. Cell 47, 649–656. https://doi.org/10.1016/0092-8674(86)90507-6

Laurin, M., Fradet, N., Blangy, A., Hall, A., Vuori, K., Côté, J.-F., 2008. The atypical Rac activator Dock180 (Dock1) regulates myoblast fusion *in vivo*. Proc. Natl. Acad. Sci. U.S.A. 105, 15446–15451. https://doi.org/10.1073/pnas.0805546105

Lejard, V., Blais, F., Guerquin, M.-J., Bonnet, A., Bonnin, M.-A., Havis, E., Malbouyres, M., Bidaud, C.B., Maro, G., Gilardi-Hebenstreit, P., Rossert, J., Ruggiero, F., Duprez, D., 2011. EGR1 and EGR2 Involvement in Vertebrate Tendon Differentiation. Journal of Biological Chemistry 286, 5855–5867. https://doi.org/10.1074/jbc.M110.153106

Lepper, C., Fan, C., 2010. Inducible lineage tracing of Pax7-descendant cells reveals embryonic origin of adult satellite cells. Genesis 48, 424–436. https://doi.org/10.1002/dvg.20630

Li, L., Cserjesi, P., Olson, E.N., 1995. Dermo-1: A Novel Twist-Related bHLH Protein Expressed in the Developing Dermis. Developmental Biology 172, 280–292. https://doi.org/10.1006/dbio.1995.0023

Liem, K.F., 2001. Functional anatomy of the vertebrates: an evolutionary perspective, 3rd ed. ed. Harcourt College publ, Fort Worth.

Linask, K.K., Ludwig, C., Han, M.-D., Liu, X., Radice, G.L., Knudsen, K.A., 1998. N-Cadherin/Catenin-Mediated Morphoregulation of Somite Formation. Developmental Biology 202, 85–102. https://doi.org/10.1006/dbio.1998.9025

Linker, C., Lesbros, C., Gros, J., Burrus, L.W., Rawls, A., Marcelle, C., 2005. β-Catenin-dependent Wnt signalling controls the epithelial organisation of somites through the activation of *paraxis*. Development 132, 3895–3905. https://doi.org/10.1242/dev.01961

Liu, N., Garry, G.A., Li, S., Bezprozvannaya, S., Sanchez-Ortiz, E., Chen, B., Shelton, J.M., Jaichander, P., Bassel-Duby, R., Olson, E.N., 2017. A Twist2-dependent progenitor cell contributes to adult skeletal muscle. Nat Cell Biol 19, 202–213. https://doi.org/10.1038/ncb3477

Liu, W., Watson, S.S., Lan, Y., Keene, D.R., Ovitt, C.E., Liu, H., Schweitzer, R., Jiang, R., 2010. The Atypical Homeodomain Transcription Factor Mohawk Controls Tendon Morphogenesis. Molecular and Cellular Biology 30, 4797–4807. https://doi.org/10.1128/MCB.00207-10

Loganathan, P.G., Nimmagadda, S., Huang, R., Scaal, M., Christ, B., 2005. Comparative analysis of the expression patterns of Wnts during chick limb development. Histochem Cell Biol 123, 195–201. https://doi.org/10.1007/s00418-005-0756-7

Lu, J., Bassel-Duby, R., Hawkins, A., Chang, P., Valdez, R., Wu, H., Gan, L., Shelton, J.M., Richardson, J.A., Olson, E.N., 2002. Control of Facial Muscle Development by MyoR and Capsulin. Science 298, 2378–2381. https://doi.org/10.1126/science.1078273

Maddin, H.C., Piekarski, N., Reisz, R.R., Hanken, J., 2020. Development and evolution of the tetrapod skull–neck boundary. Biological Reviews 95, 573–591. https://doi.org/10.1111/brv.12578

Manceau, M., Gros, J., Savage, K., Thomé, V., McPherron, A., Paterson, B., Marcelle, C., 2008. Myostatin promotes the terminal differentiation of embryonic muscle progenitors. Genes Dev. 22, 668–681. https://doi.org/10.1101/gad.454408

Mansfield, J.H., Haller, E., Holland, N.D., Brent, A.E., 2015. Development of somites and their derivatives in amphioxus, and implications for the evolution of vertebrate somites. EvoDevo 6, 21. https://doi.org/10.1186/s13227-015-0007-5

Marcelle, C., Stark, M.R., Bronner-Fraser, M., 1997. Coordinate actions of BMPs, Wnts, Shh and Noggin mediate patterning of the dorsal somite. Development 124, 3955–3963. https://doi.org/10.1242/dev.124.20.3955

Maretto, S., Cordenonsi, M., Dupont, S., Braghetta, P., Broccoli, V., Hassan, A.B., Volpin, D., Bressan, G.M., Piccolo, S., 2003. Mapping Wnt/β-catenin signaling during mouse development and in colorectal tumors. PNAS 100, 3299–3304. https://doi.org/10.1073/pnas.0434590100

Maschner, A., Krück, S., Draga, M., Pröls, F., Scaal, M., 2016. Developmental dynamics of occipital and cervical somites. Journal of Anatomy 229, 601–609. https://doi.org/10.1111/joa.12516

Masyuk, M., Abduelmula, A., Morosan-Puopolo, G., Ödemis, V., Rehimi, R., Khalida, N., Yusuf, F., Engele, J., Tamamura, H., Theiss, C., Brand-Saberi, B., 2014. Retrograde migration of pectoral girdle muscle precursors depends on CXCR4/SDF-1 signaling. Histochem Cell Biol 142, 473–488. https://doi.org/10.1007/s00418-014-1237-7

Mauger, A., 1972. Rôle du mésoderme somitique dans le développement du plumage dorsal chez l'embryon de Poulet:I. Origine, capacités de régulation et détermination du mésoderme plumigène. Development 28, 313–341. https://doi.org/10.1242/dev.28.2.313

Mayeuf-Louchart, A., Lagha, M., Danckaert, A., Rocancourt, D., Relaix, F., Vincent, S.D., Buckingham, M., 2014. Notch regulation of myogenic versus endothelial fates of cells that migrate from the somite to the limb. Proc. Natl. Acad. Sci. U.S.A. 111, 8844–8849. https://doi.org/10.1073/pnas.1407606111

McMeekan, C.P., 1940. Growth and development in the pig, with special reference to carcass quality characters. I. J. Agric. Sci. 30, 276–343. https://doi.org/10.1017/S0021859600048024

McPherron, A.C., Lawler, A.M., Lee, S.-J., 1997. Regulation of skeletal muscle mass in mice by a new TGF-p superfamily member. Nature 387, 83–90. https://doi.org/10.1038/387083a0

Meara, P.J., 1947. Meat studies; post-natal growth and development of muscle, as exemplified by the gastrocnemius and psoas muscles of the rabbit. Onderstepoort J Vet Sci Anim Ind 21, 329–466.

Melendez, J., Sieiro, D., Salgado, D., Morin, V., Dejardin, M.-J., Zhou, C., Mullen, A.C., Marcelle, C., 2021. TGFβ signalling acts as a molecular brake of myoblast fusion. Nat Commun 12, 749. https://doi.org/10.1038/s41467-020-20290-1

Mennerich, D., Schäfer, K., Braun, T., 1998. Pax-3 is necessary but not sufficient for lbx1 expression in myogenic precursor cells of the limb. Mechanisms of Development 73, 147–158. https://doi.org/10.1016/S0925-4773(98)00046-X

Messina, G., Biressi, S., Monteverde, S., Magli, A., Cassano, M., Perani, L., Roncaglia, E., Tagliafico, E., Starnes, L., Campbell, C.E., Grossi, M., Goldhamer, D.J., Gronostajski, R.M., Cossu, G., 2010. Nfix Regulates Fetal-Specific Transcription in Developing Skeletal Muscle. Cell 140, 554–566. https://doi.org/10.1016/j.cell.2010.01.027

Miao, Y., Djeffal, Y., De Simone, A., Zhu, K., Lee, J.G., Lu, Z., Silberfeld, A., Rao, J., Tarazona, O.A., Mongera, A., Rigoni, P., Diaz-Cuadros, M., Song, L.M.S., Di Talia, S., Pourquié, O., 2023. Reconstruction and deconstruction of human somitogenesis in vitro. Nature 614, 500–508. https://doi.org/10.1038/s41586-022-05655-4

Millay, D.P., 2022. Regulation of the myoblast fusion reaction for muscle development, regeneration, and adaptations. Experimental Cell Research 415, 113134. https://doi.org/10.1016/j.yexcr.2022.113134

Millay, D.P., O'Rourke, J.R., Sutherland, L.B., Bezprozvannaya, S., Shelton, J.M., Bassel-Duby, R., Olson, E.N., 2013. Myomaker is a membrane activator of myoblast fusion and muscle formation. Nature 499, 301–305. https://doi.org/10.1038/nature12343

Miller, J.B., Stockdale, F.E., 1986. Developmental origins of skeletal muscle fibers: clonal analysis of myogenic cell lineages based on expression of fast and slow myosin heavy chains. Proc. Natl. Acad. Sci. U.S.A. 83, 3860–3864. https://doi.org/10.1073/pnas.83.11.3860

Miller, K.A., Barrow, J., Collinson, J.M., Davidson, S., Lear, M., Hill, R.E., MacKenzie, A., 2007. A highly conserved Wnt-dependent TCF4 binding site within the proximal enhancer of the anti-myogenic Msx1 gene supports expression within Pax3-expressing limb bud muscle precursor cells. Developmental Biology 311, 665–678.

https://doi.org/10.1016/j.ydbio.2007.07.022

Millington, G., Elliott, K.H., Chang, Y.-T., Chang, C.-F., Dlugosz, A., Brugmann, S.A., 2017. Cilia-dependent GLI processing in neural crest cells is required for tongue development. Developmental Biology 424, 124–137. https://doi.org/10.1016/j.ydbio.2017.02.021

Mittapalli, V.R., Huang, R., Patel, K., Christ, B., Scaal, M., 2005. Arthrotome: A specific joint forming compartment in the avian somite. Developmental Dynamics 234, 48–53. https://doi.org/10.1002/dvdy.20502

Moncaut, N., Cross, J.W., Siligan, C., Keith, A., Taylor, K., Rigby, P.W.J., Carvajal, J.J., 2012. Musculin and TCF21 coordinate the maintenance of myogenic regulatory factor expression levels during mouse craniofacial development. Development 139, 958–967. https://doi.org/10.1242/dev.068015

Monsoro-Burq, A.-H., Duprez, D., Watanabe, Y., Bontoux, M., Vincent, C., Brickell, P., Douarin, N.L., 1996. The role of bone morphogenetic proteins in vertebral development. Development 122, 3607–3616. https://doi.org/10.1242/dev.122.11.3607
Montgomery, R.D., 1962. Growth of Human Striated Muscle. Nature 195, 194–195. https://doi.org/10.1038/195194a0

Moreau, C., Caldarelli, P., Rocancourt, D., Roussel, J., Denans, N., Pourquie, O., Gros, J., 2019. Timed Collinear Activation of Hox Genes during Gastrulation Controls the Avian Forelimb Position. Current Biology 29, 35-50.e4. https://doi.org/10.1016/j.cub.2018.11.009

Morin-Kensicki, E.M., Melancon, E., Eisen, J.S., 2002. Segmental relationship between somites and vertebral column in zebrafish. Development 129, 3851–3860. https://doi.org/10.1242/dev.129.16.3851

Moro, E., Ozhan-Kizil, G., Mongera, A., Beis, D., Wierzbicki, C., Young, R.M., Bournele, D., Domenichini, A., Valdivia, L.E., Lum, L., Chen, C., Amatruda, J.F., Tiso, N., Weidinger, G., Argenton, F., 2012. In vivo Wnt signaling tracing through a transgenic biosensor fish reveals novel activity domains. Developmental Biology 366, 327–340. https://doi.org/10.1016/j.ydbio.2012.03.023

Morosan-Puopolo, G., Balakrishnan-Renuka, A., Yusuf, F., Chen, J., Dai, F., Zoidl, G., Lüdtke, T.H.-W., Kispert, A., Theiss, C., Abdelsabour-Khalaf, M., Brand-Saberi, B., 2014. Wnt11 Is Required for Oriented Migration of Dermogenic Progenitor Cells from the Dorsomedial Lip of the Avian Dermomyotome. PLoS ONE 9, e92679. https://doi.org/10.1371/journal.pone.0092679

Murchison, N.D., Price, B.A., Conner, D.A., Keene, D.R., Olson, E.N., Tabin, C.J., Schweitzer, R., 2007. Regulation of tendon differentiation by scleraxis distinguishes force-transmitting tendons from muscle-anchoring tendons. Development 134, 2697–2708. https://doi.org/10.1242/dev.001933

Murphy, M., Kardon, G., 2011. Origin of Vertebrate Limb Muscle, in: Current Topics in Developmental Biology. Elsevier, pp. 1–32. https://doi.org/10.1016/B978-0-12-385940-2.00001-2

Nabeshima, Yoko, Hanaoka, K., Hayasaka, M., Esuml, E., Li, S., Nonaka, I., Nabeshima, Yo-ichi, 1993. Myogenin gene disruption results in perinatal lethality because of severe muscle defect. Nature 364, 532–535. https://doi.org/10.1038/364532a0

Nagashima, H., Koga, D., Kusumi, S., Mukaigasa, K., Yaginuma, H., Ushiki, T., Sato, N., 2020. Novel concept for the epaxial/hypaxial boundary based on neuronal development. Journal of Anatomy 237, 427–438. https://doi.org/10.1111/joa.13219

Nagashima, H., Kuraku, S., Uchida, K., Ohya, Y.K., Narita, Y., Kuratani, S., 2007. On the carapacial ridge in turtle embryos: its developmental origin,function and the chelonian body plan. Development 134, 2219–2226. https://doi.org/10.1242/dev.002618

Nagashima, H., Sugahara, F., Takechi, M., Ericsson, R., Kawashima-Ohya, Y., Narita, Y., Kuratani, S., 2009. Evolution of the Turtle Body Plan by the Folding and Creation of New Muscle Connections. Science 325, 193–196. https://doi.org/10.1126/science.1173826

Nathan, E., Monovich, A., Tirosh-Finkel, L., Harrelson, Z., Rousso, T., Rinon, A., Harel, I., Evans, S.M., Tzahor, E., 2008. The contribution of Islet1-expressing splanchnic mesoderm cells to distinct branchiomeric muscles reveals significant heterogeneity in head muscle development. Development 135, 647–657. https://doi.org/10.1242/dev.007989

Neidhardt, L.M., Kispert, A., Herrmann, B.G., 1997. A mouse gene of the paired-related homeobox class expressed in the caudal somite compartment and in the developing vertebral column, kidney and nervous system. Development Genes and Evolution 207, 330–339. https://doi.org/10.1007/s004270050120

Nimmagadda, S., Loganathan, P.G., Wilting, J., Christ, B., Huang, R., 2004. Expression pattern of VEGFR-2 (Quek1) during

quail development. Anat Embryol 208. https://doi.org/10.1007/s00429-004-0396-z

Noble, G.K., 1931. The biology of the amphibia /. McGraw-Hill, New York : https://doi.org/10.5962/bhl.title.82448

Noden, D.M., 1983. The embryonic origins of avian cephalic and cervical muscles and associated connective tissues. Am. J. Anat. 168, 257–276. https://doi.org/10.1002/aja.1001680302

Nowicki, J.L., Burke, A.C., 2000. *Hox* genes and morphological identity: axial versus lateral patterning in the vertebrate mesoderm. Development 127, 4265–4275. https://doi.org/10.1242/dev.127.19.4265

Oginuma, M., Harima, Y., Tarazona, O.A., Diaz-Cuadros, M., Michaut, A., Ishitani, T., Xiong, F., Pourquié, O., 2020. Intracellular pH controls WNT downstream of glycolysis in amniote embryos. Nature 584, 98–101. https://doi.org/10.1038/s41586-020-2428-0

Oginuma, M., Moncuquet, P., Xiong, F., Karoly, E., Chal, J., Guevorkian, K., Pourquié, O., 2017. A Gradient of Glycolytic Activity Coordinates FGF and Wnt Signaling during Elongation of the Body Axis in Amniote Embryos. Developmental Cell 40, 342-353.e10. https://doi.org/10.1016/j.devcel.2017.02.001

Okamoto, E., Kusakabe, R., Kuraku, S., Hyodo, S., Robert-Moreno, A., Onimaru, K., Sharpe, J., Kuratani, S., Tanaka, M., 2017. Migratory appendicular muscles precursor cells in the common ancestor to all vertebrates. Nat Ecol Evol 1, 1731–1736. https://doi.org/10.1038/s41559-017-0330-4

Olivera-Martinez, I., Coltey, M., Dhouailly, D., Pourquié, O., 2000. Mediolateral somitic origin of ribs and dermis determined by quail-chick chimeras. Development 127, 4611–4617. https://doi.org/10.1242/dev.127.21.4611

Olivera-Martinez, I., Missier, S., Fraboulet, S., Thélu, J., Dhouailly, D., 2002. Differential regulation of the chick dorsal thoracic dermal progenitors from the medial dermomyotome. Development 129, 4763–4772. https://doi.org/10.1242/dev.129.20.4763

Olivera-Martinez, I., Thelu, J., Dhouailly, D., 2004. Molecular mechanisms controlling dorsal dermis generation from the somitic dermomyotome. Int. J. Dev. Biol. 48, 93–101. https://doi.org/10.1387/ijdb.15272374

Ono, Y., Schlesinger, S., Fukunaga, K., Yambe, S., Sato, T., Sasaki, T., Shukunami, C., Asahara, H., Inui, M., 2023. Scleraxis-lineage cells are required for correct muscle patterning. Development 150, dev201101. https://doi.org/10.1242/dev.201101

Ordahl, C.P., Le Douarin, N.M., 1992. Two myogenic lineages within the developing somite. Development 114, 339–353. https://doi.org/10.1242/dev.114.2.339

Otto, A., Schmidt, C., Patel, K., 2006. Pax3 and Pax7 expression and regulation in the avian embryo. Anat Embryol 211, 293–310. https://doi.org/10.1007/s00429-006-0083-3

Palmeirim, I., Dubrulle, J., Henrique, D., Ish-Horowicz, D., Pourquié, O., 1998. Uncoupling segmentation and somitogenesis in the chick presomitic mesoderm. Dev. Genet. 23, 77–85. https://doi.org/10.1002/(SICI)1520-6408(1998)23:1<77::AID-DVG8>3.0.CO;2-3

Palmeirim, I., Henrique, D., Ish-Horowicz, D., Pourquié, O., 1997. Avian hairy Gene Expression Identifies a Molecular Clock Linked to Vertebrate Segmentation and Somitogenesis. Cell 91, 639–648. https://doi.org/10.1016/S0092-8674(00)80451-1

Pardanaud, L., Luton, D., Prigent, M., Bourcheix, L.-M., Catala, M., Dieterlen-Lièvre, F., 1996. Two distinct endothelial lineages in ontogeny, one of them related to hemopoiesis. Development 122, 1363–1371. https://doi.org/10.1242/dev.122.5.1363

Patapoutian, A., Yoon, J.K., Miner, J.H., Wang, S., Stark, K., Wold, B., 1995. Disruption of the mouse MRF4 gene identifies multiple waves of myogenesis in the myotome. Development 121, 3347–3358. https://doi.org/10.1242/dev.121.10.3347

Picard, C.A., Marcelle, C., 2013. Two distinct muscle progenitor populations coexist throughout amniote development. Developmental Biology 373, 141–148. https://doi.org/10.1016/j.ydbio.2012.10.018

Piekarski, N., Olsson, L., 2014. Resegmentation in the mexican axolotl, *Ambystoma mexicanum*. Journal of Morphology 275, 141–152. https://doi.org/10.1002/jmor.20204

Pinot, M., 1969. Etude expérimentale de la morphogenèse de la cage thoracique chez Fembryon de Poulet: mécanismes et origine du matériel. Development 21, 149–164. https://doi.org/10.1242/dev.21.1.149

Pouget, C., Gautier, R., Teillet, M.-A., Jaffredo, T., 2006. Somite-derived cells replace ventral aortic hemangioblasts and

provide aortic smooth muscle cells of the trunk. Development 133, 1013–1022. https://doi.org/10.1242/dev.02269

Pouget, C., Pottin, K., Jaffredo, T., 2008. Sclerotomal origin of vascular smooth muscle cells and pericytes in the embryo. Developmental Biology 315, 437–447. https://doi.org/10.1016/j.ydbio.2007.12.045

Pourquié, O., Coltey, M., Bréant, C., Le Douarin, N.M., 1995. Control of somite patterning by signals from the lateral plate. Proc. Natl. Acad. Sci. U.S.A. 92, 3219–3223. https://doi.org/10.1073/pnas.92.8.3219

Pourquié, O., Coltey, M., Teillet, M.A., Ordahl, C., Le Douarin, N.M., 1993. Control of dorsoventral patterning of somitic derivatives by notochord and floor plate. Proc. Natl. Acad. Sci. U.S.A. 90, 5242–5246. https://doi.org/10.1073/pnas.90.11.5242

Pourquié, O., Fan, C.-M., Coltey, M., Hirsinger, E., Watanabe, Y., Bréant, C., Francis-West, P., Brickell, P., Tessier-Lavigne, M., Le Douarin, N.M., 1996. Lateral and Axial Signals Involved in Avian Somite Patterning: A Role for BMP4. Cell 84, 461–471. https://doi.org/10.1016/S0092-8674(00)81291-X

Pryce, B.A., Brent, A.E., Murchison, N.D., Tabin, C.J., Schweitzer, R., 2007. Generation of transgenic tendon reporters, ScxGFP and ScxAP, using regulatory elements of the scleraxis gene. Developmental Dynamics 236, 1677–1682. https://doi.org/10.1002/dvdy.21179

Pu, Q., Abduelmula, A., Masyuk, M., Theiss, C., Schwandulla, D., Hans, M., Patel, K., Brand-Saberi, B., Huang, R., 2013. The dermomyotome ventrolateral lip is essential for the hypaxial myotome formation. BMC Dev Biol 13, 37. https://doi.org/10.1186/1471-213X-13-37

Quinn, M.E., Goh, Q., Kurosaka, M., Gamage, D.G., Petrany, M.J., Prasad, V., Millay, D.P., 2017. Myomerger induces fusion of non-fusogenic cells and is required for skeletal muscle development. Nat Commun 8, 15665. https://doi.org/10.1038/ncomms15665

Rao, J., Djeffal, Y., Chal, J., Marchianò, F., Wang, C.-H., Al Tanoury, Z., Gapon, S., Mayeuf-Louchart, A., Glass, I., Sefton, E.M., Habermann, B., Kardon, G., Watt, F.M., Tseng, Y.-H., Pourquié, O., 2023. Reconstructing human brown fat developmental trajectory in vitro. Developmental Cell 58, 2359-2375.e8. https://doi.org/10.1016/j.devcel.2023.08.001

Rees, E., Young, R.D., Evans, D.J.R., 2003. Spatial and temporal contribution of somitic myoblasts to avian hind limb muscles. Developmental Biology 253, 264–278. https://doi.org/10.1016/S0012-1606(02)00028-3

Relaix, F., Rocancourt, D., Mansouri, A., Buckingham, M., 2005. A Pax3/Pax7-dependent population of skeletal muscle progenitor cells. Nature 435, 948–953. https://doi.org/10.1038/nature03594

Relaix, F., Rocancourt, D., Mansouri, A., Buckingham, M., 2004. Divergent functions of murine Pax3 and Pax7 in limb muscle development. Genes Dev. 18, 1088–1105. https://doi.org/10.1101/gad.301004

Reshef, R., Maroto, M., Lassar, A.B., 1998. Regulation of dorsal somitic cell fates: BMPs and Noggin control the timing and pattern of myogenic regulator expression. Genes & Development 12, 290–303. https://doi.org/10.1101/gad.12.3.290

Rickmann, M., Fawcett, J.W., Keynes, R.J., 1985. The migration of neural crest cells and the growth of motor axons through the rostral half of the chick somite. J Embryol Exp Morphol 90, 437–455.

Rifes, P., Carvalho, L., Lopes, C., Andrade, R.P., Rodrigues, G., Palmeirim, I., Thorsteinsdóttir, S., 2007. Redefining the role of ectoderm in somitogenesis: a player in the formation of the fibronectin matrix of presomitic mesoderm. Development 134, 3155–3165. https://doi.org/10.1242/dev.003665

Rifes, P., Thorsteinsdóttir, S., 2012. Extracellular matrix assembly and 3D organization during paraxial mesoderm development in the chick embryo. Developmental Biology 368, 370–381. https://doi.org/10.1016/j.ydbio.2012.06.003

Rinon, A., Lazar, S., Marshall, H., Büchmann-Møller, S., Neufeld, A., Elhanany-Tamir, H., Taketo, M.M., Sommer, L., Krumlauf, R., Tzahor, E., 2007. Cranial neural crest cells regulate head muscle patterning and differentiation during vertebrate embryogenesis. Development 134, 3065–3075. https://doi.org/10.1242/dev.002501

Rios, A.C., Denans, N., Marcelle, C., 2010. Real-time observation of Wnt beta-catenin signaling in the chick embryo. Dev. Dyn. 239, 346–353. https://doi.org/10.1002/dvdy.22174

Rios, A.C., Serralbo, O., Salgado, D., Marcelle, C., 2011. Neural crest regulates myogenesis through the transient activation of NOTCH. Nature 473, 532–535. https://doi.org/10.1038/nature09970

Rodriguez-Guzman, M., Montero, J.A., Santesteban, E., Gañan, Y., Macias, D., Hurle, J.M., 2007. Tendon-muscle crosstalk

controls muscle bellies morphogenesis, which is mediated by cell death and retinoic acid signaling. Developmental Biology 302, 267–280. https://doi.org/10.1016/j.ydbio.2006.09.034

Romer, A.S., Parsons, T.S., 1986. The vertebrate body, 6th ed. ed, The Saunders series in organismic biology. Saunders College Pub, Philadelphia.

Rosenquist, G.C., 1971. The common cardinal veins in the chick embryo: Their origin and development as studied by radioautographic mapping. Anat. Rec. 169, 501–507. https://doi.org/10.1002/ar.1091690303

Rudnicki, M.A., Schnegelsberg, P.N.J., Stead, R.H., Braun, T., Arnold, H.-H., Jaenisch, R., 1993. MyoD or Myf-5 is required for the formation of skeletal muscle. Cell 75, 1351–1359. https://doi.org/10.1016/0092-8674(93)90621-V

Saberi, M., Pu, Q., Valasek, P., Norizadeh-Abbariki, T., Patel, K., Huang, R., 2017. The hypaxial origin of the epaxially located rhomboid muscles. Annals of Anatomy - Anatomischer Anzeiger 214, 15–20. https://doi.org/10.1016/j.aanat.2017.05.009

Salhotra, A., Shah, H.N., Levi, B., Longaker, M.T., 2020. Mechanisms of bone development and repair. Nat Rev Mol Cell Biol 21, 696–711. https://doi.org/10.1038/s41580-020-00279-w

Sambasivan, R., Gayraud-Morel, B., Dumas, G., Cimper, C., Paisant, S., Kelly, R.G., Tajbakhsh, S., 2009. Distinct Regulatory Cascades Govern Extraocular and Pharyngeal Arch Muscle Progenitor Cell Fates. Developmental Cell 16, 810–821. https://doi.org/10.1016/j.devcel.2009.05.008

Sanchez-Gurmaches, J., Guertin, D.A., 2014. Adipocytes arise from multiple lineages that are heterogeneously and dynamically distributed. Nat Commun 5, 4099. https://doi.org/10.1038/ncomms5099

Sanchez-Gurmaches, J., Hung, C.-M., Guertin, D.A., 2016. Emerging Complexities in Adipocyte Origins and Identity. Trends in Cell Biology 26, 313–326. https://doi.org/10.1016/j.tcb.2016.01.004

Sasaki, N., Kiso, M., Kitagawa, M., Saga, Y., 2011. The repression of Notch signaling occurs via the destabilization of mastermind-like 1 by Mesp2 and is essential for somitogenesis. Development 138, 55–64. https://doi.org/10.1242/dev.055533

Sawada, A., Shinya, M., Jiang, Y.-J., Kawakami, A., Kuroiwa, A., Takeda, H., 2001. Fgf/MAPK signalling is a crucial positional cue in somite boundary formation. Development 128, 4873–4880. https://doi.org/10.1242/dev.128.23.4873

Scaal, M., 2021. Development of the amniote ventrolateral body wall. Developmental Dynamics 250, 39–59. https://doi.org/10.1002/dvdy.193

Scaal, M., Füchtbauer, E.-M., Brand-Saberi, B., 2001. cDermo-1 expression indicates a role in avian skin development. Anat Embryol 203, 1–7. https://doi.org/10.1007/PL00008244

Schaeffer, J., Weber, I.P., Thompson, A.J., Keynes, R.J., Franze, K., 2022. Axons in the Chick Embryo Follow Soft Pathways Through Developing Somite Segments. Front. Cell Dev. Biol. 10, 917589. https://doi.org/10.3389/fcell.2022.917589

Schienda, J., Engleka, K.A., Jun, S., Hansen, M.S., Epstein, J.A., Tabin, C.J., Kunkel, L.M., Kardon, G., 2006. Somitic origin of limb muscle satellite and side population cells. Proc. Natl. Acad. Sci. U.S.A. 103, 945–950. https://doi.org/10.1073/pnas.0510164103

Schrägle, J., Huang, R., Christ, B., Pr□ls, F., 2004. Control of the temporal and spatial Uncx4.1 expression in the paraxial mesoderm of avian embryos. Anat Embryol 208. https://doi.org/10.1007/s00429-004-0404-3

Schultz, R., Elbrønd, V., 2018. Novel dissection approach of equine back muscles: new advances in anatomy and topography - and comparison to present literature. BIOMEDJ. https://doi.org/10.32392/biomed.28

Schünke, M., Schulte, E., Schumacher, U., 2021. Thieme atlas of anatomy. General anatomy and musculoskeletal system, Third edition, Latin nomenclature. ed. Thieme, New York.

Schweitzer, R., Chyung, J.H., Murtaugh, L.C., Brent, A.E., Rosen, V., Olson, E.N., Lassar, A., Tabin, C.J., 2001. Analysis of the tendon cell fate using Scleraxis, a specific marker for tendons and ligaments. Development 128, 3855–3866. https://doi.org/10.1242/dev.128.19.3855

Seale, P., Bjork, B., Yang, W., Kajimura, S., Chin, S., Kuang, S., Scimè, A., Devarakonda, S., Conroe, H.M., Erdjument-Bromage, H., Tempst, P., Rudnicki, M.A., Beier, D.R., Spiegelman, B.M., 2008. PRDM16 controls a brown fat/skeletal muscle switch. Nature 454, 961–967. https://doi.org/10.1038/nature07182

Seale, P., Sabourin, L.A., Girgis-Gabardo, A., Mansouri, A., Gruss, P., Rudnicki, M.A., 2000. Pax7 Is Required for the Specification of Myogenic Satellite Cells. Cell 102, 777–786. https://doi.org/10.1016/S0092-8674(00)00066-0

Sebo, Z.L., Jeffery, E., Holtrup, B., Rodeheffer, M.S., 2018. A mesodermal fate map for adipose tissue. Development dev.166801. https://doi.org/10.1242/dev.166801

Sefton, E.M., Gallardo, M., Tobin, C.E., Collins, B.C., Colasanto, M.P., Merrell, A.J., Kardon, G., 2022. Fibroblast-derived Hgf controls recruitment and expansion of muscle during morphogenesis of the mammalian diaphragm. eLife 11, e74592. https://doi.org/10.7554/eLife.74592

Sefton, E.M., Kardon, G., 2019. Connecting muscle development, birth defects, and evolution: An essential role for muscle connective tissue, in: Current Topics in Developmental Biology. Elsevier, pp. 137–176. https://doi.org/10.1016/bs.ctdb.2018.12.004

Seno, T., 1961. AN EXPERIMENTAL STUDY ON THE FORMATION OF THE BODY WALL IN THE CHICK. Cells Tissues Organs 45, 60–82. https://doi.org/10.1159/000141740

Serralbo, O., Marcelle, C., 2014. Migrating cells mediate long-range WNT signaling. Development 141, 2057–2063. https://doi.org/10.1242/dev.107656

Shearman, R.M., Tulenko, F.J., Burke, A.C., 2011. 3D reconstructions of quail–chick chimeras provide a new fate map of the avian scapula. Developmental Biology 355, 1–11. https://doi.org/10.1016/j.ydbio.2011.03.032

Shi, D.L., Boucaut, J.C., 1995. The chronological development of the urodele amphibian Pleurodeles waltl (Michah). Int J Dev Biol 39, 427–441.

Shih, H.P., Gross, M.K., Kioussi, C., 2007. Cranial muscle defects of Pitx2 mutants result from specification defects in the first branchial arch. Proc. Natl. Acad. Sci. U.S.A. 104, 5907–5912. https://doi.org/10.1073/pnas.0701122104

Shimizu, N., Kawakami, K., Ishitani, T., 2012. Visualization and exploration of Tcf/Lef function using a highly responsive Wnt/β-catenin signaling-reporter transgenic zebrafish. Developmental Biology 370, 71–85. https://doi.org/10.1016/j.ydbio.2012.07.016

Shufeldt, R.W., 1890. The myology of the raven (Corvus corax sinuatus.) A guide to the study of the muscular system in birds. Macmillan and co, London. https://doi.org/10.5962/bhl.title.3771

Shukunami, C., Takimoto, A., Nishizaki, Y., Yoshimoto, Y., Tanaka, S., Miura, S., Watanabe, H., Sakuma, T., Yamamoto, T., Kondoh, G., Hiraki, Y., 2018. Scleraxis is a transcriptional activator that regulates the expression of Tenomodulin, a marker of mature tenocytes and ligamentocytes. Sci Rep 8, 3155. https://doi.org/10.1038/s41598-018-21194-3

Shukunami, C., Takimoto, A., Oro, M., Hiraki, Y., 2006. Scleraxis positively regulates the expression of tenomodulin, a differentiation marker of tenocytes. Developmental Biology 298, 234–247. https://doi.org/10.1016/j.ydbio.2006.06.036

Sieiro, D., Rios, A.C., Hirst, C.E., Marcelle, C., 2016. Cytoplasmic NOTCH and membrane-derived β-catenin link cell fate choice to epithelial-mesenchymal transition during myogenesis. Elife 5. https://doi.org/10.7554/eLife.14847

Sieiro-Mosti, D., De La Celle, M., Pelé, M., Marcelle, C., 2014. A dynamic analysis of muscle fusion in the chick embryo. Development 141, 3605–3611. https://doi.org/10.1242/dev.114546

Smith, J.H., 1963. Relation of Body Size to Muscle Cell Size and Number in the Chicken ,. Poultry Science 42, 283–290. https://doi.org/10.3382/ps.0420283

Smith-Paredes, D., Vergara-Cereghino, M.E., Lord, A., Moses, M.M., Behringer, R.R., Bhullar, B.-A.S., 2022. Embryonic muscle splitting patterns reveal homologies of amniote forelimb muscles. Nat Ecol Evol 6, 604–613. https://doi.org/10.1038/s41559-022-01699-x

Soriano, P., 1997. The PDGFα receptor is required for neural crest cell development and for normal patterning of the somites. Development 124, 2691–2700. https://doi.org/10.1242/dev.124.14.2691

Spitz, F., Demignon, J., Porteu, A., Kahn, A., Concordet, J.-P., Daegelen, D., Maire, P., 1998. Expression of myogenin during embryogenesis is controlled by Six/ *sine oculis* homeoproteins through a conserved MEF3 binding site. Proc. Natl. Acad. Sci. U.S.A. 95, 14220–14225. https://doi.org/10.1073/pnas.95.24.14220

Stone, O.A., Stainier, D.Y.R., 2019. Paraxial Mesoderm Is the Major Source of Lymphatic Endothelium. Developmental Cell 50, 247-255.e3. https://doi.org/10.1016/j.devcel.2019.04.034

Sun, Y., Ren, W., Côté, J.-F., Hinds, P.W., Hu, X., Du, K., 2015. ClipR-59 Interacts with Elmo2 and Modulates Myoblast Fusion. Journal of Biological Chemistry 290, 6130–6140. https://doi.org/10.1074/jbc.M114.616680

Swinehart, I.T., Schlientz, A.J., Quintanilla, C.A., Mortlock, D.P., Wellik, D.M., 2013. *Hox11* genes are required for regional patterning and integration of muscle, tendon and bone. Development 140, 4574–4582. https://doi.org/10.1242/dev.096693

Tajbakhsh, S., Borello, U., Vivarelli, E., Kelly, R., Papkoff, J., Duprez, D., Buckingham, M., Cossu, G., 1998. Differential activation of *Myf5* and *MyoD* by different Wnts in explants of mouse paraxial mesoderm and the later activation of myogenesis in the absence of *Myf5*. Development 125, 4155–4162. https://doi.org/10.1242/dev.125.21.4155

Takahashi, Y., Takagi, A., Hiraoka, S., Koseki, H., Kanno, J., Rawls, A., Saga, Y., 2007. Transcription factors Mesp2 and Paraxis have critical roles in axial musculoskeletal formation. Developmental Dynamics 236, 1484–1494. https://doi.org/10.1002/dvdy.21178

Tallquist, M.D., Weismann, K.E., Hellström, M., Soriano, P., 2000. Early myotome specification regulates PDGFA expression and axial skeleton development. Development 127, 5059–5070. https://doi.org/10.1242/dev.127.23.5059

Thorsteinsdóttir, S., Deries, M., Cachaço, A.S., Bajanca, F., 2011. The extracellular matrix dimension of skeletal muscle development. Developmental Biology 354, 191–207. https://doi.org/10.1016/j.ydbio.2011.03.015

Tokita, M., 2006. Cranial neural crest cell migration in cockatiel *Nymphicus hollandicus* (Aves: Psittaciformes). Journal of Morphology 267, 333–340. https://doi.org/10.1002/jmor.10408

Tokita, M., Abe, T., Suzuki, K., 2012. The developmental basis of bat wing muscle. Nat Commun 3, 1302. https://doi.org/10.1038/ncomms2298

Tokita, M., Nakayama, T., Schneider, R.A., Agata, K., 2013. Molecular and cellular changes associated with the evolution of novel jaw muscles in parrots. Proc. R. Soc. B. 280, 20122319. https://doi.org/10.1098/rspb.2012.2319

Tokita, M., Schneider, R.A., 2009. Developmental origins of species-specific muscle pattern. Developmental Biology 331, 311–325. https://doi.org/10.1016/j.ydbio.2009.05.548

Tozer, S., Bonnin, M.-A., Relaix, F., Di Savino, S., García-Villalba, P., Coumailleau, P., Duprez, D., 2007. Involvement of vessels and PDGFB in muscle splitting during chick limb development. Development 134, 2579–2591. https://doi.org/10.1242/dev.02867

Valasek, P., Evans, D.J.R., Maina, F., Grim, M., Patel, K., 2005. A dual fate of the hindlimb muscle mass: cloacal/perineal musculature develops from leg muscle cells. Development 132, 447–458. https://doi.org/10.1242/dev.01545

Valasek, P., Macharia, R., Neuhuber, W.L., Wilting, J., Becker, D.L., Patel, K., 2007. Lymph heart in chick - somitic origin, development and embryonic oedema. Development 134, 4427–4436. https://doi.org/10.1242/dev.004697

Valasek, P., Theis, S., DeLaurier, A., Hinits, Y., Luke, G.N., Otto, A.M., Minchin, J., He, L., Christ, B., Brooks, G., Sang, H., Evans, D.J., Logan, M., Huang, R., Patel, K., 2011. Cellular and molecular investigations into the development of the pectoral girdle. Developmental Biology 357, 108–116. https://doi.org/10.1016/j.ydbio.2011.06.031

Valasek, P., Theis, S., Krejci, E., Grim, M., Maina, F., Shwartz, Y., Otto, A., Huang, R., Patel, K., 2010. Somitic origin of the medial border of the mammalian scapula and its homology to the avian scapula blade. Journal of Anatomy 216, 482–488. https://doi.org/10.1111/j.1469-7580.2009.01200.x

Vallecillo-García, P., Orgeur, M., Vom Hofe-Schneider, S., Stumm, J., Kappert, V., Ibrahim, D.M., Börno, S.T., Hayashi, S., Relaix, F., Hildebrandt, K., Sengle, G., Koch, M., Timmermann, B., Marazzi, G., Sassoon, D.A., Duprez, D., Stricker, S., 2017. Odd skipped-related 1 identifies a population of embryonic fibro-adipogenic progenitors regulating myogenesis during limb development. Nat Commun 8, 1218. https://doi.org/10.1038/s41467-017-01120-3

Van Swearingen, J., Lance-Jones, C., 1995. Slow and Fast Muscle Fibers Are Preferentially Derived from Myoblasts Migrating into the Chick Limb Bud at Different Developmental Times. Developmental Biology 170, 321–337. https://doi.org/10.1006/dbio.1995.1218

Varela-Lasheras, I., Bakker, A.J., Van Der Mije, S.D., Metz, J.A., Van Alphen, J., Galis, F., 2011. Breaking evolutionary and pleiotropic constraints in mammals: On sloths, manatees and homeotic mutations. EvoDevo 2, 11.

https://doi.org/10.1186/2041-9139-2-11

Varela-Lasheras, I., Bakker, A.J., Van Der Mije, S.D., Metz, J.A.J., Van Alphen, J., Galis, F., 2021. Correction to: Breaking evolutionary and pleiotropic constraints in mammals: on sloths, manatees and homeotic mutations. EvoDevo 12, 13. https://doi.org/10.1186/s13227-021-00183-0

Vasyutina, E., Lenhard, D.C., Wende, H., Erdmann, B., Epstein, J.A., Birchmeier, C., 2007. RBP-J (Rbpsuh) is essential to maintain muscle progenitor cells and to generate satellite cells. PNAS 104, 4443–4448. https://doi.org/10.1073/pnas.0610647104

Vasyutina, E., Martarelli, B., Brakebusch, C., Wende, H., Birchmeier, C., 2009. The small G-proteins Rac1 and Cdc42 are essential for myoblast fusion in the mouse. Proc. Natl. Acad. Sci. U.S.A. 106, 8935–8940. https://doi.org/10.1073/pnas.0902501106

Vasyutina, E., Stebler, J., Brand-Saberi, B., Schulz, S., Raz, E., Birchmeier, C., 2005. *CXCR4* and *Gab1* cooperate to control the development of migrating muscle progenitor cells. Genes Dev. 19, 2187–2198. https://doi.org/10.1101/gad.346205

Veeman, M.T., Slusarski, D.C., Kaykas, A., Louie, S.H., Moon, R.T., 2003. Zebrafish Prickle, a Modulator of Noncanonical Wnt/Fz Signaling, Regulates Gastrulation Movements. Current Biology 13, 680–685. https://doi.org/10.1016/S0960-9822(03)00240-9

Vermot, J., Pourquié, O., 2005. Retinoic acid coordinates somitogenesis and left–right patterning in vertebrate embryos. Nature 435, 215–220. https://doi.org/10.1038/nature03488

Vivarelli, E., Brown, W.E., Whalen, R.G., Cossu, G., 1988. The expression of slow myosin during mammalian somitogenesis and limb bud differentiation. The Journal of cell biology 107, 2191–2197. https://doi.org/10.1083/jcb.107.6.2191

Wagner, J., Schmidt, C., Nikowits, W., Christ, B., 2000. Compartmentalization of the Somite and Myogenesis in Chick Embryos Are Influenced by Wnt Expression. Developmental Biology 228, 86–94. https://doi.org/10.1006/dbio.2000.9921

Wallin, J., Wilting, J., Koseki, H., Fritsch, R., Christ, B., Balling, R., 1994. The role of *Pax-1* in axial skeleton development. Development 120, 1109–1121. https://doi.org/10.1242/dev.120.5.1109

Wan, Y., Wei, Z., Looger, L.L., Koyama, M., Druckmann, S., Keller, P.J., 2019. Single-Cell Reconstruction of Emerging Population Activity in an Entire Developing Circuit. Cell 179, 355-372.e23. https://doi.org/10.1016/j.cell.2019.08.039

Wang, B., He, L., Ehehalt, F., Geetha-Loganathan, P., Nimmagadda, S., Christ, B., Scaal, M., Huang, R., 2005. The formation of the avian scapula blade takes place in the hypaxial domain of the somites and requires somatopleure-derived BMP signals. Developmental Biology 287, 11–18. https://doi.org/10.1016/j.ydbio.2005.08.016

Wang, B., Pu, Q., De, R., Patel, K., Christ, B., Wilting, J., Huang, R., 2010. Commitment of chondrogenic precursors of the avian scapula takes place after epithelial-mesenchymal transition of the dermomyotome. BMC Dev Biol 10, 91. https://doi.org/10.1186/1471-213X-10-91

Wang, H., Noulet, F., Edom-Vovard, F., Le Grand, F., Duprez, D., 2010. Bmp Signaling at the Tips of Skeletal Muscles Regulates the Number of Fetal Muscle Progenitors and Satellite Cells during Development. Developmental Cell 18, 643–654. https://doi.org/10.1016/j.devcel.2010.02.008

Wang, H.U., Anderson, D.J., 1997. Eph Family Transmembrane Ligands Can Mediate Repulsive Guidance of Trunk Neural Crest Migration and Motor Axon Outgrowth. Neuron 18, 383–396. https://doi.org/10.1016/S0896-6273(00)81240-4

Wang, W., Kissig, M., Rajakumari, S., Huang, L., Lim, H., Won, K.-J., Seale, P., 2014. Ebf2 is a selective marker of brown and beige adipogenic precursor cells. Proc. Natl. Acad. Sci. U.S.A. 111, 14466–14471. https://doi.org/10.1073/pnas.1412685111

Wang, W., Seale, P., 2016. Control of brown and beige fat development. Nat Rev Mol Cell Biol 17, 691–702. https://doi.org/10.1038/nrm.2016.96

Ward, L., Evans, S.E., Stern, C.D., 2017. A resegmentation-shift model for vertebral patterning. Journal of Anatomy 230, 290–296. https://doi.org/10.1111/joa.12540

Watanabe, Y., Le Douarin, N.M., 1996. A role for BMP-4 in the development of subcutaneous cartilage. Mechanisms of Development 57, 69–78. https://doi.org/10.1016/0925-4773(96)00534-5

Webster, E.L., Hudson, P.E., Channon, S.B., 2014. Comparative functional anatomy of the epaxial musculature of dogs (*C anis*

familiaris) bred for sprinting vs. fighting. Journal of Anatomy 225, 317–327. https://doi.org/10.1111/joa.12208

Weintraub, H., Tapscott, S.J., Davis, R.L., Thayer, M.J., Adam, M.A., Lassar, A.B., Miller, A.D., 1989. Activation of muscle-specific genes in pigment, nerve, fat, liver, and fibroblast cell lines by forced expression of MyoD. Proc. Natl. Acad. Sci. U.S.A. 86, 5434–5438. https://doi.org/10.1073/pnas.86.14.5434

White, R.B., Biérinx, A.-S., Gnocchi, V.F., Zammit, P.S., 2010. Dynamics of muscle fibre growth during postnatal mouse development. BMC Dev Biol 10, 21. https://doi.org/10.1186/1471-213X-10-21

Wiegreffe, C., Christ, B., Huang, R., Scaal, M., 2007. Sclerotomal origin of smooth muscle cells in the wall of the avian dorsal aorta. Developmental Dynamics 236, 2578–2585. https://doi.org/10.1002/dvdy.21279

Williams, B.A., Ordahl, C.P., 1994. *Pax-3* expression in segmental mesoderm marks early stages in myogenic cell specification. Development 120, 785–796. https://doi.org/10.1242/dev.120.4.785

Williams, S., Alkhatib, B., Serra, R., 2019. Development of the axial skeleton and intervertebral disc, in: Current Topics in Developmental Biology. Elsevier, pp. 49–90. https://doi.org/10.1016/bs.ctdb.2018.11.018

Wilting, J., Aref, Y., Huang, R., Tomarev, S.I., Schweigerer, L., Christ, B., Valasek, P., Papoutsi, M., 2006. Dual origin of avian lymphatics. Developmental Biology 292, 165–173. https://doi.org/10.1016/j.ydbio.2005.12.043

Wilting, J., Brand-Saberi, B., Huang, R., Zhi, Q., Köntges, G., Ordahl, C.P., Christ, B., 1995. Angiogenic potential of the avian somite. Developmental Dynamics 202, 165–171. https://doi.org/10.1002/aja.1002020208

Wilting, J., Kurz, H., Brand-Saberi, B., Steding, G., Yang, Y., Hasselhorn, H.-M., Epperlein, H.-H., Christ, B., 1994. Kinetics and differentiation of somite cells forming the vertebral column: studies on human and chick embryos. Anat Embryol 190. https://doi.org/10.1007/BF00190107

Wilting, J., Papoutsi, M., Schneider, M., Christ, B., 2000. The lymphatic endothelium of the avian wing is of somitic origin. Dev. Dyn. 217, 271–278. https://doi.org/10.1002/(SICI)1097-0177(200003)217:3<271::AID-DVDY5>3.0.CO;2-2

Winterbottom, R., 1973. A Descriptive Synonymy of the Striated Muscles of the Teleostei. Proceedings of the Academy of Natural Sciences of Philadelphia, 125, 225–317.

Wood, W.M., Otis, C., Etemad, S., Goldhamer, D.J., 2020. Development and patterning of rib primordia are dependent on associated musculature. Developmental Biology 468, 133–145. https://doi.org/10.1016/j.ydbio.2020.07.015

Wurmser, M., Madani, R., Chaverot, N., Backer, S., Borok, M., Dos Santos, M., Comai, G., Tajbakhsh, S., Relaix, F., Santolini, M., Sambasivan, R., Jiang, R., Maire, P., 2023. Overlapping functions of SIX homeoproteins during embryonic myogenesis. PLoS Genet 19, e1010781. https://doi.org/10.1371/journal.pgen.1010781

Yang, J.T., Bader, B.L., Kreidberg, J.A., Ullman-Culleré, M., Trevithick, J.E., Hynes, R.O., 1999. Overlapping and Independent Functions of Fibronectin Receptor Integrins in Early Mesodermal Development. Developmental Biology 215, 264–277. https://doi.org/10.1006/dbio.1999.9451

Yaseen, W., Kraft-Sheleg, O., Zaffryar-Eilot, S., Melamed, S., Sun, C., Millay, D.P., Hasson, P., 2021. Fibroblast fusion to the muscle fiber regulates myotendinous junction formation. Nat Commun 12, 3852. https://doi.org/10.1038/s41467-021-24159-9

Young, M., Selleri, L., Capellini, T.D., 2019. Genetics of scapula and pelvis development: An evolutionary perspective, in: Current Topics in Developmental Biology. Elsevier, pp. 311–349. https://doi.org/10.1016/bs.ctdb.2018.12.007

Yvernogeau, L., Auda-Boucher, G., Fontaine-Perus, J., 2012. Limb bud colonization by somite-derived angioblasts is a crucial step for myoblast emigration. Development 139, 277–287. https://doi.org/10.1242/dev.067678

Yvernogeau, L., Gautier, R., Petit, L., Khoury, H., Relaix, F., Ribes, V., Sang, H., Charbord, P., Souyri, M., Robin, C., Jaffredo, T., 2019. In vivo generation of haematopoietic stem/progenitor cells from bone marrow-derived haemogenic endothelium. Nat Cell Biol 21, 1334–1345. https://doi.org/10.1038/s41556-019-0410-6

Zacharias, A.L., Lewandoski, M., Rudnicki, M.A., Gage, P.J., 2011. Pitx2 is an upstream activator of extraocular myogenesis and survival. Developmental Biology 349, 395–405. https://doi.org/10.1016/j.ydbio.2010.10.028

Zalc, A., Hayashi, S., Auradé, F., Bröhl, D., Chang, T., Mademtzoglou, D., Mourikis, P., Yao, Z., Cao, Y., Birchmeier, C., Relaix, F., 2014. Antagonistic regulation of p57kip2 by Hes/Hey downstream of Notch signaling and muscle regulatory factors

regulates skeletal muscle growth arrest. Development 141, 2780–2790. https://doi.org/10.1242/dev.110155

Zhang, Q., Vashisht, A.A., O'Rourke, J., Corbel, S.Y., Moran, R., Romero, A., Miraglia, L., Zhang, J., Durrant, E., Schmedt, C., Sampath, Srinath C., Sampath, Srihari C., 2017. The microprotein Minion controls cell fusion and muscle formation. Nat Commun 8, 15664. https://doi.org/10.1038/ncomms15664

Zhang, W., Behringer, R.R., Olson, E.N., 1995. Inactivation of the myogenic bHLH gene MRF4 results in up-regulation of myogenin and rib anomalies. Genes Dev. 9, 1388–1399. https://doi.org/10.1101/gad.9.11.1388

Zhi, Q., Huang, R., Christ, B., Brand-Saberi, B., 1996. Participation of individual brachial somites in skeletal muscles of the avian distal wing. Anat Embryol 194. https://doi.org/10.1007/BF00198534

Ziermann, J.M., Diogo, R., Noden, D.M., 2018. Neural crest and the patterning of vertebrate craniofacial muscles. Genesis 56, e23097. https://doi.org/10.1002/dvg.23097